THE ANGULAR RESOLVED PHOTOELECTRON SPECTROSCOPY OF VARIOUS POLYATOMIC MOLECULAR SYSTEMS

Thesis by

Dorothy J. Flanagan

In Partial Fulfillment of the Requirements

for the Degree of

Doctor of Philosophy

California Institute of Technology

Pasadena, California

1985

Submitted April 19, 1985

In memory of my grandfather,

Vahan Garabed Azadian

Acknowledgements

I would like to thank my advisor, Professor Aron Kuppermann for his support during this study. I would also like to thank my predecessor, Jeff Sell, for his patience and kindness during my initial work on the project and also my coworker during the later part of my time here, Charles Koerting. His drive and energy were of great assistance in all aspects of our endeavors.

I would like to acknowledge the other members of the research group with whom I have shared my tenure as a graduate student, especially fellow experimentalists, Jerry Winniczek, Dave Moll and Garth Parker, and theoreticians, Jack Kaye and Steve Cuccaro. Although our interactions have at times been turbulent, their frankness, honesty and friendship have been of great value.

I would like to thank Adria McMillan and Heidi Tanciar for their able assistance in many matters, and I am especially grateful to Heidi for typing a manuscript in this work.

I am indebted to the personnel of the chemistry department instrument and electronics shops for the repair and maintenance of the equipment used in this experiment. I would, in particular, like to thank Tony Stark, Bill Schulke and Guy Duremberg of the instrument shop and Tom Dunn of the electronic shop for their timely help and advice.

I thank the California Institute of Technology for a graduate fellowship.

I wish to thank my parents for their love and concern and for asking a question at a critical time.

Lastly, I would like to thank Rena Margulis, whose friendship and emotional support over the years have been a gift beyond price.

Abstract

This thesis describes the study of the angular resolved photoelectron spectroscopy of a series of polyatomic molecules. The spectrometer consists of a He I radiation source, a scattering chamber, and a rotatable detection system which includes a set of electrostatic lenses, a hemispherical electrostatic kinetic energy analyzer and an electron multiplier. Angular distributions are determined from the variation in intensity as the detection system is rotated about the center of the scattering chamber.

The theory of photoionization is discussed semiclassically, as the interaction of an atom or molecule treated quantum mechanically with a classical radiation field. Some recent calculations of the asymmetry parameter for valence electrons are briefly reviewed.

Photoelectron angular distributions were measured for acetylene, propyne, 1-butyne, and 2-butyne. The asymmetry parameters of propyne, 1-butyne, and 2-butyne have been determined for the first time. Trends in the asymmetry parameter, ionization potentials and band shapes were studied. It was determined that the parity favoredness rules of Chang failed to account for the behavior of the asymmetry parameter of the molecule despite the symmetry of the molecule. Instead, acetylene and its alkylated analogs follow the trends in β observed in studies of the methylated ethenes.

Additionally, the semi-empirical rule that the β values of π orbitals

are higher than for σ orbitals was violated in this series. Acetylene and propyne possess σ orbital with β values significantly higher than the π orbitals.

Two principal substituent effects were observed: 1) a systematic decrease in the first ionization potential and 2) a similar decrease in the asymmetry parameter of the $\tilde{X}$ band with increasing alkylation.

The photoelectron angular distributions were measured for formaldehyde, acetaldehyde, and acetone. The asymmetry parameter has been determined for the first time for acetaldehyde, and, with the exception of the first band, for acetone.

This study has shown that the beta values of the $\tilde{X}$ n_O bands of these molecules are, within experimental error, invariant with respect to methyl substitution, results that are consistent with the nonbonding characteristics of the molecular orbitals. The $\tilde{A}$ πC=O bands, however, show a strong decrease in the asymmetry parameter of approximately 0.2 per methylation in a manner similar to that observed previously in the methylated ethenes and ethynes. The expected systematic decrease in first ionization potential with substitution was also observed.

Lastly, HAM/3 calculations were performed to determine the ionization potentials of some substituted carbonyls and to examine the excitation energies of ethylene and its methyl and fluoro derivatives to evaluate the method's usefulness to studies in electron impact spectroscopy.

There was generally good agreement between the ionization po-

tential calculated by this method and experimentally determined values. Agreement between the calculated values of the excitation energies and the experimental were reasonable but the method was not sensitive enough to reproduce the trends observed with increasing substitution of the chromophore.

TABLE OF CONTENTS

CHAPTER 1

INTRODUCTION

Photoelectron spectroscopy encompasses the study of the energy, intensity and the angular distributions of electrons produced by the interaction of atoms and molecules with vacuum ultraviolet radiation.

Einstein's[1] relationship maintains that the kinetic energy of the ejected electrons is merely the difference between the energy of the ionizing photon, $\hbar\omega$, and the binding energy of the electron, called the ionization potential(IP). Thus by conservation of energy:

$$\hbar\omega = IP + KE \tag{1}$$

By invoking Koopmans' theorem,[2] the IP of the electron is associated with the negative of the orbital energy, E.

$$IP = -E \tag{2}$$

It must be noted that Koopmans' theorem is an approximation based on many assumptions: that there are no reorientation effects in the orbitals on ionization, and that the relativistic and correlation energy is the same in both molecule and ion.[3]

These assumptions are clearly not valid for open shell systems, for ionization of core electrons, and for some ionic excited states of closed shell molecules. However, for the ionization of valence electrons of molecules with a closed shell configuration, which is the

preponderant case occurring in ultraviolet molecular photoelectron spectroscopy, Koopmans' theorem may be properly invoked to support the conclusion that the photoelectron spectrum provides a correct representation, to a good appproximation, of the molecular orbital energy diagram.

In photoelectron spectroscopy, a photon beam of high intensity is used in the ionization process. This beam is typically of two types: the resonance line source output of a noble gas discharge lamp, helium being the gas most frequently used, or the continuous wavelength source output from a synchrotron storage ring. In either case the monochromatized radiation is directed at an assemblage of sample gas either from a molecular beam or in an ionization chamber.

The principal process of ionization that results may be schematically represented by the following:

$$\hbar\omega + M \rightarrow M^+ + e^- \qquad \text{(direct ionization)} \qquad (3)$$

Other processes that may occur are,

$$\hbar\omega + M \rightarrow A^{\cdot} + B^{\cdot} \qquad \text{(photodissociation)} \qquad (4)$$

$$\hbar\omega + M \rightarrow A^+ + B^- \qquad \text{(dissociative photoionization)} \qquad (5)$$

Also possible is,

$$\hbar\omega + M \rightarrow M^* \rightarrow M^+ + e^- \qquad \text{(autoionization)} \qquad (6)$$

where M^* may be stable, metastable or unstable(repulsive). Photoelectron spectroscopy concerns only those processes that produce electrons, direct and autoionization.

The electrons generated are discriminated by an electrostatic energy analyzer according to their kinetic energy and then detected by means of an electron multiplier. A photoelectron spectrum is the plot of the measured intensity of the electrons detected versus their kinetic energy (or the conjugate variable, ionization potential).

To aid in the association of the photoelectron bands with particular molecular orbitals, the angular distribution of the ejected electrons provides additional information on the nature of the underlying orbitals.

It was established by Bethe and Salpeter[4] that the intensity of the photoelectrons ionized from hydrogen atoms depended on the angle θ between the photon beam and the direction of the velocity vector of the electron in the following manner:

$$I(\theta) = a + b\cos^2(\theta) \tag{7}$$

Cooper and Zare[5] extended this to the case of atoms and molecules ionized by linearly polarized light:

$$\frac{d\bar{\sigma}}{d\Omega} = \frac{\sigma^{tot}}{4\pi}[1 + \beta P_2(\cos\theta)] \tag{8}$$

While Cooper and Manson[6] derived a similar relation for unpolarized light:

$$\frac{d\bar{\sigma}}{d\Omega} = \frac{\sigma^{tot}}{4\pi}[1 - \frac{1}{2}\beta P_2(\cos\theta)] \tag{9}$$

where the $\cos^2\theta$ distribution is preserved in the second order Legendre polynomial,

$P_2(\cos\theta) = \frac{1}{2}(3\cos^2\theta - 1)$, and β is the asymmetry parameter that reflects the departure from isotropy.

Experiments using synchrotron radiation sources use the expression in equation 8 to determine the asymmetry parameter since synchrotron radiation is elliptically polarized.

Arc discharge lamps, such as the one in the experiment in this thesis, generate unpolarized light; hence equation 9 is the appropriate expression for determining β. It must be stressed that the β determined in both cases can be shown to be, for a given energy, rigorously identical.

It has been demonstrated experimentally that the angular distributions of photoelectrons are sensitive to differences in orbital angular momentum, yielding disparate anisotropy parameters for σ and π orbitals within the same molecule. In general, π orbitals have higher β values and σ orbitals have more symmetric distributions.[7] This empirical relationship may be used to aid in elucidating the photoelectron spectrum of molecules.

This work continues the work of D. Mintz and J. Sell of this research group who studied the angular distributions of Ar,[8] Ne,[8] N_2[9] and a homologous series of linear alkenes and dienes[8,10] and CO,[11] SF_6,[12] the halogenated benzenes[13,14] and ethylenes,[14,15] furan, thiophene and pyrrole.[16]

It is the intent of this work to characterize the effects of various functional groups on the angular distribution of the electrons and to examine substituent effects on the observed values. In this manner the perturbation interaction of the substituents on the chromophore may be explored, as well as the implications of band shape and ionization potentials of the molecules under consideration.

REFERENCES

1. A. Einstein, *Amer. J. Phys.* translated by A. Arons and M. Peppard, **33,** 367 (1965).
2. T. Koopmans, *Physica,* **1**, 104 (1933).
3. W. G. Richards, *Int. J. Mass Spect.*, **2**, 419 (1969).
4. H. A. Bethe and E. Salpeter, *Quantum Mechanics of One and Two Electron Atoms* (Springer-Verlag, Berlin, 1957)
5. J. Cooper and R. N. Zare, *J. Chem. Phys.*, **48**, 942 (1968).
6. J. Cooper and S. Manson, *Phys. Rev.*, **177**, 157 (1967).
7. P. R. Keller, D. Mehaffy, J. Taylor, F. A. Grimm, and T. A. Carlson, *J. Electron Spectroscopy,* **27**, 223 (1982) and references within.
8. D. M. Mintz, Ph.D Thesis, California Institute of Technology, 1976.
9. D. M. Mintz and A. Kuppermann, *J. Chem. Phys.*, **69**, 3953 (1978).
10. D. M. Mintz and A. Kuppermann, *J. Chem. Phys.*, **71**, 3499 (1979).
11. J. A. Sell, A. Kuppermann, and D. M. Mintz, *J. Electron Spectroscopy*, **16**, 127 (1979).
12. J. A. Sell and A. Kuppermann, *Chem. Phys.*, **33**, 379 (1978).
13. J. A. Sell and A. Kuppermann, *Chem. Phys.*, **33**, 367 (1978).
14. J. A. Sell, D. M. Mintz and A. Kuppermann, *Chem. Phys. Lett.*, **58**, 601 (1978).
15. J. A. Sell and A. Kuppermann, *J. Chem. Phys.*, **71**, 4703 (1979).
16. J. A. Sell and A. Kuppermann, *Chem. Phys. Lett.*, **61**, 355 (1979).

CHAPTER 2

THEORY

2.1 Theory of Photoionization

In this section, the theory of photoionization will be considered. It is sufficient for this purpose to consider this process semiclassically[1] as the interaction of one electron atoms (molecules) treated quantum mechanically, with a classical radiation field.

The Schrödinger equation of motion for a particle of mass m and charge e^- in a classical radiation field is given by the following relationship:

$$i\hbar\frac{d\Psi}{dt} = [-\frac{\hbar^2}{2m}\nabla^2 + \frac{ie\hbar}{mc}\mathbf{A}\cdot\nabla + \frac{ie\hbar}{2mc}\nabla\cdot\mathbf{A} + \frac{e^2}{2mc^2}\mathbf{A}^2 + e\phi + V]\Psi \quad (1)$$

where the radiation field is characterized by the vector potential **A** and the scalar potential ϕ, and V represents the binding potential of the particle. Under this treatment, **A** and ϕ characterize a field sufficiently weak to be regarded as a perturbation to the system.

The following relationship can be derived between the vector and scalar potentials **A** and ϕ and the electric and magnetic field vectors:

$$\mathbf{E} = -\frac{1}{c}\frac{d\mathbf{A}}{dt} - \nabla\phi \quad (2)$$

and,

$$\mathbf{H} = \nabla \times \mathbf{A} \quad (3)$$

consistent with Maxwell's equations.

It can be shown[1] that if the charge and the current densities are zero (completely empty space) then it is possible to invoke the Coulomb Gauge without loss of generality. So that:

$$\nabla \cdot \mathbf{A} = 0 \tag{4}$$

and

$$\phi = 0 \tag{5}$$

It is further possible to simplify the Schrödinger equation by considering the relative magnitudes of the second term in $\nabla \cdot \mathbf{A}$ and the fourth term in $\mathbf{A}^2$. It can be demonstrated[1] that the ratio of the $\mathbf{A}^2$ term to $\nabla \cdot \mathbf{A}$ is approximately $e\mathbf{A}/pc$ where p is the momentum of the particle. This ratio is of the order of 10^{-5}. Thus to a first approximation the term in $\mathbf{A}^2$ may be neglected in the perturbation hamiltonian.

The Schrödinger equation now may be expressed in terms of an unperturbed hamiltonian, $\mathbf{H}_0$, of the particle, and a perturbation hamiltonian, $\mathbf{H}'$, representing the interaction of the particle with the radiation field.

$$i\hbar \frac{d\Psi}{dt} = (\mathbf{H}_0 + \mathbf{H}')\Psi \tag{6}$$

where

$$\mathbf{H}_0 = -\frac{\hbar^2}{2m}\nabla^2 + V(r) \tag{7}$$

and

$$\mathbf{H}' = \frac{ie\hbar}{2m}\mathbf{A} \cdot \nabla \tag{8}$$

Thus the wave equation for $\mathbf{A}$ is yielded:

$$\nabla^2 \mathbf{A} - \frac{1}{c^2}\frac{d^2\mathbf{A}}{dt^2} = 0 \tag{9}$$

whose solutions are given by:

$$\mathbf{A}(r,t) = \mathbf{A}_0 \exp[i(\mathbf{k}\cdot\mathbf{r} - \omega t)] + \mathbf{A}_0^* \exp[-i(\mathbf{k}\cdot\mathbf{r} - \omega t)] \tag{10}$$

These are plane wave solutions representing a real potential with a propagation vector $\mathbf{k}$ and a real polarization vector $|\mathbf{A}_0|$. ω is the frequency of the radiation and is equal to kc where k is the magnitude of $\mathbf{k}$. The intensity of the radiation is obtained from the polarization vector by the relationship:

$$I = \frac{\omega^2 |\mathbf{A}_0^2|}{2\pi c} \tag{11}$$

The solution represented by equation 10 is general. It corresponds to both the absorption and emission of a photon. Clearly in the case of photoelectron spectroscopy only the absorption process is relevant; thus only the first term need be considered.

$$\mathbf{A}(r,t) = \mathbf{A}_0 \exp[i(\mathbf{k}\cdot\mathbf{r} - \omega t)] \tag{12}$$

The time dependent solution of the Schrödinger equation may be expanded in the usual manner in terms of a complete basis set of stationary states of the unperturbed hamiltonian, $\mathbf{H}_0$:

$$\mathbf{\Psi}(r,t) = \sum_n c_n(t)\phi_n \exp[-i\frac{E_n t}{\hbar}] \tag{13}$$

where E_n is the energy of the n^{th} stationary state and $c_n(t)$ is the coefficient of expansion.

Applying time dependent perturbation theory, if the system is initially in a given state n, at time $t = 0$, then to first order, the probability of finding the system in a state ℓ after the perturbation has ceased is the probability amplitude squared:

$$|C_\ell^1(t)|^2 = |-\frac{\langle\phi_\ell|\mathbf{H}'^0|\phi_n\rangle}{\hbar}\frac{\exp[i(\omega_{\ell n}-\omega)t]-1}{\omega_{\ell n}-\omega}|^2 \tag{14}$$

where the matrix element is,

$$\langle\phi_\ell|\mathbf{H}'^0|\phi_n\rangle = \frac{ie\hbar}{mc}\int \phi_\ell^* \exp[i(\mathbf{k}\cdot\mathbf{r})]\mathbf{A}_0\cdot\nabla\phi_n d^3r \tag{15}$$

and $\omega_{\ell n}$ is the frequency corresponding to the energy difference between the two eigenstates, ϕ_ℓ and ϕ_n, of the unperturbed hamiltonian, $\mathbf{H}_0$. Since photoionization results in a transition to a continuum of states, the transition probability must be integrated over all possible final energy states.

Defining a probability density of final states $\rho(k)$, where $\mathbf{k}$ is the wave vector of the ejected electron, the transition probability per unit time, W, may be formalized:

$$W = \frac{1}{t_0}\int |c_\ell^1(t)|^2\rho(k)dE(k) \tag{16}$$

where t_0 is the lifetime of the perturbation, the duration of the interaction of the radiation field with the particle.

Fermi's golden rule #2 is obtained if the density of states $\rho(k)$ varies slowly with k:

$$W = \frac{2\pi}{\hbar}\rho(k)|\langle\phi_\ell|\mathbf{H}'^0|\phi_n\rangle|^2 \tag{17}$$

The density of final states is determined from the allowed levels in a cube of length, L, where $E = \frac{\hbar^2 k^2}{2m}$.

$$\rho(k) = \frac{mL^3}{8\pi^3\hbar^2}kd\Omega \tag{18}$$

where $d\Omega = \sin(\theta)d\theta d\phi$. Thus, the transition probability becomes :

$$W = \frac{e^2L^3}{4\pi^2\hbar c}\frac{k}{m}|\langle\phi_\ell|\exp[i\mathbf{k}\cdot\mathbf{r}]\mathbf{A}_0\cdot\nabla|\phi_n\rangle|^2 d\Omega \tag{19}$$

A differential cross section, $\frac{d\sigma}{d\Omega}$, is obtained by dividing by the total incident current density, $\frac{\omega^2}{2\pi c}|\mathbf{A}_0|^2\frac{1}{\hbar\omega}$:

$$\frac{d\sigma}{d\Omega} = \frac{e^2kL^3}{2\pi mc\omega}|\langle\phi_\ell|\exp[i\mathbf{k}\cdot\mathbf{r}]\nabla_A|\phi_n\rangle|^2 \tag{20}$$

where ∇_A is the component of the gradient operator along the polarization vector $\mathbf{A}_0$.

The exponential term, $\exp[i(\mathbf{k}\cdot\mathbf{r})]$, may be expanded in a Taylor series. In the dipole expansion only the first term is retained. Thus,

$$\exp[i(\mathbf{k}\cdot\mathbf{r})] \approx 1 \tag{21}$$

The second term $\mathbf{k}\cdot\mathbf{r}$ has a magnitude approximately $\frac{1}{300}$ of the first term for photoionization with He I radiation providing justification for the dipole approximation.

By considering the commutator relationship:

$$[\mathbf{r}, \mathbf{H}] = \frac{i\hbar}{m}\mathbf{p} \tag{22}$$

equation 20 may be further simplified.

For eigenstates of **H**:

$$\int \phi_\ell^*[\mathbf{r}, \mathbf{H}]\phi_n d^3r = (E_\ell - E_n) \int \phi_\ell^* \mathbf{r} \phi_n d^3r \tag{23}$$

since the hamiltonian is hemitian. So:

$$\langle \phi_\ell | \nabla_A | \phi_n \rangle = -\langle \phi_\ell | r_A | \phi_n \rangle \frac{m\omega}{\hbar} \tag{24}$$

where r_A is the component of **r** along the direction of polarization.

The differential cross section may therefore be written as,

$$\frac{d\sigma}{d\Omega} = \frac{e^2 L^3 k m \omega}{2\pi c \hbar^2} |\langle \phi_\ell | r_A | \phi_n \rangle|^2 \tag{25}$$

The apparent dependence of this expression on L, the length of the box used to determine the density of states, is eliminated by considering the nature of the wave functions of the final state. These are continuous and are box normalized. Thus ϕ_n is proportional to $L^{-\frac{3}{2}}$ rendering the differential cross section independent of L, as is required physically.

Bethe and Salpeter[2] derived an equivalent expression for the differential cross section :

$$\frac{d\sigma}{d\Omega} = \frac{2\pi e^2 \hbar^2}{m^2 c \nu} |D_{\Omega b}^{k_\nu j}|^2 \tag{26}$$

where

$$D_{\Omega b}^{k_\nu j} = \int u_\Omega \exp[i\mathbf{k}\cdot\mathbf{r}]\frac{\partial u_b}{\partial x}d\tau \tag{27}$$

and ν is the frequency of the incident photon.

The continuum wave function u_Ω is given by :

$$u_\Omega(r) = \sqrt{\frac{k}{(2\pi)^3}}\{\exp[i\mathbf{k}\cdot\mathbf{r}] + V(r)\} \tag{28}$$

where V(r) is the scattered part of the eigenfunction of the atomic hamiltonian, and u_b is the initial atomic wavefunction.

Bethe and Salpeter ascertained that, for the angular distribution of electrons of hydrogenic atoms, the differential cross section has the form:

$$\frac{d\sigma}{d\Omega} = a + b\cos^2(\theta) \tag{29}$$

where a and b are system dependent parameters. In the formalism previously developed, it can be seen that the matrix element, $\langle\phi_\ell|r_A|\phi_n\rangle$, does not depend on the direction of $\mathbf{A}_0$ or $\mathbf{k}$, the propagation vector of the electron. Since ϕ_n represents a discrete state with quantum numbers n, ℓ and m, the differential cross section must also depend on m, and the direction of quantization of ϕ_n.

Experimentally, however, it is not possible to resolve the rotational states using the instrument under consideration in this thesis; thus an average differential cross section is measured, $\frac{d\bar{\sigma}}{d\Omega}$, where the average is taken over all allowed m values of the initial state, $m = -\ell, \ldots \ell$, leaving θ as the only source of angular dependence.

If the polarization vector is taken to lie along the x axis, then

$$\langle \phi_\ell | r_A | \phi_n \rangle = \int \phi_\ell x \phi_n d^3r \tag{30}$$

It can further be shown that $\frac{d\bar{\sigma}}{d\Omega}$ is invariant to reversal of the direction of electron propagation, $\mathbf{k} \rightarrow -\mathbf{k}$. The final wavefunction has the form of the sum of a plane wave and an incoming spherical wave, $\phi_\ell = N(\exp[i\mathbf{k}\cdot\mathbf{r}] + V(r))$; therefore reversing the propagation vector $\mathbf{k}$ has the same effect as reversing the position vector $\mathbf{r}$ and the direction of quantization of ϕ_n. Thus $x \rightarrow -x$ while the volume element, d^3r, is unaltered; hence $\langle \phi_\ell | x | \phi_n \rangle$ is antisymmetric with respect to reversal of the propagation vector.

Since $k\cos\theta = k_x$, changing the sign of $\mathbf{k}$ changes the sign of $\cos\theta$. As the differential cross section is proportional to the square of the matrix element, it must be an even function of $\cos\theta$, and hence invariant to reversal.

This function can, subsequently, be shown to be $\frac{d\bar{\sigma}}{d\Omega} = a + b\cos^2(\theta)$. The coordinates of the position vector, $\mathbf{r}$, may be given in spherical polar coordinates, where $\mathbf{k}$ is defined to be the polar axis and (r, θ', ϕ') are the basis of the system (see Figure 1). Using the spherical harmonics addition theorem:

$$\begin{aligned} x = \mathbf{A}_0 \cdot \mathbf{r} &= r\cos\theta'' \\ &= r(\cos\theta\cos\theta' + \sin\theta\sin\theta'\cos\theta') \end{aligned} \tag{31}$$

The matrix element was shown, however, to depend on θ only, from the contribution of linear terms in $\cos\theta$ and $\sin\theta$. The average

differential cross section, $\frac{d\bar{\sigma}}{d\Omega}$, is obtained by summing over the allowed m values.

From symmetry arguments, the coefficient of the cross terms in $\cos\theta\sin\theta$ must vanish. So,

$$\begin{aligned}\frac{d\bar{\sigma}}{d\Omega} &= \alpha\sin^2\theta + \beta'\cos^2\theta \\ &= \alpha + \beta\cos^2\theta\end{aligned} \tag{32}$$

Cooper and Zare[3] extended the theory of photoionization from hydrogenic atoms to the more useful case of atoms and molecules. For photoionization by linearly polarized light, they derived a form similar to that of Bethe and Salpeter:

$$\frac{d\bar{\sigma}}{d\Omega} = \frac{\sigma}{4\pi}[1 + \beta P_2(\cos\theta)] \tag{33}$$

where P_2 is the second order Legendre polynomial, $P_2(\cos\theta) = \frac{1}{2}(3\cos^2\theta - 1)$ and β is an asymmetry parameter that reflects the distribution's departure from isotropy.

For hydrogenic atoms β has the form:

$$\beta = \frac{\ell(\ell+1)\sigma_{\ell-1}^2 + (\ell+1)(\ell+2)\sigma_{\ell+1}^2 - 6\ell(\ell+1)\sigma_{\ell+1}\sigma_{\ell-1}\cos(\delta_{\ell+1} - \delta_{\ell-1})}{(2\ell+1)[\ell\sigma_{\ell-1}^2 + (\ell+1)\sigma_{\ell+1}^2]} \tag{34}$$

where ℓ is the orbital angular momentum of the initial state, $\delta_{\ell\pm1}$ are phase shifts and $\sigma_{\ell\pm1}$ are radial dipole integrals for the $\ell+1$ and $\ell-1$ outgoing spherical waves.

$$\sigma_{\ell\pm1} = \int_0^\infty r R_{n\ell}(r) G_{k\ell\pm1}(r)\,dr \tag{35}$$

where $R_{n\ell}(r)$ is the radial wavefunction of the initial state and $G_{k\ell\pm1}(r)$ is the radial wavefunction divided by kr from the continuum state.

Because the differential cross section must be positive, β is constrained to lie in the range $-1 \leq \beta \leq 2$. If $\beta = 0$, it is easily seen that the angular distribution is isotropic; if $\beta = 2$, then a $\cos^2\theta$ distribution exists peaked in the direction of the photon polarization vector, and if $\beta = -1$, there is a $\sin^2\theta$ distribution peaked plane perpendicular to the polarization vector.

Tully, Berry, and Dalton[4] have derived the same expression for the differential cross section of a molecule starting from a form similar to equation 25 for ionization by polarized light:

$$\frac{d\sigma}{d\Omega} = \frac{\sigma}{4\pi}[1 + \beta P_2(\cos\theta)] \tag{36}$$

where θ is the angle between the momentum vector of the electron and the polarization vector of the radiation. It was assumed in this derivation that: 1) the molecules are randomly oriented, 2) the dipole approximation is valid and 3) photoejection is fast compared to molecular rotation during the photoionization process.

Cooper and Manson[5] derived the expression for the differential cross section for unpolarized light:

$$\frac{d\bar{\sigma}}{d\Omega} = \frac{\sigma}{4\pi}[1 - \frac{\beta}{2}P_2(\cos\theta)] \tag{37}$$

where θ is the angle between the photon beam and the propagation direction of the electron. This expression is critical to the experiment

since the discharge lamp employed produces unpolarized radiation. The derivation of this expression proceeds from consideration of unpolarized radiation as an incoherent superposition of two beams polarized in the plane and perpendicular to the plane defined by the photon beam and the electron ejection vector. The derivation will be considered in more detail in an appendix to this section because of its importance.

2.2 Calculations of the Asymmetry Parameter

In recent years, calculation of asymmetry parameters has focused intensively on K-shell ionizations,[e.g.,6-9] transitions that are accessible only with x-radiation and thus beyond the scope of the experiment discussed in this thesis.

In a recent paper, Manson and Starace[10] have discussed the calculation of s-subshell asymmetry parameters as well as given a concise overview of the theory of the photoelectron angular distributions of atoms in general. The theory is presented within the framework of the angular momentum transfer formulation and the electric dipole approximation.

For valence electrons there have been a few fairly recent calculations using the Xα method. Grimm *et al.*[11] have used the multiple scattering method with muffin-tin potentials and overlapping spherical potentials to calculate the asymmetry parameters for N_2, CO, CO_2, COS, and CS_2, which they compared with experimental values determined from their own apparatus and values taken from the literature. Their calculations

gave reasonable correlation, generally within 0.3, although the results for CS_2 are considerably poorer, due in part to difficulty in convergence.

Gustafsson[12] has applied the method to the angular distribution of photoelectrons from linear molecules. In particular, he has succeeded in using the MS Xα technique in calculations of CO adsorbed on Ni(111) and Pt(111) to model experimental results.

Thiel[13] has briefly reviewed some of the more current calculations of asymmetry parameters for the vacuum ultraviolet in a paper examining the energy dependence of the asymmetry parameter in linear molecules by partitioning the contributions into diagonal and off-diagonal components with respect to the angular momentum. His results give reasonable agreement when compared to experimental results for CO_2 and N_2.

2.3 Appendix

In the right handed coordinate system of Figure 2a, let the photon beam propagate along the z axis and let the xz plane contain the polarization vector of the beam. Also let $\mathbf{k}_e$ be the momentum vector of the ejected electron.

The expression for the differential cross section for a polarized beam is proportional to $1 + \beta P_2(\cos\theta)$ where θ is the angle between the axis of polarization, x, and the electron vector, $\mathbf{k}_e$.

The expression for the differential cross section of an unpolarized beam is proportional to $1 - \frac{1}{2}\beta P_2(\cos\theta')$ where θ' is the angle between the axis of propagation, z, and the electron vector, $\mathbf{k}_e$.

To relate these two expressions, a set of spherical polar coordinates (r, α, ϕ) must be defined. Let α be the same as θ' above, and let ϕ be the angle between the x axis and the projection of $\mathbf{k}_e$ in the xy plane.

It is now necessary to express θ in terms of α and ϕ. To do this, the trigonometric relationship that defines the angle θ between two vectors **A** and **B** must be used:

$$\cos\theta = \cos\theta_A \cos\theta_B + \sin\theta_A \sin\theta_B \cos(\phi_A - \phi_B) \qquad (1a)$$

Consider now, the angle θ between the x axis and $\mathbf{k}_e$, the electron vector.

$$\cos\theta = \cos\alpha_x \cos\alpha_k + \sin\alpha_x \sin\alpha_k \cos(\phi_x - \phi_k) \qquad (2a)$$

For the x axis: $\alpha_x = 90$, and $\phi_x = 0$.

For the $\mathbf{k}_e$ vector: $\alpha_x = \theta'$, and $\phi_k = \phi$.

Therefore,

$$\cos\theta = \cos(90)\cos\theta' + \sin(90)\sin\theta'\cos(-\phi) \qquad (3a)$$

Since cosine is a symmetric function this yields:

$$\cos\theta = \sin\theta'\cos\phi \qquad (4a)$$

If the axis of polarization is shifted, the angle ϕ is altered, but the angle θ' is invariant to rotation about the axis of propagation, z. (See Figure 2c.) So unpolarized light will have the same θ' dependence as polarized light but will average the ϕ dependence over

all orientations. Since ϕ is a continuous variable, the differential cross section is integrated over 2π and the result divided by 2π to normalize the intensity contribution at each polarization angle.

$$\frac{d\sigma}{d\Omega} = \frac{1}{2\pi}\int_0^{\infty} \frac{d\sigma(\phi)}{d\Omega} \tag{5a}$$

However, as $\frac{d\sigma}{d\Omega} \propto [1 + \frac{\beta}{2}(3\cos^2\theta - 1)]$, substituting equation 4a yields:

$$\frac{d\sigma(\phi)}{d\Omega} \propto [1 + \frac{\beta}{2}(3\sin^2\theta'\cos^2\phi - 1)] \tag{6a}$$

Integrating this expression over all ϕ orientations and dividing by 2π results in :

$$\frac{d\sigma}{d\Omega} = 1 + \frac{\beta}{4}[3\sin^2\theta' - 2] \tag{7a}$$

which, through simple algebraic manipulations, quickly yields:

$$\frac{d\sigma}{d\Omega} = [1 - \frac{\beta}{2}P_2(\cos\theta')] \tag{8a}$$

as desired.

REFERENCES

1. L. Schiff, *Quantum Mechanics*, third edition (McGraw-Hill, New York, 1968).
2. H. A. Bethe and E. Salpeter, *Quantum Mechanics of One and Two Electron Atoms* (Springer-Verlag, Berlin, 1957).
3. J. Cooper and R. N. Zare, in *Lectures in Theoretical Physics*, S. Geltman, K. Mahanthappa and N. Brittens, editors (Gordon and Breach, New York, 1969).
4. J. Tully, R. Berry, and B. Dalton, *Phys. Rev.*, **176**, 95 (1968).
5. J. Cooper and S. Manson, *Phys. Rev.*, **177**, 157 (1969).
6. O. Baschenko and V. I. Nefedov, *J. Electron Spectroscopy*, **17**, 405 (1979).
7. O. Baschenko and V. I. Nefedov, *J. Electron Spectroscopy*, **21**, 153 (1980).
8. D. Dill, S. Wallace, J. Siegel, and J. L. Dehmer, *Phys. Rev. Lett.*, **41**, 1230 (1978).
9. D. Dill, J. R. Swanson, S. Wallace, and J. L. Dehmer, *Phys. Rev. Lett.*, **45**, 1393 (1980).
10. S. Manson and A. Starace, *Rev. Mod. Phys.*, **54**, 389 (1982).
11. F. A. Grimm, T. A. Carlson, W. B. Dress, P. Agron, J. O. Thomson, and J. W. Davenport, *J. Chem. Phys.*, **72**, 3041 (1980).
12. T. Gustafsson, *Surf. Sci.*, **94**, 593 (1980).
13. W. Thiel, *Chem. Phys. Lett.*, **87**, 249 (1982).

FIGURE CAPTIONS

Figure 1. Coordinate system showing **P**, the polarization vector; **k**, the propagation vector of the electron; and **r**, the position vector, the domain over which the vector potential **A** acts.

Figure 2. Appendix coordinate systems.

FIGURE 1.

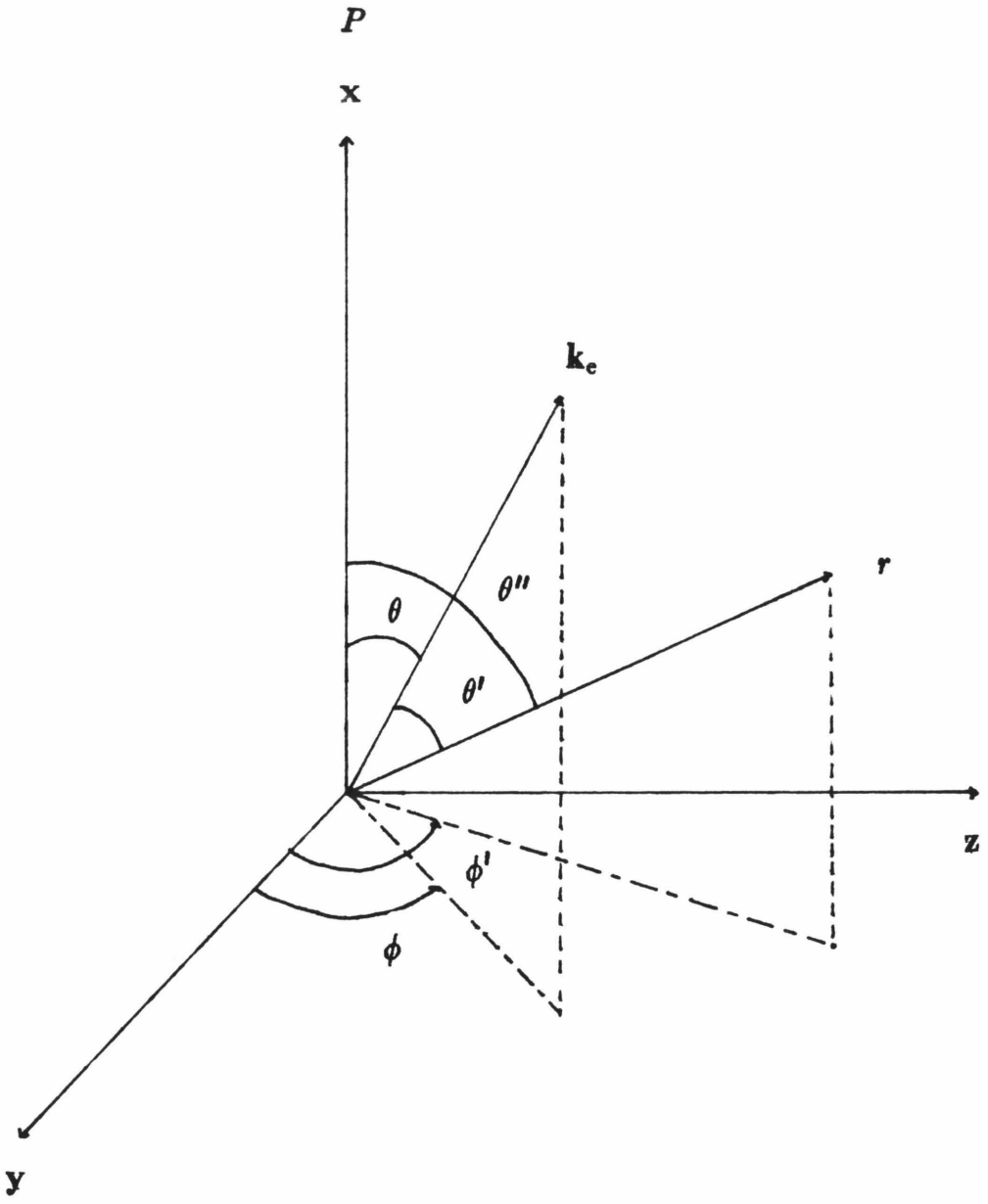

FIGURE 2.

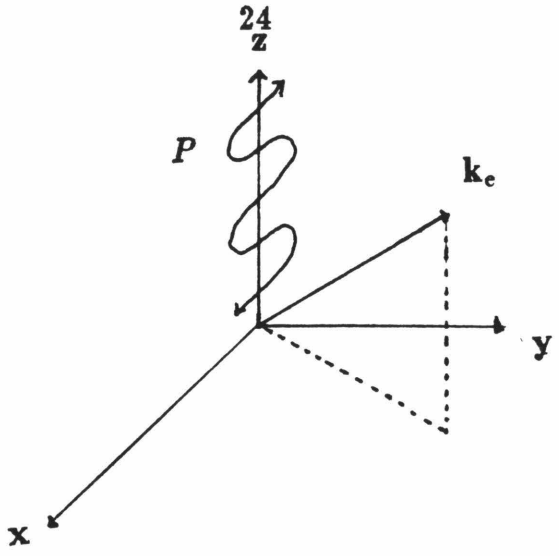

a

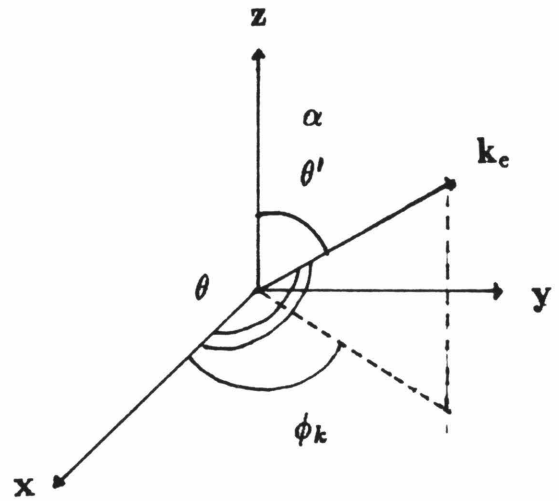

b

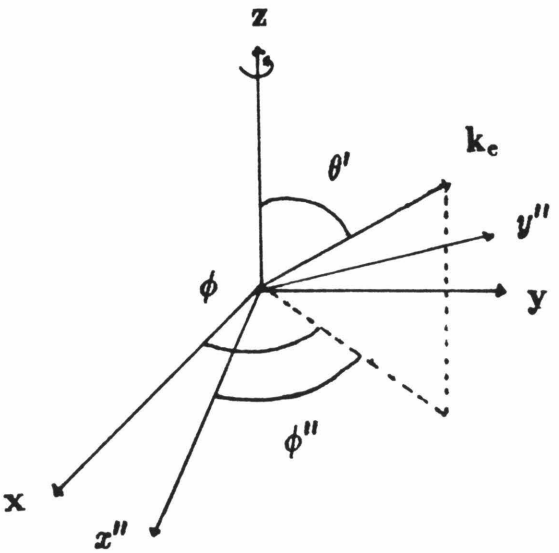

c

CHAPTER 3

EXPERIMENTAL

3.1 Experimental Introduction

This section seeks to briefly outline the major experimental components and capabilities of the multiple angle photoelectron spectrometer (MAPS). The apparatus was primarily designed and built under the auspices of D. Mason and D. Mintz. Further details about the construction and operation of the spectrometer can be obtained by consulting their theses[1,2] and reference 3.

A block diagram of the apparatus is given in Figure 1. Ultra high purity helium flows into the discharge lamp within the vacuum chamber. The photons produced are collimated and enter the scattering chamber which contains sample vapors at pressures between 1 and 10 mtorr, depending on the compound. The photons (nearly monochromatic at 584 Å) ionize molecules of the sample gas and the electrons produced traverse through a slot in the scattering chamber to be collimated and decelerated by a set of electrostatic lenses before entering the hemispherical analyzer. The electrons passing through the potential field of the analyzer are energy discriminated and those that emerge are recollimated and reaccelerated by another pair of electrostatic lenses into the front cone of a Spiraltron electron multiplier. The Spiraltron generates a low voltage pulse for each electron impacting its surface;

this pulse is then shaped and amplified by a preamplifier external to the vacuum chamber. These pulses pass through an optical isolator which further strengthens the signal and eliminates low voltage noise. The PDP-8e computer, functioning as a multichannel scaler, converts the pulse string into counting rates and stores the results in memory. By varying the energy, for which the analyzer discriminates, a photoelectron spectrum is obtained that may be displayed on an oscilloscope or plotted by an X-Y plotter by means of a digital to analog converter.

The detector subsystem, consisting of the electrostatic lenses, the hemispherical analyzer and the electron multiplier may be rotated about the center of the scattering chamber from an angle of 45° to an angle of 120° with respect to the photon beam; thus the variation of intensity with angle may be obtained.

Due to the relatively low kinetic energy of valence electrons ionized by He I radiation, the main vacuum chamber is lined with μ metal and located within three pairs of matched Helmholtz coils which reduce the ambient magnetic field to less than approximately 0.2 mgauss, to prevent distortions of the angular distributions by magnetic fields.

The major constituents of MAPS will be further considered in the following sections.

3.2 Vacuum System

The internal parts of the spectrometer are mounted on a bracket attached to an 18 inch flange on the main vacuum chamber (Figures 2

and 3). This flange is bolted to a cart and may be rolled away from the chamber to provide access.

The vacuum chamber is pumped by a Varian-NRC six inch oil diffusion pump mounted at the bottom of the chamber. The diffusion pump is trapped by a Granville-Phillips 278 liquid nitrogen trap which has been retrofitted to operate with a Polycold PCT-200 cold trap chiller. The Polycold is fundamentally a sophisticated freon compressor using Freon 14 (tetrafluoromethane) as the refrigerant. It is capable of providing cooling down to 133° K, which is warmer than liquid nitrogen (77° K), but more than adequate for the medium high vacuum required by MAPS.

Formerly, the diffusion pump was backed by a smaller oil diffusion pump acting as a booster. This pump has been removed because of metal failure due to thermal stress. The main diffusion pump is now backed directly by a 6.1 liter/sec mechanical pump.

The base pressure of the vacuum system with no gas entering the chamber from the discharge lamp or the sample inlet is 2×10^{-7} torr. Typical pressures in the main chamber when the apparatus is taking spectra is about 8×10^{-6} to 1×10^{5} torr, which is monitored by a Bayard-Alpert type ionization gauge tube and a Veeco RG-830 gauge controller.

3.3 Helium Discharge Lamp

MAPS now utilizes two different lamps. A cross-sectional view of

the old lamp is given in Figure 3 and the new in Figure 5. The new helium discharge lamp is based very loosely on the design of a lamp by Heinzmann and Schönhense[4,5] and its operating characteristics are described in the thesis of C. Koerting.[6] However, both the old and new lamps operate in fundamentally the same way. Ultra high purity helium (99.999%) is further purified by passing it through a zeolite trap immersed in liquid nitrogen, removing any condensable contaminants, principally water vapor. The helium enters the discharge lamp via an inlet line on the main flange. A discharge is induced through a quartz capillary between the anode, held at approximately +550 volts, and the cathode, which is held at ground. The lamp housing is water-cooled to prevent overheating.

To reduce the amount of helium entering the main chamber and to prevent the self absorption of the radiation (584Å) by ground state helium atoms, the lamp has two stages of differential pumping by two mechanical pumps. Photon flux is measured by a photocathode in the rear of the scattering chamber.

The lamp is powered by a current limited DC power supply. At the normal He backing pressure of about 5 torr measured external to the vacuum chamber, the typical operational current is maintained at 150 ma.

The salient differences in the new lamp design are 1) a reversal of the relative position of the anode and the cathode and 2) the use of a narrower and longer quartz capillary. The benefits are twofold: the first

and most important is an approximate two orders of magnitude increase in intensity to $\sim 10^{13}$ photons/sec allowing the apparatus to accumulate an equivalent spectrum in a much shorter time span. This avoids the problems of long term stability. Secondly, since the direction of the arc is reversed, the internal surfaces are less subject to contamination improving the stability of the lamp and necessitating less maintenance and cleaning.

3.4 Scattering Chamber and Sample Inlet System

The scattering chamber, Figure 6, consists of three coaxial cylinders. The interior and exterior cylinders are made of gold plated copper and rotate with the energy analyzer to which they are connected. The medial shell is fixed to the mounting bracket.

Sample vapors enter the chamber through a 1/2 inch aperture in the base. The pressure in the chamber is monitored with either a Baratron capacitance manometer or, under exceptional circumstances, a Shultz-Phelps ionization gauge, the Baratron being the greatly preferred device since it measures absolute pressures independent of the nature of the sample and has no filament to be fouled by corrosive samples.

Due to the design characteristics of the chamber it has been found that the pressure of the sample within the chamber will vary with the angle of the detector. Thus signal intensity varies with both angle and pressure. The pressure dependency can be eliminated by modulating the intensity by the pressure. As a consequence, spectra must be taken at

pressures where the intensity varies linearly with the pressure ($\sim$ 1 to 10 mtorr) and the pressure must be measured frequently.

The sample inlet system is composed of a glass manifold line mounted external to the vacuum chamber. The inlet system is evacuated to 10 mtorr using a mechanical pump with a LN_2 trap before being loaded with sample.

For gaseous compounds, a 5 liter ballast flask is attached to the manifold and the line filled to a pressure of about an atmosphere (11 to 15 psi).

For condensed samples the ballast is omitted. The sample vapor is permitted to reach its equilibrium vapor pressure in the manifold. If condensation proves to be a problem, some vapor is trapped out using LN2, until the vapor is undersaturated .

The sample is then admitted into the system through a Philips-Granville variable leak valve. A pneumatically controlled shutoff valve is positioned between the variable leak and the sample inlet feedthrough on the main flange and is interlocked to cut off the sample gas flow in case of a pumping failure.

Between samples the glass manifold system is disassembled, cleaned, and baked overnight in the glass shop's annealing oven to avoid cross-contamination.

3.5 Energy analyzer and Detector

The energy analyzer and detector subsystem consist of two sets of

electrostatic lens assemblies, a hemispherical analyzer and a Spiraltron electron multiplier and is shown in Figure 7. This subsystem is mounted on a 20 cm diameter gear and is rotatable in a vertical arc about the axis of the scattering chamber. Physical restrictions in the vacuum chamber constrict the rotation between angles of 40° and 120° with respect to the collimated output of the lamp.

The hemispherical analyzer and the lens elements are made from gold plated OFHC copper and are coated with Aero-Dag©, an aerosol suspension of micron sized graphite particles, to smooth out the potential surfaces.

Electrons ejected from the sample molecules proceed from the scattering chamber and are decelerated by the first set of electrostatic lenses from an initial energy T to a kinetic energy V, usually 1.5 volts. The voltage difference T-V, the sphere center voltage, serves as the reference for the lens voltages except for the one immediately attached to the scattering chamber which is tied to ground.

The energy analyzer is operated such that only electrons with a kinetic energy of 1.5 eV completely traverse the hemispheres; all others are deflected into the sides of the analyzer. Constant resolution is maintained by operating at a constant transmission energy. The electrons that emerge from the analyzer are reaccelerated by a second set of lenses to 6.5 eV and focused into the front cone of the Spiraltron electron multiplier. To facilitate collection the front cone is biased at approximately +50 to +75 volts.

The multiplier cascade provides an electron gain of 10^8. The charge pulses from the copper plate of the Spiraltron are converted into voltage pulses by an RC differentiating network, which are amplified and discriminated by preamp affixed to the main flange. Lastly, the pulses pass through an optical isolator which further improves the signal while eliminating low voltage noise.

Counting rates for samples vary from rates as low as fractions of a count per second for some organic molecules to over 5000 counts per second for the Ar $^2P_{3/2}$ peak at 1 mtorr using the new lamp.

3.6 Computer and other hardware

A twelve bit Digital PDP-8e computer with 12K of memory controls most of the data taking for the experiment. The computer has three I/O peripherals, a Teletype 43 terminal, a 300 char/sec high speed paper tape reader and a high speed paper tape punch.

Additional devices used by the computer are a 120 Hz real time clock and three channels of digital to analog conversion (DAC), one that operates the energy scanning of the instrument and two for driving the x and y inputs of the oscilloscope and plotter displays.

The computer is interfaced to the experiment at three levels. The first, a 12-bit counter with a six digit display, displays the number of counts (electrons detected) accumulated in a preset fixed time interval. The second interface is composed of a 4-bit sense register and 12-bit drive register. The sense register monitors status logic levels in four

lines connected to critical devices in the apparatus, for example, the vacuum system via diffusion pump power. The drive register permits the computer to apply voltages to control or activate various devices: the angle drive motor, an audio alarm, pen motion on the XY plotter and others. Lastly, there is an analog to digital converter (ADC) through which the computer controls a multiplexer which can monitor analog voltages from many devices such as the Baratron manometer, the lens and analyzer voltages and the electrometer which measures lamp intensities. These voltages are sampled frequently in the course of data taking and are stored in memory and printed on the terminal.

Also crucial to the experiment but not under computer control are three pairs of matched 10 ft. square Helmholtz coils. These are separately powered by three DC power supplies. Additional magnetic shielding is provided by a single layer of μ metal lining the vacuum chamber. These two devices reduce the ambient magnetic field within the interaction region to less than 0.2 mgauss. The field strengths are monitored frequently and are kept within acceptable limits through systematic degaussing and through adjustments in the fields produced by the Helmholtz coils.

This is absolutely mandatory if reproducible, accurate results are to be obtained. Unacceptable magnetic fields are the single most important factor in the failure of MAPS to achieve fully operational status at any given time. The acceptability of the fields is ultimately based on the apparatus' ability to routinely reproduce a value of $0.88 \pm .02$ for the

$^2P_{3/2}$ state of argon previously reported,[3,7-11] as well as the mandatory symmetry of the intensity about 90° .

The principal source of magnetic fields affecting the instrument is, of course, the earth's magnetic field but other "stray" fields have been found as well. Many of the LN_2 tanks have been magnetized to such an extent that their proximity to the apparatus produces unacceptable fields within the chamber. Also changes in the field strengths of the NMR magnets in nearby laboratories may raise the measured field in the chamber by a factor of 3. Most critically, the internal parts of the spectrometer may themselves accumulate residual magnetism, if they are composed of magnetically susceptible materials. This includes 316 stainless steel, normally considered nonmagnetic, and nickel. Even the μ metal shielding has been found to need occasional reannealing to remove induced magnetism. Whenever reasons of strength or other important physical properties did not preclude it, all magnetically susceptible components have been systematically replaced.

3.7 Data Acquisiton and Software

The role of the PDP-8e has been drastically reduced in this experiment; its function now is restricted almost exclusively to data acquistion. Although the capacity to perform data reduction remains, with the exception of argon, all spectra are now reduced and plotted from the division's VAX-11/780.

The division of computer memory and method of operation of the

8e have been described elsewhere.[12] In the process of taking a spectrum, the counter interface accumulates the number of electrons detected in a fixed time interval determined by the operator with the lens and sphere voltages at a fixed value. This total count is deposited in a memory location. The computer then increments an internal register and outputs it to the DAC, driving the lens and sphere voltages. The counts accumulated in the same time period at these new settings are deposited in the next sequential memory location. Thus each location in the data buffer corresponds to a given voltage interval and contains the counts accumulated while the analyzer was set to that ionization potential. Due to the nature of memory partitioning in the PDP-8e, the storage buffer is restricted to a maximum of 511 channels. Each channel, however, has a capacity of over 8 million counts.

The computer scans a voltage interval determined by the user and pauses to read the sample pressure before reinitiating the scan. The total amount of time spent in each channel is user selected. After the last scan the computer averages the pressure of the sample and records this on the terminal. By using this average pressure, partial correction is made for fluctuations in the sample pressure over the duration of the spectrum.

The data may be partially reduced from the data taking program. A routine devised by Savitzky and Golay[13] is used to smooth the spectrum and a derivative algorithm is used to locate the band maxima.

Parameters associated with the spectrum are printed to the terminal along with the ionization potentials and intensities of the located peaks.

A full photoelectron spectrum is generally taken for each system studied. The spectrum typically covers a range of 12 eV and is taken at an angle of 54.7° with respect to the light source. This angle, often referred to as the "magic angle," corresponds to a zero in the second Legendre order polynomial and thus at this angle all dependency of the intensity on the asymmetry parameter is eliminated. At this angle then, the ratio of two peak intensities will be equal to the ratio of their respective integral cross sections, ignoring any discrimination on the basis of kinetic energy by the analyzer.

Angular distributions are determined by taking spectra at nine detector angles between 45° and 120° with respect to the photon beam. Since this procedure can take up to 12 hours to complete, the process has been essentially automated by having the computer accept commands from paper tape rather than from the terminal console.

If the molecule being examined has a well-defined vibrational structure, the angular distribution is taken by scanning over a very narrow energy range (approximately 60 meV) centered on the peak maxima in the well-resolved region. A β value is calculated for this region only. For bands lacking well-resolved structure a β value is determined every few meV throughout the band.

Although the instrument's background signal has been found to remain fairly constant over extended lengths of time, a new set of

background spectra is taken after each sample, or approximately every week in the case of protracted examination of a sample. Variations are principally caused by absorption of the sample on graphite coated surfaces and to a lesser extent to drift in the preamp threshold settings. The background is strongly angle dependent and must be taken separately for each of the nine angles in the distribution. The background signal itself is typically between 0 and 3 counts/sec and depends on the electron kinetic energy, reaching a maximum at zero electron energy. The signal has been found to be approximately independent of sample pressure. Since some organic samples have intensities of this magnitude, it is imperative that the background be subtracted before the asymmetry parameter is calculated.

It is also necessary to correct for the angular dependence of the volume of the region of intersection of the photon beam and the detector acceptance cone. At larger angles, the detector samples a smaller volume than at smaller angles because of the geometry. This may be corrected by modulating the intensity at θ by $\sin\theta$.

The procedure for calculating the asymmetry parameter is straightforward. The background is first subtracted from the intensities, which are then further corrected for the variation in acceptance volume at each angle and the sample pressure. The corrected intensities are subjected to a weighted least squares fit to the form:

$$I(\theta) = A + B\sin^2(\theta) \qquad (1)$$

The values of A and B are determined from the linear regression analysis together with their variances, σ_A^2 and σ_B^2. The value of β can be determined from A and B by the expression, $\beta = \frac{4B}{2A+3B}$ and the value of the variance, σ_β^2, by propagating the variances of σ_A^2 and σ_B^2.

3.7.1 Programs

As stated previously, the role of the PDP-8e in this experiment has been reduced to little more than a multichannel scaler.

The software for MAPS has been substantially rewritten to transfer the bulk of data analysis for the PDP-8e to the divisional VAX-11/780. The reasons for this are manifest. The 8e possesses no operating system and thus is incapable of any file structure. All programming must be done in machine assembler through the arduous and tedious medium of paper tape. Additionally, it has severely restricted memory and storage capacity. The transfer of data reduction to the VAX takes advantage of the greatly increased speed, storage, peripherals and sophisticated plotting and statistical packages available on the VAX-11 as well as the convenience of programming in Fortran.

In the process, considerable improvement has been made in the software, especially in background handling, that yields more uniform results with lower scatter. From the user's point of view the conversion of software to Fortran is of great benefit in understanding the code, in the ease of making alterations and the ability to transfer the programs without exceptional difficulty to other computers if the necessity should

occur.

The new programming fundamentally has five functions: 1) to transfer data 2) to parameterize the background 3) to reorganize spectral data 4) to calculate beta values and 5) to plot.

These five functions and software utilization will be considered in detail in Appendix 2.

REFERENCES

1. D. Mason, M.S. Thesis, California Institute of Technology, 1973.
2. D. Mintz, Ph.D Thesis, California Institute of Technology, 1975.
3. D. Mason, D. Mintz, and A. Kuppermann, *Rev. Sci. Instrum.*, **48**, 926 (1977).
4. U. Heinzmann and G. Schönhense, in *VIth International Conference on Vacuum Ultraviolet Radiation* (Plenun Press, New York, 1980).
5. G. Schönhense, Thesis, Westfälishe Wilhelms-Universitat, Münster 1978.
6. C. F. Koerting, Ph.D Thesis, California Institute of Technology, 1985.
7. T. Carlson and A. Jonas, *J. Chem. Phys.*, **55**, 4913 (1971).
8. D. Kennedy and S. Manson, *Phys. Rev. A*, **5**, 227 (1972).
9. J. Dehmer, W. Chupka, J. Berkowiz and W. Jivery, *Phys. Rev. A*, **12**, 1966 (1975).
10. W. Hancock and J. Samson, *J. Electron Spectroscopy*, **9**, 211 (1976).
11. D. Holland, A. Parr, D. Ederer, J. Dehmer, and J. West, *Nuclear Instrum. Meth.*, **195**, 331 (1982).
12. J. Sell, Ph.D Thesis, California Institute of Technology, 1978.
13. A. Savitzky and M. Golay, *Anal. Chem.*, **36**, 1627 (1962).

FIGURE CAPTIONS

Figure 1. Block diagram of MAPS: He–cylinder of UHP helium, ZT–zeolite trap at 77° K for lamp helium supply, RB–lamp ballast resistor, LPS–lamp power supply, SC–scattering chamber, PC–photocathode, CL–set of electrostatic lenses, ANALYZER–hemispherical electrostatic analyzer, ML–set of electrostatic lenses, S–Spiraltron electron multiplier, CPS–Spiraltron cathode power supply, APS–Spiraltron anode power supply, RC–differentiating network for Spiraltron pulses, INTER–counting system interface to experiment, PDP-8e–Digital PDP 8e minicomputer, and OUTPUT–computer peripheral devices.

Figure 2. Side view of the spectrometer where the main flange has been separated from the vacuum chamber. (Figure is not drawn to scale.)

Figure 3. General view of the photoelectron spectrometer vacuum system. The internal components of the spectrometer have been removed to show the supporting brackets.

Figure 4. Cross-sectional view of the old lamp. Hatched and stippled parts are of aluminum except for the stainless steel lamp anode, A, and constitute the lamp body or housing. K–tungsten cathode, C-quartz discharge capillary, HV–high voltage power lead, S–starter electrode, He–helium inlet, OA–lamp flux collimating capillary, DP–differential pumping lines, WAT–water cooling inlet, M–mica insulating spacer, CE–cooling water envelope within the housing.

Flow directions are indicated by the arrows.

Figure 5. Cross-sectional view of the new lamp. He–helium inlet, H_2O–water inlet, K–berylium-copper cathode, A–berylium copper anode, DC–quartz discharge capillary, CCh–cooling channels, CC–light collimating capillary. Direction of the water and helium flows are indicated by the arrows. Hatched and stippled parts of the lamp show the different materials used in the construction of the lamp and are explained in the legend on the figure.

Figure 6. External and cross sectional views of the sample scattering chamber. Hatched portions are sections of the inner and outer cylinders. IS–inner shell, MS–middle shell, OS–outer shell, GI–sample inlet, HS–helical slot, GS–guide screw for the helical slot, LI–light inlet. Motion of the outer shell and flow of the sample are shown with vertical arrows.

Figure 7. Cross sectional view of the electron analyzer and sample chamber in the plane of the electron trajectories. Hatched areas encompass BN–a boron nitride mounting block for the Spiraltron, S, and the part of the inner shell of the scattering chamber, CIS. COS–outer shell of scattering chamber, PC–photocathode, LE–light entrance, C1, HC, HM, M1–electrostatic lens elements, LS–aluminum lens supports, OS–outer hemisphere of analyzer, OSC–outer sphere corrector electrode, IS–inner hemisphere of analyzer, ISC–inner sphere corrector electrode, AF,CF–electrical feedthroughs for the electron multiplier, AR–resistor from the

multiplier anode to anode plate A.

FIGURE 1.

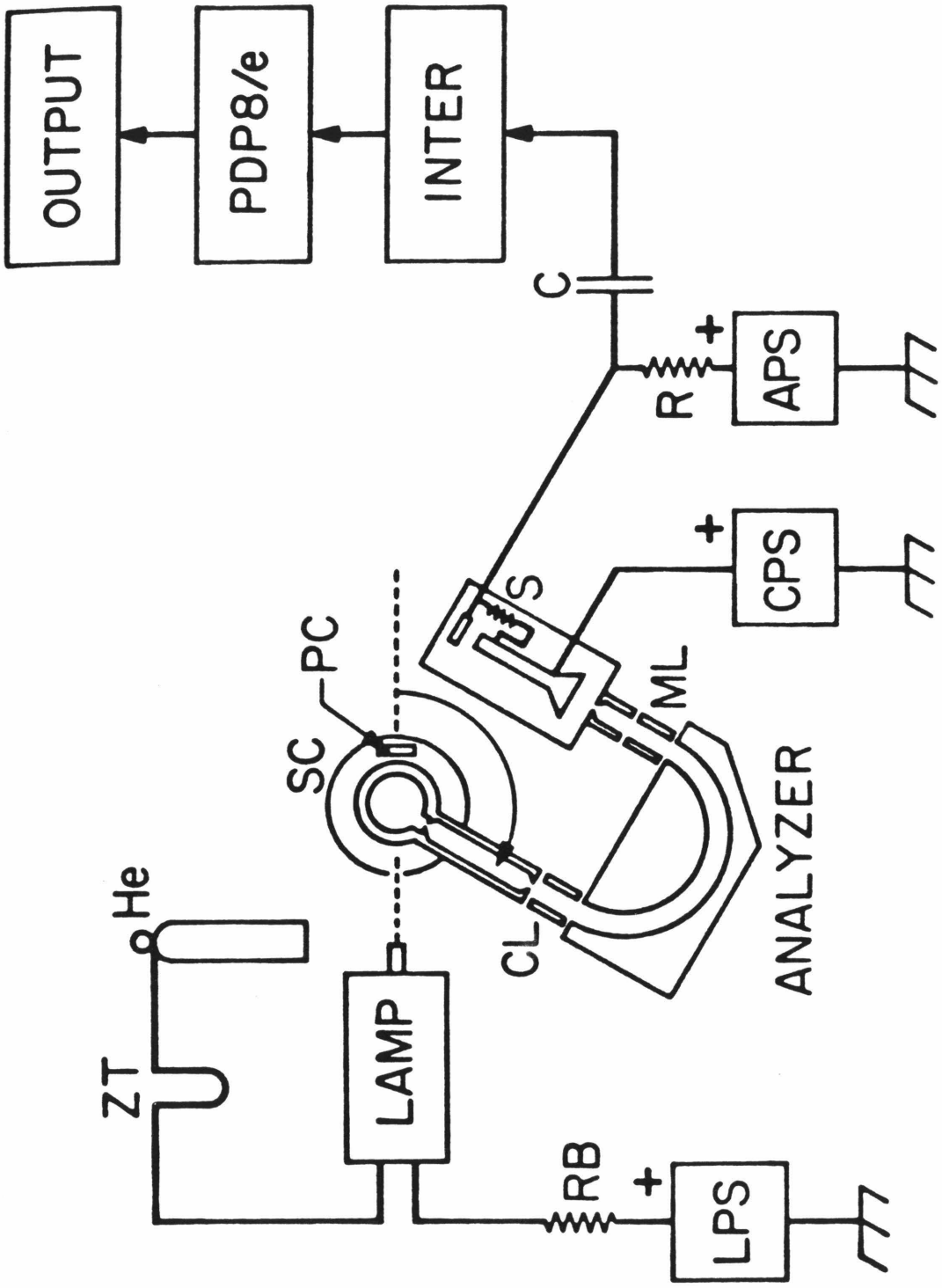
OUTPUT
PDP8/e
INTER
C
R
APS
CPS
S
PC
SC
ML
ANALYZER
CL
He
ZT
LAMP
RB
LPS

FIGURE 2.

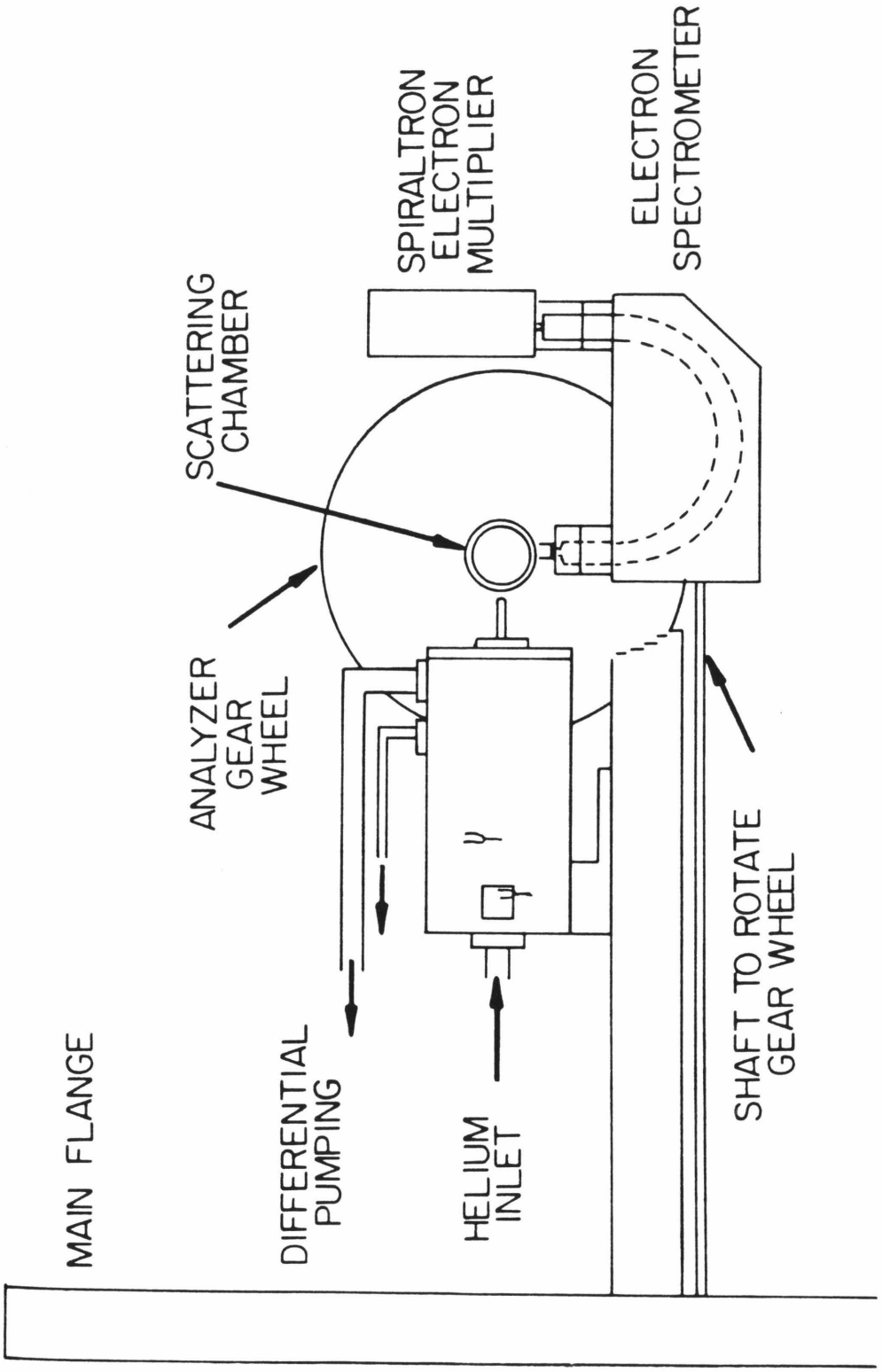
SPIRALTRON ELECTRON MULTIPLIER
ELECTRON SPECTROMETER
SCATTERING CHAMBER
ANALYZER GEAR WHEEL
MAIN FLANGE
DIFFERENTIAL PUMPING
HELIUM INLET
SHAFT TO ROTATE GEAR WHEEL

FIGURE 3.

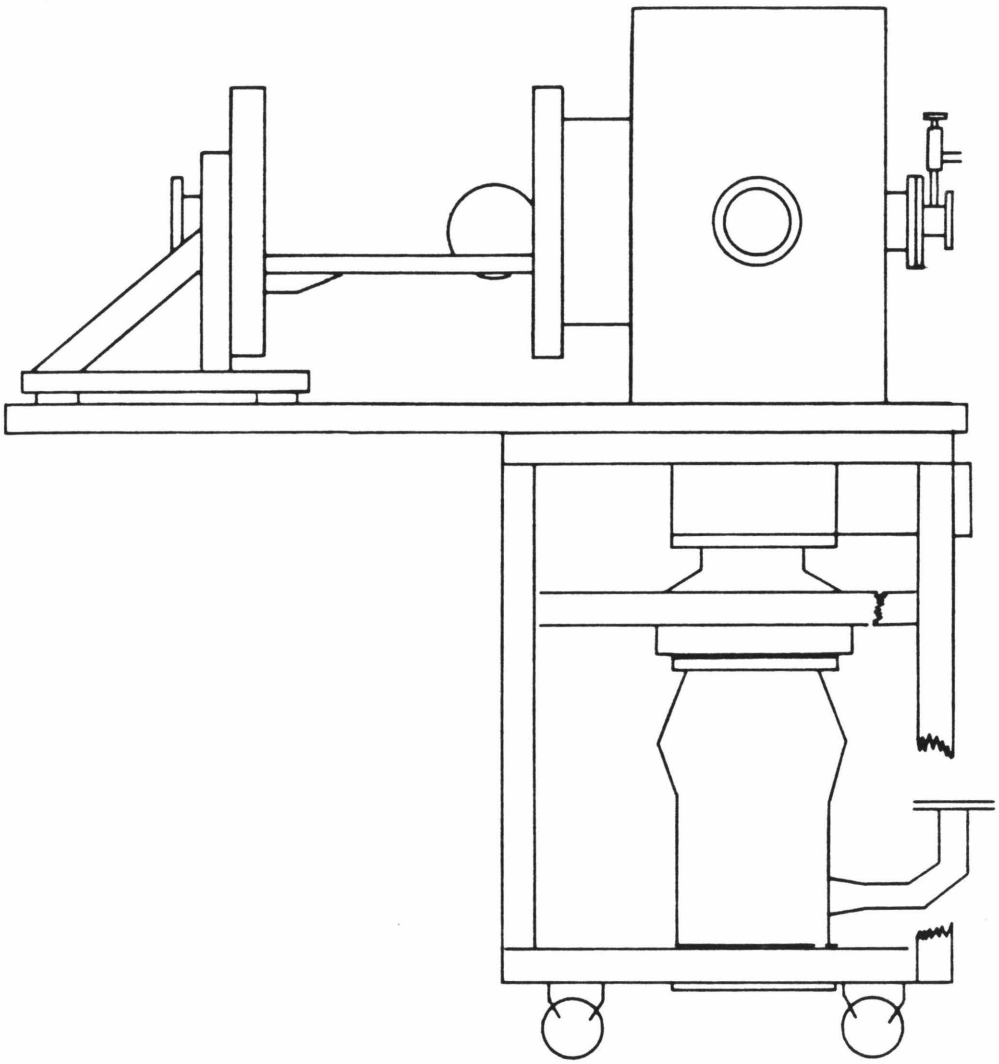

FIGURE 4.

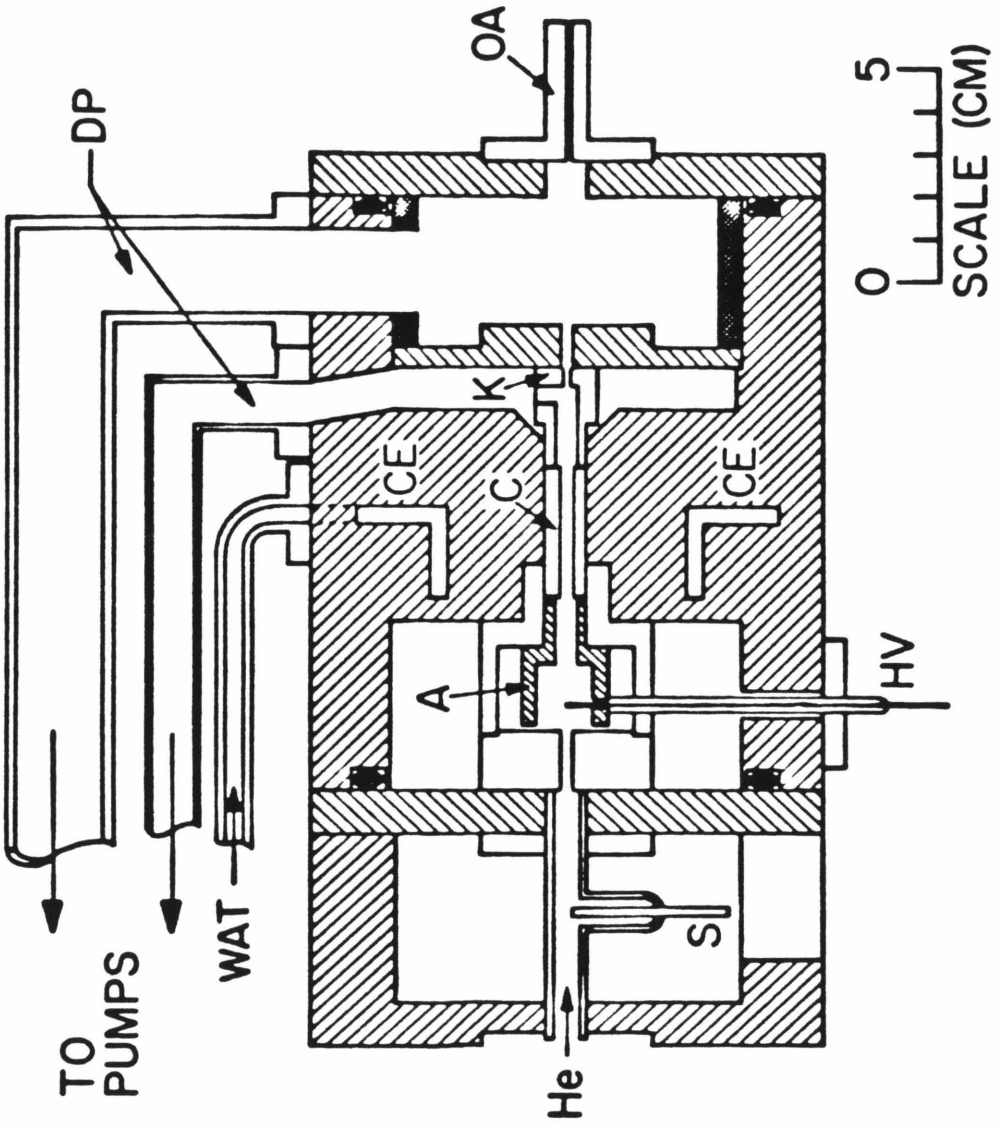

FIGURE 5.

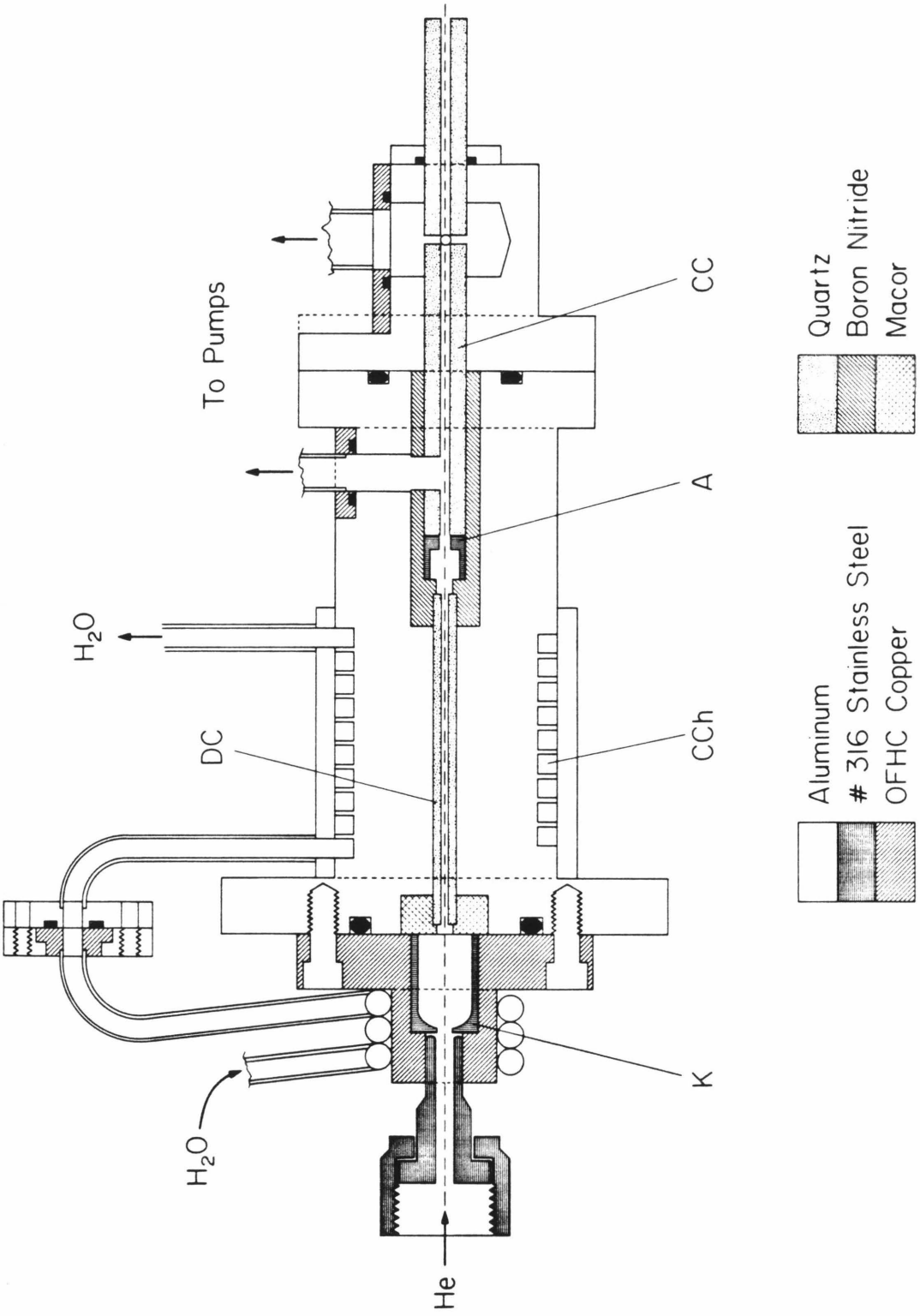
To Pumps
CC
A
H_2O
DC
CCh
K
H_2O
He
Quartz
Boron Nitride
Macor
Aluminum
316 Stainless Steel
OFHC Copper

FIGURE 6.

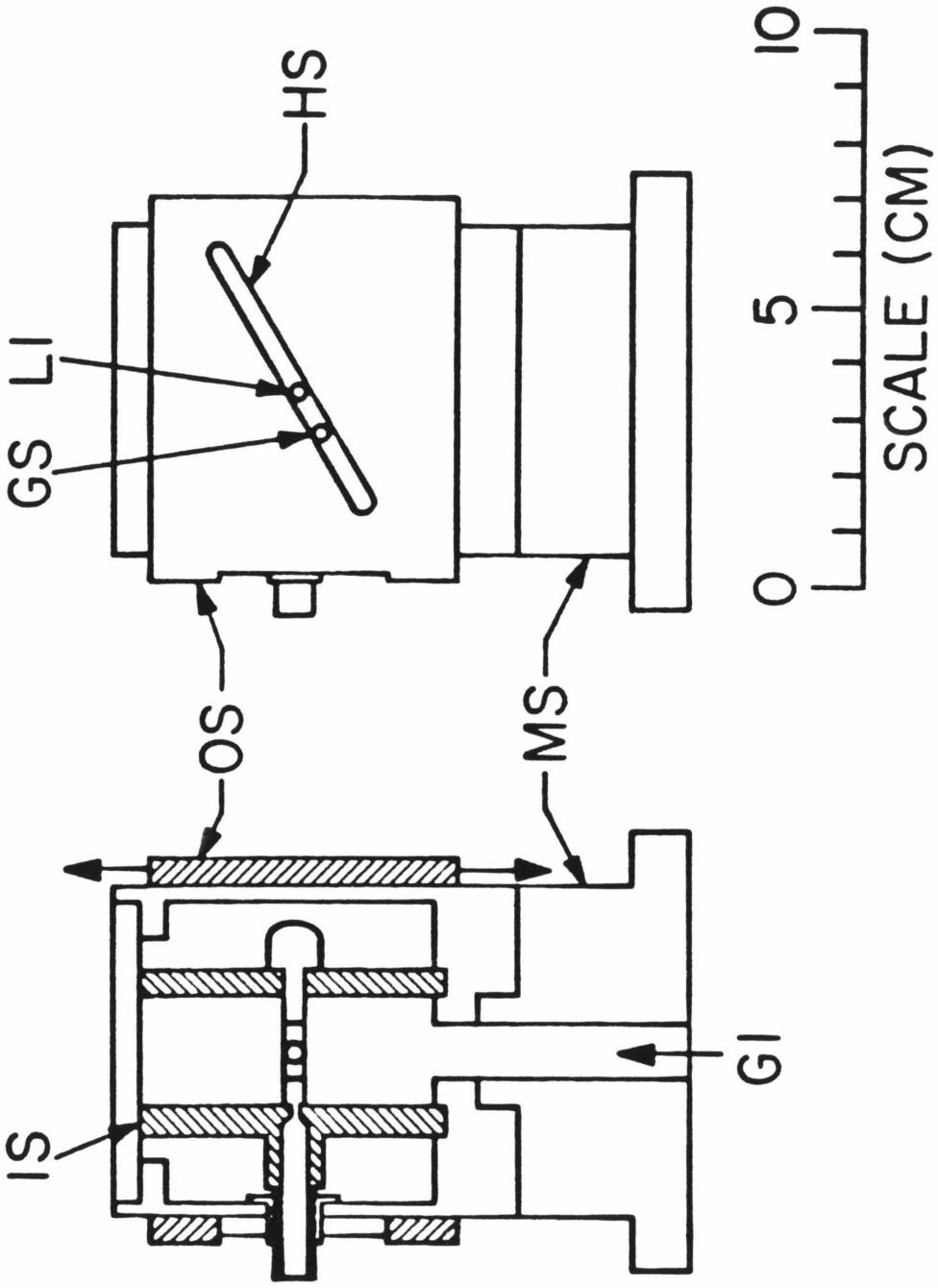

FIGURE 7.

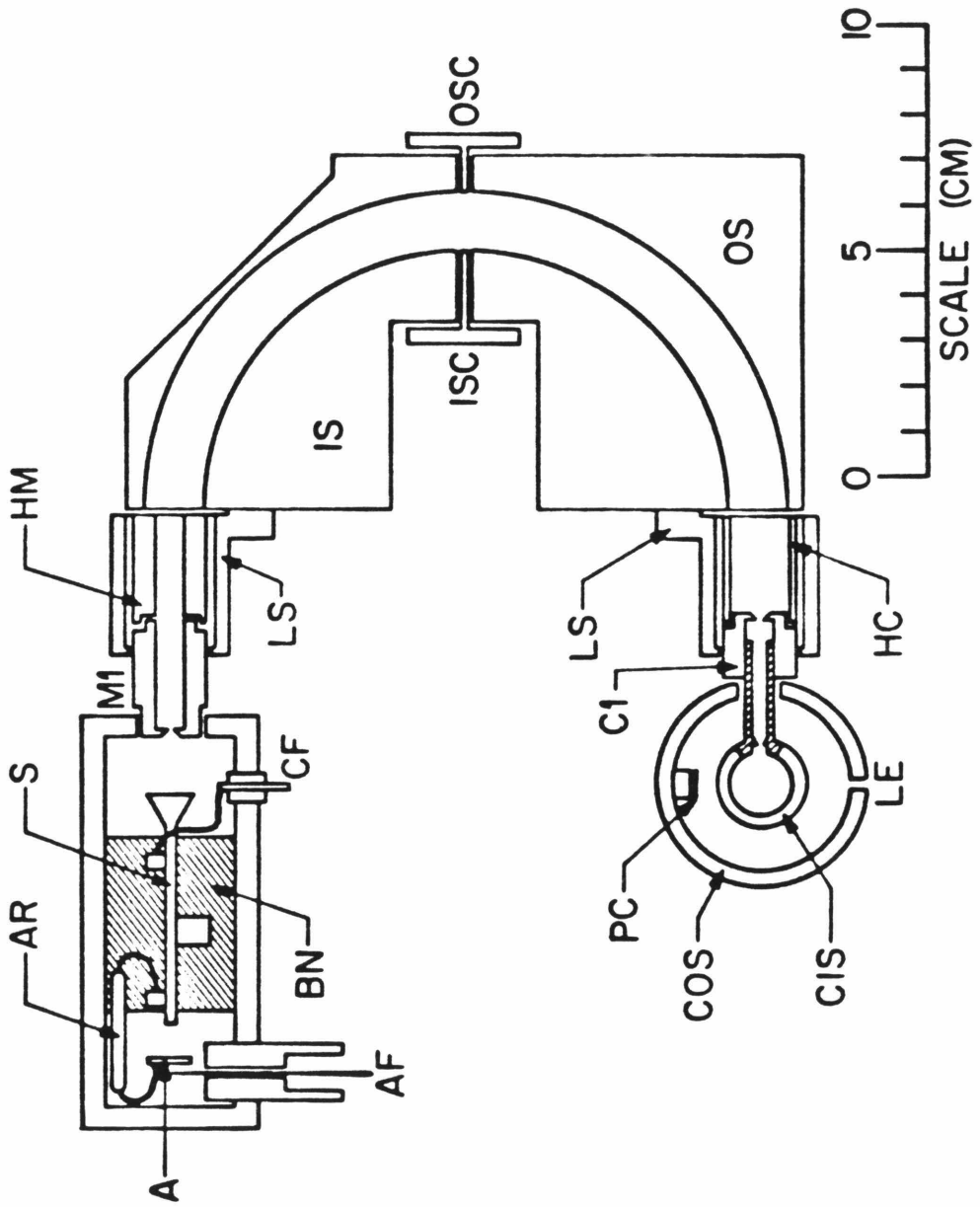
OSC
OS
IS
ISC
HM
LS
M1
CF
S
AR
BN
AF
A
LS
C1
HC
LE
PC
COS
CIS
0
5
10
SCALE (CM)

CHAPTER 4

HAM/3 CALCULATIONS

4.1 Introduction

The HAM/3 method was introduced in 1977 by Åsbrink, Fridh, and Lindholm in three relatively short letters in Chemical Physics Letters.[1-3] This method, a semi-empirical MO SCF theory, was formulated in an intuitive way, to calculate electron spectroscopic data: ionization potentials, electron affinities and excitation energies.

From 1977 to 1979 there was a good deal of critical debate over the method and some relatively pithy commentary.[4-7] While the method clearly demonstrated its ability to calculate the desired data with speed and accuracy,[*e.g.*,2,3,6-15] the validity of its theoretical basis was questioned. In 1979 and 1980, Åsbrink *et al.*, in collaboration with de Bruijn, Chong and Manne,[16-18] showed that through suitable transformation and an unconventional use of the idempotency of the density matrix, the HAM/3 method was a proper Hartree-Fock derivative with energy expressions similar to those in CNDO.

In 1980, the HAM/3 program was made available through the Quantum Chemistry Program Exchange (QCPE)[19] and was acquired. This program has the capacity to handle up to 60 atoms and 122 orbitals of the following elements: H, C, N, O, F. The program has been used in this study to calculate the ionization potentials of formaldehyde and

some substituted carbonyls in conjunction with an experimental study, and to examine the excitation energies of ethylene and its methyl and fluoro derivatives to determine the methods usefulness to studies in electron impact spectroscopy also performed by this research group.

4.2 Background Review of the Hartree-Fock SCF Method

This section will briefly review the Hartree Fock Self Consistent Field (HF-SCF) molecular orbital theory[20] as background for consideration of the HAM/3 method.

The total hamiltonian operator for the interactions of the particles of a molecular system is given by :

$$\mathbf{H_T} = \sum_{A<}\sum_{B}\frac{z_A z_B}{r_{AB}} - \sum_{A}\sum_{i}\frac{z_A}{r_{Ai}} + \sum_{i<}\sum_{j}\frac{1}{r_{ij}} - \sum_{i}\frac{\hbar^2}{2m}\nabla_i^2 - \sum_{A}\frac{\hbar^2}{2M_A}\nabla_A^2 \tag{1}$$

where A and B are the nuclear centers and i and j are the electrons. The terms of this hamiltonian represent nuclear repulsion, nuclear-electronic attractions, electronic repulsions, the electronic kinetic energies and the nuclear kinetic energy respectively. As usual:

$$\mathbf{H_T}\Psi = E\Psi \tag{2}$$

and

$$E = \frac{\langle\Psi|\mathbf{H_T}|\Psi\rangle}{\langle\Psi|\Psi\rangle} \tag{3}$$

In the Born-Oppenheimer approximation, the kinetic energy of the nuclei is neglected and their interaction is reduced to a sum of electrostatic repulsions.

The new hamiltonian, **H**, is:

$$\mathbf{H} = -\sum_{A}\sum_{i}\frac{z_A}{r_{Ai}} + \sum_{i<}\sum_{j}\frac{1}{r_{ij}} - \sum_{i}\frac{\hbar^2}{2m}\nabla_i^2 \tag{4}$$

and the energy is expressed as,

$$E = \sum_{A<}\sum_{B}\frac{z_A z_B}{r_{AB}} + \frac{\langle\Psi|\mathbf{H}|\psi\rangle}{\langle\Psi|\Psi\rangle} \tag{5}$$

where Ψ is now purely electronic.

It is further possible to break up **H** into two terms, H1 and H2, where H1 contains all single electron terms (nuclear attraction and the kinetic energies), and H2 contains all two electron operators (the electron-electron repulsion terms).

Thus:

$$\mathbf{H} = H1 + H2 \tag{6}$$

where

$$H1 = -\sum_{i}(\sum_{A}\frac{z_A}{r_{Ai}} + \frac{\hbar^2}{2m}\nabla_i^2) \tag{7}$$

and

$$H2 = \sum_{i<}\sum_{j}\frac{1}{r_{ij}} \tag{8}$$

Substituting equation 6 into equation 5 yields:

$$E = \sum_{A<}\sum_{B}\frac{z_A z_B}{r_{AB}} + \frac{1}{\langle\Psi|\Psi\rangle}(\langle\Psi|H1|\Psi\rangle + \langle\Psi|H2|\Psi\rangle) \tag{9}$$

where the first term represents nuclear-nuclear repulsions and the last two, the total electronic energy of the system, represents one electron interactions and electron-electron repulsions.

The total wavefunction Ψ may, to a first approximation, be expressed as a composite function of one electron orbitals, neglecting the effects of electronic correlation. Thus the global electronic wavefunction is represented as a normalized product of antisymmetrized one electron functions, usually expressed as a Slater determinant:

$$\Psi = (n!)^{-\frac{1}{2}} |\psi_p^\alpha(1)\psi_p^\beta(2)\cdots\psi_z^\alpha(n-1)\psi_z^\beta(n)| \tag{10}$$

where each orbital is doubly occupied. $\psi_p^\alpha(1)$ is a one electron molecular wave function, p, containing electron 1 with spin α and so forth and $(n!)^{-\frac{1}{2}}$ is the normalization factor where n is the number of electrons.

By replacing Ψ in the total electronic energy with the expression in equation 10 and assuming the single electron molecular orbitals are orthonormal, the one electron term becomes:

$$\begin{aligned} E1 &= \langle\Psi|H1|\Psi\rangle \\ &= 2\sum_p \langle\psi_p(i)|H1|\psi_p(i)\rangle \end{aligned} \tag{11}$$

and the two electron term is:

$$E2 = \langle\Psi|H2|\Psi\rangle$$

$$= 2\sum_p\sum_q [\langle\psi_p(i)\psi_q(j)|H2|\psi_p(i)\psi_q(j)\rangle - \frac{1}{2}\langle\psi_p(i)\psi_q(j)|H2|\psi_p(j)\psi_q(i)\rangle] \tag{12}$$

where p and q are one electron orbital indices and $\psi_p(i)$ is now spinless.

In the LCAO-MO approximation each molecular orbital is expanded in a normalized linear combination of atomic orbitals:

$$\psi_p(i) = \frac{1}{\sqrt{N_p}}\sum_k c_k^p \phi_k(i) \tag{13}$$

where $\phi_k(i)$ are individual atomic orbitals and c_k^p are variational parameters (expansion coefficients). N_p is the normalization constant:

$$N_p = \sum_k \sum_\ell c_k^p c_\ell^p S_{k\ell} \tag{14}$$

where $S_{k\ell}$ is the overlap between atomic orbitals k and ℓ.

Substituting into equation 11 yields:

$$\begin{aligned} E1 &= 2 \sum_p \frac{1}{N_p} \langle \sum_k c_k^p \phi_k(i) | H1 | \sum_i c_i^p \phi_i(i) \rangle \\ &= 2 \sum_k \sum_\ell (\sum_p \frac{c_k^p c_\ell^p}{N_p} \langle \phi_k(i) | H1 | \phi_\ell(i) \rangle) \end{aligned} \tag{15}$$

By making the following notational changes:

$$P_{k\ell} = 2 \sum_p \frac{c_k^p c_\ell^p}{N_p} \tag{16}$$

and

$$H_{k\ell} = \langle \phi_k(i) | H1 | \phi_\ell(i) \rangle \tag{17}$$

the above collapses to:

$$E1 = \sum_k \sum_\ell P_{k\ell} H_{kl} \tag{18}$$

The electron-electron repulsion can be treated in a like manner:

$$\begin{aligned} E2 = \frac{1}{2} \sum_k \sum_\ell \sum_m \sum_n P_{k\ell} P_{mn} [&\langle \phi_k(i) \phi_m(j) | H2 | \phi_\ell(i) \phi_n(j) \rangle \\ - \frac{1}{2} &\langle \phi_k(i) \phi_m(j) | H2 | \phi_\ell(i) \phi_n(i) \rangle] \end{aligned} \tag{19}$$

where the first integral is the Coulomb repulsion and is usually represented by $\langle k\ell|mn\rangle$ and the second is the exchange integral and is expressed as $\langle kn|lm\rangle$.

Therefore:

$$E2 = \frac{1}{2}\sum_{k}\sum_{\ell} P_{kl} \sum_{m}\sum_{n} P_{mn}(\langle kl|mn\rangle \quad - \frac{1}{2}\langle kn|lm\rangle) \tag{20}$$

The total energy may be expressed as:

$$E = \sum_{A<}\sum_{B} \frac{z_A z_B}{r_{AB}} + \sum_{k}\sum_{\ell} P_{k\ell}[H_{k\ell} + \frac{1}{2}\sum_{m}\sum_{n} P_{mn}(\langle kl|mn\rangle - \frac{1}{2}\langle kn|lm\rangle)] \tag{21}$$

The electron population, P, and hence the variational parameters, c, must be determined. Using the variational method, the total energy is minimized with respect to the variational parameters:

$$\frac{\partial E}{\partial c_k^p} = 0 \tag{22}$$

for all k and p.

This yields a set of linear homogeneous equations for all k:

$$\frac{\partial E}{\partial c_k^p} = \sum_{\ell} c_\ell^p (F_{k\ell} - E^p S_{k\ell}) = 0 \tag{23}$$

The Fock matrix is defined as follows:.

$$F_{k\ell} = H_{k\ell} + \sum_{m}\sum_{n} P_{mn}(\langle k\ell|mn\rangle - \frac{1}{2}\langle kn|\ell m\rangle) \tag{24}$$

and the molecular orbital energy is:

$$E^p = \sum_{m}\sum_{n} \frac{c_m^p c_n^p}{N_p} F_{mn} \tag{25}$$

The necessary condition for all equations to hold is a zero determinant.

$$|F_{k\ell} - E^p S_{k\ell}| = 0 \tag{26}$$

By solving the secular determinant, E^p is obtained for each molecular orbital. Substituting these energies back into equation 23 and using the normalization condition, $N = \sum_k \sum_\ell c_k c_\ell S_{k\ell} = 1$, and orthogonality, the coefficients, c_k, and the electronic distribution, P_{kl} can be determined.

The problem is the Fock matrix elements themselves depend on c_m and P_{mn}. To circumvent this dilemma, an initial charge distribution is assumed and from this an initial set of P_{mn} is determined. The Fock matrix elements that result are calculated and the secular determinant solved. This yields a first order approximation for E^p and ψ_p. The coefficients, c_p, are then used to determine a new set of P_{mn} values and the entire process is iterated until consistent values are achieved, a self consistent field.

It should be noted that even if the Hartree-Fock energy described above could be determined exactly, it does not equal the true electronic energy. Correction would have to be made for errors due to electronic correlation and relativistic effects.

The relativistic error increases with the number of inner shell electrons whose average velocity reaches a significant fraction of the speed of light, thus increasing their relativistic mass. Usually this energy

makes very little contribution to the bond energy and is neglected.

The correlation error stems from the one electron approximation, that the motion of each electron is independent of the motion of the other electrons in the system. This error is sometimes minimized through a process of configuration interaction (CI) or, in many semi-empirical methods, absorbed into the parameterization of the integrals.

4.3 The HAM/3 method

The HAM/3 method differs from other semi-empirical methods in that it begins by parameterizing the atomic orbitals then evaluates the integrals rather than by using empirical values to replace the integrals themselves.

The HAM method uses the Slater expression for the energy, E_μ, of one electron, μ, in an atom A[1]:

$$E_\mu = -\zeta_\mu^2 \tag{27}$$

where ζ_μ is the orbital exponent (a function of energy), $\zeta_\mu = (z_A - S_\mu)/n_\mu$, z is the nuclear charge, S is the shielding and n, the principal quantum number.

Slater evaluated the shielding in terms of constants, $\sigma_{\nu\mu}$, and obtained for atoms:

$$E_T = -\sum_\mu \frac{P_{\mu\mu}}{n_\mu^2}[z_A - (P_{\mu\mu} - 1)\sigma_{\mu\mu} - \sum_{\nu\neq\mu} P_{\nu\nu}\sigma_{\nu\mu}]^2 \tag{28}$$

where $P_{\mu\mu}$ is the density matrix element, the number of electrons in orbital μ.

It was found in the HAM method that the best total energies were achieved when $\sigma_{\nu\mu}$ were functions rather than fixed constants. By trial and error, the following function was selected:

$$\sigma_{\nu\mu} = a_{\nu\mu} - \frac{b_{\nu\mu} + c_{\nu\mu} z_A}{\varsigma_\mu} \tag{29}$$

where a, b and c are constants and ς_μ is the orbital exponent of the shielded orbital. The shielding constants have been determined by using the total energies of 311 different atomic species having $n = 1$ or 2.[1]

To generalize to molecules, the LCAO approximation is made.

$$\psi_i = \sum_\mu c_{\mu i} \phi_\mu \tag{30}$$

As in HF-SCF, the total energy is a function of the density matrix elements, $P_{\mu\nu}$ and these elements in turn are functions of $c_{\mu i}$, the expansion coefficients

$$P_{\mu\nu} = \sum_i q_i c_{\mu i} c_{\nu i} \tag{31}$$

where q_i is the charge in orbital i.

By using the variational method, Roothan's equations are obtained:

$$\sum_\nu \left(\frac{\partial E}{\partial P_{\mu\nu}} - \epsilon_i S_{\mu\nu}\right) c_{\nu i} = 0 \tag{32}$$

where the Fock matrix element is given by:

$$F_{\mu\nu} = \frac{\partial E}{\partial P_{\mu\nu}} \tag{33}$$

and E is the total energy.

The energy can be partitioned into elements,

$$E = \sum_{\mu\nu} E_{\mu\nu} \tag{34}$$

where $E_{\mu\nu}$ is the energy of the electronic charge, $P_{\mu\nu}S_{\mu\nu}$ in the region $\mu\nu$.

The diagonal terms, $E_{\mu\mu}$ can be expressed as:

$$E_{\mu\mu} = -P_{\mu\mu}\varsigma_{\mu}^{2} \tag{35}$$

using the atomic orbital exponents as before. In the off-diagonal elements, the charge in the bond is divided between the two centers:

$$E_{\mu_A\nu_B} = -P_{\mu\nu}S_{\mu\nu}[\frac{1}{2}(\varsigma_{\mu}^{2} + \varsigma_{\nu}^{2})]f_{\mu\nu} \tag{36}$$

where $f_{\mu\nu}$ is a parameter that depends on the type of bond (ss, sp, etc.) and the internuclear distance, R_{AB}.

An additional term is added to the total energy for interatomic electrostatic interactions:

$$\sum_{A>B} Q_A Q_B \gamma_{AB} \tag{37}$$

where Q_A and Q_B are the gross atomic charges and γ_{AB} is parameterized.

To generated the Fock matrix elements, the total effective number of electrons in ϕ_μ is first formulated.

$$T_\mu = P_{\mu\mu} + \sum_{B\neq A}\sum_{\nu_B}^{B} \frac{1}{2}(P_{\mu\nu}S_{\mu\nu} + P_{\nu\mu}S_{\nu\mu})f_{\mu\nu} \tag{38}$$

Then,

$$E1 = -\sum_{\mu} T_{\mu}\zeta_{\mu}^2 + \sum_{A>B} Q_A Q_B \gamma_{AB} \tag{39}$$

where E1 is the total energy including the electrostatic term above.

So,

$$\begin{aligned} F_{\mu\mu} &= \frac{\partial E1}{\partial P_{\mu\mu}} \\ &\approx -\zeta_{\mu}^2 + \sum_{\nu}^{A} \sigma_{\mu\nu} \frac{2}{n_{\nu}} \zeta_{\nu} T_{\nu} - \sum_{B} Q_B \gamma_{AB} \end{aligned} \tag{40}$$

and

$$F_{\mu_A\nu_B} \approx \frac{1}{2} S_{\mu_A\nu_B} [F_{\mu_A\mu_A} + F_{\nu_B\nu_B} - (\zeta_{\mu_A}^2 + \zeta_{\nu_B}^2)(f_{\mu_A\nu_B} - 1)] \tag{41}$$

The Fock matrix elements are treated in the usual way and the overlap is not neglected.

It should be noted that in the HAM/3 method not only are the orbital coefficients, $c_{\mu i}$, subjected to the variational process but the wavefunctions, ϕ_{μ}, are as well, through the dependence of ζ_{μ} on the P matrix; thus the HAM SCF results yield an optimized basis set.

It has been shown[17] that if a transition state is formed by removing one half of an electron either from a specific orbital i or diffusely where the decrease in electron density is distributed homogeneously over all valence orbits, the eigenvalues of the orbitals correspond to the ionization potentials of the molecules. In a like manner, if one half an electron is added the electron affinities are determined. Lastly, if a transition state is formed where one half an electron is removed from orbital i and one

half an electron is added to orbital a, the excitation energy between states i and a may be calculated.

4.4 Calculations

Unless otherwise indicated all geometries were taken from reference 21.

4.4.1 Ionization Potentials of some Substituted Carbonyls

The ionization potentials of formaldehyde, trans-acrolein (2-propenal), ketene, and acetone have been calculated by the HAM/3 method. The ionization potentials that were determined are tabulated in Tables 1 through 4 along with experimental and other theoretical values for comparison. There is generally good agreement between the values calculated with this method and experimentally determined values.

4.4.2 Excitation Energies of the Methyl and Fluoroethenes

The first singlet and triplet excitation energies for the methylethenes and the fluoroethenes are given in Tables 5 and 6 where they are contrasted with experimental values determined by electron impact.[28,29] Although agreement between the values is very reasonable, in some cases excellent, examination reveals that overall, in this highly simplistic treatment of the problem, the method is not sensitive enough to reproduce the trends in the excitation energies with substitution of the chromophore.

REFERENCES

1. L. Åsbrink, C. Fridh, and E. Lindholm, *Chem. Phys. Lett.*, **52**, 63 (1977).
2. L. Åsbrink, C. Fridh, and E. Lindholm, *Chem. Phys. Lett.*, **52**, 69 (1977).
3. L. Åsbrink, C. Fridh, and E. Lindholm, *Chem. Phys. Lett.*, **52**, 72 (1977).
4. S. de Bruijn, *Chem. Phys. Lett.*, **52**, 76 (1977).
5. S. de Bruijn, *Theo. Chem. Acta*, **50**, 313 (1979).
6. D. Chong, *Theo. Chem. Acta*, **51**, 55 (1979).
7. L. Åsbrink, C. Fridh, and E. Lindholm, *Chem. Phys.*, **27**, 159 (1978).
8. L. Åsbrink, C. Fridh, and E. Lindholm, *Inter. J. Quantum Chem.*, **13**, 331 (1978).
9. C. Fridh, L. Åsbrink, and E. Lindholm, *Chem. Phys.*, **27**, 169 (1978).
10. L. Åsbrink, C. Fridh, and E. Lindholm, *Tetrahedron Lett.*, **52**, 4627 (1977).
11. C. Fridh, *J. Chem. Soc. Faraday Trans. II*, **74**, 190 (1978).
12. E. Lindholm, G. Bieri, L. Åsbrink, and C. Fridh, *Inter. J. Quantum. Chem.*, **14**, 737 (1978).
13. L. Åsbrink, C. Fridh, and E. Lindholm, *J. Electron Spectroscopy*, **16**, 65 (1979).
14. C. Fridh, L. Åsbrink, and E. Lindholm, *Physica Scripta*, **20**, 603 (1979).

15. G. Bieri and L. Åsbrink, *J. Electron Spectroscopy*, **20**, 149 (1980).

16. L. Åsbrink, C. Fridh, E. Lindholm, and S. de Bruijn, *Chem. Phys. Lett.*, **66**, 411 (1979).

17. L. Åsbrink, C. Fridh, E. Lindholm, S. de Bruijn, and D. Chong, *Physica Scripta*, **22**, 475 (1980).

18. E. Lindholm, L. Åsbrink, and P. Manne, *Physica Scripta*, **28**, 377 (1983).

19. L. Åsbrink, C. Fridh, and E. Lindholm, *Q.C.P.E.*, program 393.

20. G. Klopman and R. Evans, in *Semi Empirical Methods of Electronic Structure Calculation, part A: Techniques*, G. A. Segal, editor (Plenum Press, New York, 1977).

21. K. Hellwege, *Landolt-Bornstein numerical data and functional relationship in science and technology, New Series, Group II, Vol. 7* (Springer-Verlag, Berlin, 1976).

22. H. Bock, T. Hirabayashi, and S. Mohmand, *Chem. Ber.*, **114**, 2595 (1981).

23. W. Von Neissen, G. Bieri, and L. Åsbrink, *J. Electron Spectroscopy*, **21**, 175 (1980).

24. P. Masclet and G. Mouvier, *J. Electron Spectroscopy*, **14**, 77 (1978).

25. H. Van Dam and A. Oskam, *J. Electron Spectroscopy*, **13**, 273 (1978).

26. G. Bieri, L. Åsbrink, and W. Von Niessen, *J. Electron Spectroscopy*, **27**, 129 (1982).

27. V. Young and K. Cheng, *J. Chem. Phys.*, **65**, 3187 (1976).

28. W. Flicker, O. Mosher, and A. Kuppermann, *Chem. Phys. Lett.*, **36**, 56 (1975).

29. M. Coggiola, W. Flicker, O. Mosher, and A. Kuppermann, *J. Chem. Phys.*, **65**, 2655 (1976).

TABLE 1

Ketene Vertical Ionization Potentials (eV)

Band/orbital[a]	HAM/3	Experimental[a,b]		HAM/3[a]	CEPA[a]	RSPT[a]
$\tilde{X}$ $2b_1$	9.67(π)	9.8	9.64	9.70	9.50	9.14
$\tilde{A}$ $2b_2$	14.29	14.2	14.2	14.38	14.46	14.23
$\tilde{B}$ $1b_1$	15.27(π)	15.0	15.0	15.28	15.08	15.56
$\tilde{C}$ $1b_2$	16.31	16.3	16.3	16.45	16.79	16.61
$\tilde{D}$ $7a_1$	16.83	16.8	16.8	16.75	17.04	16.70
$\tilde{E}$ $6a_1$	18.36	18.2	18.2	18.26	18.57	18.44
$\tilde{F}$ $5b_1$	24.30			24.32		
$\tilde{G}$ $4b_1$	38.95			35.96		

a Reference 6.

b Reference 22.

TABLE 2

Formaldehyde Vertical Ionization Potentials (eV)				
Band/orbital[a]	HAM/3	Experimental[a]	HAM/3[a]	GF[a]
$\tilde{X}$ $2b_2(n_O)$	10.72	10.9	10.72	10.84
$\tilde{A}$ $1b_1(\pi_{CO})$	14.82(π)	14.5	14.80	14.29
$\tilde{B}$ $5a_1$	16.47	16.1	16.44	16.36
$\tilde{C}$ $1b_2$	17.35	17.0	17.33	17.13
$\tilde{D}$ $4a_1$	21.24	21.4	21.23	21.57
$\tilde{E}$ $3a_1$	34.39	34.2	34.31	35.9

a Reference 23.

TABLE 3

Acrolein Vertical Ionization Potentials (eV)

Band/orbital[a]	HAM/3	Experimental[a,b,c]			HAM/3[a]	GF[a]
$\tilde{X}$ $13a'(n_O)$	9.86	10.1	10.11	10.11	9.87	10.19
$\tilde{A}$ $2a''(\pi_{CC})$	10.91(π)	11.0	10.93	10.94	10.91	10.67
$\tilde{B}$ $1a''(\pi_{CO})$	13.74(π)	13.8	13.67	13.67	13.75	13.27
$\tilde{C}$ $12a'$	13.89	13.8		14.00	13.89	13.89
$\tilde{D}$ $11a'$	14.84	14.8	14.76	14.82	14.85	14.71
$\tilde{E}$ $10a'$	15.42	16.2	15.5	15.53	15.43	15.9
$\tilde{F}$ $9a'$	15.69	15.4	16.1	16.36	15.69	15.77
$\tilde{G}$ $8a'$	19.00	16.2		19.02	19.00	19.62
$\tilde{H}$ $7a'$	20.56	18.8		21.35	20.56	20.73
$\tilde{I}$ $6a'$	24.93	20.9			24.93	26.97
$\tilde{J}$ $5a'$	32.64	24.6			32.64	34.43

a Reference 23.

b Reference 24.

c Reference 25.

TABLE 4

Acetone Vertical Ionization Potentials (eV)

Band/orbital[a]	HAM/3[b]	Experimental[a,c]		GF[a]
$\tilde{X}$ $5b_2(n_O)$	9.95	9.8	9.71	9.85
$\tilde{A}$ $2b_1(\pi_{CO})$	12.52	12.6	12.59	12.65
$\tilde{B}$ $4b_2$	13.20	~13.4	13.40	13.45
$\tilde{C}$ $8a_1$	13.95	14.1	13.95	14.05
$\tilde{D}$ $1a_2$	14.14	~14.4		14.40
$7a_1$	14.70	15.7		15.66
$3b_2$	14.78	15.7		15.93
$1b_1$	15.55	~16.0	15.52	16.08
$6a_1$	17.70	18.0	17.75	18.21
$2b_2$	22.50	23.0		23.78
$5a_1$	24.02	24.6		25.42
$4a_1$	32.48			29.36

a Reference 26.

b And reference 26 except entries 14.14 and 13.95 reversed.

c Reference 27.

TABLE 5

Excitation Energies of the Methylethenes (eV)

$R_1R_2C=CR_3R_4$	Calculated[a]		Experimental[b]	
$R_1R_2R_3R_4$	singlet	triplet	singlet	triplet
H H H H	7.75	4.38	7.6	4.32
	7.77	4.40		
Me H H H	7.61	4.38	7.17	4.28
	7.51	4.29		
Me H Me H				
cis	7.38	4.22	7.10	4.21
	7.44	4.28		
trans	7.30	4.17	6.95	4.24
Me Me H H[c]	7.34	4.21	6.60	4.22
	7.57	4.28		
Me Me Me H	7.17	4.09	6.97	4.16
Me Me Me Me	7.12	4.10	6.57	4.10

a Multiple entries have different geometries.

b Reference 28.

c Geometry adapted from data for tetramethylethene and trans 1,2 dimethylethene.

TABLE 6

Excitation Energies of the Fluoroethenes (eV)				
$R_1R_2C=CR_3R_4$	Calculated[a]		Experimental[b]	
$R_1R_2R_3R_4$	singlet	triplet	singlet	triplet
H H H H	7.75	4.38	7.6	4.32
	7.77	4.40		
F H H H	7.41	4.23	7.50	4.40
F H F H				
cis	7.11	4.05	7.82	4.28
	7.11	4.00		
trans	7.02	3.95	7.39	4.18
F F H H	7.54	4.43	7.50	4.63
	7.55	4.43		
F F F H	7.12	4.11	7.65	4.43
F F F F	6.90	3.97	8.84	4.68

a Multiple entries have different geometries.

b Reference 29.

CHAPTER 5

DISCUSSION AND RESULTS

Paper 1: The Angular Resolved Photoelectron Spectroscopy of Some Alkylated Alkynes

The Angular Resolved Photoelectron Spectroscopy of Some Alkylated Alkynes[a]

D. J. Flanagan[b] and A. Kuppermann

Arthur Amos Noyes Laboratory of Chemical Physics,[c]

California Institute of Technology, Pasadena, CA 91125

(received)

Abstract

The photoelectron angular distributions have been taken on acetylene, propyne, 1-butyne and 2-butyne using He I radiation (584 Å). Their respective bands are discussed on the basis of the asymmetry parameter β and other experimental and theoretical criteria.

---

[a] This work was supported in part by the U. S. Department of Energy, Contract No. DE-AM03-F00767, Project Agreement No. DE-AT03-76ER72004.

[b] Work performed in partial fulfillment of the requirements for the Ph.D degree in Chemistry at the California Institute of Technology.

[c] Contribution No.

I. INTRODUCTION

Angular resolved photoelectron spectroscopy has demonstrated its power to detect autoionization and shape resonances in ionization processes and elucidate the nature of the orbitals involved in valence orbital photoionization.[1]

Experimentally this process involves using He I radiation at 584 Å to ionize an electron from a valence orbital.

The energetics of this process is described by the equation:

$$\hbar\omega = IP + KE \tag{1}$$

where $\hbar\omega$ is the photon energy, IP the ionization potential, and KE the kinetic energy of the ejected electron. By Koopmans' theorem,[2] IP is equal to the negative of the orbital energy, $IP = -E$.

Cooper and Manson[3] derived the following expression for the differential cross section for the interaction of unpolarized radiation with atomic or molecular targets, expanding the work of Bethe and Salpeter[4] and Cooper and Zare[5] on the interaction of polarized radiation with hydrogenic atoms and atoms and molecules, respectively,

$$\frac{d\bar{\sigma}}{d\Omega} = \frac{\sigma^{TOT}}{4\pi}[1 - 1/2\beta P_2(\cos\theta)] \tag{2}$$

where P_2 is the second order Legendre polynomial, $P_2(\cos\theta) = 1/2[3\cos^2\theta - 1]$, and β is an asymmetry parameter that reflects the departure from isotropy of the angular distribution. Its range is restricted to values between -1 and 2. σ^{TOT} is the total ionization cross section for a photon

with energy $\hbar\omega$ to eject an electron from a molecule in a given initial state to produce an ion in a given final state.

It has been shown experimentally that the angular distributions are sensitive to the differences in orbital angular momentum, yielding in the same molecule different values of β for σ and π orbital ionization.[1] In general, π orbitals have higher β values and σ orbitals have more symmetric distributions. It should be noted that β also depends on the energy of the outgoing electron and it is possible to determine the energy dependence by examining the variation of β with photon wavelength. This is typically done using synchrotron radiation. Because this radiation is usually ellipically polarized, β is commonly, but not exclusively, determined by examining the variation in intensity as a function of the angle between the polarization vector and the ejected electrons rather than the angle between the photon beam and the electrons. Regardless of method, the β values determined are equivalent. As a result of this energy dependence, caution must be exercised in comparing β values for bands in different molecules when the ionization potentials differ.

Acetylene and its alkylated analogs have been chosen for this study because acetylene represents the simplest alkyne and a study of the homologous series permits examination of substituent effects including induction and possible hyperconjugation in a manner similar to the study of the substituted ethenes undertaken by previous workers.[6,7] The angular distributions of propyne, 1-butyne, and 2-butyne are presented

here for the first time.

Additionally of interest is the theoretical work of Dill, Fano and Chang on the homogeneous diatomics and their possible applicability to acetylene. Dill and Fano[8-10] have developed arguments predicting the asymmetry parameter in homogeneous diatomic molecules based on angular momentum transfer. Their utility has been demonstrated in recent studies, such as that by Southworth *et al.*[11] on H_2 and D_2, where the experimentally obtained values of β compare well with the prediction. Chang[43] has extended these arguments to develop parity favoredness rules for the β values of homogeneous diatomic molecules based on the symmetry of the transitions:

$$\beta[\Sigma^{\pm} \rightarrow \Sigma^{\pm}] > \beta[\Sigma \rightarrow \Pi] \tag{3}$$

and

$$\beta[\Sigma^{\pm} \rightarrow \Sigma^{\mp}] = -1 \tag{4}$$

The validity of these rules has been verified by the experimentally measured values of β for selected homogenous diatomic molecules. Since the basis of these rules is the symmetry of states involved in the transition and since acetylene belongs to the same point group as the homogenous diatomics, a study of acetylene and the symmetry perturbed propyne can verify whether the rules are applicable for systems other than the homogeneous diatomic molecules.

Finally, the experimentally determined orbital energies can be

compared to those determined by theoretical calculations.[12–17]

II. EXPERIMENTAL

The variable angle spectrometer used in these experiments is described in detail elsewhere.[18] A block diagram of the apparatus is given in Figure 1. Briefly, the radiation source consists of a He I (584 Å) discharge lamp which ionizes sample vapors contained within a cylindrical scattering chamber. The electrons ionized are energy-analyzed by means of a hemispherical electrostatic analyzer and detected by a spiraltron electron multipier. Both analyzer and electron multiplier are mounted on a rotatable gear. Spectra are taken at nine angles between 45 degrees and 120 degrees with respect to the photon beam.

The ambient magnetic field in the photon-molecule interaction region of the spectrometer is reduced to less than 0.2 mgauss by lining the chamber with μ metal and by the use of three sets of matched Helmholtz coils. This avoids deflection of the relatively slow electrons by that field which would otherwise occur, thereby preventing distortions in the angular distributions.

The background has been systematically parameterized by a least squares fit to a fifth order polynomial and subtracted from all spectra. Resolution for the angular distributions was less than 40 meV and for the vibrational spectra was approximately 20 meV full width at half maximum of the Ar $^2P_{3/2}$ peak which also provided energy calibration for the spectra. The accuracy of the β measurements was determined

by the apparatus' ability to consistantly reproduce a $\beta = 0.88 \pm .02$ for Ar $^2P_{3/2}$ which has been determined independently in several laboratories.[18–23]

All samples were from commerical sources. Acetylene (Matheson 96% purity), propyne (Matheson 96% purity) and 1-butyne (Air Products 95% purity) are permanent or liquified gases and were used without further purification. 2-Butyne (Farchan $\geq$ 98% purity) is a liquid and was subjected to several freeze-pump-thaw cycles and then was vaccuum distilled before utilization.

III. RESULTS AND DISCUSSION

1. Acetylene C_2H_2

1.1 Full Scan

The photoelectron spectrum shown in Figure 2 was taken at a detector angle of 54.7°, the so-called "magic angle" which corresponds to a zero in the second order Legendre polynomial. The ionization potential range was 11.3 to 20.0 eV. This spectrum reveals the presence of three distinct bands labelled $\tilde{X}\,^2\Pi_u$, $\tilde{A}\,^2\Sigma_g^+$, and $\tilde{B}\,^2\Sigma_u^+$. Vibrational structure is clearly in evidence on all three bands but is most distinct on the $\tilde{X}$ and $\tilde{B}$ bands.

The ground state MO description of the acetylene molecule is:

$$(1\sigma_g 1sc)^2(1\sigma_u 1sc)^2(2\sigma_g)^2(2\sigma_u)^2(3\sigma_g)^2(1\pi_u)^4 \equiv {}^1\Sigma_g^+ \qquad (5)$$

where g and u indicate the molecular inversion symmetries. The lowest

set of σ orbitals is composed of core 1s orbitals on the carbons as noted. The other sets are from the carbon 2s and 2pz orbitals and the hydrogen 1s atomic orbitals. The π_u orbitals are composed of carbon 2px and 2py orbitals.

Ionization of the highest energy electron would remove one of the degenerate π orbital electrons, resulting in an ion in the $^2\Pi_u$ state. The second ionic state should result from the removal of a $3\sigma_g$ electron and be a $^2\Sigma_g^+$ state. The third state should result from the removal of a $2\sigma_u$ electron and be $^2\Sigma_u^+$. Removal of an electron from a bonding orbital generally increases internuclear separation and would be expected to cause a shift in the Franck-Condon envelope of the $\tilde{X}$ band to higher vibrational states and to result in a smaller vibrational energy spacing. However, the principal vibrational progression present has a maximum intensity at $\nu' = 0$. Analysis of the Franck-Condon factors in this band by Heilbronner et al.[24] support the predictions of Griffith and Goodman[25] and later of Chu and Goodman[26] of a linear configuration in the electronic ground state of the cation. The frequency of the primary vibrational progression is 1770±50 cm^{-1} which is smaller than the observed neutral molecular vibrational frequency of 1983 cm^{-1} for the ν_3 (C≡C) stretching frequency as expected[27] (Figure 3). This also agrees fairly well with the frequency of 1830 cm^{-1} obtained by Turner *et al.*[28]

Further vibrational structure of much lower intensity is visible at higher resolution on the $\tilde{X}$ $^2\Pi_u$ band consistent with the presence of

bending modes deduced by Parr *et al.*[29] and observed by Dehmer and Dehmer[30]. Features were seen at 0.036, 0.087 and 0.171 eV above the principal ν_3 progression by Dehmer and Dehmer[30] and at 0.036, 0.086 and 0.172 by Parr *et al.*[29] Parr has tentatively assigned the feature at 0.036 (290 cm^{-1}) to a trans bending mode and those at 0.086 and 0.172 to a cis bending mode (694 cm^{-1}) and its harmonic. Dehmer and Dehmer also assign the structure to cis and/or trans bending modes but, based on their present evidence, decline to make a more definitive assignment. The vibrational features of this band and the bands that follow are summarized in Table 1. Neither Renner-Teller nor spin-orbit splitting is resolved for this band.

The $\tilde{A}\ ^2\Sigma_g^+$ band also shows vibrational fine structure (Figure 4). Due to its complexity, this structure is not as readily interpreted as that of the $\tilde{X}$ band. The figure displays at least three different modes with appreciable overlap. This is consistent with the cis-bent equilibrium configuration for the $\tilde{A}\ ^2\Sigma_g^+$ state of $C_2H_2^+$ postulated by Rosmus *et al.*[14] Consequently, transitions to the $\tilde{A}$ state from the linear ground state of C_2H_2 should lead to vibrational excitation of the bending mode of the C-H bonds as well as the expected stretching modes. Additionally the bent configuration of the ion would result in a double minimum in the potential surface with frequency doubling possible for quanta exceeding the barrier.[31]

The unusual shape of this band is readily seen in the presence of

an anomalous decrease in intensity in the region about 16.6 eV. Present data do not permit an explanation of this feature. The threshold for the photoionization appearance potential of dissociative ionization to C_2H^+ occurs at 16.8 eV,[32] within the range of the $\tilde{A}$ state. The thermochemical limit might be lower.[33] However, a photoelectron-photoion coincidence study by Eland[33] shows that this channel is not open from the $\tilde{A}$ state for levels below 17.3 eV. Above 17.3 the molecular ion is fully predissociated to C_2H^+, possibly reappearing at 17.6 eV. Additionally, analysis shows the formation of the dissociation products to be spin forbidden and possibly symmetry forbidden as well, depending on whether the ground state of C_2H^+ is $^3\Sigma^-$ or $^3\Pi$.

Other possible influences on band shape are possible isomerization to a vinylidene configuration[14] or internal conversion and dissociation. Although expected, the fluorescence from the $\tilde{A}$ to $\tilde{X}$ states has never been observed.[33]

Finally, the unlikely possiblity of contribution of intensity on the later part of the band from a $\tilde{X}$ band shake up was briefly considered. This is inconsistent with the observed β values, and calculations indicate the intensity of such a satellite would be less than 0.02% of the primary.[34] Although it would lie within the range of this band, it would have miniscule influence on the band shape.

The third band $\tilde{B}\ ^2\Sigma_u^+$ shows a vibrational progression with a frequency of 2,430 cm^{-1} and a second mode at 1920 cm^{-1} as indicated in Figure 5. Baker and Turner[35] have ascribed these frequencies

to the C-H symmetric stretch and C≡C stretch, respectively. This interpretation is consistent with the Franck-Condon principle, the orbital being antibonding between the two carbons and strongly bonding between the carbons and hydrogens.[36]

1.2 Angular Distributions

Angular distributions were measured over each of the resolvable vibrational peaks of the $\tilde{X}$ band of the spectrum. Each distribution involved the measurement of nine fixed angle spectra. Since the structure of the $\tilde{A}$ and $\tilde{B}$ bands is not sufficiently well resolved to limit the scanning to the peak maxima of the vibrational progressions, angular distributions were taken over the entire band. The results are summarized in Table 2, and plots of the β values vs. ionization potential are presented in Figures 2, 6 and 7.

$\tilde{X}\ ^2\Pi_u$ Band

It is immediately observed that the value of β in this band varies only slightly with ν'. Good agreement is acheived between the results obtained here and those reported by Kreile and Schweig[37] for this molecule and are consistent with the results of Keller *et al.*[38] for the first two orbitals using synchrotron radiation. The β value of close to unity is comparable to that obtained from ionization from other C-C π bonds. For example, a β value of $1.25 \pm .05$ over the range of the $\tilde{X}$ band for the ethylene has been obtained by this apparatus[39] and a vertical β value of 1.20 has been reported by others[40].

$\tilde{A}\ ^2\Sigma_g^+$ Band

The β values for this band are significantly lower in magnitude than those of the $\tilde{X}\ ^2\Pi_u$ band ranging from a maximum of 0.69 to a minimum of -0.12 with a value of 0.55 observed at the vertical ionization potential. This lowering of β in Σ over Π bands has also been observed in the β spectrum of ethylene and other molecules.[1,6,7,38–41]

$\tilde{B}\ ^2\Sigma_u^+$ BAND

A significant increase in the β value is observed relative to those in the $\tilde{A}\ ^2\Sigma_g^+$ band where the value of β at the vertical ionization potential for this band is 1.10 with maximum and minimum values of 1.85 and 0.63. Error bars for the lower electron energy range of this band are high due to poor counting statistics from the low ionization cross section. Nevertheless, the values here are comparable to those seen in the $\tilde{X}\ ^2\Pi_u$ band, contradicting the rule that Σ bands display significantly lower β values than Π bands in the same unsaturated hydrocarbon. This is compatible with the suggestion of Machado and Leal *et al.*[42] that the $\tilde{B}\ ^2\Sigma_u^+$ excitation channel is stongly perturbed by coupling with the $\tilde{X}\ ^2\Pi_u$ channel.

Part of the motivation for the study of this molecule was to determine if the β values of acetylene, which has the same symmetry as the homogeneous diatomic molecules ($D_{\infty h}$), obey the parity favoredness rules developed by E. Chang[43] for these molecules. From theoretical considerations linking angular momentum transfer to parity favoredness,

Chang has concluded that the β values for $\Sigma^{\pm}$ to $\Sigma^{\pm}$ transitions should be larger than those for Σ to Π transitions, while the β values for $\Sigma^{\pm}$ to $\Sigma^{\mp}$ transitions are negative unity. The photoelectron spectrum of acetylene contains one Σ to Π band and two Σ^{+} to Σ^{+} bands. In both our data and that of Kreile and Schweig,[37] the β values associated with the $\tilde{X}\ ^2\Pi_u$ band are clearly higher than those of the $\tilde{A}\ ^2\Sigma_g^+$ band, plainly in disagreement with Chang's rules, although the β values of the $\tilde{X}$ and the $\tilde{X}\ ^2\Sigma_u^+$ bands are comparable.

2. PROPYNE C_3H_4

2.1 Full Scan

This molecule, a methyl substituted acetylene, was chosen to examine the effects of symmetry reduction and substitution on the angular distributions. However, in the course of studying this molecule it quickly became clear that its properties more closely resembled those of its isomer, allene, which has a nearly identical photoelectron spectrum,[44] than acetylene. In fact, some evidence exists that they share common ion states with cyclopropene,[45] its other isomer.

The ionization potentials and vibrational frequencies associated with this molecule are given in Table 3. It is immediately noticed that the first ionization potential is 1.02 eV lower than that of acetylene. The most noticeable fine structure is observed on the $\tilde{X}$ band. Visible is a main progression at 1965 cm^{-1} associated with the C≡C stretching mode plus overtones of three other modes, one of which has been previously

unreported. These overtone frequencies are associated with the C-C stretching mode (865 cm^{-1}) and with methyl bending mode (1410 cm^{-1}) induced by interaction of the C-C π orbitals with pseudo-π orbitals of the methyl group causing orbital delocalization over the three carbon skeleton. The third mode, at 357 cm^{-1}, which has not been previously observed, can be attributed to a ≡C-H bending by comparison with the ethynyl bending mode in C_2H_2.

The second broad band in the photoelecton spectrum consists of two overlapping features. The $\tilde{A}$ band has vibrational fine structure on the leading edge at frequencies of 1,335 cm^{-1}, 897 cm^{-1}, and a previously unobserved mode at 487 cm^{-1}. These may be attributed to the C-C single bond stretch and the methyl deformation modes and the last probably to ≡C-H bend. There is excellent agreement with Carlier *et al.*[36] on the first two frequencies. Turner et al.[28] observe only a frequency of about 1300 cm^{-1} under their experimental resolution.

The $\tilde{B}$ and $\tilde{C}$ bands are broad features with vibrational structure that has not been observed by this apparatus under high resolution(15-20 meV). The $\tilde{B}$ band has a possible progression at 620 cm^{-1} under low resolution (35-40 meV). Under these conditions the $\tilde{C}$ band also has fine structure of a complex nature which has not been analyzed here.

2.2 Angular Distributions

$\tilde{X}$ 2e

The β value across this band shows a modest variation with

vibrational state (Figure 8). These β values are 0.3 lower than those for the $\tilde{X}$ band in acetylene. However, to within experimental error the β value for the $\tilde{X}$ band vertical ionizational potential of propyne and allene are identical.

The lower β values observed can be accounted for by two possible mechanisms: 1) an inductive effect of the methyl group or 2) hyperconjugation of the C≡C π bonds with the C-H pseudo-π methyl bonds or a combination of the two.

There is some evidence that allene, propyne, and cyclopropene ions share a common ion state and may spontaneously isomerize to this common form.[45] The effect is uncertain since by the Franck-Condon principle it is explicitly assumed that the ionization will occur much faster than any nuclear rearrangement.

$\tilde{A}$ 1e $\tilde{B}$ 7a

Although caution must be exercised in the comparison, it is clear that the trends of the β values for this molecule and that of allene for these two bands and for the $\tilde{C}$ band are remarkably similar although the β values themselves are uniformly lower in allene. The magnitude of the β values are much closer to that of acetylene where the correspondence between the sigma bands is $\tilde{B}$ propyne $\rightarrow$ $\tilde{A}$ acetylene and $\tilde{C} \rightarrow \tilde{B}$, respectively. This is not unexpected considering the close similarity between these molecules and the fact that the βs of σ type orbitals tend to be less sensitive to inductive effects, than π orbitals.

Nevertheless, it is clear that the features between 13.8 and 16.8 eV consist of two overlapped bands: the first $\tilde{A}$ being a π type with β values closer to that of the $\tilde{X}$ band, falling off rapidly over the band, and the second $\tilde{B}$ being a σ type with a β value of approximately 0.4.

$\tilde{C}$ 6a1

In this band we see the same anomalous behavior observed in acetylene, where the β value for a proported σ orbital has equal or greater magnitude than the π band.

Plots of the β values for the full spectrum and the individual band are given in Figures 8, 11, 12 and 13 and are summarized in Table 4.

3. 1-Butyne

3.1 Full Scan

Discernible in the photoelectron spectrum of this molecule are four broad features, the first two of which possess resolvable vibrational structure under high resolution scanning (Figure 14).

The first feature labelled I is attributed to the $\tilde{X}$ band, ionization from the π orbitals. Present here are two vibrational progressions with frequencies 1927 cm^{-1} and 940 cm^{-1} and a third previously unreported at 1490 cm^{-1} (Figure 15). The first two may be assigned to νC$\equiv$C, and νC-C alpha to the triple bond, the third to νC-C of the two C-C bonds in phase.[36] These values compare well with those achieved by P. Carlier and J. Dubois *et al.*[36] presented in Table 5. The presence of the single bond

stretching frequencies in this band is indicative of some delocalization of the triple bond over the four carbon skeleton. It is observed that first ionization potential of this molecule is 0.18 eV lower than that seen in propyne. The inductive effect of an ethyl group is slightly greater than that of a methyl group. On the other hand, a greater potential exists in this molecule for delocalization. The first effect is to increase the electron density; the second is to reduce it.

Three overlapped bands II, III and IV, are in evidence in the second broad feature. The leading edge, band II, contains vibrational structure that is resolvable but complex (Figure 16).

Visible on band II is a vibrational progression with a frequency of 1299 cm^{-1} attributable to in-phase stretching of the two C-C bonds. Other structure is present that at the moment defies satisfactory assignment.

The third feature labelled by the single numeral, V, is held by other workers to consist of two degenerate bands[44]. Finally, there is the fourth feature, VI, which like I represents a single band.

3.2 Angular Distributions

Since the ionization potentials of 1-butyne and propyne differ only by 0.2 eV and since the β values of the $\tilde{X}$ bands of these molecules are uniform within experimental error over the bandwidths, the β value for the $\tilde{X}$ band of this molecule, $0.71 \pm .02$, is directly comparable to that of propyne at $0.72 \pm .03$, which is within experimental error of the

same value, and allene at 0.70±.05, but differs from the $\tilde{X}$ band value of acetylene by 0.3.

It was found in the methylated ethylenes that β π strongly decreased with increasing methyl substitution. This was attributed to increasing hyperconjugation with the methyl groups. If this effect is extended to the alkynes, one would expect empirically the amount of hyperconjugation possible between the π orbital and the ethyl group to be roughly equal to that of the methyl group and thus β π values that are roughly equivalent. This is, in fact, observed.

The β values for this band and the other bands are summarized in Table 6 and plotted in Figures 14, 17, 18 and 19.

β values drop rapidly across II, reach a minimum over band III, and then rise again over the last part of band IV.

In V the β values average 0.58, and in the last band they are slightly lower, averaging 0.53 to approximately 0.45.

The β values over the entire molecule are much more homogeneous than in either acetylene or propyne, varying only about 0.4. Also lacking in this molecule, consequentially, is the rise in the higher ionization potential σ bands, V and VI, to values exceeding unity as seen in the other two molecules although the β values are greater than for II, III and IV, parallelling the trend observed in acetylene and propyne.

4. 2-Butyne

4.1 Full Scan

The spectrum of this molecule (Figure 21) bears a strong superficial resemblence to that of propyne, containing three broad features. The first feature, the $\tilde{X}$ band, shows two vibrational progressions: a primary progression at 2115 cm^{-1} and a subsidiary set of envelopes at a frequency of 370 cm^{-1}. The first frequency may be assigned to the carbon triple bond stretching mode, the second to bending $\equiv$C-CH_3. Carlier and Dubois[36] report only the primary progression at a frequency of 2110 cm^{-1} for this band while Bieri and Asbrink[12] report three frequencies: 2400, 1520 and 1050 cm^{-1}. This contradicts those observed here. It is seen in Figure 22 that a single mode at a frequency of 370 will adequately account for the overtones on the primary sequence. This assignment is based in part on the the presence of clearly observed but not strongly resolved shoulders on the primary progression at 370 cm^{-1}. If these shoulders were unresolved, then a report of two frequencies at two and three times the fundamental would be invoked to account for the structure and thus would explain the discrepancy between the two results.

The second broad feature contains three bands, $\tilde{A}$, $\tilde{B}$, and $\tilde{C}$, the maxima of which are resolvable in the high resolution spectra. Figure 23 shows the presence of two frequencies on the $\tilde{A}$ band, one at 1251 cm^{-1} and a complex overlay of peaks at a frequency of 389 cm^{-1}. The first may be assigned to in-phase deformation of the methyl group,[36] the latter to the bending mode above. The frequency of 1251 agrees

well with that of 1270 observed by Carlier and Dubois *et al.*[36] and less well with the frequency of 1450 reported by Bieri and Asbrink[12]. The frequency of 389 cm^{-1} is previously unreported for this band.

The third broad feature contains a single band, $\tilde{D}$, which has substantial overlap with the $\tilde{C}$ band.

The $\tilde{E}$ band of this molecule with a reported vertical ionization potential of 21.1 eV has not been studied because part of the band is beyond the region accessible by He I radiation, although it can be observed by He II.[12]

The ionization potentials and vibrational frequencies are listed in Table 7. It is observed that the vertical ionization potential of the molecule is lower than that of propyne and 1-butyne by 0.79 and 0.60 eV, respectively.

4.2 Angular Distributions

$\tilde{X}$

The trend of decreasing β value with alkyl substitution is confirmed and continued in this band. The values show very little fluctuation over the width of the band and thus not dependent on vibrational state.

$\tilde{A}$, $\tilde{B}$, $\tilde{C}$, $\tilde{D}$

All the higher ionization bands and $\tilde{X}$ as well show a remarkable uniformity in β. The average β value of all the band lies within 0.1 of each other, although both the $\tilde{A}$ and $\tilde{D}$ bands show considerable oscillatory

behavior. The discontinuity in β over the $\tilde{B}$ band represents an artifact in the data.

The crucial aspect of the angular distribution of this molecule is that no distinction can be made between the π and σ orbitals on the basis of the asymmetry parameter. Due to the extreme homogeneity of the β values the empirical rule, the β value of a π orbital will be greater than a σ orbital in a given molecule, is not valid here.

Plots of the angular distributions are given in Figures 21, 24, 25 and 26, and are summarized in Table 8.

5. Substituent Effects

Two principal substituent effects were observed in the course of this study: 1) the systematic variation of the first ionization potential with alkylation and 2) the variation of the β value of the π orbital with alkyl substitution.

5.1 Variation of Ionization Potential With Substituent

By Koopmans' theorem any effect of substituent on the orbital energy will be reflected in a change in ionization potential. There is a very dramatic substituent effect in the first ionization potential of the alkylated alkynes examined in this study. It is clearly seen in Table 9 that the effect of alklyation on the first ionization energy is nonlinear; the effect of two methyl groups is not twice the magnitude of one. While substituent effects certainly exist for the other ionization potentials, correlation is much less facile due to increased uncertainty in determining

onset caused by overlapping features.

Bachiri *et al.*[46] have quantized the effects of various substituents on alkynes and other systems of molecules through the use of empirical site functionals for the chromophore and are able to predict with very high degrees of precision the effect of substitution on the first ionization potential.

These functionals are nonlinear analytic functions empirically selected to be stable under linear regression based on a set of n parameters characterizing the functional site and an additional parameter characterizing the polarization effect of the substituent.

Although the approach is completely empirical, the accuracy of prediction is within 30 meV for all the molecules in this study and for many others as well.

Substituent effects are traditionally divided into two parts, inductive and conjugative (or hyperconjugative). To effectively distinguish between the two types of effects requires a detailed knowledge of the bonding interactions of the π orbitals and the pseudo-π orbitals of the alkyl group. This in turn necessitates high quality calculations of molecular orbitals. There is no lack of molecular orbital calculations (of diverse qualities) available on acetylene, but for the rest of the series high quality calculations are not available. This is especially true for 1-butyne which possesses low symmetry (C_s).

Ensslin *et al.*[47] have examined the hyperconjugative effects of methyl mono- and di- substitution of acetylene on the orbital shifts

using a modified CNDO/2 program. It was determined that the hyperconjugative destabilization of the acetylene π orbital is less than the inductive one and in 2-butyne hyperconjugation contributes 1 eV to the orbital shift and the inductive effect, 1.7 eV, where the effects of the two methyl groups are non additive. The experimental drop in ionization potential between acetylene and 2-butyne is 1.81 eV.

5.2 Variation of β with Substituent

With the exception of acetylene, which shows a modest drop in β with vibrational excitation, the β values of these molecules in this series are invariant with vibrational state over the range of the $\tilde{X}$ band. This may be cautiously used as an indication that β does not vary significantly with electron energy in the region at issue and the variations in β reflect a purely substituent effect.

The vertical β_π for acetylene (1.01±.03) drops by 0.29 on a single methyl substitution 0.72±.03 in propyne. This study yields no difference in the β value for ethyl substitution *vis-a-vis* methyl substitution; the β value for 1-butyne at 0.71±.02 is within experimental error of the value for propyne. Two methyl substitutions cause a further drop of 0.17 to a value of 0.55±.03 in 2-butyne. Thus, as in the variation of ionization potential, disubstitution has a less than linear effect on the asymmetry parameter.

By reciprocity, if the β of the π orbitals are decreased by alkyl substitution, the β of the σ orbitals must be increased. This trend is,

in fact, observed but is more difficult to correlate due to the overlap of bands, higher uncertainties and oscillations present in the asymmetry parameter.

These substituent effects compare with those seen by Mintz *et al.*[7] in the methylated ethenes, where a similar trend of decreasing β value of the π orbitals was seen with increasing methylation.

IV. CONCLUSIONS

Photoelectron angular distributions have been taken for acetylene, propyne, 1-butyne, and 2-butyne. The last three have been reported here for the first time.

In the course of this study it has been determined that the parity favoredness rules of Chang[43] for predicting the asymmetry parameter of homogeneous diatomic molecules fails to account for the behavior observed in acetylene. Instead, acetylene and its alkylated analogs follow the trends in β observed in studies of the methylated ethenes.[7]

In addition, the semi-empirical rule that the asymmetry parameters for π orbitals are higher than for σ orbitals in the same molecule is clearly violated in this series. Acetylene and propyne possess σ orbitals with β values significantly higher than the π orbitals. In 1- butyne and 2- butyne the β values are nearly equivalent in the π orbital and some or all of the σ bands.

Finally, two principal substituent effects have been observed in this series: 1) a systematic decrease in first ionization potential and

2) a similar decrease in the asymmetry parameter of the $\tilde{X}$ band with increasing alkylation.

REFERENCES

1. P. R. Keller, D. Mehaffy, J. Taylor, F. A. Grimm and T. A. Carlson, *J. Electron Spectroscopy*, **27**, 223 (1982).

2. T. Koopmans, *Physica*, **1**, 104 (1933).

3. J. Cooper and S. Manson, *Phys. Rev.*, **177**, 157 (1969).

4. H. Bethe and E. Salpeter, *Quantum Mechanics of One and Two Electron Atoms* (Springer-Verlag, Berlin, 1957).

5. J. Cooper and R. Zare, in *Lectures in Theoretical Physics*, edited by S. Geltman, K. Mahanthappa and N. Britten (Gordon and Breach, New York, 1969) Vol xi-c.

6. D. C. Mason, A. Kuppermann, D. M. Mintz in *Electron Spectroscopy*, edited by D. A. Shirley (North-Holland Publishing Co., Amsterdam, 1972) pp. 269-275.

7. D. M. Mintz and A. Kuppermann, *J. Chem. Phys.*, **70**, 3151 (1979).

8. D. Dill, *Phys. Rev. A*, **6**, 160 (1972).

9. U. Fano and D. Dill, *Phys. Rev. A*, **6**, 185 (1972).

10. D. Dill and U. Fano, *Phys. Rev. Lett.*, **29**, 1203 (1972).

11. S. Southworth, W. D. Brewer, C. M. Truesdale, P. H. Kobrin, D. W. Lindle, and D. A. Shirley, *J. Electron Spectroscopy*, **26**, 43 (1982).

12. G. Bieri and L. Asbrink, *J. Electron Spectroscopy*, **20**, 149 (1980).

13. G. Bieri, A. Schmelzer, L. Asbrink, and M. Jonsson, *Chem. Phys.*, **49**, 213 (1980).

14. P. Rosmus, P. Botschwina, and J. P. Maier, *Chem. Phys. Lett.*, **84**, 71 (1981).

15. L. Asbrink, C. Fridh, and E. Lindholm, S. de Bruijn, and D. P. Chong, *Physica Scripta*, **22**, 475 (1980).

16. M. V. Andreocci, P. Bitchev, P. Carusi, A. Furlani, *J. Electron Spectroscopy*, **16**, 25 (1979).

17. M. Raimondi and M. Simonetta, *Molecular Physics*, **34**, 745 (1977).

18. D. Mason, D. Mintz, and A. Kuppermann, *Rev. Sci. Instrum.*, **48**, 926 (1977).

19. T. Carlson and A. Jonas, *J. Chem. Phys.*, **55**, 4913 (1971).

20. D. J. Kennedy and S. T. Manson, *Phys. Rev. A*, **5**, 227 (1972).

21. J. L. Dehmer, W. A. Chupka, J. Berkowitz and W. T. Jivery, *Phys. Rev. A*, **12**, 1966 (1975).

22. W. Hancock and J. Samson, *J. Electron Spectroscopy*, **9**, 211 (1976).

23. D. M. P. Holland, A. C. Parr, D. L. Ederer, J. L. Dehmer and J. B. West, *Nuclear Instruments and Methods*, **195**, 331 (1982).

24. E. Heilbronner, K. Muszkat and J. Schaublin, *Helv. Chem. Acta*, **54**, 58 (1971).

25. M. Griffin and L. Goodman, *J. Chem. Phys.*, **47**, 4494 (1967).

26. S. Y. Chu and L. Goodman, *J. Amer. Chem. Soc.*, **97**, 7 (1975).

27. G. Herzberg, *Molecular Spectra and Molecular Structure III: Electronic Spectra and Electronic Structure of Polyatomic Molecules* (Van Nostrand Reinhold Co., New York, 1966).

28. D. Turner, C. Baker, A. Baker and C. Brundle, *Molecular Photoelectron Spectroscopy* (Wiley, London, 1970).

29. A. C. Parr, J. West, D. Holland, and J. Dehmer, *J. Chem. Phys.*, **76**, 4349 (1982).

30. P. Dehmer and J. Dehmer, *J. Electron Spectroscopy*, **28**, 145 (1982).

31. J. H. D. Eland, *Photoelectron Spectroscopy* (John Wiley & Sons, New York, 1974).

32. T. Hayaishi, S. Iwata, M. Sasunuma, E. Ishiguro, Y. Morioka, Y. Iida and N. Nakamura, *J. Phys. B*, **15**, 79 (1982).

33. J. H. D. Eland, *Int. J. Mass. Spect.*, **31**, 161 (1979).

34. B. V. McKoy, private communication.

35. C. Baker and D. W. Turner, *Proc. Roy. Soc. A*, **308**, 19 (1968).

36. P. Carlier, J. Dubois, P. Masclet, and G. Mouvier, *J. Electron Spectroscopy*, **7**, 55 (1975).

37. J. Kreile and A. Schweig, *Chem. Phys. Lett.*, **69**, 71 (1980).

38. P. Keller, D. Mehaffy, J. Taylor, F. Grimm, and T. Carlson, *J. Electron Spectroscopy*, **27**, 223 (1982).

39. J. Sell and A. Kuppermann, *J. Chem. Phys.*, **71**, 3499 (1979).

40. T. Carlson and G. McGuire, *J. Electron Spectroscopy*, **1**, 209 (1973).

41. J. A. Sell and A. Kuppermann, *Chem. Phys. Lett.*, **61**, 355 (1979).

42. L. E. Machado, E. P. Leal, G. Csanak, B. V. McKoy, and P. W. Langhoff, *J. Electron Spectroscopy*, **25**, 1 (1982).

43. E. Chang, *J. Phys. B*, **11**, L293 (1978).

44. G. Bieri, F. Burger, E. Heilbronner and J. Maier, *Helv. Chem. Acta,* **60**, 2213 (1977).

45. E. Jemmis, J. Chandrasekhar and P. von Rague' Schleur, *J. Amer. Chem. Soc.,* **101**, 2848 (1979).

46. M. Bachiri, P. Carlier, and J. E. Dubois and G. Mouvier, *J. Chim. Phys.,* **77**, 899 (1980).

47. W. Ensslin, H. Bock, and G. Becker, *J. Amer. Chem. Soc.,* **96**, 2757 (1974).

48. G. Bieri, E. Heilbronner, T. Jones, E. Kloster-Jensen and J. Maier, *Physica Scripta,* **16**, 202 (1977).

49. R. Cavell and D. Allison, *J. Chem. Phys.,* **69**, 159 (1978).

50. J. A. Pople, H. B. Schlegel, R. Krishman, D. J. Defrees, J. S. Binkley, M. J. Frish, R. A. Whiteside, R. F. Hout, and W. J. Hehre, *Int. J. Quantum Chem. Symp.,* **15**, 269 (1981).

51. D. Mintz, Ph.D thesis, California Institute of Technology, 1976.

52. F. Cleveland, M. Murray, and H. Taufen, *J. Chem. Phys.,* **10**, 172 (1942).

53. N. L. Allinger and A. Y. Meyer, *Tetrahedron,* **31**, 1807 (1975).

54. G. Herzberg, *Molecular Spectra and Molecular Structure II: Infrared and Raman Spectra of Polyatomic Molecules* (Van Nostrand Reinhold Co, New York, 1945).

55. M. Tanimoto, K. Kuchitsu, and Y. Morino, *Bull. Chem. Soc. Jap.,* **42**, 2519 (1969).

TABLE 1b: Calculated IP of C_2H_2 (eV)

Band	Ham/3[a]	Ham/3[b]	GF[b]	VB[c]	CEPA[d]	SCF[d]	PNO CI[d]	STO-3G[e]	CNDO/S[e]
$\tilde{X}$	11.56	11.59	11.17	11.40	11.17	9.86	10.93	9.48	11.61
$\tilde{A}$	17.17	17.19	17.07	17.18	17.30	17.52	17.38	16.59	17.57
$\tilde{B}$	19.72	19.73	19.10	19.33	19.23	20.18	19.56	19.29	23.47

a) Geometry source references 27.

b) Reference 12.

c) Reference 17.

d) Reference 14.

e) Reference 13.

TABLE 1a: Vibrational Structure in C_2H_2

Band	Assignment	Ionic Frequency (cm^{-1})		Molecular Frequency (cm^{-1})[a]	
		This Work	Other Work[b,c]		
$\tilde{X}^2\Pi_u$	$\nu_2(\nu C \equiv C)^b$	1770	1830[d], 1800, 1792, 1806	1973	1983
	ν_4(cis bend)[e]	319	290, 290	612	
	ν_5(trans bend)[e]	700	694, 701	730	
$\tilde{A}^2\Sigma_g^+$					
$\tilde{B}^2\Sigma_u^+$	$\nu_1(\nu C - H)^{f,g}$	1920	1900, 1700	3372	3369
	$\nu_2(\nu C \equiv C)^{f,g}$	2430	2510, 2650	1973	1983

a) References 27 and 28.

b) References 28, 29, 30,and 36.

c) Reported in eV.

d) G. Bieri, E. Heilbronner, T. Jones, E. Kloster-Jensen, and J. Maier, *Physica Scripta*, **16**, 202 (1977).

e) Reference 29.

f) Reference 28.

g) Reference 36.

TABLE 2. β Values and IPs for C_2H_2 at 584 Å

Band/Orbital	Ionization Potential (eV)		Beta[a]	
	This Work	Other Work[b,c]	This Work	Other Work[d]
$\tilde{X}^2\Pi_u/1\pi_u$	1.40	11.40, 11.40, 11.43,	$\nu = 0$ 1.01±.03	1.02±.03
		11.49, 11.403±.003	$\nu = 1$ 0.93±.03	0.99± .01
			$\nu = 2$ 0.95±.03	0.93±.03
			$\nu = 3$ 0.84±.08	
$\tilde{A}^2\Sigma_g^+/3\sigma_g$	16.46	16.37, 16.74, 16.76,	vert: 0.55±.08	0.24±.02
		16.7, 16.375±.008	max: 0.69±.19	0.41±.04
			min: -0.12±.15	0.12±.05
$\tilde{B}^2\Sigma_u^+/2\sigma_u$	18.66	18.38, 18.72, 18.71,	vert: 1.10±.09	1.08± .05
		18.7, 18.404±.020	max: 1.85±.42	1.25±.06
			min: 0.63±.14	0.42±.07

a) Beta is measured at each maxima on vibrationally resolvable bands; the vertical, maximum and minimum beta values are indicated for vibrationally unresolved bands.

b) Adiabatic ionization potential.

c) References 2, 28, 36, 37; R. Cavel, and D. Allison, *J. Chem. Phys.*, **69**, 159 (1978).

d) Reference 37.

TABLE 3a: Vibrational Structure and IPs of C_3H_4

Band/orbital	Vertical IP (eV)		Vibrational Frequency (cm^{-1})				Assignment
			ionic		molecular		
	This work	Other work[b,c,d,e]	This work	Other work[c,e]	Other work[c,f]		
$\tilde{X}$ $2e(\pi)$	10.38[a]	10.37[a], 10.54, 10.364±.005[a], 10.36[a]	1,965	1,940 2000±50	2,142.0	2142	$\nu_3(\nu C \equiv C)^g$
			1,410	1440±50	1,382	1382	$\nu_4(\sigma CH3)^e$
			865	940 930±50	930.7	931	$\nu_5(\nu C - C)^g$
			357			328	$\nu_{10}(\equiv C - H)$ bend
$\tilde{A}$ $1e(\pi)$	14.60	13.69, 14.6, 13.906±.015, 14.5	1,335	1,290 1340±100	1,382	1382	$\nu_4(\sigma CH3)^g$
			897	900±100	930.7	931	$\nu_5(\nu C - C)^e$
			487				
$\tilde{B}$ $7a1$	15.54	15.2, 15.4, 14.93±.05, 15.2					
$\tilde{C}$ $6a1$	17.60	17.2, 17.4, 17.10±.03, 17.2					

a) Adiabatic ionization potential.
b) Reference 12.
c) Reference 27.
d) Reference 28.
e) Reference 36.
f) J. A. Pople, *et al. J.Quantum Chem.: Quant. Chem. Symp.*, **15**, 269 (1981).
g) Reference 4.

TABLE 3b: Calculated IP of C_3H_4 (eV)

Band	Ham/3[a]	Ham/3[b]	STO-3G[b]	CNDO/2[c]
$\tilde{X}$	10.30	10.30	8.80	15.04
$\tilde{A}$	14.72	14.63	15.15	19.28
$\tilde{B}$	14.93	15.05	15.17	22.69
$\tilde{C}$	17.66	17.73	17.99	24.34

a) Geometry source references 27.

b) Reference 12.

c) Reference 16.

TABLE 4: β Values for Propyne and Allene

Band	β Propyne[a] (ν_3,ν_4,ν_5)	β Allene[b] vertical beta
$\tilde{X}$	(0,0,0) 0.72±.03 (0,0,1) 0.73±.04 (0,1,0) 0.71±.07 (1,0,0) 0.73±.06 (1,0,1) 0.57±.09 (1,1,0) 0.73±.09 (2,0,0) 0.66±.07	0.70±.05
$\tilde{A}$	vert: 0.46±.05 max: 1.26±.23 min: 0.30±.09	0.65±.05
$\tilde{B}$	vert: 0.36±.10 max: 0.83±.13 min: 0.26±.08	0.10±.05
$\tilde{C}$	vert: 1.22±.17 max: 1.84±.41 min: 0.85±.18	0.55±.10

a) Convention as above.

b) D. Mintz, Ph.D Thesis, California Institute of Technology, 1976.

TABLE 5a: Ionization Potentials and Vibrational Frequencies of 1-Butyne

Band/orbital[a]	Vertical IP (eV)		Vibrational Frequency (cm^{-1})			Assignment
			ionic		molecular	
	This work	Other work[a,b]	This work	Other work[b]	Other work[d]	
I/3a″,12a′	10.19	10.3(10.20[c]),10.178±.005	1927	1980±50	2118[b,e]	$\nu(C \equiv C)^b$
			948	890±50	840(?)	$\nu(\equiv C - C-)^b$
			1490		1438(?)	$\nu(\equiv C - C-)$ in phase
II	12.70	12.8, 12.07±.02	1089		1068(?)	$\nu(\equiv C - C-)$ in phase
III	13.33	13.4				
IV	14.08	14.2				
V	15.78	15.8, 15.18±.05				
VI/8a′	17.23	17.2				

a) Reference 44.
b) Reference 36.
c) Adiabatic ionization potential.
d) F. Cleveland, M. Murray, and H. Taufen, *J. Chem. Phys.*, **10**, 172 (1942).
e) Reference 46.

TABLE 5b: Calculated IPs of 1-Butyne (eV)

Band	Ham/3[a]
$\tilde{X}$	9.84
$\tilde{A}$	9.99
$\tilde{B}$	12.61
$\tilde{C}$	12.88
$\tilde{D}$	13.08
$\tilde{E}$	15.07
$\tilde{F}$	15.40
$\tilde{G}$	17.06
$\tilde{H}$	19.98

a) Geometry source reference 53.

TABLE 6: β Values of 1-Butyne

Band	β^a
I	vert: 0.71±.02 max: 0.72±.10 min: 0.68±.05
II	vert: 0.36±.05 max: 1.03±.24 min: 0.31±.04
III	vert: 0.31±.07 max: 0.47±.12 min: 0.17±.08
IV	vert: 0.29±.04 max: 0.68±.13 min: 0.21±.08
V	vert: 0.44±.11 max: 0.97±.14 min: 0.28±.16
VI	vert: 0.63±.06 max: 0.74±.17 min: 0.36±.14

a) Convention as above.

TABLE 7a: Ionization Potentials and Vibrational Frequencies of 2-Butyne

Band/orbital[a]	Vertical IP (eV)		Vibrational Frequency (cm^{-1})			Assignment
			ionic		molecular	
	This work[a]	Other work[c,d,e,f]	This work	Other work[c,d]	Other work[g,h]	
$\tilde{X}/2e_u$	9.59	9.59[b], 9.61, 9.79, 9.562±.005	2115	2400, 2110±50 1520 1050	2313, 2240	$\nu(C \equiv C)$[d]
			370		374, 371	$\equiv C - CH_3$ bend
$\tilde{A}/5a1_g$	14.17	14.3, 14.0, 14.1(13.42[b]), 13.437±.02	1251	1450,1270±200	1379, 1380	in phase def CH_3[d]
			389		374, 371	$\equiv C - CH_3$ bend
$\tilde{B}/1e_g$	14.52	14.9, 14.5, 14.5				
$\tilde{C}/1e_u$	14.98	15.3, 15.0, 14.9				
$\tilde{D}/4a2_g$	16.28	16.3, 15.8, 16.1				
$\tilde{E}/4a1_g$		21.1, 20.63, 21.1				

a) Apparent maxima of overlapping bands.
b) Adiabatic ionization potential.
c) Reference 12.
d) Reference 36.
e) Reference 44.
f) Reference 47.
g) reference 50.
h) G. Herzberg, *Molecular Spectra and Molecular Structure II: Infrared and Raman Spectra of Polyatomic Molecules* (Van Nostrand Reinhold Co., New York, 1945).

TABLE 7b: Calculated IPs of 2-Butyne (eV)

Band	Ham/3[a]	Ham/3[b]	STO-3G[b]
$\tilde{X}$	9.41	9.47	8.22
$\tilde{A}$	13.87	14.19	14.48
$\tilde{B}$	14.07	14.01	14.74
$\tilde{C}$	14.12	14.25	15.18
$\tilde{D}$	15.17	15.27	16.36
$\tilde{E}$	20.19	20.33	23.30

a) Geometry source reference 55.

b) Reference 12.

TABLE 8: β Values of 2-Butyne

Band	β^a
$\tilde{X}$	vert: 0.55±.03 max: 0.61±.05 min: 0.49±.05
$\tilde{A}$	vert: 0.56±.05 max: 0.95±.06 min: 0.41±.08
$\tilde{B}$	vert: 0.51±.06 max: 0.63±.08 min: 0.43±.09
$\tilde{C}$	vert: 0.38±.14 max: 0.67±.09 min: 0.29±.08
$\tilde{D}$	vert: 0.69±.13 max: 0.98±.10 min: 0.26±.22

a) Convention as above.

TABLE 9: Variation of IP with Substituent

Molecule	IP(eV)	Delta[a]*	Delta[b]	Delta[c]
H-C≡C-H	11.40			
H-C≡C-CH_3	10.38	1.02	1.02	1.02
H-C≡C-CH_2CH_3	10.19	1.21	0.19	
CH_3C≡C-CH_3	9.59	1.81	0.60	0.79

a) Delta IP-IP(C_2H_2).

b) Delta IPm-IPn.

c) Delta IP of methyl species only.

FIGURE CAPTIONS

Figure 1. Block diagram of MAPS: He–cylinder of UHP helium, ZT–zeolite trap at 77°K for lamp helium supply, RB–lamp ballast resistor, LPS–lamp power supply, SC–scattering chamber, PC–photocathode, CL–set of electrostatic lenses, ANALYZER–hemispherical electrostatic analyzer, ML–set of electrostatic lenses, S–Spiraltron electron multiplier, CPS–spiraltron cathode power supply, APS–Spiraltron anode supply, RC–differentiating network for Spiraltron pulses, INTER–counting system interface to experiment, PDP 8e–Digital PDP 8e microcomputer, and OUTPUT–computer peripheral devices.

Figure 2. Photoelectron spectrum at a detector angle of 54.7°(lower panel) and the β spectrum (upper panel) of acetylene.

Figure 3. High resolution (15 meV) vibrational spectrum of acetylene $\tilde{X}\ ^2\Pi_u$ band at a detector angle of 54.7°. Dashed lines indicate marginally resolved features.

Figure 4. High resolution (15 meV) vibrational spectrum of acetylene $\tilde{A}\ ^2\Sigma_g^+$ band, at a detector angle of 54.7°.

Figure 5. High resolution spectrum (15 meV) vibrational spectrum of acetylene $\tilde{B}\ ^2\Sigma_u^+$ band at a detector angle of 54.7°.

Figure 6. Photoelectron spectrum (lower panel) and β spectrum (upper panel) of acetylene $\tilde{A}\ ^2\Sigma_g^+$ band.

Figure 7. Photoelectron spectrum (lower panel) and β spectrum (upper

FIGURE 1.

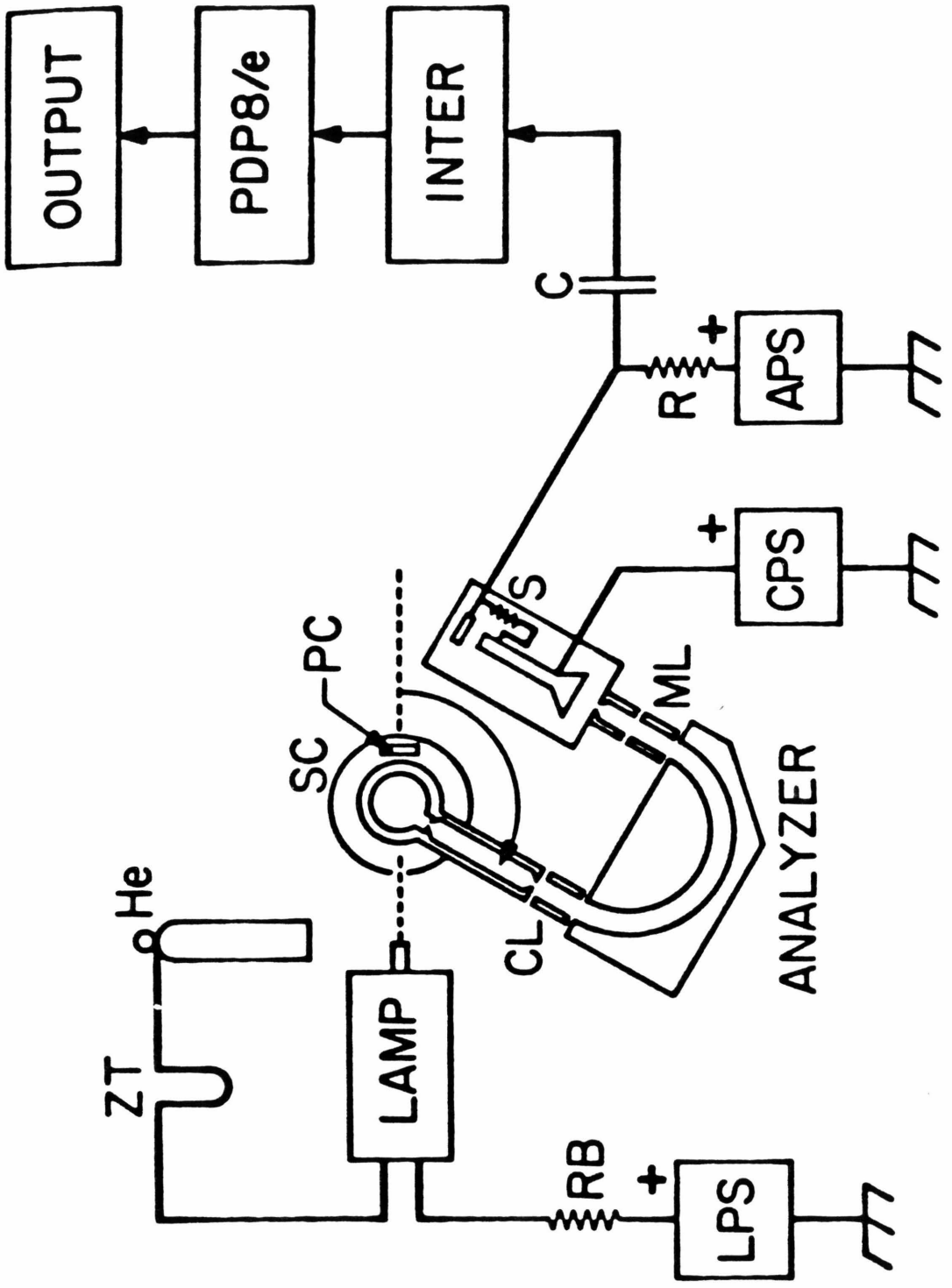
OUTPUT
PDP8/e
INTER
C
R
APS
CPS
S
PC
SC
ML
ANALYZER
CL
He
ZT
LAMP
RB
LPS

FIGURE 2.

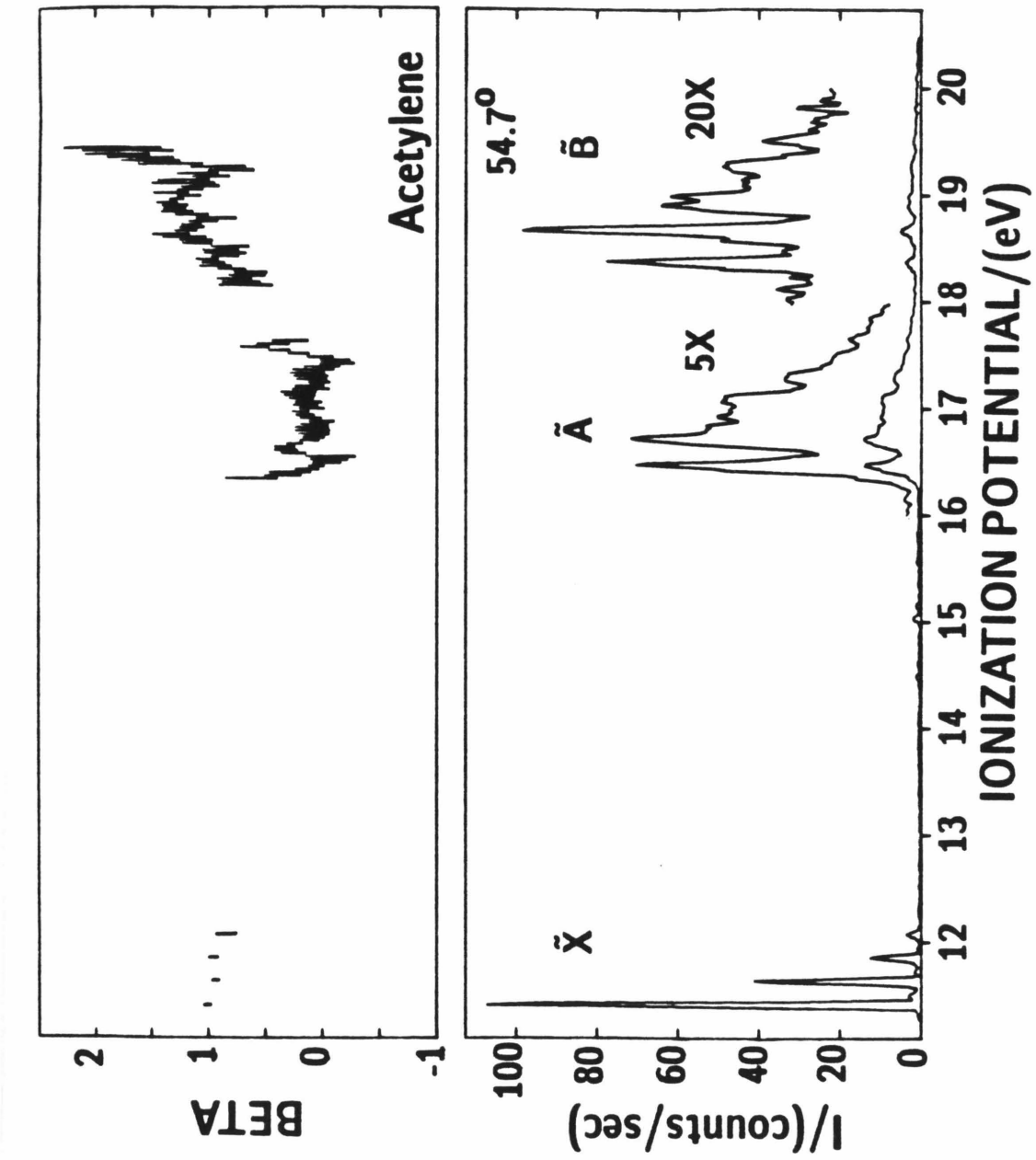
Acetylene
BETA
2
1
0
-1
X̃
Ã
B̃
5X
20X
54.7°
I/(counts/sec)
100
80
60
40
20
0
12
13
14
15
16
17
18
19
20
IONIZATION POTENTIAL/(eV)

FIGURE 3.

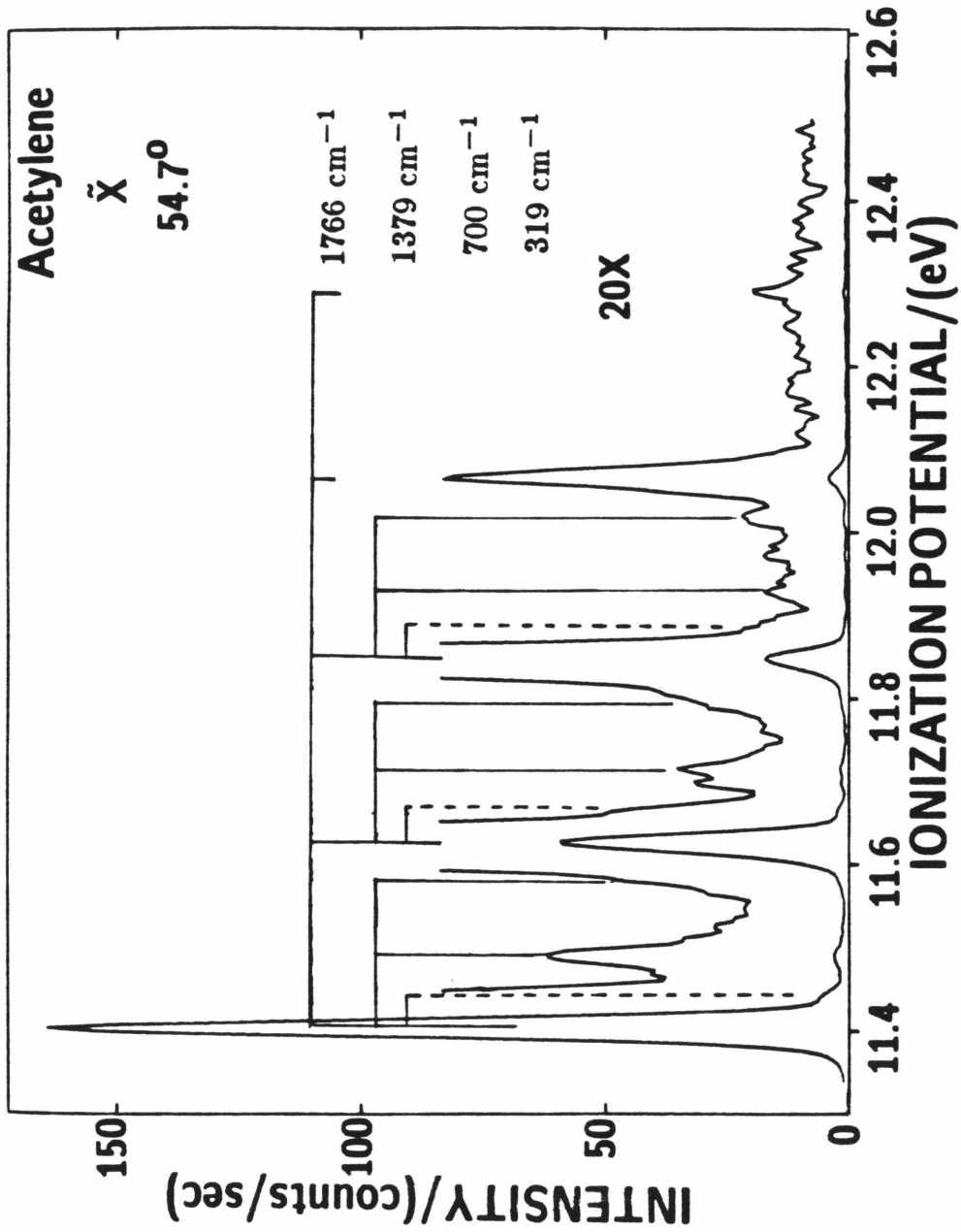
Acetylene
$\tilde{X}$
54.7°
1766 cm^{-1}
1379 cm^{-1}
700 cm^{-1}
319 cm^{-1}
20X
INTENSITY/(counts/sec)
150
100
50
0
11.4
11.6
11.8
12.0
12.2
12.4
12.6
IONIZATION POTENTIAL/(eV)

FIGURE 4.

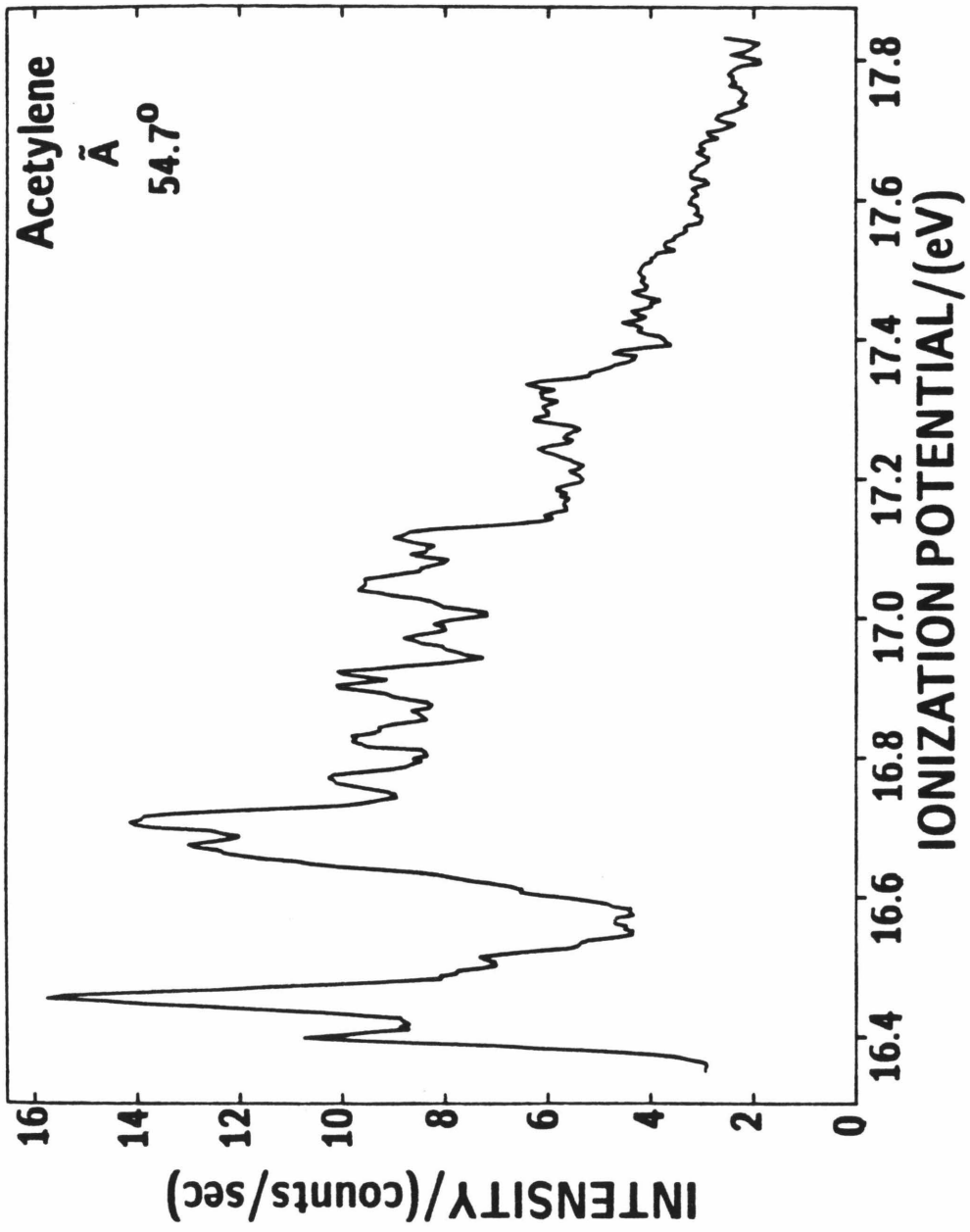
Acetylene
Ã
54.7°
INTENSITY/(counts/sec)
0
2
4
6
8
10
12
14
16
16.4
16.6
16.8
17.0
17.2
17.4
17.6
17.8
IONIZATION POTENTIAL/(eV)

FIGURE 5.

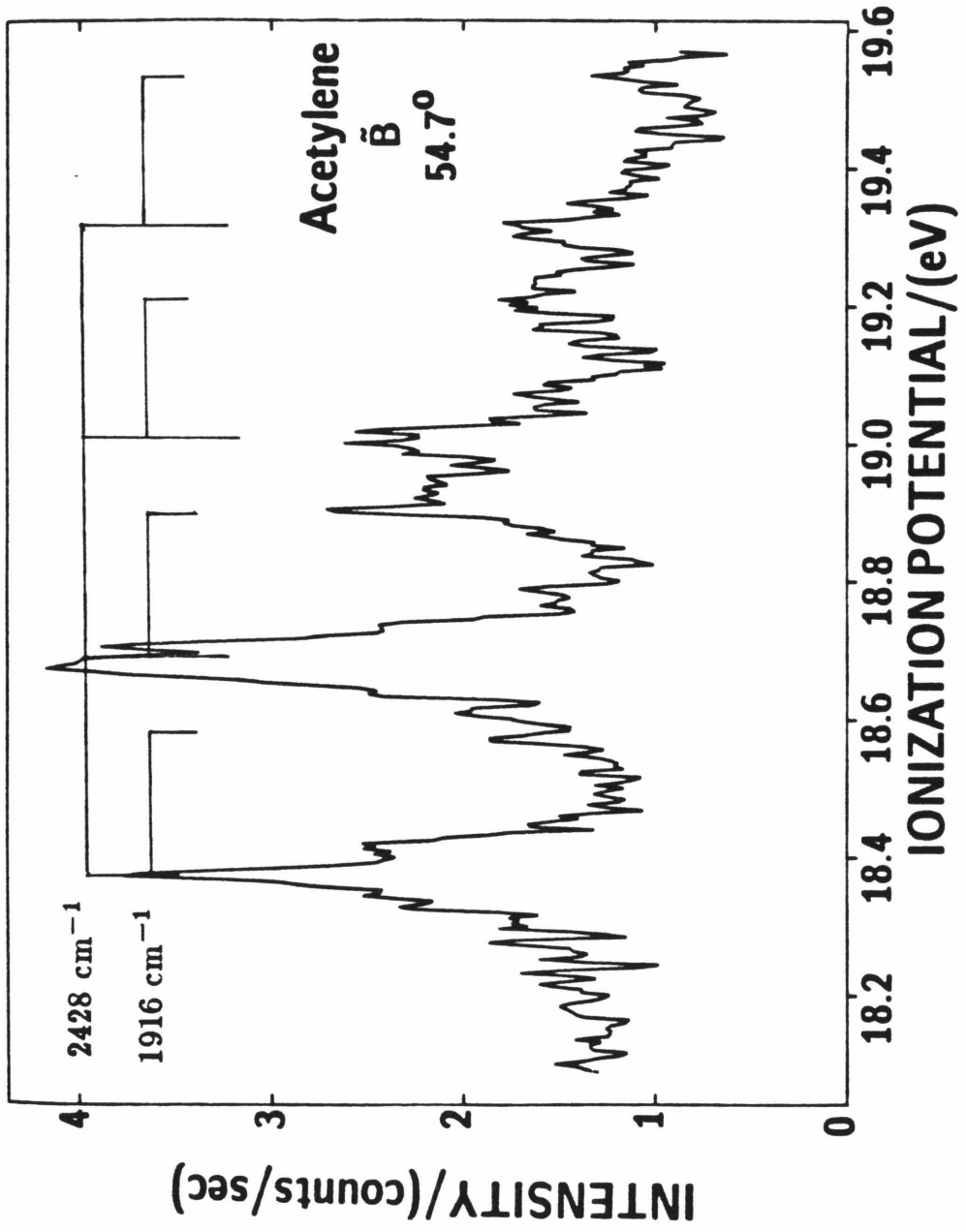
Acetylene
B̃
54.7°
2428 cm⁻¹
1916 cm⁻¹
INTENSITY/(counts/sec)
IONIZATION POTENTIAL/(eV)
0
1
2
3
4
18.2
18.4
18.6
18.8
19.0
19.2
19.4
19.6

FIGURE 6.

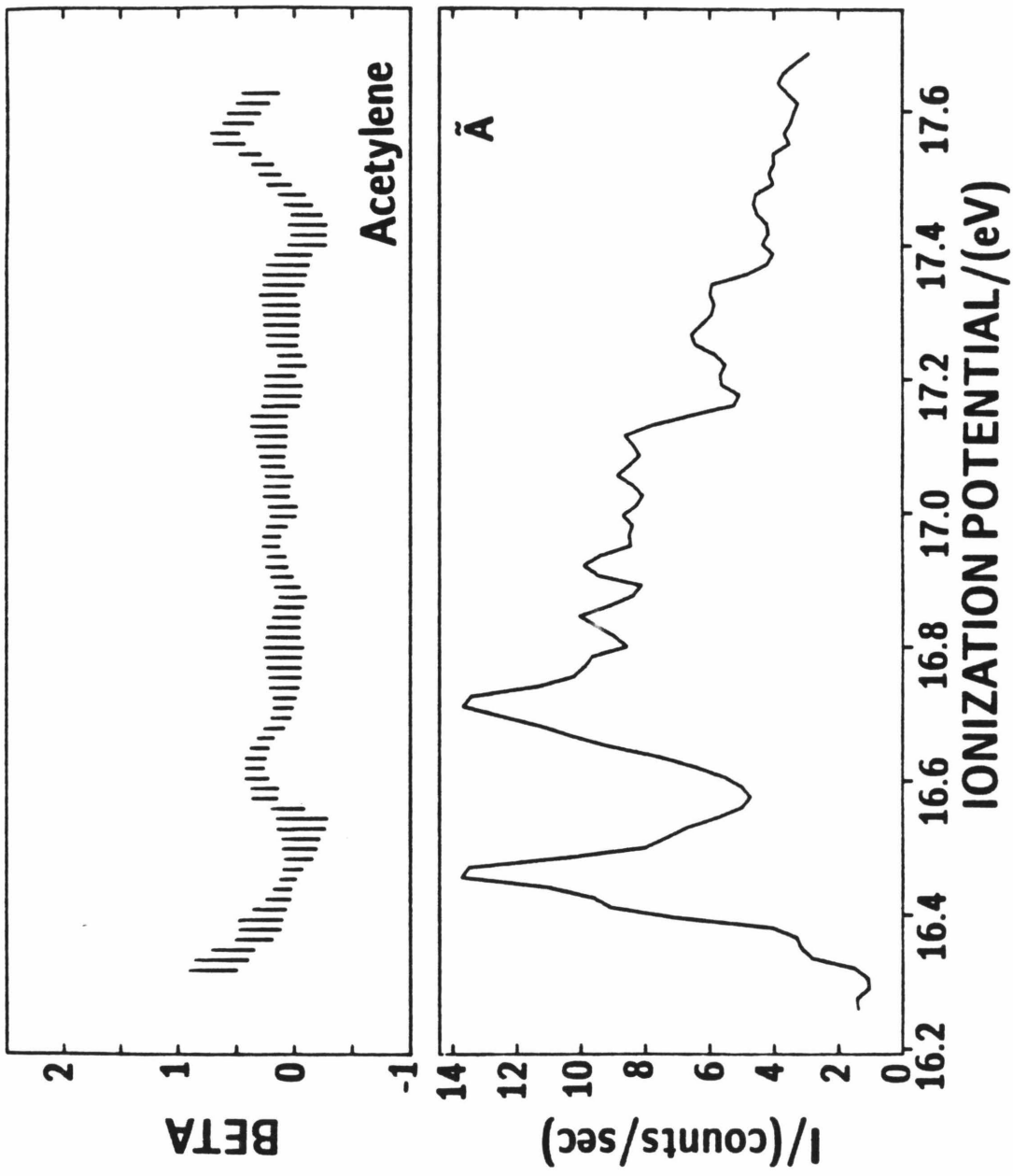
Acetylene
BETA
2
1
0
-1
Ã
I/(counts/sec)
14
12
10
8
6
4
2
0
16.2
16.4
16.6
16.8
17.0
17.2
17.4
17.6
IONIZATION POTENTIAL/(eV)

FIGURE 7.

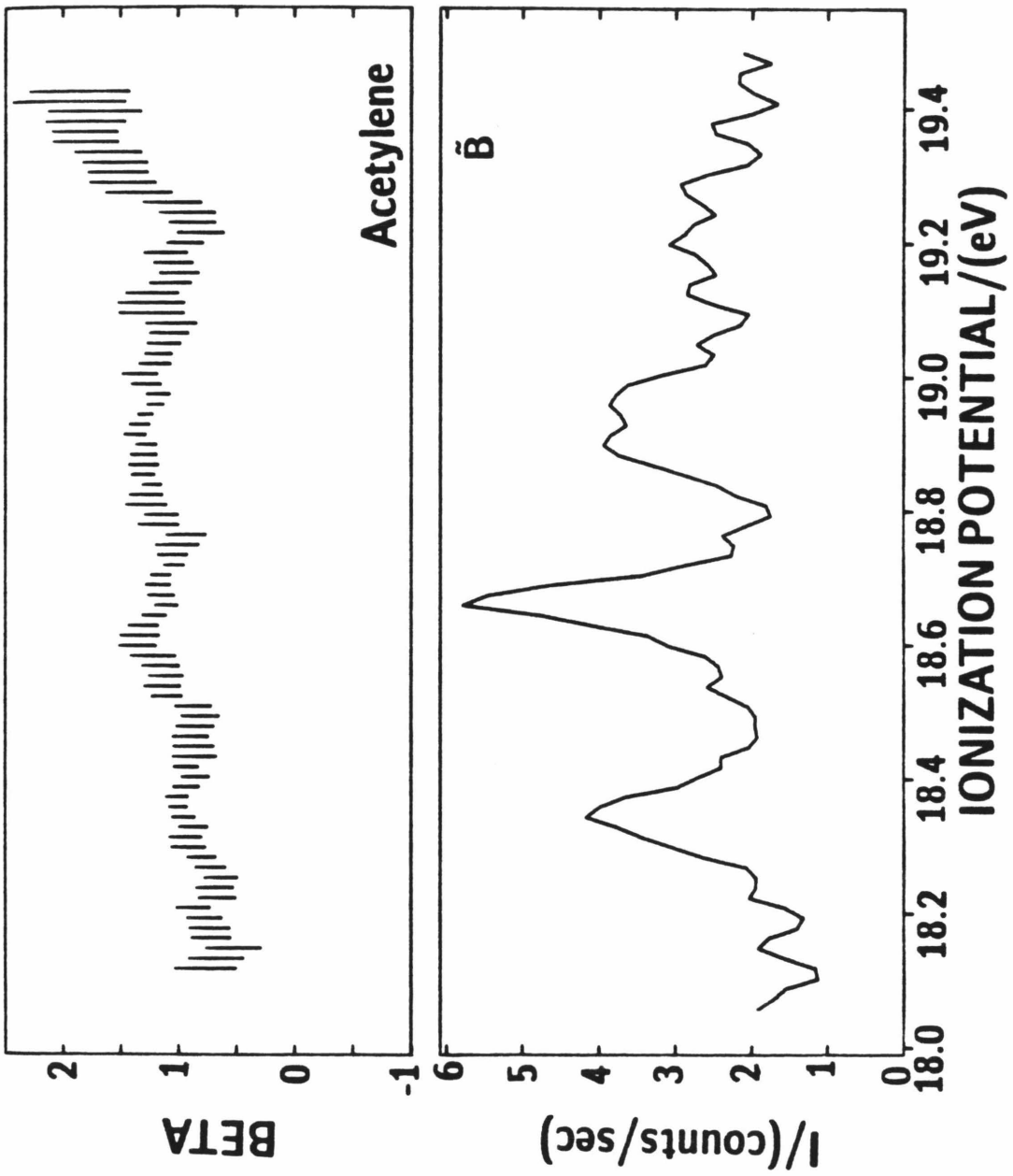
Acetylene
BETA
2
1
0
-1
B̃
I/(counts/sec)
6
5
4
3
2
1
0
18.0
18.2
18.4
18.6
18.8
19.0
19.2
19.4
IONIZATION POTENTIAL/(eV)

FIGURE 8.

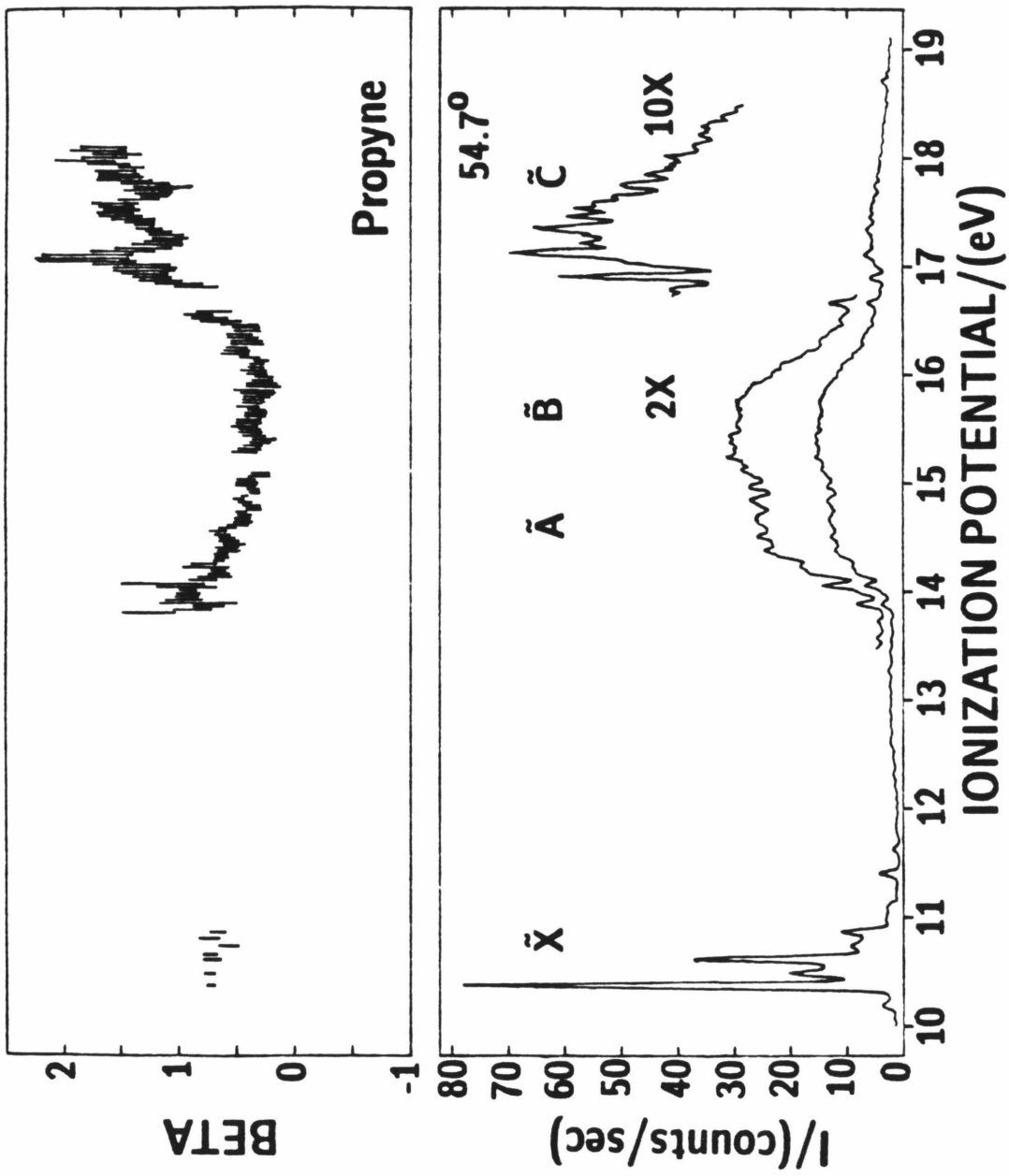
Propyne
BETA
2
1
0
-1
I/(counts/sec)
80
70
60
50
40
30
20
10
0
54.7°
X̃
Ã
B̃
2X
C̃
10X
10
11
12
13
14
15
16
17
18
19
IONIZATION POTENTIAL/(eV)

FIGURE 9.

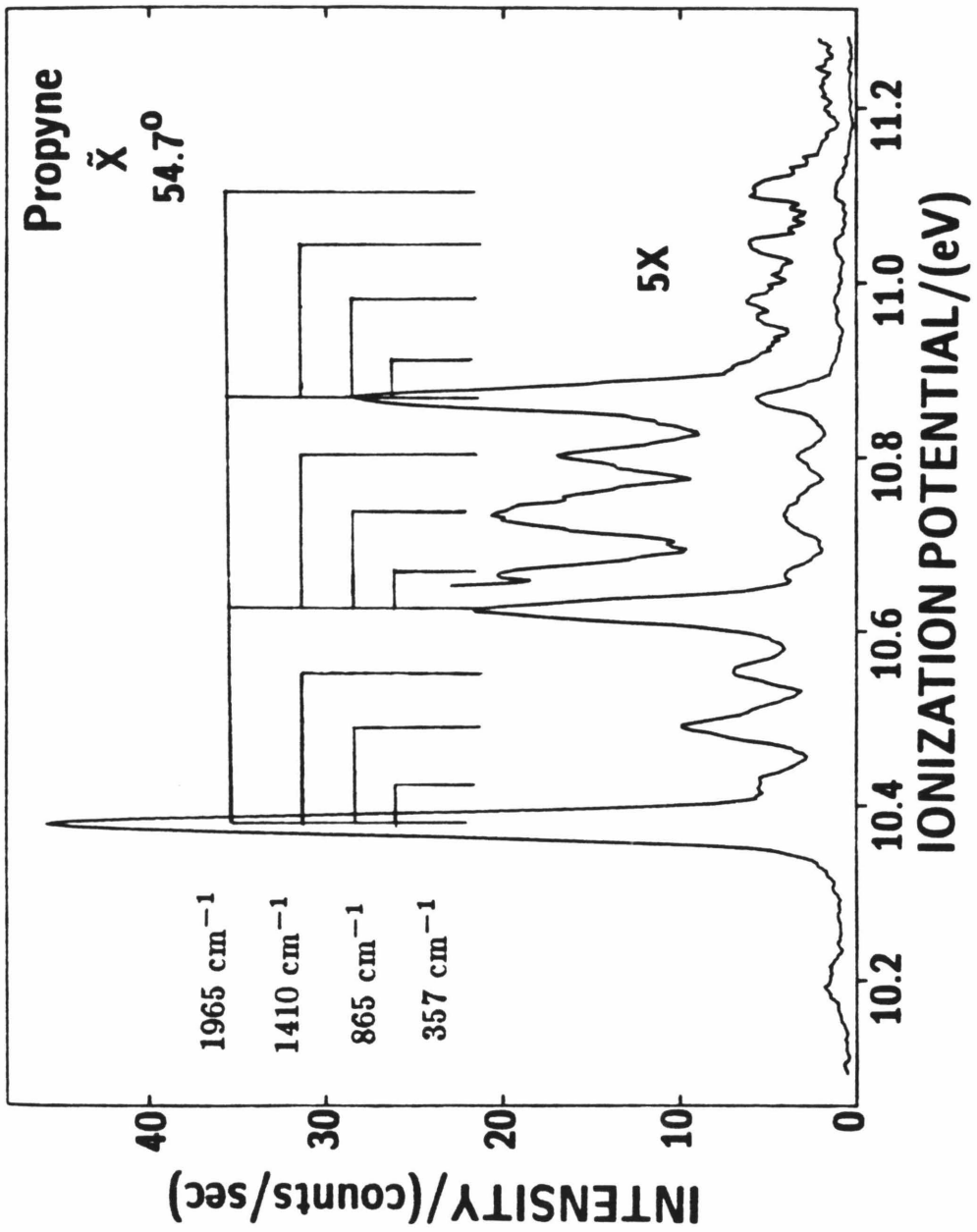
Propyne
$\tilde{X}$
54.7°
5X
1965 cm^{-1}
1410 cm^{-1}
865 cm^{-1}
357 cm^{-1}
INTENSITY/(counts/sec)
0
10
20
30
40
10.2
10.4
10.6
10.8
11.0
11.2
IONIZATION POTENTIAL/(eV)

FIGURE 10.

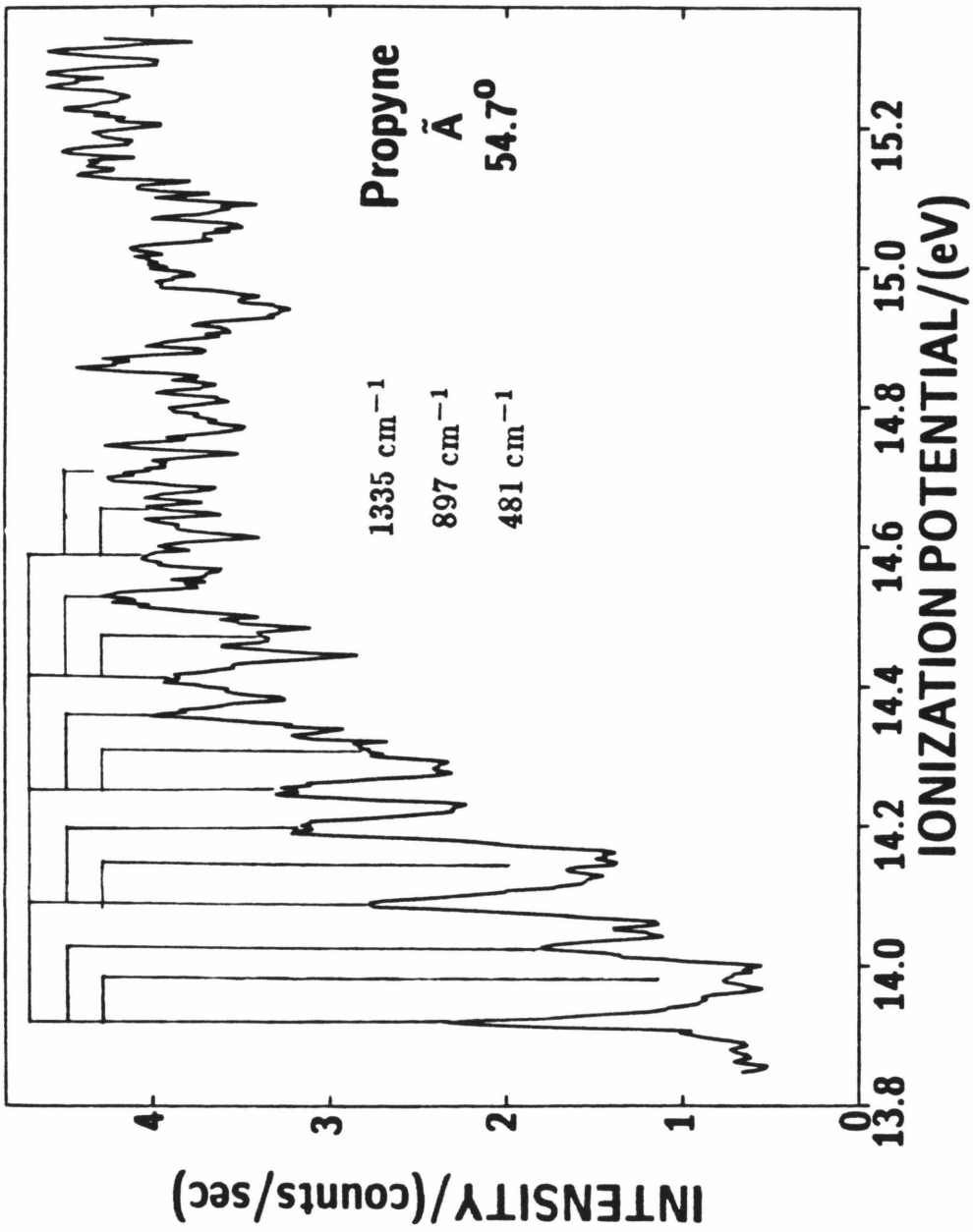
Propyne
Ã
A
54.7°
1335 cm⁻¹
897 cm⁻¹
481 cm⁻¹
INTENSITY/(counts/sec)
IONIZATION POTENTIAL/(eV)
0
1
2
3
4
13.8
14.0
14.2
14.4
14.6
14.8
15.0
15.2

FIGURE 11.

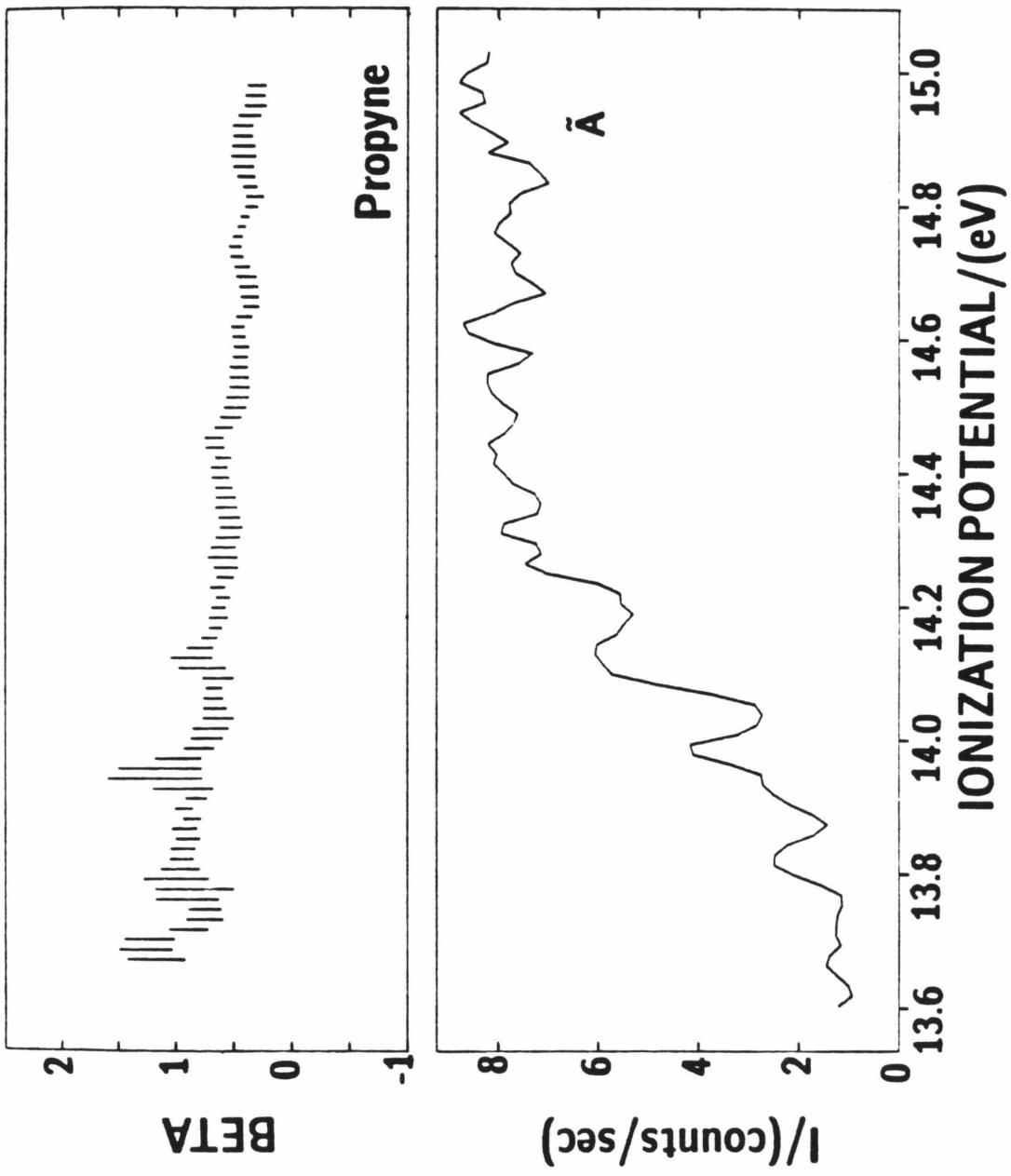
Propyne
BETA
2
1
0
-1
Ã
I/(counts/sec)
8
6
4
2
0
13.6
13.8
14.0
14.2
14.4
14.6
14.8
15.0
IONIZATION POTENTIAL/(eV)

FIGURE 12.

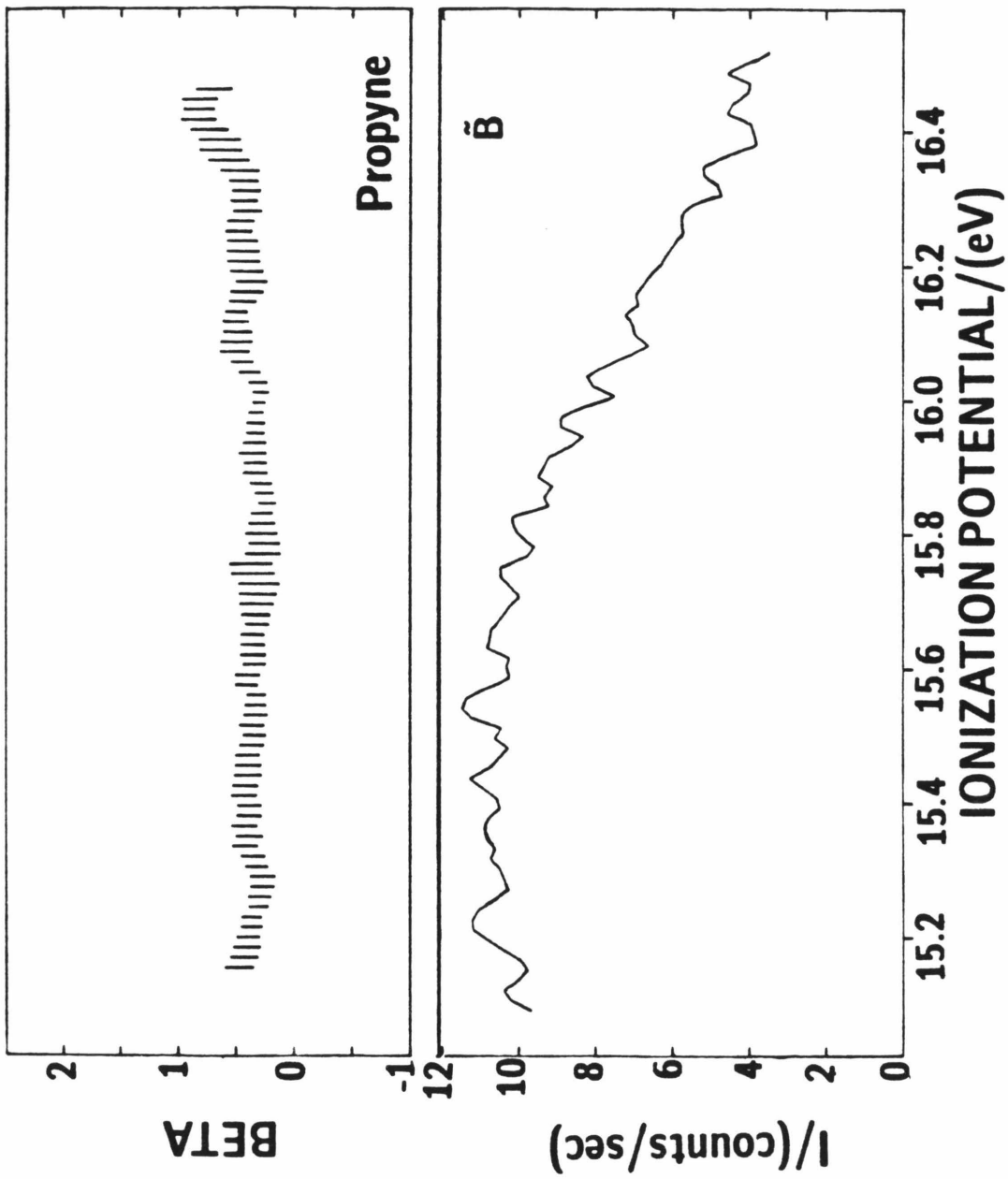
Propyne
BETA
2
1
0
-1
B̃
I/(counts/sec)
12
10
8
6
4
2
0
15.2
15.4
15.6
15.8
16.0
16.2
16.4
IONIZATION POTENTIAL/(eV)

FIGURE 13.

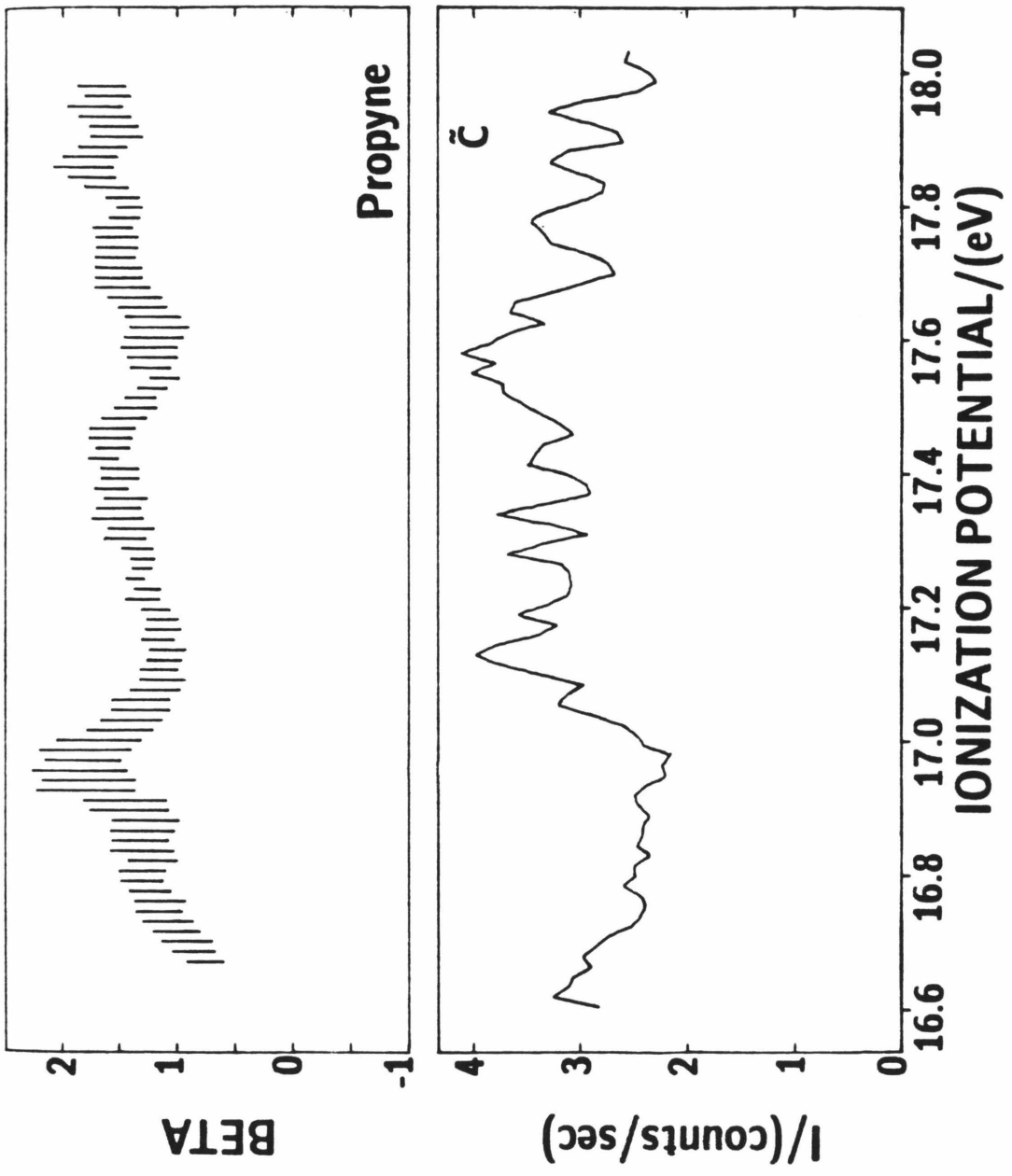
Propyne
BETA
2
1
0
-1
$\tilde{C}$
I/(counts/sec)
4
3
2
1
0
16.6
16.8
17.0
17.2
17.4
17.6
17.8
18.0
IONIZATION POTENTIAL/(eV)

FIGURE 14.

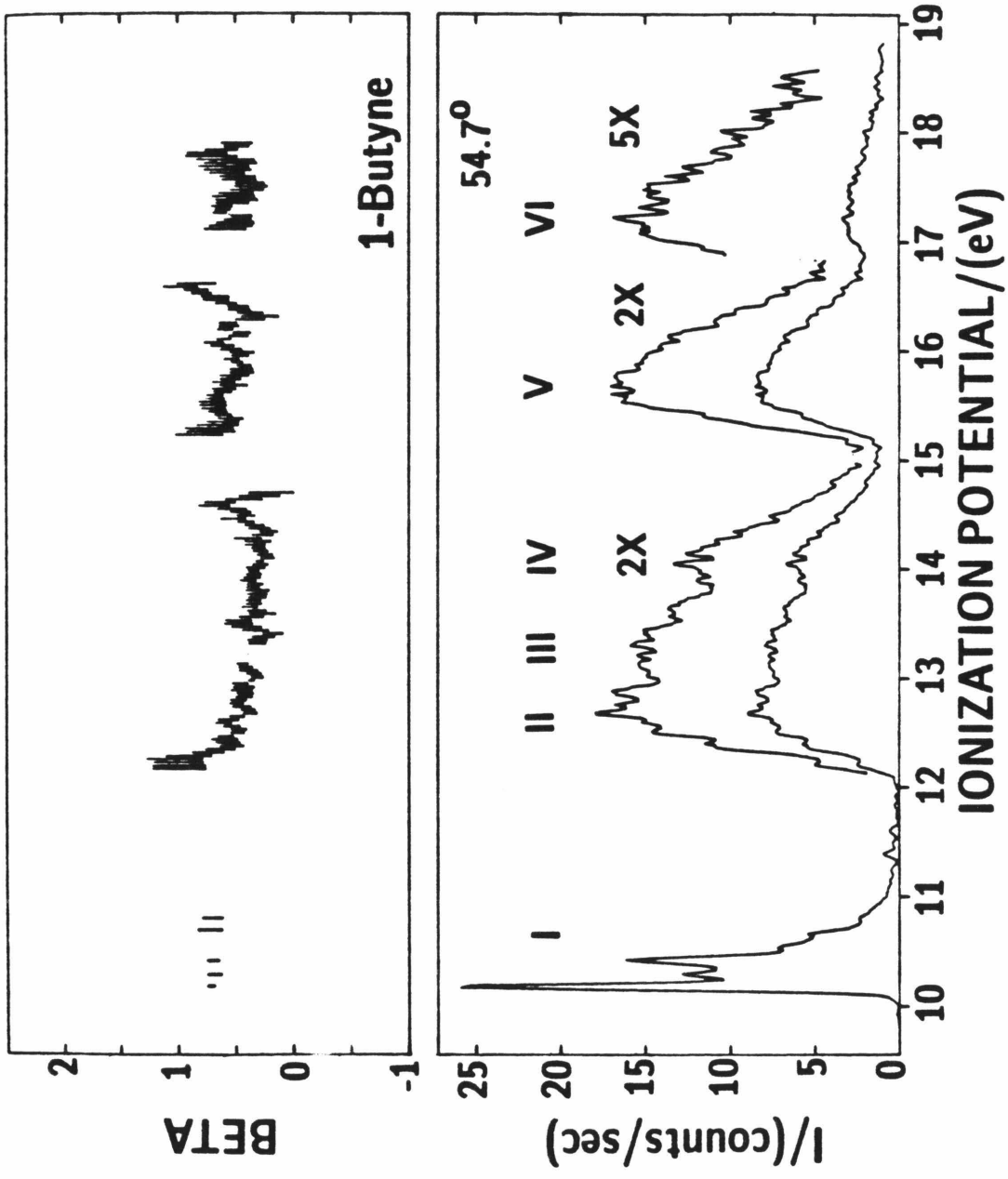
1-Butyne
BETA
2
1
0
-1
I
II
III
IV
V
VI
2X
2X
5X
54.7°
I/(counts/sec)
25
20
15
10
5
0
10
11
12
13
14
15
16
17
18
19
IONIZATION POTENTIAL/(eV)

FIGURE 15.

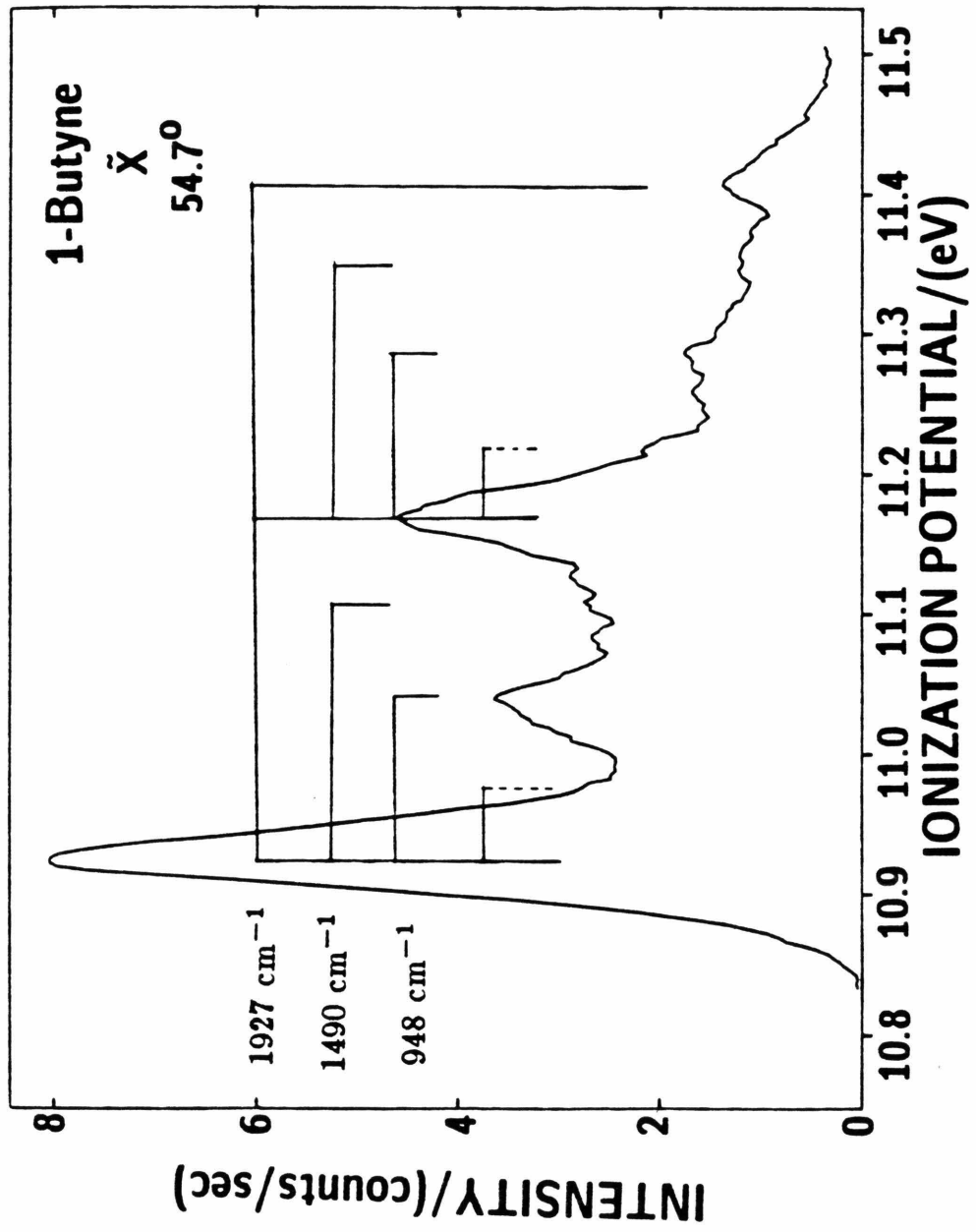
1-Butyne
$\tilde{X}$
54.7°
1927 cm^{-1}
1490 cm^{-1}
948 cm^{-1}
INTENSITY/(counts/sec)
IONIZATION POTENTIAL/(eV)
0
2
4
6
8
10.8
10.9
11.0
11.1
11.2
11.3
11.4
11.5

FIGURE 16.

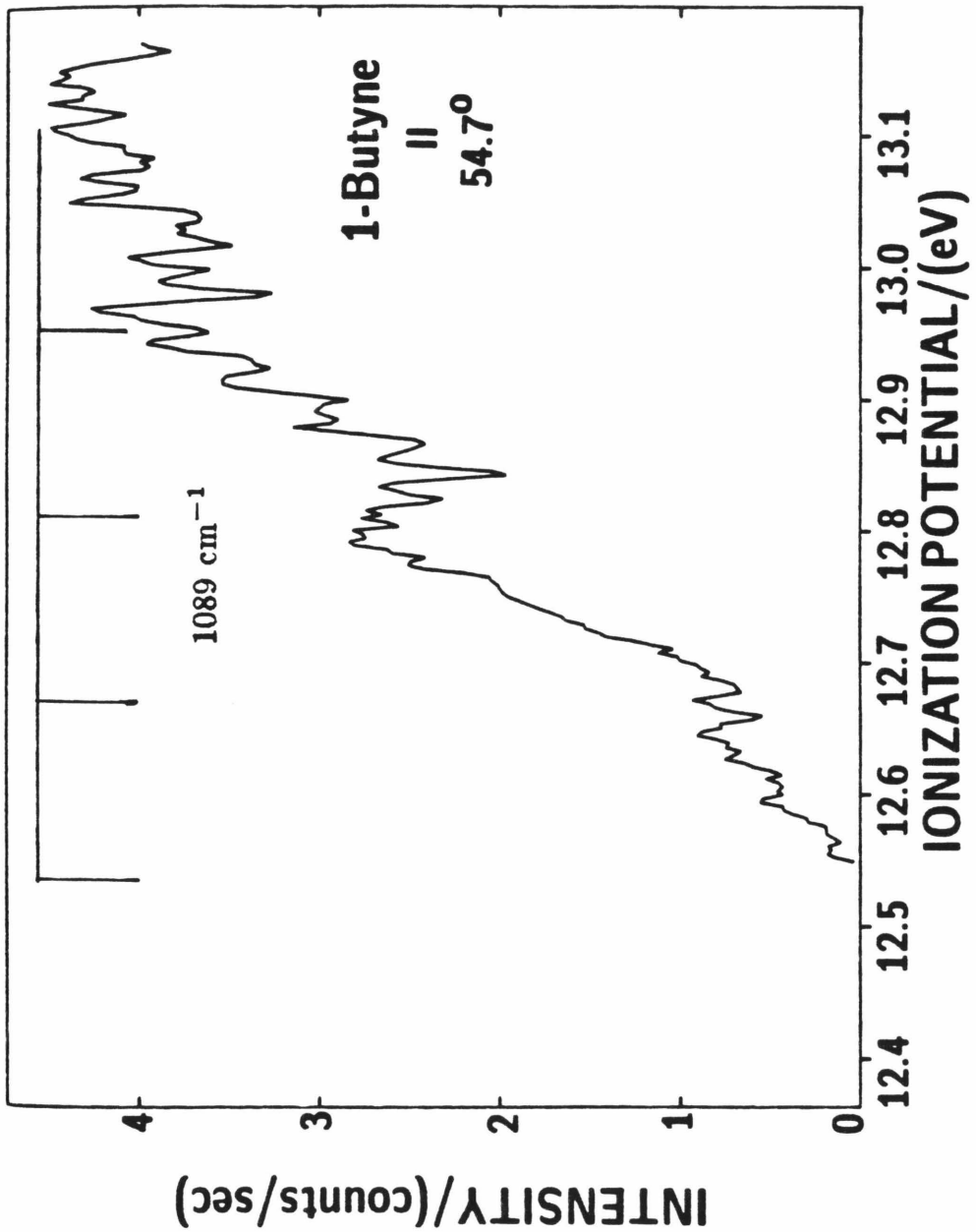
1-Butyne
II
54.7°
1089 cm⁻¹
INTENSITY/(counts/sec)
IONIZATION POTENTIAL/(eV)
0
1
2
3
4
12.4
12.5
12.6
12.7
12.8
12.9
13.0
13.1

FIGURE 17.

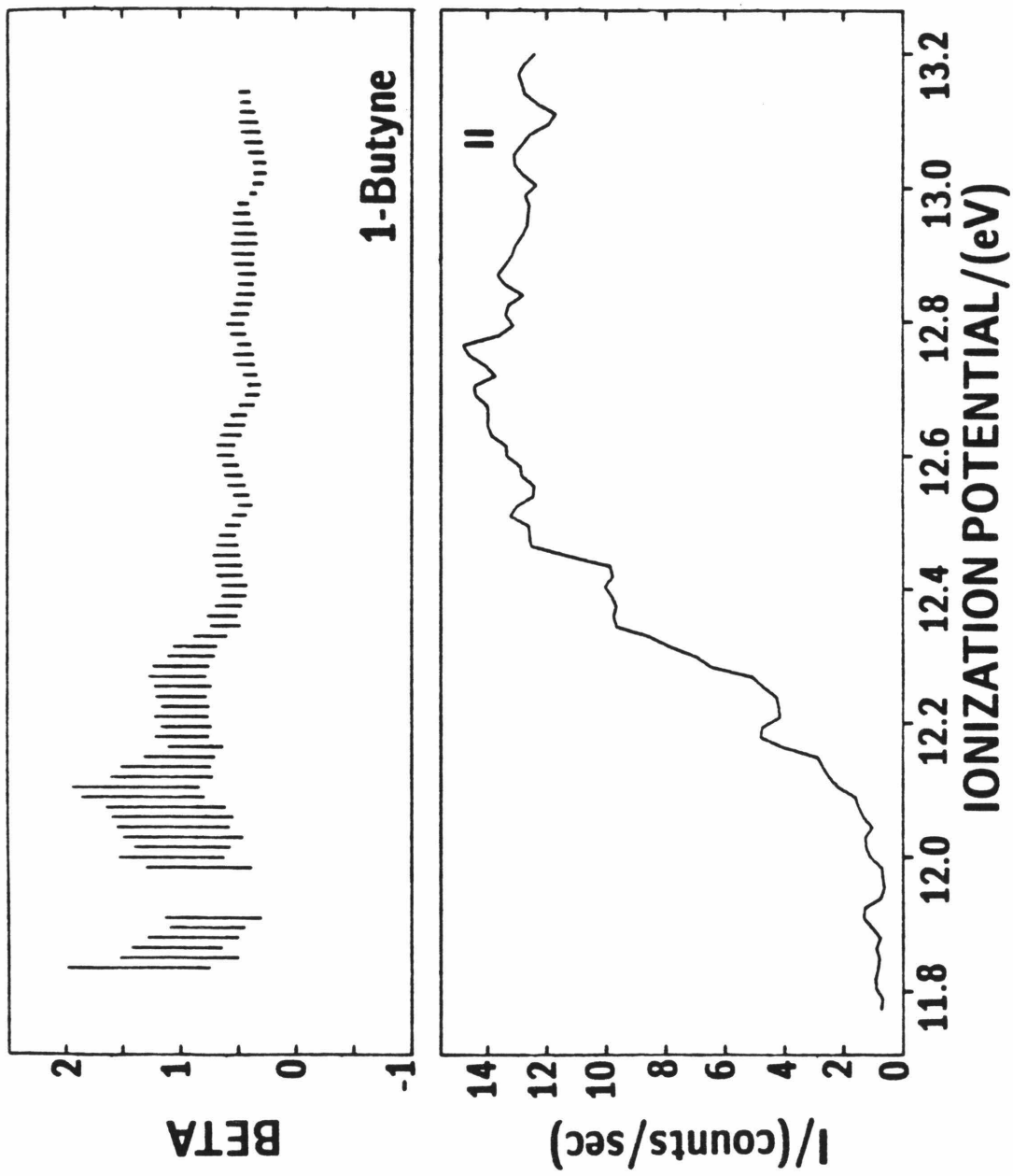
1-Butyne
BETA
2
1
0
-1
II
I/(counts/sec)
14
12
10
8
6
4
2
0
11.8
12.0
12.2
12.4
12.6
12.8
13.0
13.2
IONIZATION POTENTIAL/(eV)

FIGURE 18.

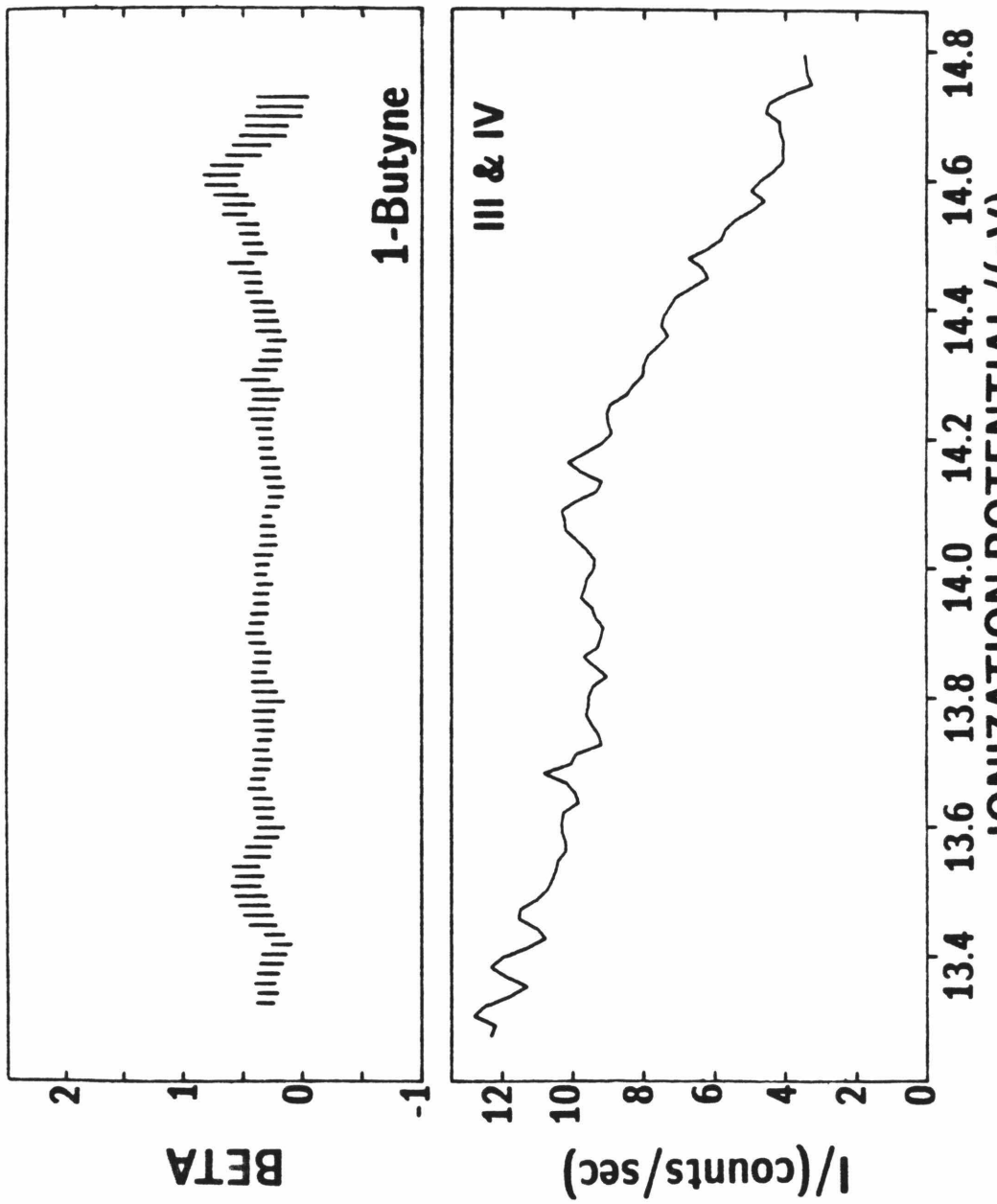
1-Butyne
BETA
2
1
0
-1
III & IV
I/(counts/sec)
12
10
8
6
4
2
0
13.4
13.6
13.8
14.0
14.2
14.4
14.6
14.8
IONIZATION POTENTIAL/(eV)

FIGURE 19.

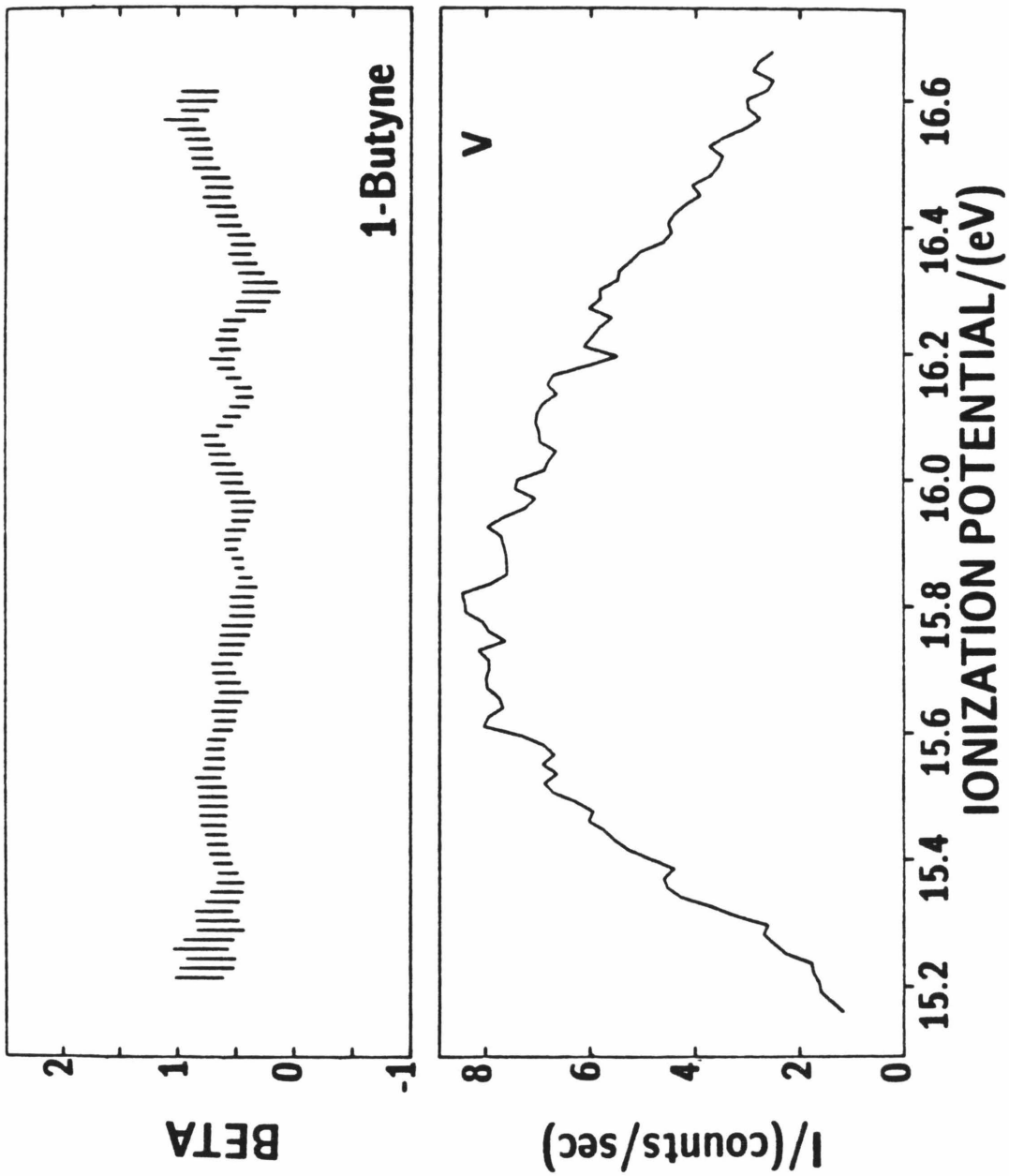
1-Butyne
BETA
2
1
0
-1
V
I/(counts/sec)
8
6
4
2
0
15.2
15.4
15.6
15.8
16.0
16.2
16.4
16.6
IONIZATION POTENTIAL/(eV)

FIGURE 20.

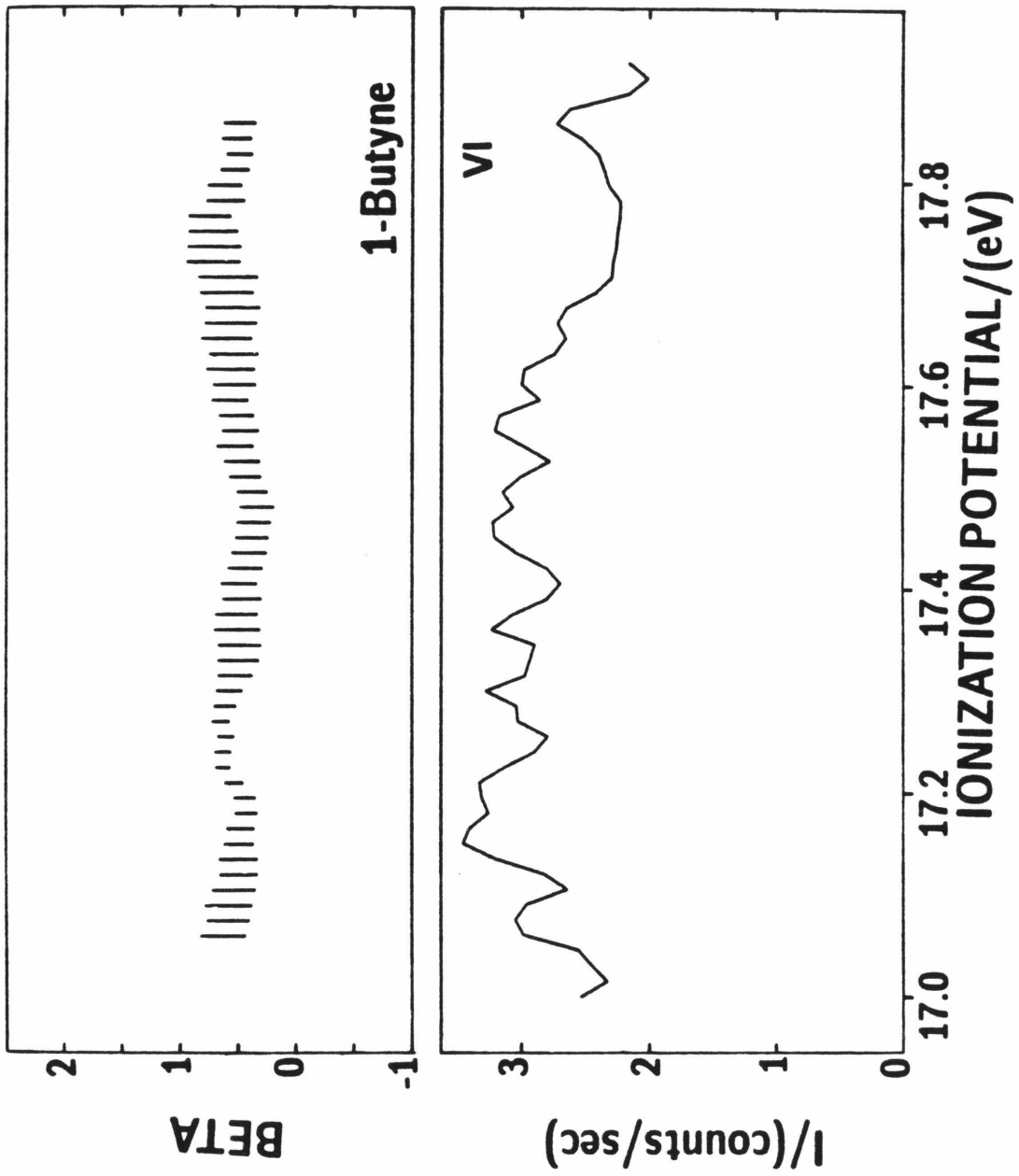
1-Butyne
BETA
2
1
0
-1
VI
I/(counts/sec)
3
2
1
0
17.0
17.2
17.4
17.6
17.8
IONIZATION POTENTIAL/(eV)

FIGURE 21.

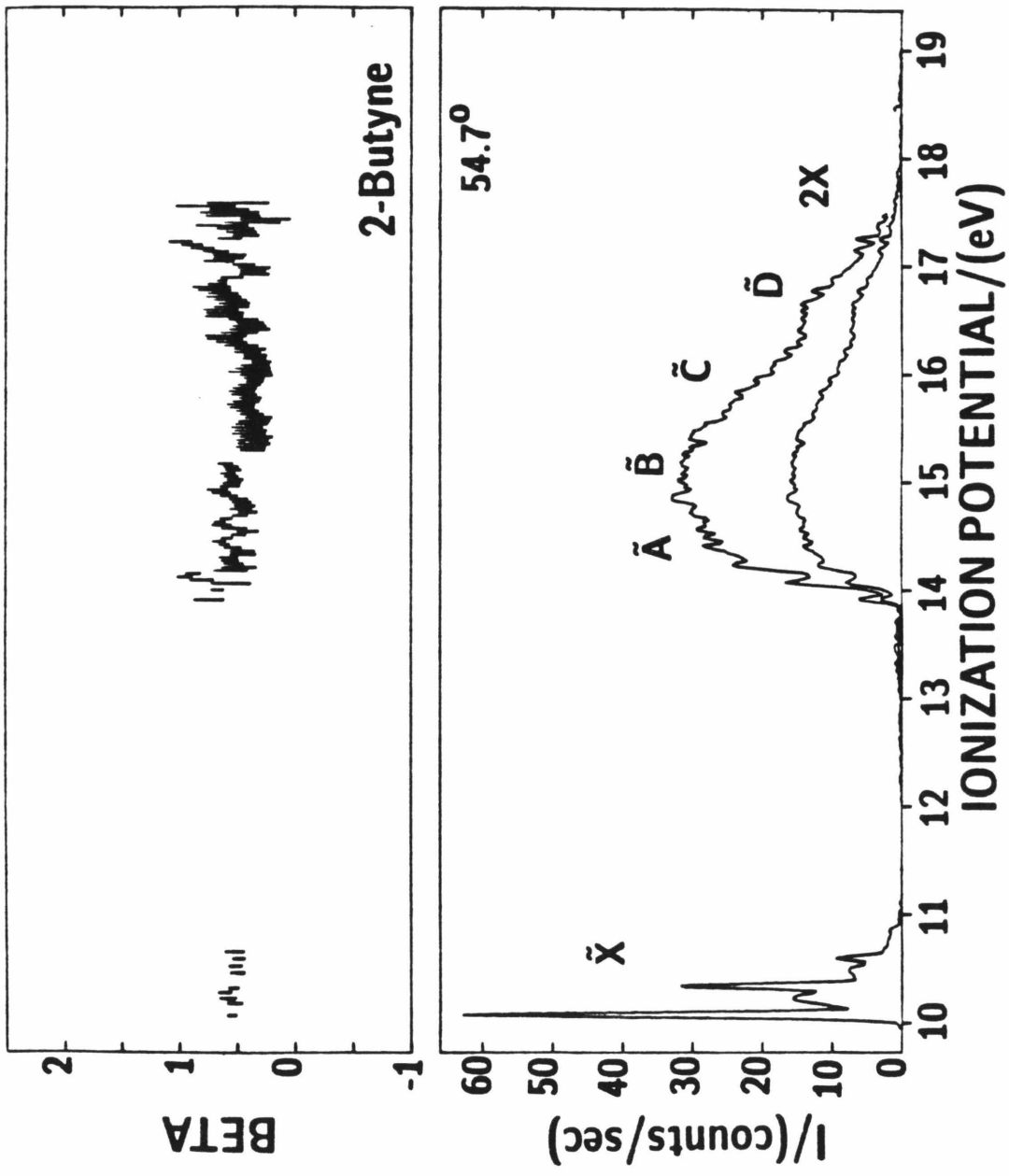
2-Butyne
BETA
2
1
0
-1
54.7°
X̃
Ã
B̃
C̃
D̃
2X
I/(counts/sec)
60
50
40
30
20
10
0
10
11
12
13
14
15
16
17
18
19
IONIZATION POTENTIAL/(eV)

FIGURE 22.

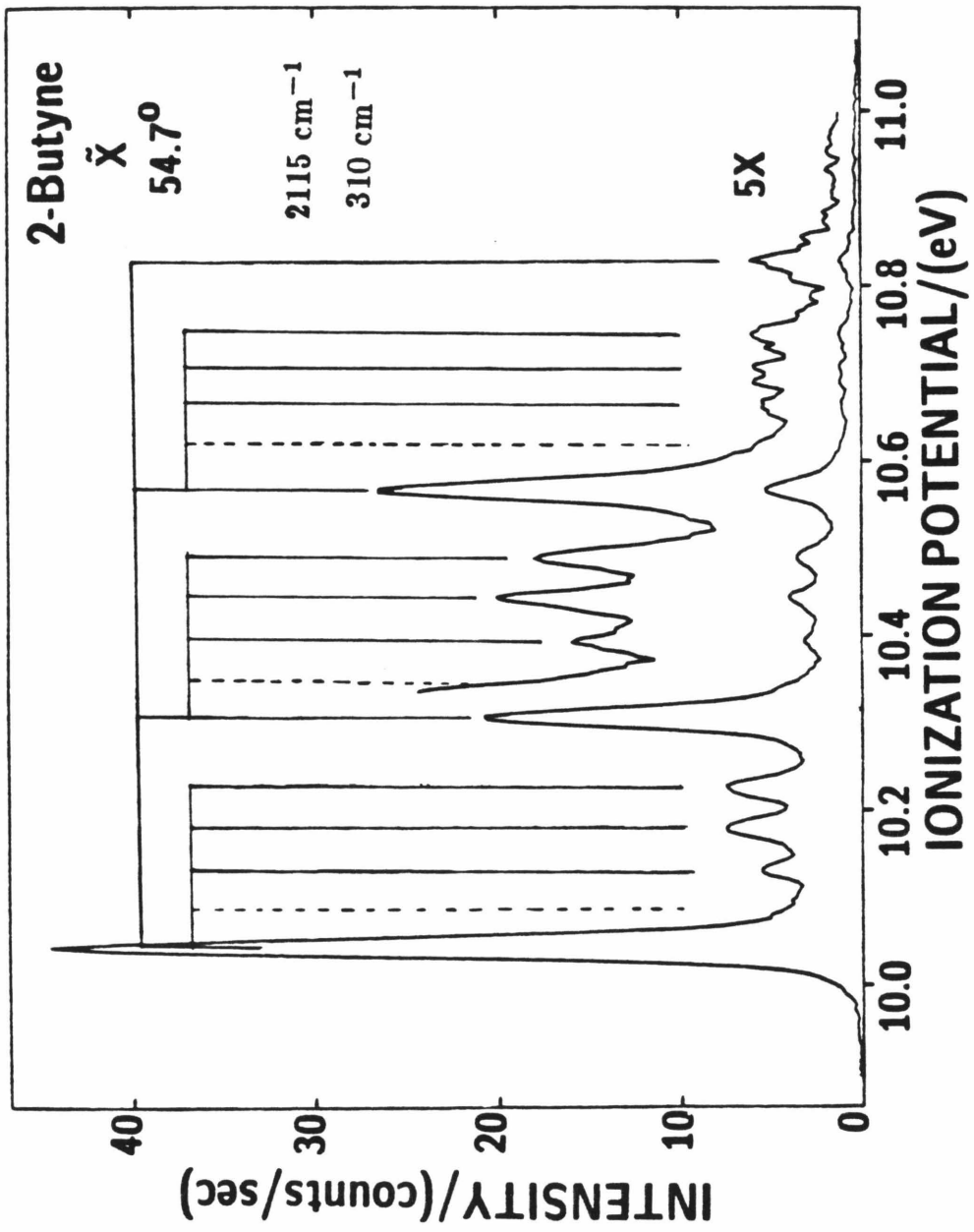
2-Butyne
$\tilde{X}$
54.7°
2115 cm^{-1}
310 cm^{-1}
5X
INTENSITY/(counts/sec)
0
10
20
30
40
10.0
10.2
10.4
10.6
10.8
11.0
IONIZATION POTENTIAL/(eV)

FIGURE 23.

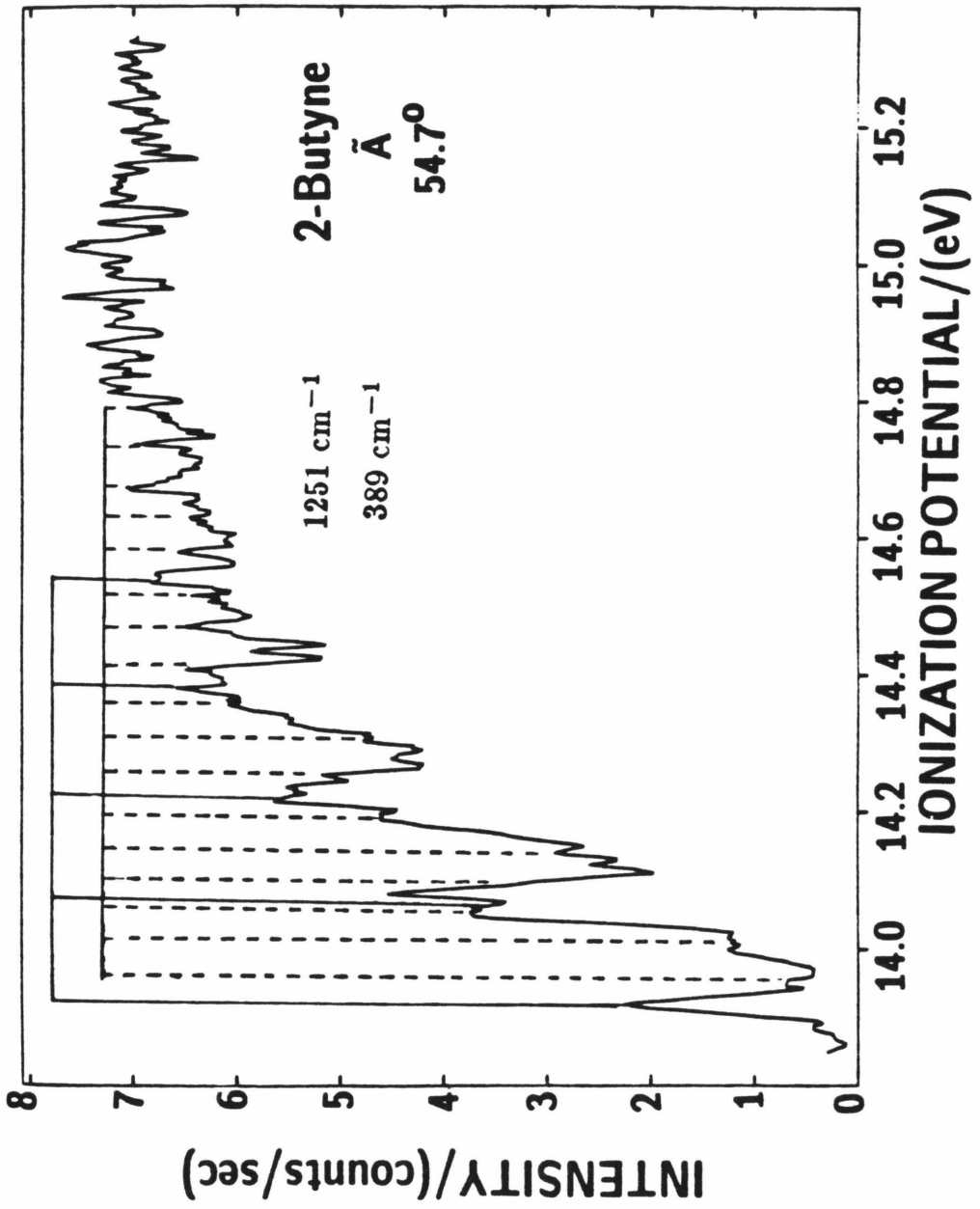
2-Butyne
Ã
54.7°
1251 cm⁻¹
389 cm⁻¹
INTENSITY/(counts/sec)
IONIZATION POTENTIAL/(eV)
0
1
2
3
4
5
6
7
8
14.0
14.2
14.4
14.6
14.8
15.0
15.2

FIGURE 24.

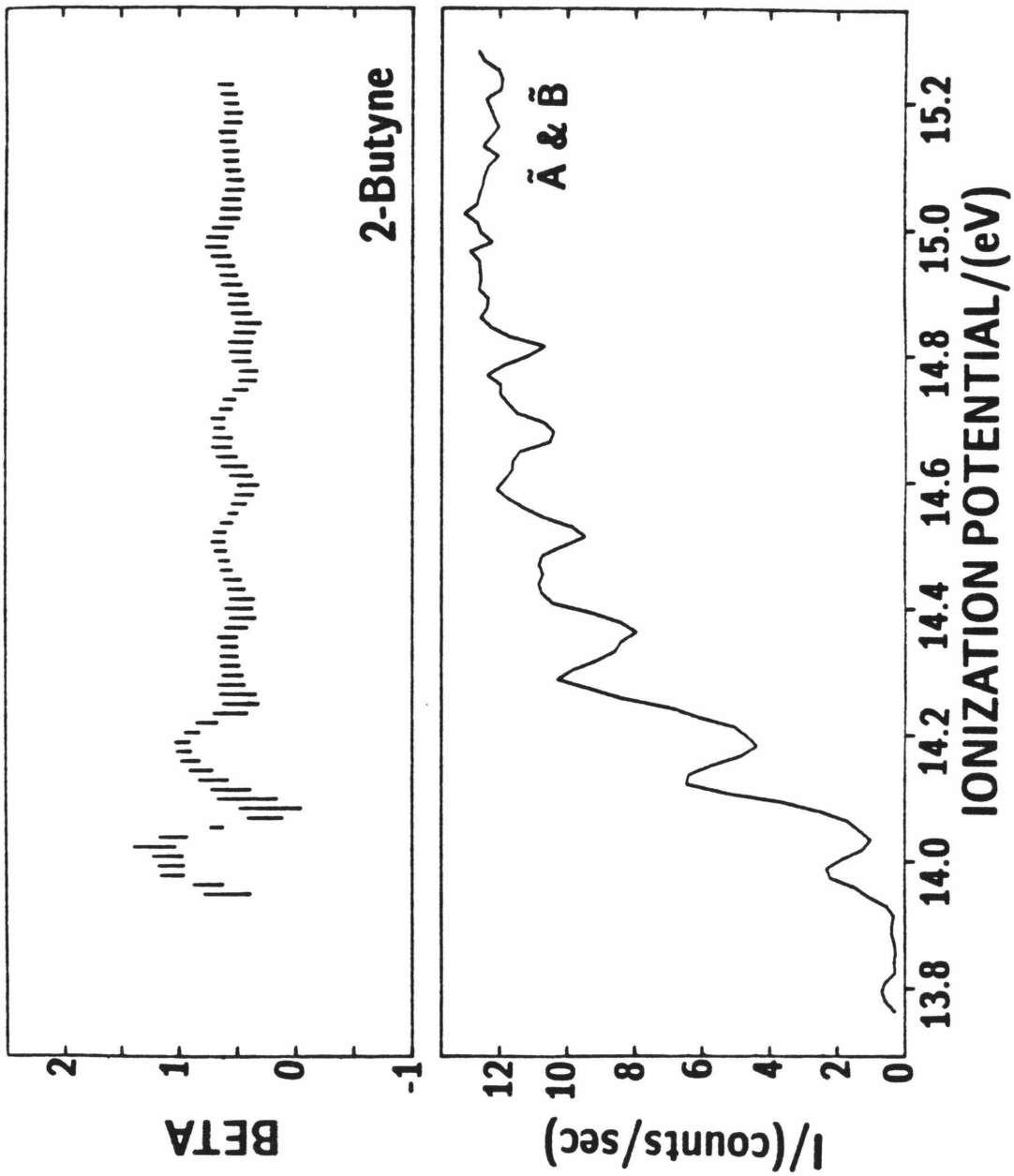
2-Butyne
BETA
2
1
0
-1
Ã & B̃
I/(counts/sec)
12
10
8
6
4
2
0
13.8
14.0
14.2
14.4
14.6
14.8
15.0
15.2
IONIZATION POTENTIAL/(eV)

FIGURE 25.

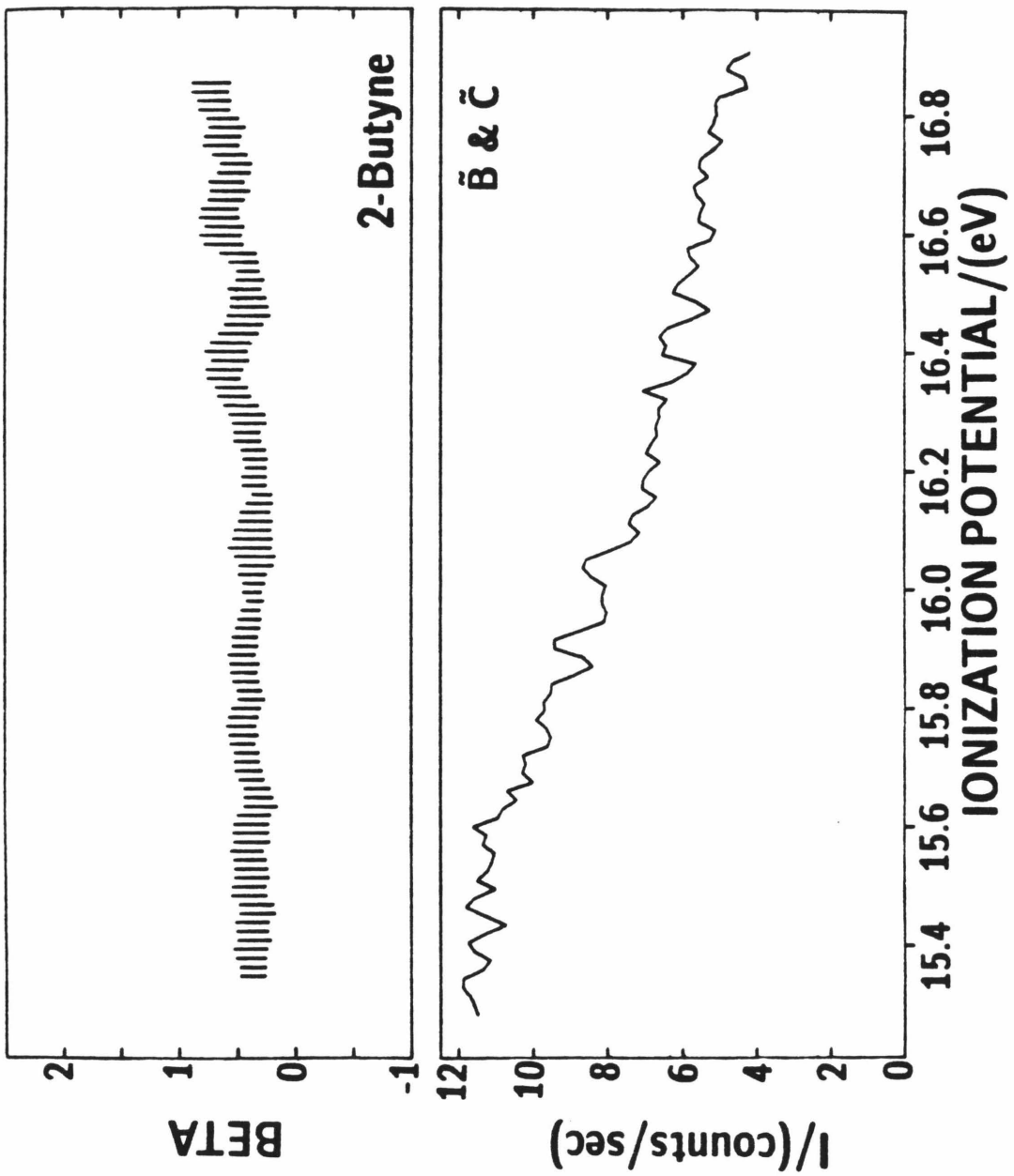
2-Butyne
BETA
2
1
0
-1
B̃ & C̃
I/(counts/sec)
12
10
8
6
4
2
0
15.4
15.6
15.8
16.0
16.2
16.4
16.6
16.8
IONIZATION POTENTIAL/(eV)

FIGURE 26.

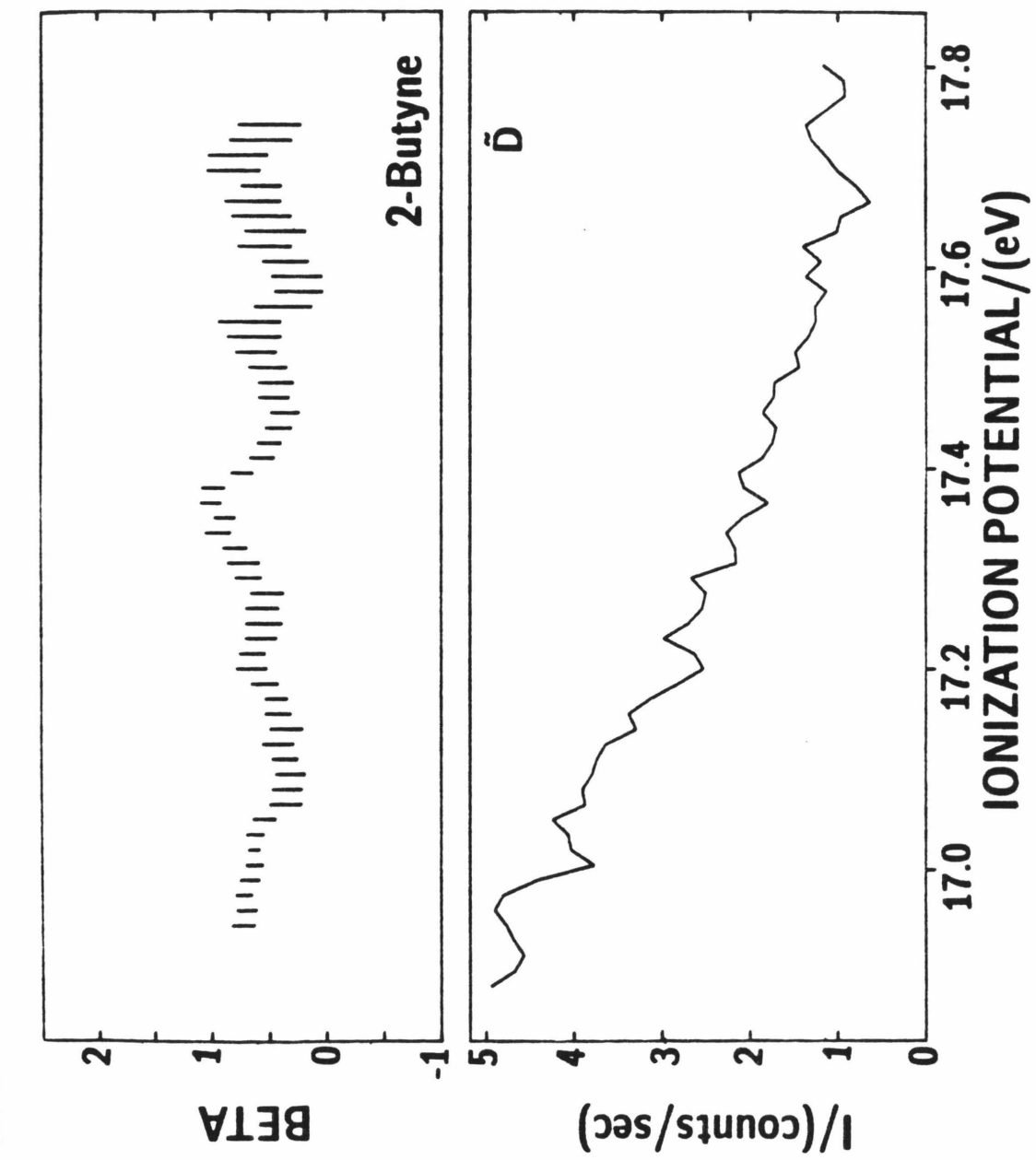
2-Butyne
BETA
2
1
0
-1
D̃
I/(counts/sec)
5
4
3
2
1
0
17.0
17.2
17.4
17.6
17.8
IONIZATION POTENTIAL/(eV)

CHAPTER 6

RESULTS AND DISCUSSION

Paper 2: The Angular Resolved Photoelectron Spectroscopy of Formaldehyde, Acetaldehyde, and Acetone.

The Angular Resolved Photoelectron Spectroscopy of Formaldehyde, Acetaldehyde, and Acetone[a]

D. J. Flanagan[b] and A. Kuppermann

Arthur Amos Noyes Laboratory of Chemical Physics,[c]

California Institute of Technology, Pasadena, CA 91125

(received)

Abstract

Photoelectron angular distributions have been measured for formaldehyde, acetaldehyde, and acetone using He I radiation. The asymmetry parameters of acetaldehyde and for all but the first band of acetone are presented here for the first time. The bands of these molecules are discussed in terms of the anisotropy parameter, substituent effects and other experimental and theoretical criteria.

---

[a] This work was supported in part by the U. S. Department of Energy, Contract No. DE-AM03-F00767, Project Agreement No. DE-AT03-76ER72004.

[b] Work performed in partial fulfillment of the requirements for the Ph.D degree in Chemistry at the California Institute of Technology.

[c] Contribution No.

1. INTRODUCTION

This study continues the work of this group in the "chemical scanning" of chromophores, that is, examining the effects of substituents on the principal chromophore of a series of homologous molecules. Previous studies have been made with the halogenated and methylated ethenes,[1-4] alkylated ethynes[5] and the heterosubstituted three and five membered rings.[6,7]

Measurement of the angular distributions of the photoelectrons of atoms and molecules has proven useful in examining the symmetry, energy and bonding characteristics of the orbitals from which the electron is photoionized, information that cannot be derived from the fixed angle photoelectron spectrum alone.[8-11]

Experimentally, this process involves the use of He I radiation at 584 Å to ionize valence electrons. The energetics of this process are described by $\hbar\omega = IP + KE$, where $\hbar\omega$ is the photon energy, IP, the ionization potential, and KE, the kinetic energy of the photoejected electron. By Koopmans' theorem,[12] the ionization potential is equal to the negative orbital energy, $IP = -E$.

The angular distribution of the photoelectrons generated by the interaction of unpolarized radiation with a randomly oriented sample can be expressed in terms of the differential cross section, $\frac{d\sigma}{d\Omega}$, as follows,[13-15]

$$\frac{d\sigma}{d\Omega} = \frac{\sigma_{TOT}}{4\pi}[1 - 1/2\beta P_2(\cos\theta)]$$

where $P_2(\cos\theta)$ is the second order Legendre polynomial, σ_{TOT} is the

total ionization cross section for a photon with energy $\hbar\omega$ to eject an electron from a molecule in a given initial state to produce a given final state, θ is the angle between the velocity vector of the ejected electron and the incident photon beam, and β is the asymmetry or anisotropy parameter for the state-to-state process being considered. Since the cross section must be positive, β is constrained to values between -1 and 2.

In this study the results of measurements of the asymmetry parameter for formaldehyde, acetaldehyde, and acetone are presented, the homologous series which permits an assessment of the effects of methylation on the carbonyl chromophore. The angular distributions of formaldehyde have been examined previously by Keller and coworkers[16] using synchrotron radiation and the $\tilde{X}$ band of acetone has been measured by Kobayashi;[17] however, this is the first unified treatment of this series, planned to obtain from the asymmetry parameters information on the bonding and other characteristics of the orbitals of these molecules.

2. EXPERIMENTAL

The variable angle photoelectron spectrometer used for this study is described elsewhere in detail.[18] A block diagram of the apparatus is given in Figure 1. Briefly the radiation source consists of a He I discharge lamp which ionizes sample vapors contained within a cylindrical scattering chamber. The sample vapor pressures are typically of the order of a few millitorr in this region. The electrons ejected from the sample are

energy analyzed by means of a 6.8 cm radius hemispherical electrostatic analyzer. Both the analyzer and the electron multiplier are mounted on a rotatable gear. Spectra are recorded at nine angles between 45 and 120 degrees with respect to the beam of incident photons.

The ambient magnetic field in the photon-molecule interaction region has been reduced to less than 0.2 mgauss by lining the vacuum chamber with mu metal and by the use of three pairs of orthogonal Helmholtz coils. This shielding is sufficient to prevent distortions in the angular distributions by deflections of the relatively slow electrons that would otherwise result from the presence of these fields.

The background has been systematically parameterized by a least squares fit to a fifth order polynomial and subtracted from the spectra. The resolution for the spectra used in the angular distribution measurements was between 40 to 50 meV. The fixed angle spectra used to determine vibrational structure had higher resolution, in the 15 to 20 meV range. The resolution was measured as the full width at half maximum of the $Ar^+ {}^2P_{3/2}$ line, which also provided the energy calibration for the spectra. The accuracy of the β measurements was determined by the apparatus' ability to consistently reproduce a $\beta = 0.88 \pm .02$ for $Ar^+ {}^2P_{3/2}$ which has been determined in several laboratories independently.[13–23]

All samples were obtained from commercial sources. Acetone (Mallinckrodt 99.5%) and acetaldehyde (Baker 99+%), liquids at room temperature, were thoroughly degassed by several freeze-pump-thaw cycles. Acetone was then vacuum distilled before utilization. To prevent

the formation of a polymeric condensate, acetaldehyde was not vacuum distilled. Formaldehyde was generated by continuous pyrolysis of paraformaldehyde (Celanese 91-93%) at moderate temperatures ($\sim$ 60° C); the temperature was regulated to produce a constant vapor pressure of approximately 2 millitorr within the sample scattering chamber. The paraformaldehyde was prepared by first grinding the sample into a fine powder, which was carefully degassed at room temperature. The sample was then continuously pumped under pyrolysis conditions, except for periodic monitoring of the photoelectron spectrum for the presence of H_2O, which is the principal contaminant. Sample pumping was discontinued when the H_2O $\tilde{X}$ peak at 12.6 eV was minimized. It should be noted that due to the nature of paraformaldehyde it is not possible to totally prevent the presence of water vapor since it is incorporated into the condensate. However, the height of the H_2O $\tilde{X}$ band which is the most intense is only 1-2% of the height of the $\tilde{X}$ $\nu = 0$ formaldehyde band and no other water bands can be discerned. The presence of extra bands due to contaminants was not observed in acetone and acetaldehyde.

3. RESULTS AND DISCUSSION

3.1 Formaldehyde

The photoelectron spectrum of formaldehyde, Figure 2, reveals four bands accessible to He I radiation. The first three of these bands possess resolvable vibrational structure while the vibrational structure of the fourth band is partially resolvable. A high resolution spectrum, Figure

3, of the first band, $\tilde{X}\ ^2B_2$, whose vertical and adiabatic ionization potential is 10.89 eV, arises from ionization of the essentially nonbonding O $2b_2$ orbital.[24] This band shows the presence of all three symmetric vibrational modes of this molecule:[25,26] ν_1, C-H stretch at 2580 cm^{-1}, ν_2 C-O stretch at 1610 cm^{-1}, and ν_3 HCH bend at 1190 cm^{-1}; however, all modes are only weakly excited.

The high resolution spectrum, Figure 4, of the second band $\tilde{A}\ ^2B_1$ has a vertical ionization potential of 14.40 eV and an adiabatic ionization potential of 14.10 eV. This band, which also has well-resolved structure consisting of an envelope of weakly split doublets, originates from ionization of the C-O π bonding orbital $1b_1$,[24] where the maximum of the band falls on the third doublet. The principal progression results from excitation of the ν_2 stretching mode (1190 cm^{-1}) expected to be present on this band. The splitting is the result of excitation of overtones of ν_3 vibrational quanta (1385 cm^{-1}), which, for this band, is nearly degenerate with ν_2, the separation becoming more pronounced with higher ionization potential as more anharmonicity is present in the ν_2 spacing. This structure is consistent with the interpretation of Cederbaum and Domke.[27,28]

There had been in the past literature a dispute over the identification of the orbitals corresponding to the third and fourth ionization bands. Initially the assignment of Turner *et al.*[29] was $1b_2$ and $5a_1$ respectively for these two orbitals; however, subsequent experimental and

theoretical work support the reverse order.[e.g.,24,27,28,30,31] These include an (e,2e) electron impact coincidence study by Hood *et al.*[31] and a very elegant many body Green's Function study by Cederbaum *et al.*[27,28] Additionally, comparing the beta values of the third, $5a_1$, band to those of the 5σ orbital in CO,[10] lends credence to this ordering and it is this ordering that will be used in the present study.

The third band, $\tilde{B}\ ^2A_1$, with an adiabatic ionization potential of 15.82 eV, and a vertical ionization potential of 15.98 eV, derives from the ionization from a $5a_1$ orbital, which is a delocalized orbital predominantly C-H bonding and slightly C-O σ bonding.[24] Like the $\tilde{A}$ band it shows a strongly excited ν_2 progression at approximately 1248 cm^{-1}. This band overlaps extensively with the fourth band ($\tilde{C}\ ^2B_2$) due to ionization of a $1b_2$ electron which has C-O π bonding characteristics. This fourth band has an only partially resolvable progression in ν_3 at a frequency of 1416 cm^{-1}. This progression gives an approximate upper limit of 16.21 eV for the adiabatic ionization potential of this last band. The high resolution spectrum of both of these bands is shown in Figure 5. Without a detailed Franck-Condon analysis of the vibrational states it is not possible to precisely determine the vertical ionization potential of the $\tilde{C}$ band because of the near coincidences in some of the vibrational lines of the $\tilde{B}$ and $\tilde{C}$ bands; however, a reasoned consideration of the band shapes and the Franck-Condon envelope of the $\tilde{B}$ band yields 16.76 eV as a best estimate under these circumstances.

The vibrational frequencies measured for this molecule agree well with those determined by Turner *et al.*[29] The ionization potentials and vibrational frequencies of this molecule determined by this work and other work[24–27,29,30,32–35] are summarized in Table 1.

The asymmetry parameters calculated for this molecule are displayed over the full spectrum in Figure 2. These values are summarized in Table 2 where values determined by other workers[16] are also presented.

The beta values for the $\tilde{X}$ band are independent of vibrational quantum and equal 0.31. This is slightly higher than the value of Keller and coworkers[16] at 0.27 but within experimental error of it. These values are read off from plots of beta versus photon energy (since their values were from a study use synchrotron radiation) and hence are only approximate.

The $\tilde{A}$ band beta values are also independent of vibrational quantum number having a mean value over the band of 0.72 , which is higher than the value of Keller *et al.*[16] at 0.62.

Bands $\tilde{B}$ and $\tilde{C}$ overlap; therefore it is reasonable to assume that the beta values, especially in the region of greatest overlap, reflect contributions from both orbitals. It is seen that the beta values for the $\tilde{B}$ band rise from lower values on the first few peaks where the contribution of the $\tilde{C}$ band is nonexistent, or of very low magnitude, to higher values on the latter peaks where the $\tilde{C}$ band contribution is more substantial. Also present is an extension of the oscillatory behavior that is exhibited

in the beta values across the $\tilde{C}$ band. Such undulations are frequently observed in the angular distributions of continuous structureless, or nearly structureless, features. The mean value over the oscillations is very close to the vertical beta value of 0.54 with a very slight decline in beta observed with increasing ionization potential over the range of the band. An average value of the $\tilde{B}$ band may be determined from the first few peaks to be approximately 0.49.

This value of beta for the $\tilde{B}$ band compares favorably with Keller *et al.*[16] results of 0.52; however, our value for the $\tilde{C}$ band is again higher, 0.54 vs. 0.42, although this disagreement is not unreasonable considering the variation in beta observed over the band.

Overall agreement between these two studies is good with the general trends reproduced, although there would appear to be a nearly systematic discrepancy of approximately 0.05 between the two sets of results.

3.2 Acetaldehyde

The photoelectron spectrum of acetaldehyde, Figure 6, has five strong features and a weak feature accessible with He I radiation. However, calculations of the ionization potentials of this molecule[36] reveal the presence of seven molecular orbitals in this range. The first feature is well isolated and displays the band profile, with a strong adiabatic transition with short vibrational progression, associated with an essentially nonbonding orbital, and can be ascribed with confidence

to the n_O $10a'$ orbital ($\tilde{X}\ ^2A'$). The last weak feature between 19 and 20 eV can be associated with the $6a''$ orbital which is an inner valence orbital of the "s-type" composed principally of antibonding C 2s orbitals. The ionization potential of orbitals of this type are compatible with this energy range and their bands typically have low total cross sections. The intervening four features, which overlap considerably, correspond then to five orbitals. On the basis of the calculated ionization potentials[36] and the enhanced cross section clearly discernible, it is reasonable to assign two orbitals to the feature between 15 and 16 eV.

The high resolution spectrum of the $\tilde{X}$ band, seen in Figure 7, shows the typical profile of a nonbonding orbital with the most intense transition being the adiabatic and the other transitions having much lower amplitudes. The adiabatic and vertical ionization potentials for this band coincide at 10.22 eV in good agreement with the values from other experimental studies.[33,36–44] This band contains resolvable vibrational structure: a principal progression with a frequency of 1260 cm^{-1} which accounts for the peaks observed in Figure 6, and structure of much lower intensity at 1130, 915, and 730 cm^{-1}. With the exception of the 915 cm^{-1} frequency, which is observed here only as a shoulder, and has not been previously reported; these transitions occur at frequencies in reasonable agreement with those published previously.[34,40,41,43,44] Cvitas *et al.*[44], whose acetaldehyde and deuteroacetaldehyde spectra have the highest resolution of all these studies (<15 meV), also observe a

very low amplitude feature at 2570 cm^{-1} which is insufficiently resolved in this study from the second quanta of the 1260 cm^{-1} mode to be so assigned. While there is good general agreement in these works on the frequencies of this band, there is no accord on the assignments of these frequencies. Cvitas and coworkers[44], however, have the most comprehensive study of the vibrational structure present and their assignments are the most definitive (see Table 3). The frequency at 1260 cm^{-1} is designated ν_7, a mode corresponding roughly to a CH_3 deformation plus a C-C stretch. Because of the low symmetry of this molecule, this mode and most of the others are delocalized motions. The 1130 cm^{-1} frequency can be assigned to ν_6, a CH bending mode; the 730 cm^{-1} to ν_9, a C-C stretch plus a CH_3 rocking motion. The additional frequency of 2570 cm^{-1} observed by Cvitas *et al.*[44] is assigned to ν_3, a C-H stretch, while the frequency of 915 cm^{-1} observed in this work can be tenatively assigned to ν_8, where the frequency reduction in this mode going from the molecule to the ion (see Table 3) is comparable to that of ν_6 and ν_9.

The second band $\tilde{A}\ ^2A''$ arises from the $2a''$ molecular orbital which is principally C-O π bonding. The adiabatic ionization potential is at 12.63 eV and the vertical ionization potential is 13.24 eV which compares with those of other studies.[33,36–44] There is visible a vibrational progression at 1270 cm^{-1} up the leading edge of the band which is confirmed in the works of other groups.[33,34,37,43,44] An additional mode,

which is not resolved in Figure 6, was tentatively assigned by Chadwick and Katrib[42] and later confirmed by Cvitas *et al.*[44] at 440 cm^{-1} . These modes correspond to ν_4, the C-O stretching mode and to ν_{10}, the CCO bending mode.

Band $\tilde{B}$ $^2A'$ originates from the $9a'$ orbital which is a pseudo-π orbital involving the CH_3 group.[24] This band between 13.7 and 14.8 eV has a vertical ionization potential at 14.14 eV and overlaps to a considerable extent with the neighboring $\tilde{A}$ and $\tilde{C}(\tilde{D})$ bands. No vibrational structure is observed on this band.

Bands $\tilde{C}$ ($^2A'$) and $\tilde{D}$ ($^2A''$) lie principally between 14.8 and 16.0 eV again with significant overlap with adjacent peaks. In this study only a single maximum at 15.30 eV is observed in this region, which for lack of a better descriptive method is the measured vertical ionization potential for both the $\tilde{C}$ and $\tilde{D}$ bands. The other studies of this molecule[33,36,37,38–44] report these two bands with coincident maxima with the exception of Kimura *et al.*,[38] who report the vertical ionization potential of the $\tilde{D}$ band as a shoulder observed at 15.6 eV. These two bands originate from ionization of the $8a'$ and $1a''$ orbitals although there is disagreement as to which orbital is assigned to which band;[24,36] the issue is moot from the experimental point of view. Respectively, the $8a'$ and $1a''$ orbitals can be characterized as σ C-C and CH_3 pseudo-π bonding.[24] No vibrational structure is resolved on this band.

The last strong feature in the spectrum at 16 to 17 eV is the $\tilde{E}$ $^2A'$ band issuing from the $7a'$ orbital. This orbital is characterized as σ

C-O bonding.[24] Cvitas *et al.*[44] identify a vibrational progression in the ν_4 C-O stretching mode at 1200 cm^{-1} on this band. Although there is some faint evidence of structure, the resolution in this study of this band is insufficient to confirm or deny the presence of this mode. The vertical ionization potential of this band is 16.38 eV in good agreement with other studies of this molecule.[33,36–44]

The last feature in the He I spectrum corresponds to ionization from the antibonding orbital mentioned above. Due to its low cross section and position in a region of the spectrum where instrumental effects (notably, rising background) are greatest, there is less certainty in the literature about the vertical ionization potential of this band;[33,36–44] however the value of 19.15 eV reported here is consonant with the majority of values. This band also lacks vibrational fine structure.

Table 3 summarizes the ionization potentials and vibrational structure determined by the various studies of this molecule.

The asymmetry values for this molecule are reported here for the first time and are summarized in Table 4 as well as displayed over the full spectrum in Figure 6. For most of the bands the beta value at the vertical ionization potential is a good measure of the average value over the band.

The measured beta values for the $\tilde{X}$ band of 0.31 are in excellent agreement with those determined in the corresponding band in formaldehyde. The value of beta on the second vibrational peak is slightly lower

than that observed on the adjacent peaks but is within experimental error. This agreement conforms with the nature of the molecular orbitals; the orbital is substantially localized in both molecules to the O nonbonding electrons. Methyl substitution would be expected to have little effect on the beta values except to the extent that the asymmetry parameter depends on electron energy as the orbital is destabilized by substitution. Here, however, as in formaldehyde, the beta values of this band show no discernible energy dependence.

The $\tilde{A}$ bands in acetaldehyde and formaldehyde also correlate, originating from ionization of the π C=O bonding orbital; however, the beta values are more diverse than in the $\tilde{X}$ bands. At low ionization potential the beta values are higher than in the latter part of the band where the values level off. It is difficult to specify the extent to which this falloff is a consequence of an inherent energy dependence or to a result of overlap with the $\tilde{B}$ band which has a lower asymmetry parameter. Regardless, the mean value of 0.52 is 0.20 lower than the asymmetry parameter of the corresponding band in formaldehyde, a strong substituent effect reflecting perhaps the antibonding contribution of the methyl group carbon to the molecular orbital in acetaldehyde.[24]

The $\tilde{B}$ band whose molecular orbital is principally localized in the methyl functional[24] does not correlate with a formaldehyde band. The mean value of the asymmetry parameter for this band is 0.40 and, aside from the oscillations, there is no variation of beta with energy over the apparent range of this band. This lower value is consistent with well-

known trends in beta with the percent of π character in the orbital.

The $\tilde{C}$ and $\tilde{D}$ bands are essentially coincident, so there is no possiblity of deconvoluting the contribution of each to the observed beta values. The average value over this region is 0.52 with a 0.14/eV rise in beta in evidence in this range. The two orbitals of these bands, as in the $\tilde{B}$ band, do not correlate with formaldehyde orbitals, one being a CH_3 pseudo-π orbital localized in the substituent and the other a σ C-C bonding orbital.[24]

The $\tilde{E}$ band of this molecule should correlate with the $\tilde{B}$ band of formaldehyde, both being σ C-O bonding. The average value here is 0.70 which, unlike the other bands, differs substantially from the vertical beta of 0.81, but other than the seemingly ubiquitous oscillations, the beta values do not vary discernibly with electron energy. These values are somewhat higher than expected considering the nature of the orbital; in general, the beta values for π orbitals are higher in the same molecule than for σ band but here the betas are about 0.2 higher than the π C-O $\tilde{A}$ band of this molecule. The beta values are also higher by approximately the same amount than in the corresponding band in formaldehyde. Indeed, these values agree suprisingly well with the $\tilde{A}$ π band in that molecule.

The last band in acetaldehyde, ($\tilde{F}$), is a C 2s antibonding orbital. The standard deviation of the asymmetry parameters of this band is higher than for the other bands due primarily to the fact that the band has a low cross section in a region where the instrumental background

is high, resulting in a less than optimal signal-to-noise ratio for this band. The average value here, 0.48, agrees well with the vertical beta of 0.50; however, there is a distinct overall decline in beta with energy of -0.33/eV. It also does not correlate with any band in the formaldehyde spectrum.

3.3 Acetone

The valence bands of acetone are displayed in Figure 8. There is an additional band acessible to He I radiation, a C 2s band, as in acetaldehyde, beyond 18 eV which is not presented in this spectrum, although a high resolution spectrum of this band is shown in Figure 10. Figure 8 contains five strong features which, from molecular orbital calculations,[24,36] represent ionization from eight orbitals.

The first feature which is well isolated is plainly the $\tilde{X}$ $5b_2$ band, the molecular orbital being primarily localized on the nonbonding oxygen orbital as anticipated, but there is a small amount of electron density on the carbon chain as well.[24] The high resolution spectrum of this band, Figure 9, reveals a more complex structure than is apparent in Figure 8. There is some, admittedly tenuous, evidence that the vertical transition here is not adiabatic; there seems to be an extremely faint shoulder on the vertical transition, although this departure from expected band shape could proceed from the delocalization of the orbital rather than being due to an unresolved vibrational transition. That structure that can be definitely identified is consistent with that observed by Brundle *et al.*[35] and Rao[34]; the principal progression at 1190 cm^{-1} may be

assigned, based on optical studies of acetone and perdeuteroacetone,[45] to ν_4, a methyl deformation mode, and the higher frequency overtone at 350 cm^{-1} to ν_8, conforming with the 10-20% reduction in frequency observed in the homologs in the ion states *vis-a-vis* the neutral states. The vertical and perhaps adiabatic ionization potential for this band is 9.72 eV in good agreement with other studies[17,33,35,37–39,46] as is the appearance of the spectrum in general. This further drop in ionization potential over formaldehyde and acetaldehyde is indicative of an additional destabilization of the orbital with alkyl substitiution.

The second feature corresponds to the $\tilde{A}\ ^2B_2$ band which may be assigned from theoretical calculations to the $2b_2$ orbital which is C=O π bonding. Brundle *et al.*[35] assigned this band to the $4b_1$ methyl group orbital based partially on a study of the perfluoro effect and partially on intuition since good calculations were not available. This feature and the two that follow overlap considerably, and thus the ionization potentials are those of the apparent maxima. A vibrational progression at 1290 cm^{-1} is observed on this band, almost certainly the C-O stretching frequency, although the reduction in frequency is greater than anticipated, approximately 25% over the neutral. This progression is not resolved in other studies[33,35–39] and because of this the vertical ionization potential of this band differs from the others where the vertical ionization potential is closer to the band centroid, as far as that concept applies.

The third feature is the $\tilde{C}$ band, from the $4b_1$ CH_3 pseudo-π bonding orbital which in this molecule is also slightly C-O π bonding.[24] The vertical ionization potential of this band is 13.53 eV.

The fourth feature of Figure 8, based on the observed cross section and theoretical calculations,[24,36] represents two bands with extensive overlap, ionization from the $8a_1$ and $1a_2$ orbitals although the calculations give different orderings. These orbitals are predominantly (σ C-C, σ C-O) and π CH_3 bonding, respectively.[24] Some of the studies of this molecule report coincident vertical ionization potentials for these bands[37,39] while others[35,36,38] report the second ionization potential as the energy of a shoulder on this feature. While the shoulder is clearly present in the spectrum, due to its broad slope, it is distinctly difficult to specify its precise position, 14.4 eV being a reasonable approximate location. The principal maximum falls at 14.06 eV.

The fifth and final feature of Figure 8 contains three bands, $\tilde{E}$,$\tilde{F}$,and $\tilde{G}$, ionization from the $7a_1$, $3b_2$, and $1b_1$ orbitals, although again the ordering is in dispute.[24,36] These orbitals have the bonding characteristics, σ C-O, (σ C-C, n_O) and π CH_3, respectively. The number of ionization potentials reported on this feature varies from study to study depending on the resolution (or lack thereof) of weak shoulders. The first vertical ionization potential corresponds to the absolute maximum of this feature, 15.65 eV. A second and third can be tenuously placed at 16.1 eV and 16.3 eV, but these latter shoulders

are nebulous at best.

Ionization from the $6a_1$ orbital is acessible to He I radiation. This band characterized as the C "s-type," has a considerably lower intensity than the other bands and is presented here only as the high resolution spectrum, Figure 10. The vertical ionization potential is 18.15 eV with an observed vibrational frequency of 1400 cm^{-1} (ν_5) in agreement with Brundle *et al.*[35]

These results are tabulated in Table 5.

With the exception of the first band, the angular distribution of acetone are reported here for the first time. The measured asymmetry parameters are summarized in Table 6 and displayed over the full spectrum in Figure 8.

The beta values of the $\tilde{X}$ band, approximately 0.34, agree remarkably well with the $\tilde{X}$ bands of formaldehyde and acetaldehyde with which it is correlated. The small difference, 0.03, which is within experimental error, could also represent a very slight energy dependence of the asymmetry parameters over the 1.1 eV that the orbital energy decreases with methyl substitution, or perhaps, an effect of orbital delocalization.

Kobayashi[17] has measured an asymmetry parameter of 0.64 ± 0.04, for this band at a photon energy of 21.2 eV, in substantial disagreement with the value determined here. Because of the very reasonable agreement in the anisotropy parameters determined in the $\tilde{X}$ bands of the three molecules under investigation and the agreement with the results of Keller *et al.*[16] for formaldehyde, the value determined in this study is

strongly believed to be the correct one and that the deviation from this value observed by Kobayashi represents some systematic error perhaps due to instrumental effects (insufficient shielding).

The $\tilde{A}$ band's average beta value of 0.24 is reasonably close to that of the vertical value of 0.17. As can be deduced from this, there is an -0.15/eV energy dependence over this band, although some of this dependence may be due to overlap with the $\tilde{B}$ band. Even excluding this energy dependence, which would decrease the beta value further, this is a significant lowering of the asymmetry parameter, 0.18, over the correlated $\tilde{A}$ band in acetaldehyde. Extrapolating the beta value to the vertical ionization potential of the acetaldehyde band yields a reduction of 0.28 with the second methyl substitution. This is in concordance with the trends observed in the methylated ethenes[4] and the alkylated ethynes[5] previously studied by this group.

The $\tilde{B}$ band has nearly identical average and vertical beta values, 0.18 and 0.17, respectively, with an essentially zero energy dependence (0.06/eV). This orbital is considerably more delocalized than the $9a'$ orbital in acetaldehyde,[24] although they could probably be considered correlated. In which case, extrapolating to the acetaldehyde vertical ionization potential, the reduction in beta is 0.18, a value comparable to the reduction observed in the $\tilde{A}$ bands.

It is necessary, because of the extensive overlap, to treat the $\tilde{C}$ and $\tilde{D}$ bands as a single entity. The vertical ionization potential, being the absolute maxima of the bands at 14.06 eV, has an associated asymmetry

parameter of 0.21. The average value is 0.18 with a nearly flat energy dependence (-0.04/eV) over the band. If, again, correlation is assumed between these two orbitals and those in acetaldehyde, which are similar in characterization[24] and in general band shape, although, as in $\tilde{B}$ the acetone orbitals naturally possess greater delocalization, there is again a large drop in beta, approximately 0.3.

The $\tilde{E}$, $\tilde{F}$, and $\tilde{G}$ bands are also treated as coincident due to the extensive overlap, the vertical ionization potential being taken as 15.65 eV. The vertical beta is 0.32, which is very close to the average 0.34. The behavior of the asymmetry parameter on this peak is noteworthy; the values start out high over the initial portions of the structure then drop to a fairly constant value over the remaining part of the feature. Since these higher values occur on a rapidly rising region of the spectrum caution must be observed in any interpretation; however, this behavior would be consistent with the values if the first portion corresponding to a band that differed in character (*vis-a-vis* the asymmetry parameter) from the remaining two. In a simplistic approach this might be taken as credence for the ordering $1b_1$, $7a_1$, $3b_2$[24] for these orbitals since $1b_1$ has at least nominally π type character while the other orbitals are σ bonding. However, in this molecule, as evidenced by the other bands, π character does not guarantee higher beta values and in all likelihood the π/σ designation may have very little significance considering the degree of delocalization in these orbitals. Moreover, oscillatory behavior, which is not pronounced on the rest of the band, and energy dependence, as

well as the experimental artifact mentioned above, cannot be totally ruled out.

The effects of alkyl substitution on the ionization potentials have not been subjected to close scrutiny in this study, although the expected shifts to lower ionization potential with methyl substitution have of course been noted. These effects on aldehydes and ketones have been extensively studied by other workers,[33,34,37,47–49] using such techniques as Taft polarization constants (σ^*), induction correlations, and theoretical modeling to examine the effects of substitution on delocalization and shifts in ground versus ion state energies.

4. SUMMARY AND CONCLUSIONS

The photoelectron angular distributions have been obtained for formaldehyde, acetaldehyde, and acetone using He I radiation at scattering angles between 45 and 120°. The asymmetry parameter has been determined for the first time for acetaldehyde and for acetone except for the first band which has been measured by Kobayashi.[17]

In the course of this study it has been seen that within experimental error the asymmetry parameter of the $\tilde{X}$ n_O bands of this series is invariant with respect to methyl substitution, while the $\tilde{A}$ C-O π bands show a strong decrease in the asymmetry parameter, approximately 0.2-0.25, with each methylation. The correlations among the other bands is not secure enough to draw definite conclusions about the substituent effects on their asymmetry parameters.

Lastly, a systematic decrease in ionization potential with methylation is noted, an effect that has been extensively analyzed in previous studies.[33,34,37,47–49]

REFERENCES

1. D. C. Mason, A. Kuppermann, and D. M. Mintz, in *Electron Spectroscopy*, edited by D. A. Shirley (North-Holland Publishing Co., Amsterdam, 1972).

2. J. A. Sell, D. M. Mintz, and A. Kuppermann, *Chem. Phys. Lett.*, **58**, 601 (1978).

3. D. M. Mintz and A. Kuppermann, *J. Chem. Phys.*, **71**, 3499 (1979).

4. D. M. Mintz and A. Kuppermann, *J. Chem. Phys.*, **70**, 3151 (1979).

5. D. J. Flanagan, C. F. Koerting, and A. Kuppermann, *The Angular Resolved Photoelectron Spectroscopy of Some Alkylated Alkynes*, manuscript in preparation.

6. C. F. Koerting, D. J. Flanagan, and A. Kuppermann, *The Angle Resolved Photoelectron Spectroscopy of Cyclopropane, Ethylene Oxide and Ethyleneimine*, manuscript in preparation.

7. J. A. Sell and A. Kuppermann, *J. Chem. Phys.*, **71**, 4703 (1979).

8. P. R. Keller, D. Mehaffy, J. Taylor, F. A. Grimm, and T. A. Carlson, *J. Electron Spectroscopy*, **27**, 223 (1982).

9. R. M. White, T. A. Carlson, and D. P. Spears, *J. Electron Spectroscopy*, **3**, 59 (1974).

10. T. A. Carlson and C. P. Anderson, *Chem. Phys. Lett.*, **10**, 561 (1971).

11. D. M. Mintz, Ph.D Thesis, California Institute of Technology, Pasadena, CA (1976).

12. T. Koopmans, *Physica*, **1**, 104 (1933).

13. J. Cooper and R. Zare, in *Lectures in Theoretical Physics*, edited by S. Geltman, K. Mahanthappa, and N. Britten (Gordon and Breach, New York, 1969) Vol xi-c.

14. J. Cooper and S. Manson, *Phys. Rev.*, **177**, 157 (1969).

15. H. Bethe and E. Saltpeter, *Quantum Mechanics of One and Two Electron Atoms* (Springer-Verlag, Berlin, 1957).

16. P. R. Keller, J. W. Taylor, F. A. Grim, T. A. Carlson, *Chem. Phys.*, **90**, 147 (1984).

17. T. Kobayashi, *Phys. Lett.*, **69A**, 31 (1978).

18. D. Mason, D. Mintz, and A. Kuppermann, *Rev. Sci. Inst.*, **48**, 926 (1977).

19. T. Carlson and A. Jonas, *J. Chem. Phys.*, **55**, 4913 (1971).

20. D. J. Kennedy and S. T. Manson, *Phys. Rev. A*, **5**, 227 (1972).

21. J. L Dehmer, W. A. Chupka, J. Berkowitz, and W. T. Jivery, *Phys. Rev. A*, **12**, 1966 (1975).

22. W. Handcock and J. Samson, *J. Electron Spectroscopy*, **9**, 211 (1976).

23. D. M. P. Holland, A. C. Parr, D. L. Ederer, and J. B. West, *Nuclear Instruments and Methods*, **195**, 331 (1982).

24. K. Kimura, S. Katsumata, Y. Achiba, T. Yamazaki, and S. Iwata, *Handbook of HeI Photoelectron Spectra of Fundamental Organic Molecules* (Japan Scientific Societies Press, Tokyo, 1981).

25. J. A. Pople, H. B. Schlegel, R. Krishnan, D. J. Defrees, J. S. Binkley, M. J. Frish, R. A. Whiteside, R. F. Hout, and W. J. Hehre, *Int. J Quantum Chem. Symp.*, **15**, 269 (1981).

26. G. Hertzberg, *Molecular Spectra and Molecular Structure III: Electronic Spectra and Electronic Structure of Polyatomic Molecules* (Van Nostrand Reinhold Co., New York, 1966).

27. L. S. Cederbaum, W. Domke, and W. von Niessen, *Chem. Phys. Lett.*, **34**, 60 (1975).

28. W. Domke and L. S. Cederbaum, *J. Chem. Phys.*, **64**, 612 (1976).

29. A. D. Baker, C. Baker, C. R. Brundle, and D. W. Turner, *Int. J. Mass Spectrosc.*, **1**, 285 (1968).

30. W. von Niessen, G. Bieri, and L. Åsbrink, *J. Electron Spectroscopy*, **21**, 175 (1980).

31. S. T. Hood, A. Hamnett, and C. E. Brion, *Chem. Phys. Lett.*, **41**, 428 (1976).

32. J. E. Mentall, E. P. Gentieu, M. Krauss, and D. Neumann, *J. Chem. Phys.*, **55**, 5471 (1971).

33. R. Hernandez, R. Masclet, and G. Mouvier, *J. Electron Spectroscopy*, **10**, 333 (1977).

34. C. N. R. Rao, *Indian J. Chem.*, **13**, 950 (1975).

35. C. R. Brundle, M. B. Robin, N. A. Kuebler, and H. Basch, *J. Amer. Chem. Soc.*, **94**, 1451 (1972).

36. G. Bieri, L. Åsbrink, and W. von Niessen, *J. Electron Spectroscopy*, **27**, 129 (1982).

37. W-C. Tam, D. Yee, and C. E. Brion, *J. Electron Spectroscopy*, **4**, 77 (1980).

38. K. Kimura, S. Katsumata, T. Yamazaki, and H. Wakabayashi, *J. Electron Spectroscopy*, **6**, 41 (1975).

39. H. Ogata, J. Kitayama, M. Koto, S. Kojima, Y. Nihei, and H. Kamada, *Bull. Chem. Soc. Japan.*, **47**, 958 (1974).

40. K. Johnson, I. Powis, C. J. Danby, *Chem. Phys.*, **70**, 329 (1982).

41. S. P. McGlynn and J. L. Meeks, *J. Electron Spectroscopy*, **6**, 269 (1975).

42. D. Chadwick and A. Katrib, *J. Electron Spectroscopy*, **3**, 39 (1974).

43. J. L. Meeks, J. F. Arnett, D. Larson, and S. P. McGlynn, *Chem. Phys. Lett.*, **30**, 190 (1975).

44. T. Cvitas, H. Gusten, and L. Klasinc, *J. Chem. Phys.*, **64**, 2549 (1976).

45. M. Lawson and A. B. F. Duncan, *J. Chem. Phys.*, **12**, 329 (1944).

46. J. Kelder, H. Cerfontain, B. R. Higginson, and D. R. Lloyd, *Tetrahedron Lett.*, **9**, 739 (1974).

47. W. C. Tam and C. E. Brion, *J. Electron Spectroscopy*, **3**, 467 (1974).

48. D. W. Davis, U. C. Singh, and P. A. Kollman, *J. Molec. Structure (THEOCHEM)*, **105**, 99 (1983).

49. B. W. Levitt and L. S. Levitt, *Chem. Ind.(London)*, 725 (1972).

TABLE 1. Formaldehyde

Band/Orbital	Ionization Potential (eV)		Vibrational Frequencies (cm^{-1})		
	This Work*	Other Work*	This Work	Other Work[a]	Molecular[b,c]
$\tilde{X}\ ^2B_2/^2b_2$	10.89	$10.87 \pm .01$[d] 10.88(4)[a] 10.88(5)±0.005[f] 10.9[g] 10.88[h]	2580 ν_1 1610 ν_2 1190 ν_3	2560±50[e] ν_1 1590±50 ν_2 1210±50 ν_3	ν_1 2780, 2783 ν_2 1744, 1746 ν_3 1503, 1500
$\tilde{A}\ ^2B_1/^2b_1$	[14.10,14.40]	[14.09(5),14.38(8)][a] 14.10(3)±0.005[f] 14.5[g,i] 14.50[h]	1190 ν_2 1350 ν_3	1210±50 ν_2	
$\tilde{B}\ ^2A_1/^2a_1$	[15.82,15.98]	[15.85(4),16.00(9)][a] 16.1[g] 16.00[h]	1250 ν_2	1270±50 ν_2 or ν_3	
$\tilde{C}\ ^2B_2/^1b_2$	[~16.21,16.76]	[16.25(4),16.78][a] ~17.0[g] 16.60[h]	1420 ν_3	1400±50 ν_3	

a) Reference 29.
b) Reference 26.
c) Reference 25.
d) Reference 32.
e) Reference 34.
f) Reference 33.
g) Reference 30.
h) Reference 24.
i) Reference 35.

* The first entry in brackets is the adiabatic ionization potential the second the vertical, for the $\tilde{X}$ band they are the same.

TABLE 1a. Formaldehyde

Band/Orbital	Calculated Ionization Potentials				
	Ham/3	CI[a]	SCF-MO[a]	MB-GF[b]	Ham/3[c]
$\tilde{X}\ {}^2B_2/{}^2b_2$	10.72	10.32	11.96	10.81	10.72
$\tilde{A}\ {}^2B_1/{}^2b_1$	14.82	14.15	14.53	14.62	14.80
$\tilde{B}\ {}^2A_1/{}^2a_1$	16.47	15.59	17.51	16.20	16.44
$\tilde{C}\ {}^2B_2/{}^1b_2$	17.35	17.12	19.06	17.36	17.33

a) Reference 24.
b) Reference 27.
c) Reference 30.

TABLE 2. Formaldehyde β values

Band/Orbital	β	
	This Work	Other Work[a]
$\tilde{X}\ ^2B_2/^2b_2$	ν=0 $0.31 \pm .05$ (β_{vert})	$0.27 \pm .05$
	ν=1 $0.31 \pm .05$	
	ν=2 $0.31 \pm .07$	
$\tilde{A}\ ^2B_1/^2b_1$	ν=0 $0.77 \pm .09$	$0.65 \pm .05$
	ν=1 $0.71 \pm .05$	
	ν=2 $0.76 \pm .07$ (β_{vert})	
	ν=3 $0.74 \pm .03$	
	ν=4 $0.71 \pm .11$	
	ν=5 $0.72 \pm .07$	
	ν=6 $0.76 \pm .05$	
	ν=7 $0.69 \pm .08$	
	ν=8 $0.63 \pm .15$	
$\tilde{B}\ ^2A_1/^2a_1$	ν=0 $0.39 \pm .03$	$0.52 \pm .06$
	ν=1 $0.45 \pm .03$ (β_{vert})	
	ν=2 $0.62 \pm .04$	
	ν=3 $0.52 \pm .01$	
	ν=4 $0.70 \pm .04$	
	ν=5 $0.56 \pm .04$	
$\tilde{C}\ ^2B_2/^1b_2$	vert: $0.54 \pm .04$	$0.42 \pm .05$
	max: $0.62 \pm .08$	
	min: $0.30 \pm .15$	

a) Reference 16.

TABLE 3. Acetaldehyde

Band/Orbital	Ionization Potential (eV)		Vibrational Frequencies (cm^{-1})		
	This Work†	Other Work†	This Work	Other Work	Molecular[a,b]
$\tilde{X}\ ^2A'/10a'$	10.22	10.19[c]	1260 ν_7	1260 ν_7[d]	ν_1 3005, 2967
		10.20[e,f]		1260 ν_6,ν_7[g]	ν_2 2917, 2840
		10.21[d,h]		1303 ν_4[e,f]	ν_3 2822, 2736
		10.22(9)±0.005[i]			ν_4 1743, 1743
		10.24[g,j]	1130 ν_6	1100 ν_6[d],ν_8[g]	ν_5 1441, 1441
		10.26[k]		1129 ν_4[l]	ν_6 1400, 1390
		10.3[m]			ν_7 1352
			730 ν_9	700 ν_9,ν_{10}[g]	ν_8 1113
				770 ν_9[d]	ν_9 919
			915 ν_8?	2570 ν_3[d]	ν_{10} 509
$\tilde{A}\ ^2A''/2b''$	[12.63,13.24]	[12.54,13.15][g]	1270 ν_4	1210 ν_4[d]	
		[12.61,13.20][e,f]		1230 ν_5[e,f]	
		12.62±0.01[i*]		1270 ν_6,ν_7[g]	
		13.09[c]			
		13.15[j]		440 ν_{10}[d]	
		13.2[h,m]		(460)[g]	
		13.24[f]			

Band/Orbital	Ionization Potential (eV)		Vibrational Frequencies (cm^{-1})		
	This Work†	Other Work†	This Work	Other Work	Molecular[a,b]
$\tilde{B}$ $^2A'/9a'$	14.14	13.93[c*] 14.10[e,j] 14.1[g,h] 14.15[k] 14.17[d] 14.19[f] 14.2[m]			
$\tilde{C}$ $^2A'/8a'$	15.30	15.09[c*] 15.3[e,f,h] 15.34[k] 15.36[d] 15.40[j] 15.4[g,m]			
$\tilde{D}$ $^2A''/1a''$	15.30	15.4[g,m] (15.6)[k]			

Band/Orbital	Ionization Potential (eV)		Vibrational Frequencies (cm^{-1})		
	This Work†	Other Work†	This Work	Other Work	Molecular[a,b]
$\tilde{E}$ $^2A'/7a'$	16.38	16.32[d] 16.40[c] 16.4[e,g,h,j] 16.47[k] 16.5[m]		1200 ν_4	
(C 2s) $^2A'/6a'$	19.15	~19[g] ~19.00[h] 19.0[e,f] 19.1[k] 19.4[m] 19.54[d]			

† first number in brackets is the adiabatic ionization potential
the second is the vertical ionization potential.

* adiabatic ionization potential

a) Reference 25.
b) Reference 26.
c) Reference 39.
d) Reference 44.
e) Reference 41.
f) Reference 43.
g) Reference 42.
i) Reference 33.
h) Reference 37.
j) Reference 40.
k) Reference 38.
l) Reference 34.
m) Reference 36.

TABLE 3a. Acetaldehyde

Band/Orbital	Calculated Ionization Potentials			
	SCF-MO[a]	CI[a]	HAM/3[b]	GF[b]
$\tilde{X}\ ^2A'/10a'$	11.57	9.47	10.13	10.26
$\tilde{A}\ ^2A''/2b''$	13.57	12.88	13.15	13.35
$\tilde{B}\ ^2A'/9a'$	15.15	13.89	13.78	14.09
$\tilde{C}\ ^2A'/8a'$	16.63	14.96	14.80	15.25
$\tilde{D}\ ^2A''/1a''$	16.94	15.62	14.98	15.54
$\tilde{E}\ ^2A'/7a'$	18.44	16.31	15.90	16.33
(C 2s) $^2A'/6a'$			19.58	19.65

a) Reference 24.
b) Reference 36.

TABLE 4. Acetaldehyde β values

Band	β This Work
$\tilde{X}$	ν=0 $0.32 \pm .04$ (β_{vert}) ν=1 $0.27 \pm .04$ ν=2 $0.31 \pm .07$
$\tilde{A}$	vert: $0.53 \pm .05$ max: $0.97 \pm .11$ min: $0.27 \pm .06$ ave: 0.52
$\tilde{B}$	vert: $0.34 \pm .06$ max: $0.59 \pm .08$ min: $0.23 \pm .10$ ave: 0.40
$\tilde{C}$,$\tilde{D}$	vert: $0.46 \pm .08$ max: $0.66 \pm .07$ min: $0.26 \pm .10$ ave: 0.52
$\tilde{E}$	vert: $0.81 \pm .06$ max: $0.88 \pm .08$ min: $0.53 \pm .14$ ave: 0.48
($\tilde{F}$)	vert: $0.50 \pm .09$ max: $0.86 \pm .15$ min: $0.15 \pm .15$ ave: 0.48

TABLE 5. Acetone

Band/Orbital	Ionization Potential (eV)†		Vibrational Frequencies (cm^{-1})		
	This Work	Other Work	This Work	Other Work	Molecular[a]
$\tilde{X}\ ^2B_2/5b_2$	9.72	9.70(9) ± .005[b] 9.71[e,f,g] 9.70[h] 9.72[c,i] 9.8[j]	1190 ν_7	1210[c,d] ν_4[c],ν_3[d] 360 ν_8[c]	ν_1 3019 ν_2 2937 ν_3 1731 ν_4 1435 ν_5 1364
$\tilde{A}\ ^2B_1/2b_1$	12.78	11.93±0.01[b*] 12.6[c,e,j] 12.59[h] 12.62[f]	1290 ν_3		ν_6 1066 ν_7 777 ν_8 385
$\tilde{B}\ ^2B_1/4b_1$	13.53	13.5[e] ~13.4[j] 13.4[c] 13.41[h] 13.70[f]			
$\tilde{C}\ ^2A_1/8a_1$	14.06	14.1[e,j] 14.04[h] 13.9[c] 14.18[f]			

Band/Orbital	Ionization Potential (eV)†		Vibrational Frequencies (cm^{-1})		
	This Work	Other Work	This Work	Other Work	Molecular[a]
$\tilde{D}\ ^2A_2/1a_2$	(14.4)	~14.4[j] (14.8)[h] 14.5[c]			
$\tilde{E}\ ^2A_1/7a_1$	15.65	15.6[e,h] 15.7[j] 15.55[c]			
$\tilde{F}\ ^2B_2/3b_2$	(16.1)	(16.1)[h] 15.7[j]			
$\tilde{G}\ ^2B_1/1b_1$	(16.3)	(16.6)[h] 16.0[j]			
(C 2s) $^2A_1/6a_1$	18.16	18.0[e,j] 17.73[c] 18.1[h]	1400	1370 ν_5[c]	

† Ionization potentials in parentheses indicate the position of shoulders.

* Adiabatic ionization potential.

a) Reference 25.
b) Reference 33.
c) Reference 35.
d) Reference 34.
e) Reference 37.
f) Reference 39.
g) Reference 46.
h) Reference 38.
i) Reference 17.
j) Reference 36.

TABLE 5a. Acetone

Band/Orbital	Calculated Ionization Potentials			
	SCF-MO[a]	HAM/3[b]	GF[b]	HAM/3
$\tilde{X}$ $^2B_2/5b_2$	11.20	9.95	9.85	9.95
$\tilde{A}$ $^2B_1/2b_1$	13.02	12.52	12.65	12.52
$\tilde{B}$ $^2B_1/4b_1$	14.62	13.21	13.45	13.20
$\tilde{C}$ $^2A_1/8a_1$	15.09	14.14	14.05	14.14
$\tilde{D}$ $^2A_2/1a_2$	15.46	13.95	14.40	13.95
$\tilde{E}$ $^2A_1/7a_1$	17.23	14.70	15.66	14.70
$\tilde{F}$ $^2B_2/3b_2$	17.69	14.78	15.93	14.78
$\tilde{G}$ $^2B_1/1b_1$	17.18	15.55	16.08	15.55
(C 2s) $^2A_1/6a_1$		17.70	19.65	

a) Reference 24.
b) Reference 36.

TABLE 6. Acetone β values

Band	β	
	This Work	Other Work[a]
$\tilde{X}$	ν=0 0.34 ± .04 (β_{vert}) ν=1 0.36 ± .06 "ν=2" 0.36 ± .10	0.64 ± .04
$\tilde{A}$	vert: 0.17 ± .03 max: 0.50 ± .05 min: 0.08 ± .10 ave: 0.24	
$\tilde{B}$	vert: 0.17 ± .04 max: 0.29 ± .06 min: 0.11 ± .06 ave: 0.18	
$\tilde{C}$,$\tilde{D}$	vert: 0.21 ± .07 max: 0.26 ± .08 min: 0.07 ± .08 ave: 0.18	
$\tilde{E}$,$\tilde{F}$,$\tilde{G}$	vert: 0.32 ± .07 max: 0.62 ± .07 min: 0.62 ± .07 ave: 0.34	

a) Reference 17.

FIGURE CAPTIONS

Figure 1. Block diagram of MAPS: He–cylinder of UHP helium, ZT–zeolite trap at 77°K for lamp helium supply, RB–lamp ballast resistor, LPS–lamp power supply, SC–scattering chamber, PC–photocathode, CL–set of electrostatic lenses, ANALYZER–hemispherical electrostatic analyzer, ML–set of electrostatic lenses, S–Spiraltron electron multiplier, CPS–Spiraltron cathode power supply, APS–Spiraltron anode power supply, RC–differentiating network for Spiraltron pulses, INTER–counting system interface to experiment, PDP 8e–Digital PDP 8e minicomputer, and OUTPUT–computer peripheral devices.

Figure 2. Photoelectron spectrum (lower panel) and the asymmetry parameters (upper panel) for formaldehyde. The spectrum was taken at 54.7°. Channel width was 20 meV. Total acquisition time per channel was 60 s.

Figure 3. High resolution photoelectron spectrum of the $\tilde{X}$ band of formaldehyde taken at 54.7°. Channel width was 4 meV. Total acquisition time per channel was 110 s. Position of the vibrational lines, the assignment of the corresponding vibrational modes and their frequencies are given in the figure.

Figure 4. High resolution photoelectron spectrum of the $\tilde{A}$ band of formaldehyde taken at 54.7°. Channel width was 4 meV. Total acquisition time per channel was 60 s. Position of the vibrational

lines, the assignment of the corresponding vibrational modes and their frequencies are given in the figure.

Figure 5. High resolution photoelectron spectrum of the $\tilde{B}$ and $\tilde{C}$ bands of formaldehyde taken at 54.7°. Channel width was 4 meV. Total acquisition time per channel was 60 s. Position of the vibrational lines, the assignment of the corresponding vibrational modes and their frequencies are given in the figure.

Figure 6. Photoelectron spectrum (lower panel) and the asymmetry parameters (upper panel) for acetaldehyde. The spectrum was taken at 54.7°. Channel width was 20 meV. Total acquisition time per channel was 75 s.

Figure 7. High resolution photoelectron spectrum of the $\tilde{X}$ band of acetaldehyde taken at 54.7°. Channel width was 3 meV. Total acquisition time per channel was 50 s. Position of the vibrational lines, the assignment of the corresponding vibrational modes and their frequencies are given in the figure.

Figure 8. Photoelectron spectrum (lower panel) and the asymmetry parameters (upper panel) for acetone. The spectrum was taken at 54.7°. Channel width was 25 meV and total acquisition time per channel was 35 s.

Figure 9. High resolution photoelectron spectrum of the $\tilde{X}$ band of acetone taken at 54.7°. Channel width was 5 meV. Total acquisition time per channel was 35 s. Position of the vibrational lines, the assignment of the corresponding vibrational modes and their

frequencies are given in the figure.

Figure 10. High resolution photoelectron spectrum of the C 2s band of acetone taken at 54.7°. Channel width was 4 meV. Total acquisition time per channel was 22.5 s. Position of the vibrational lines, the assignment of the corresponding vibrational modes and their frequencies are given in the figure.

FIGURE 1.

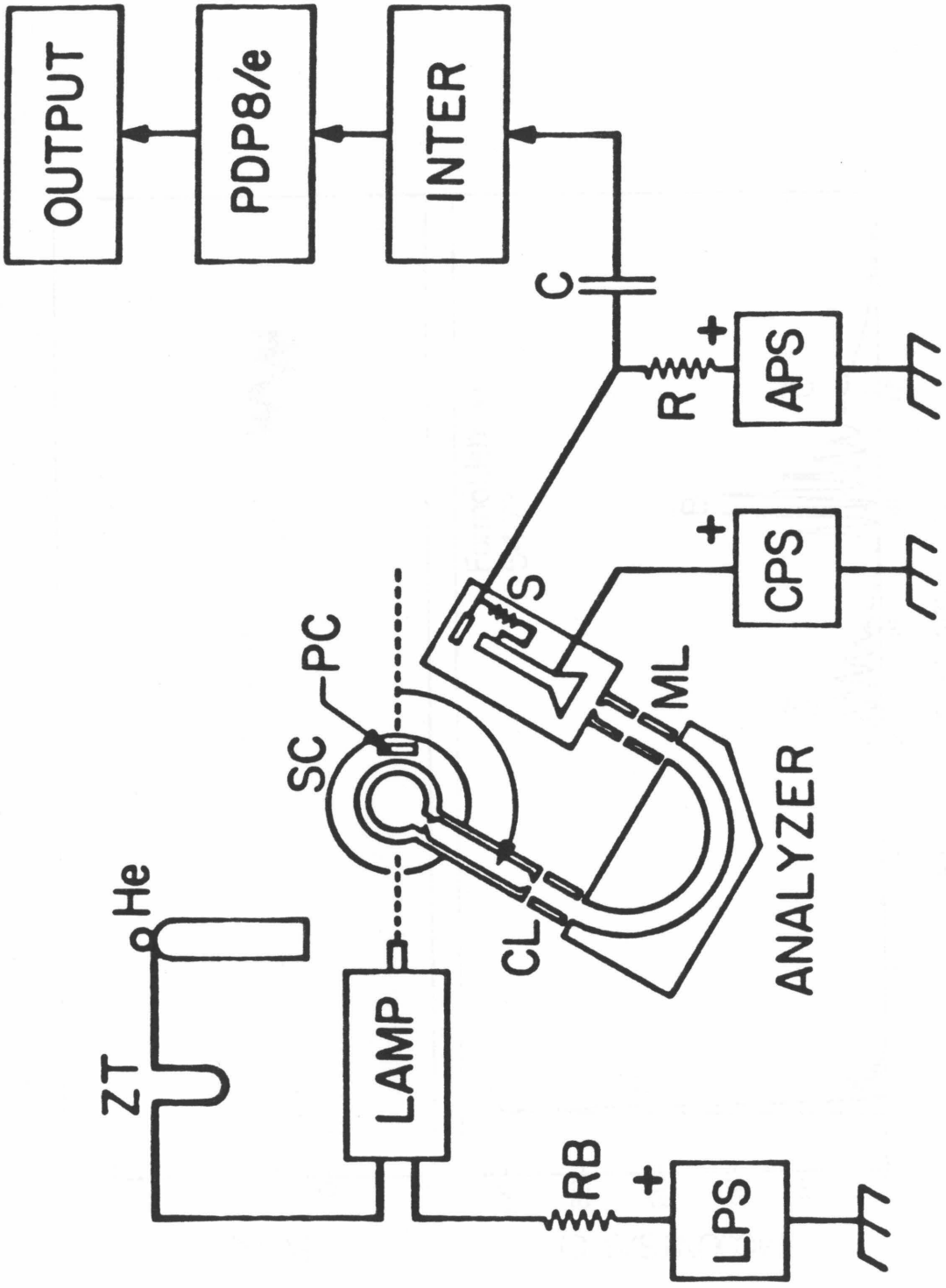
OUTPUT
PDP8/e
INTER
C
R
APS
CPS
S
PC
SC
ML
ANALYZER
He
CL
ZT
LAMP
RB
LPS

FIGURE 2.

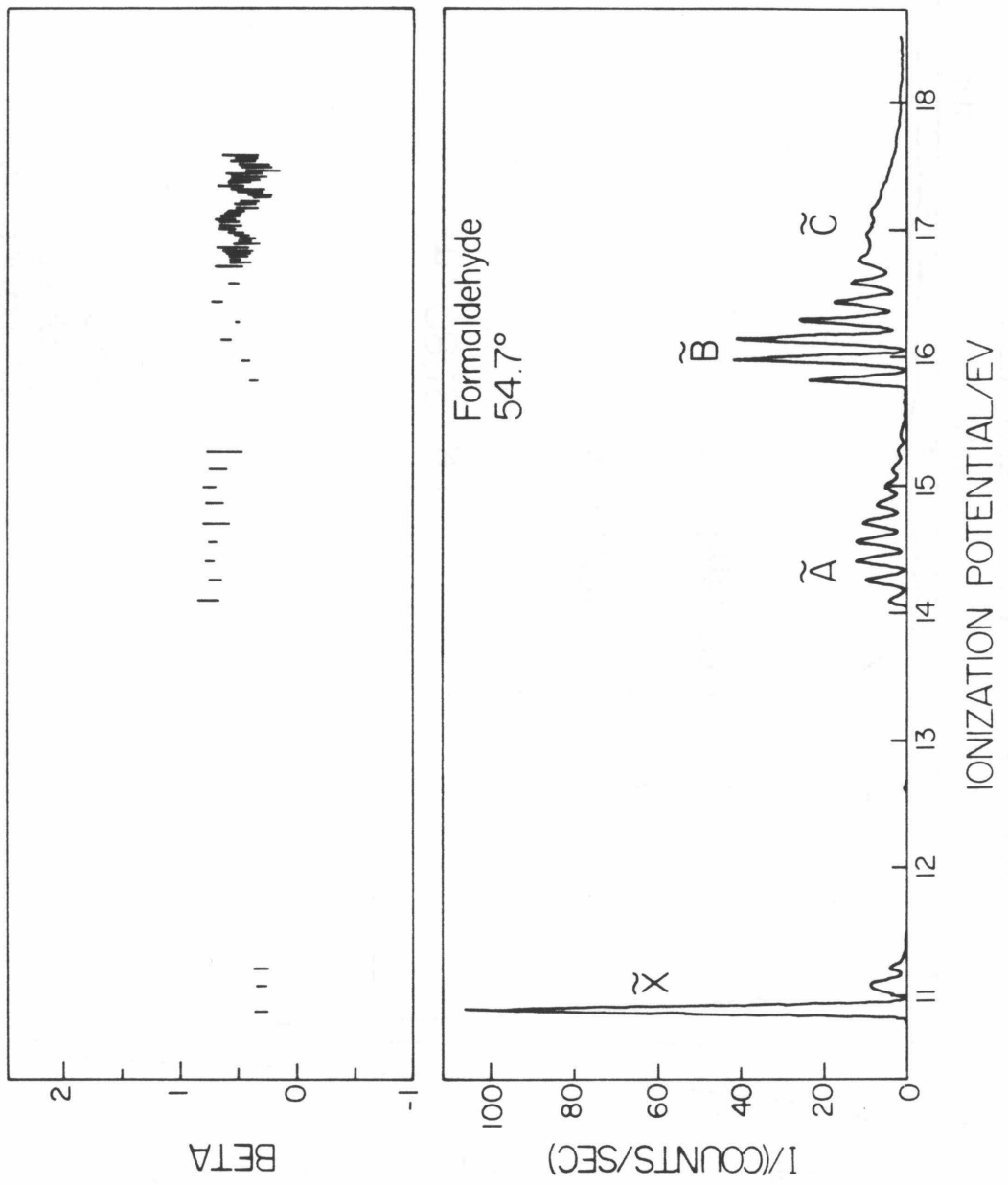
BETA
2
1
0
-1
I/(COUNTS/SEC)
100
80
60
40
20
0
Formaldehyde
54.7°
X̃
Ã
B̃
C̃
11
12
13
14
15
16
17
18
IONIZATION POTENTIAL/EV

FIGURE 3.

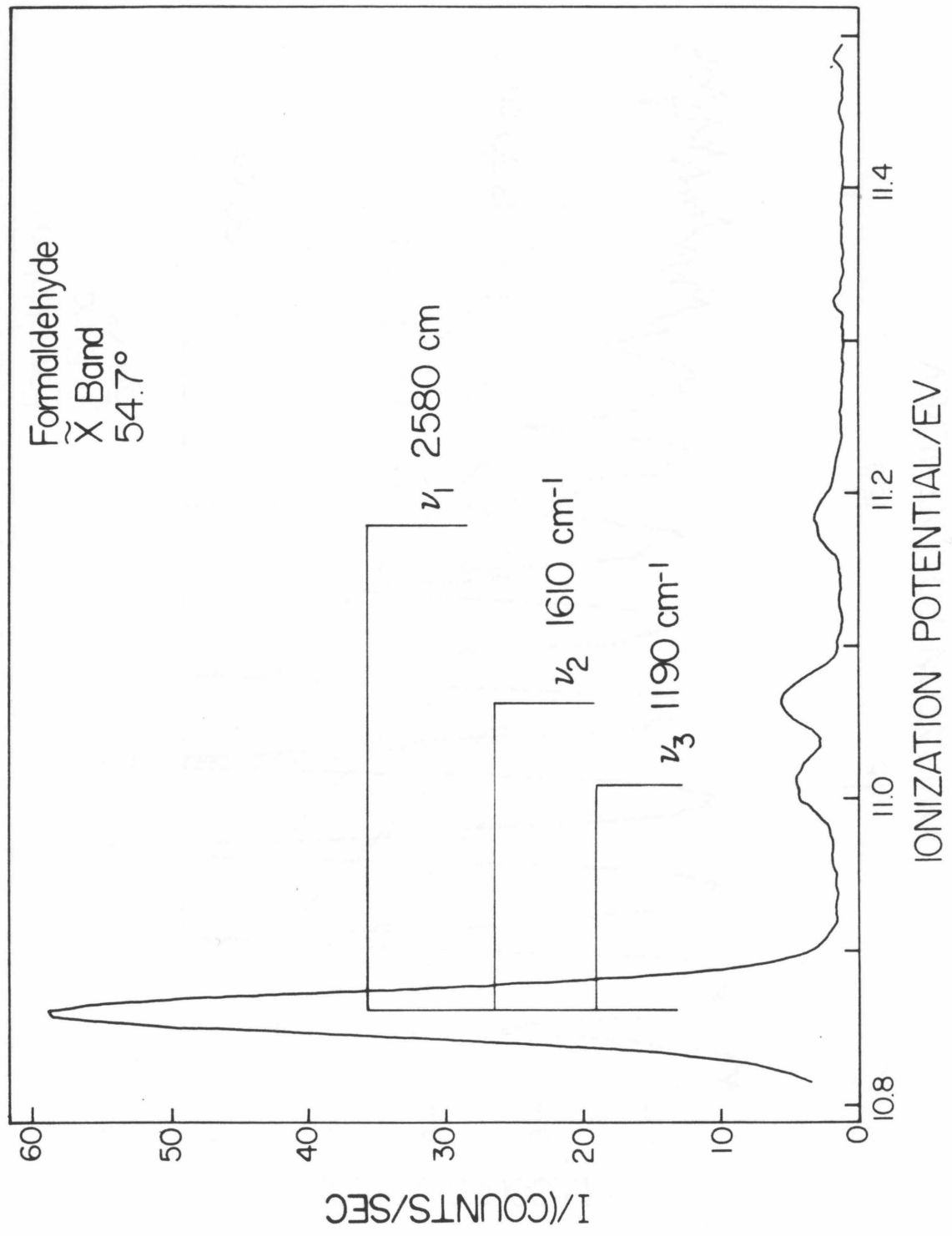
Formaldehyde
$\tilde{X}$ Band
54.7°
ν_1 2580 cm
ν_2 1610 cm^{-1}
ν_3 1190 cm^{-1}
I/(COUNTS/SEC
0
10
20
30
40
50
60
10.8
11.0
11.2
11.4
IONIZATION POTENTIAL/EV

FIGURE 4.

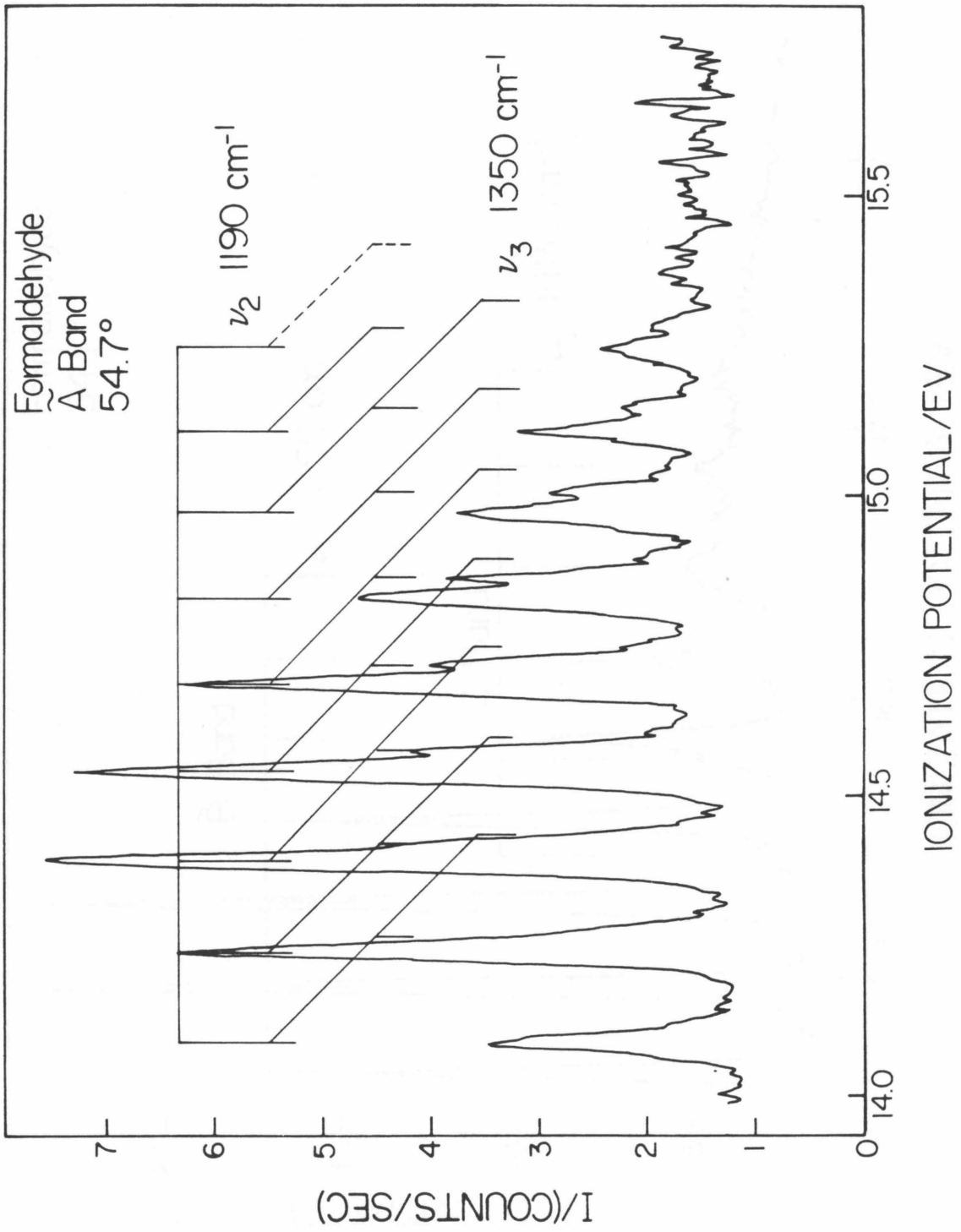
Formaldehyde
Ã Band
54.7°
ν2 1190 cm-1
ν3 1350 cm-1
I/(COUNTS/SEC)
IONIZATION POTENTIAL/EV
0
1
2
3
4
5
6
7
14.0
14.5
15.0
15.5

FIGURE 5.

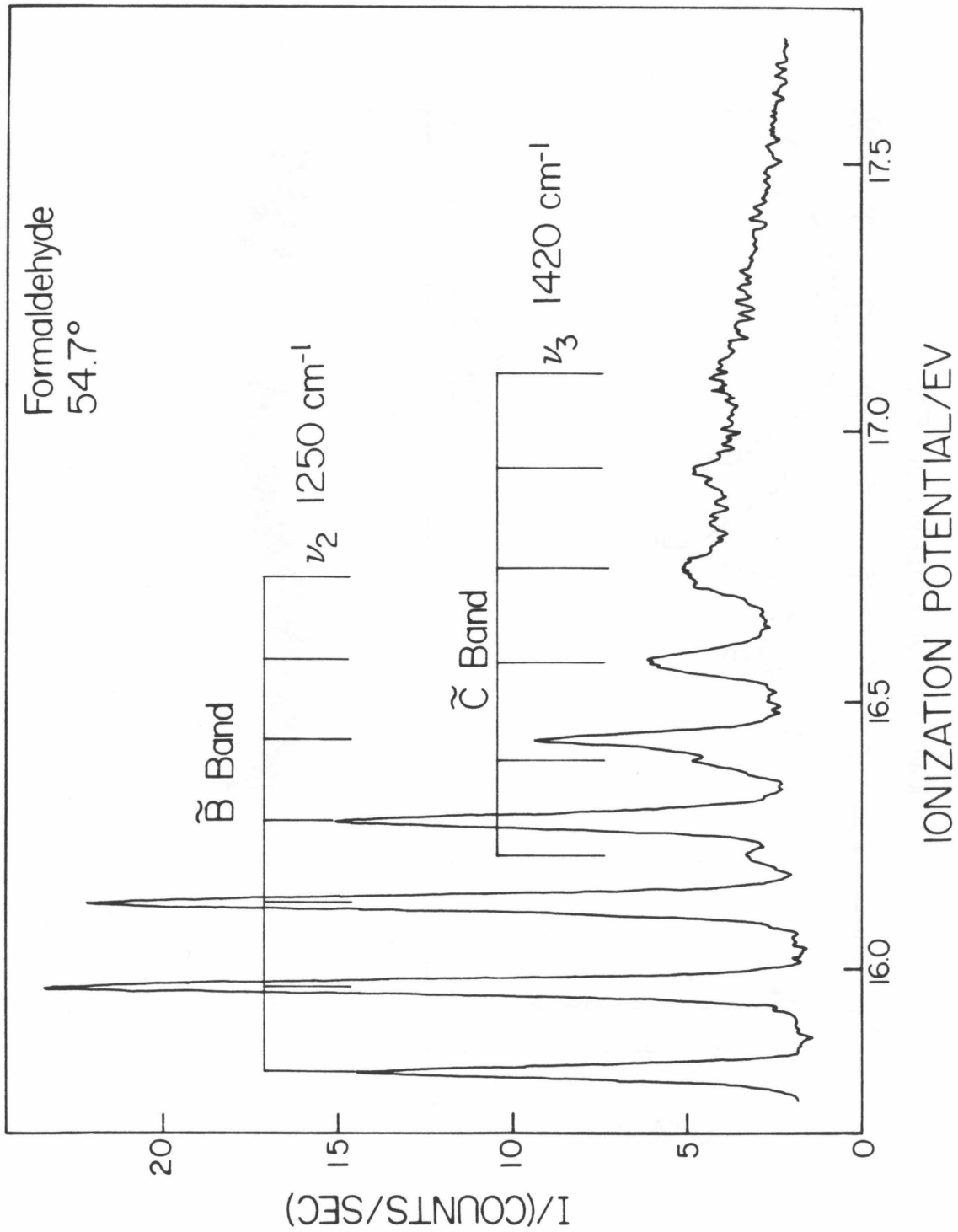
Formaldehyde
54.7°
$\tilde{B}$ Band
ν_2 1250 cm^{-1}
$\tilde{C}$ Band
ν_3 1420 cm^{-1}
I/(COUNTS/SEC)
20
15
10
5
0
16.0
16.5
17.0
17.5
IONIZATION POTENTIAL/EV

FIGURE 6.

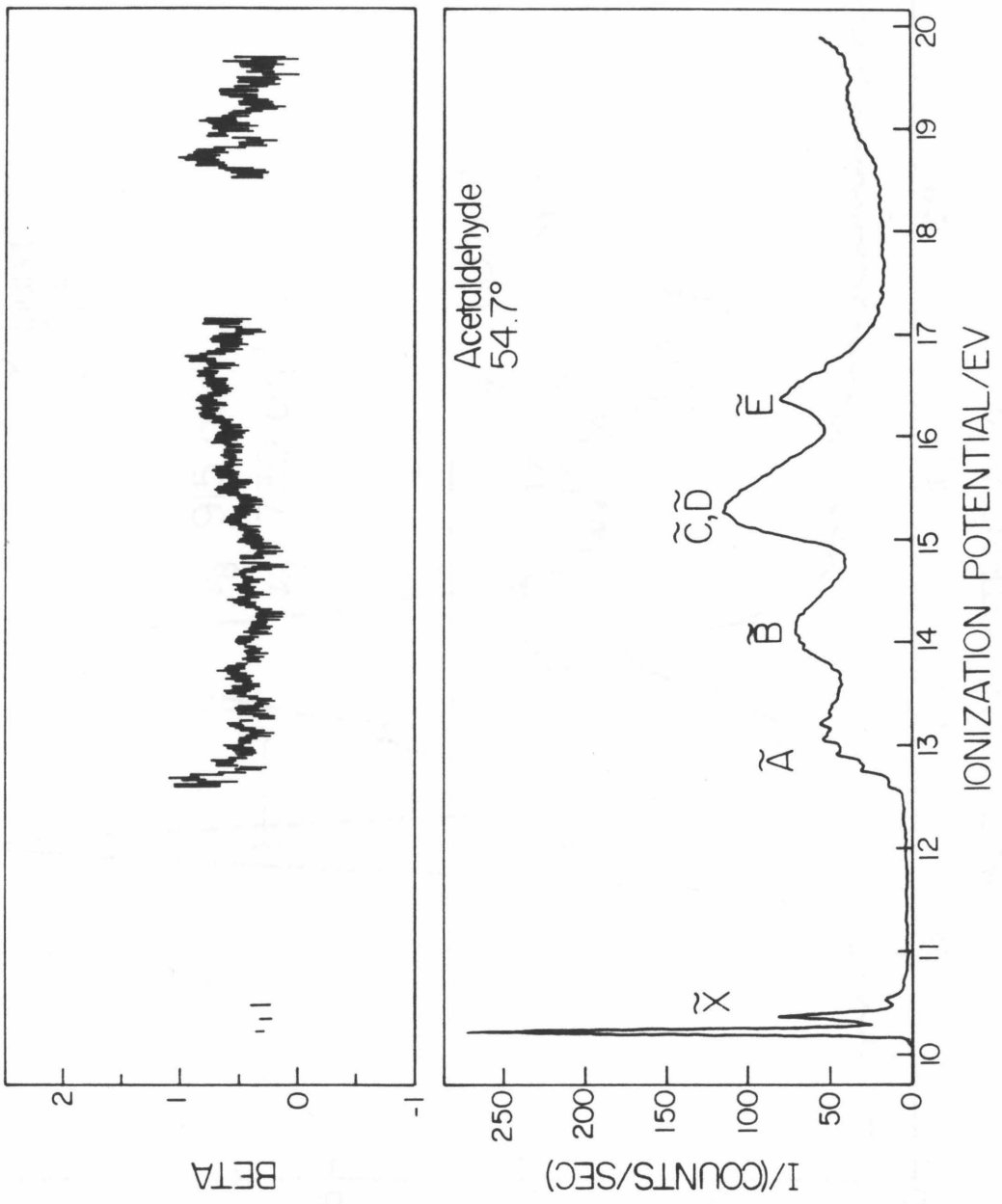
BETA
2
1
0
-1
Acetaldehyde
54.7°
I/(COUNTS/SEC)
250
200
150
100
50
0
10
11
12
13
14
15
16
17
18
19
20
IONIZATION POTENTIAL/EV
X̃
Ã
B̃
C̃,D̃
Ẽ

FIGURE 7.

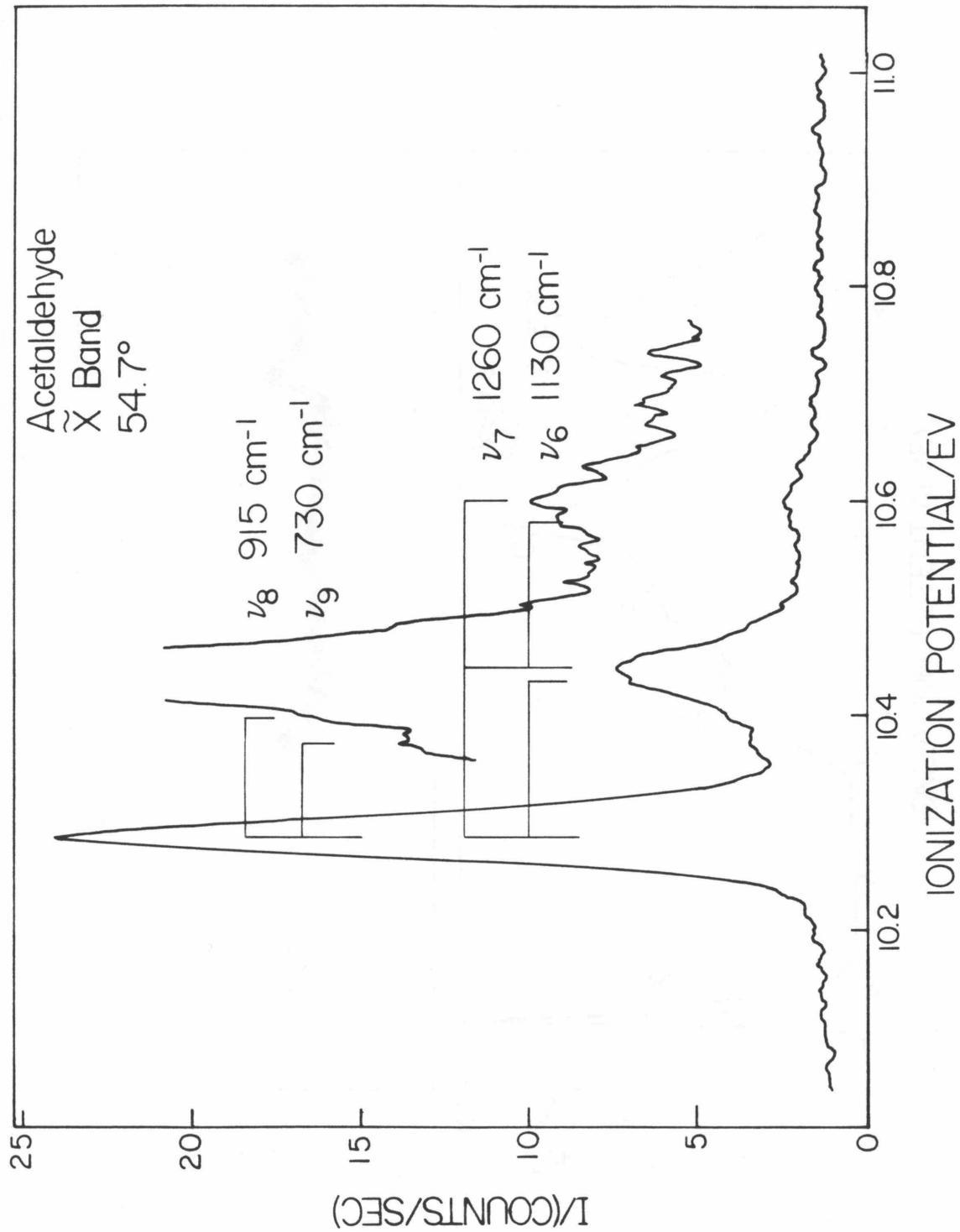
Acetaldehyde
X̃ Band
54.7°
ν8 915 cm-1
ν9 730 cm-1
ν7 1260 cm-1
ν6 1130 cm-1
I/(COUNTS/SEC)
IONIZATION POTENTIAL/EV
0
5
10
15
20
25
10.2
10.4
10.6
10.8
11.0

FIGURE 8.

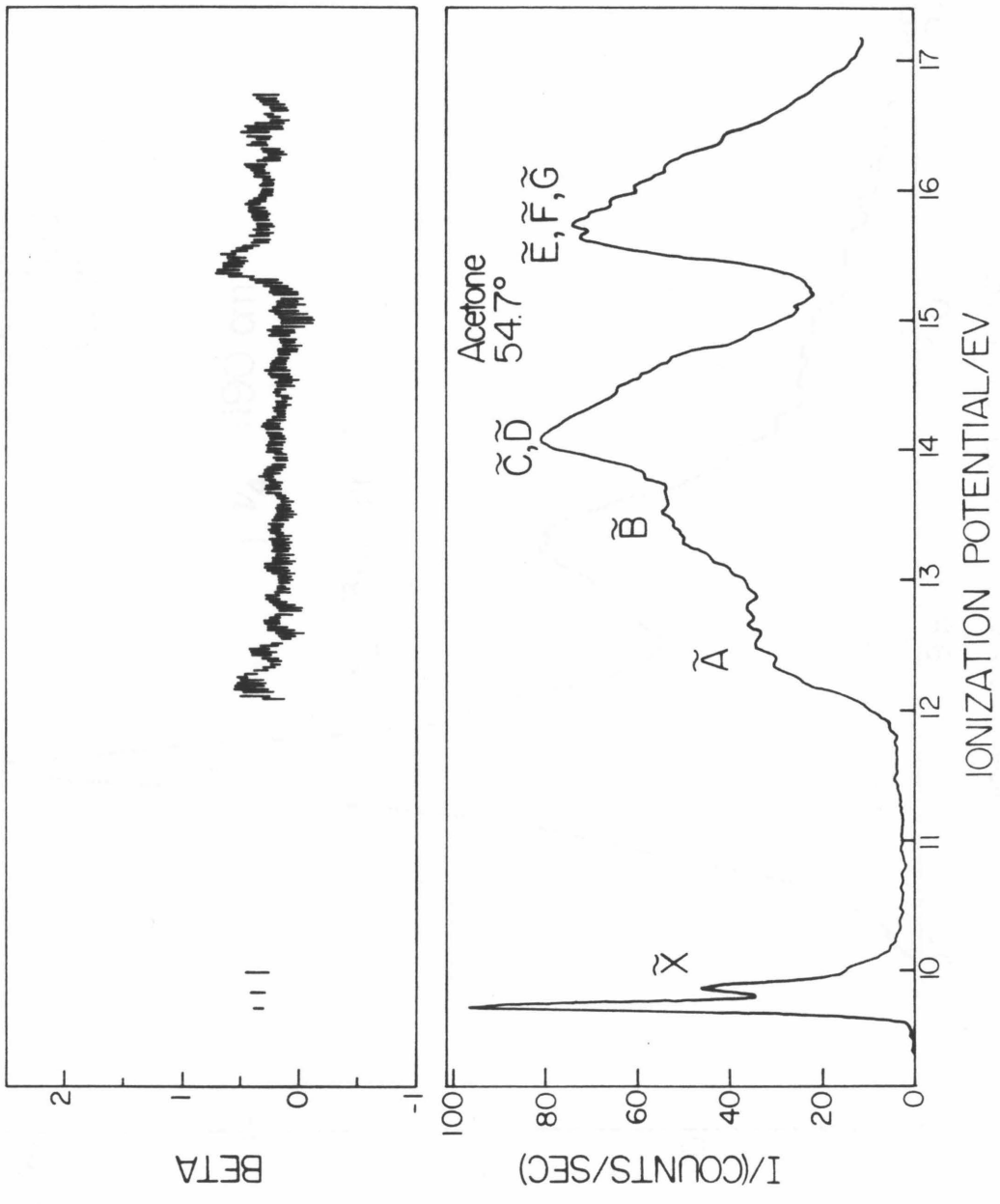
BETA
2
1
0
-1
I/(COUNTS/SEC)
100
80
60
40
20
0
Acetone
54.7°
X̃
Ã
B̃
C̃,D̃
Ẽ,F̃,G̃
10
11
12
13
14
15
16
17
IONIZATION POTENTIAL/EV

FIGURE 9.

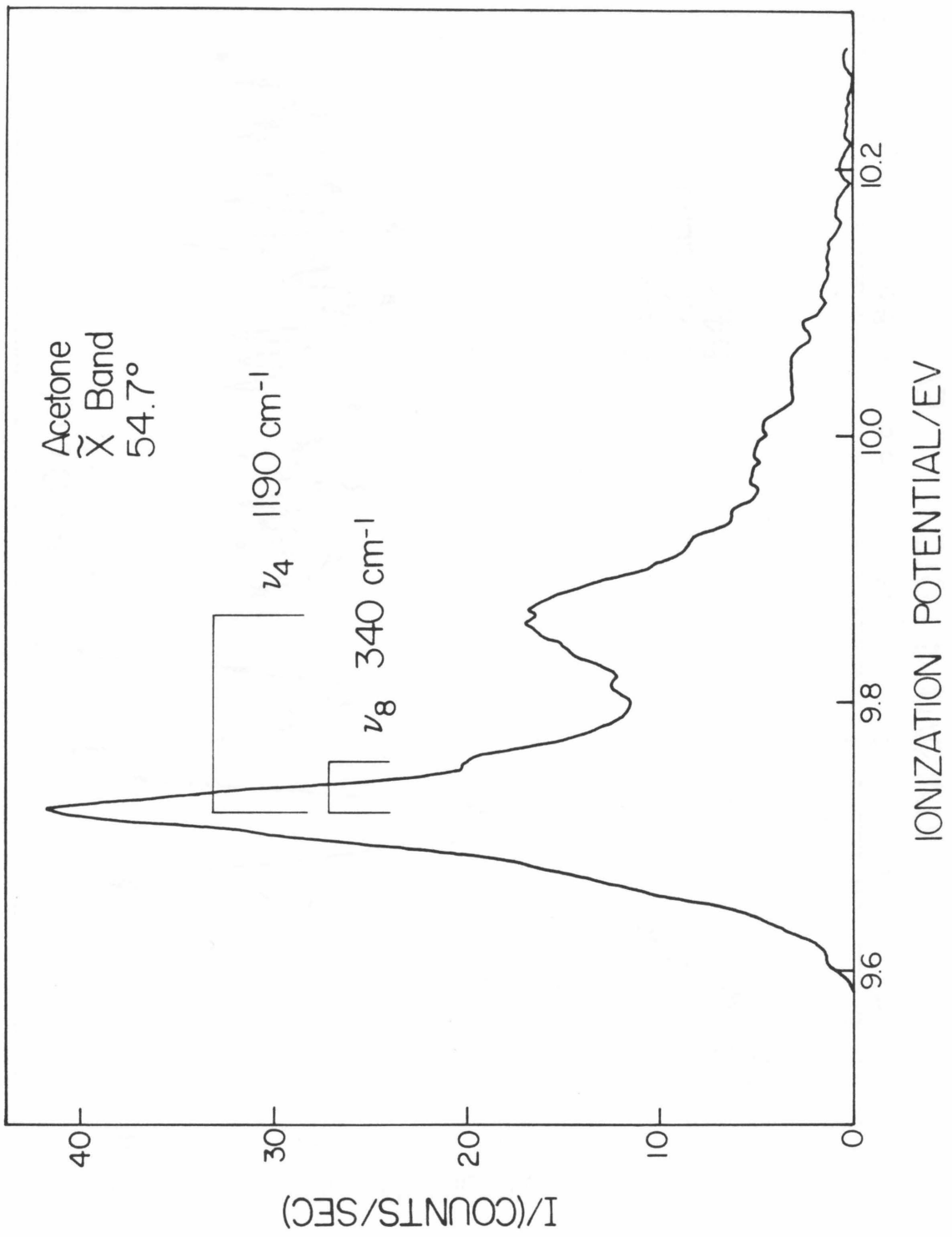
Acetone
$\tilde{X}$ Band
54.7°
ν_4 1190 cm^{-1}
ν_8 340 cm^{-1}
I/(COUNTS/SEC)
0
10
20
30
40
9.6
9.8
10.0
10.2
IONIZATION POTENTIAL/EV

FIGURE 10.

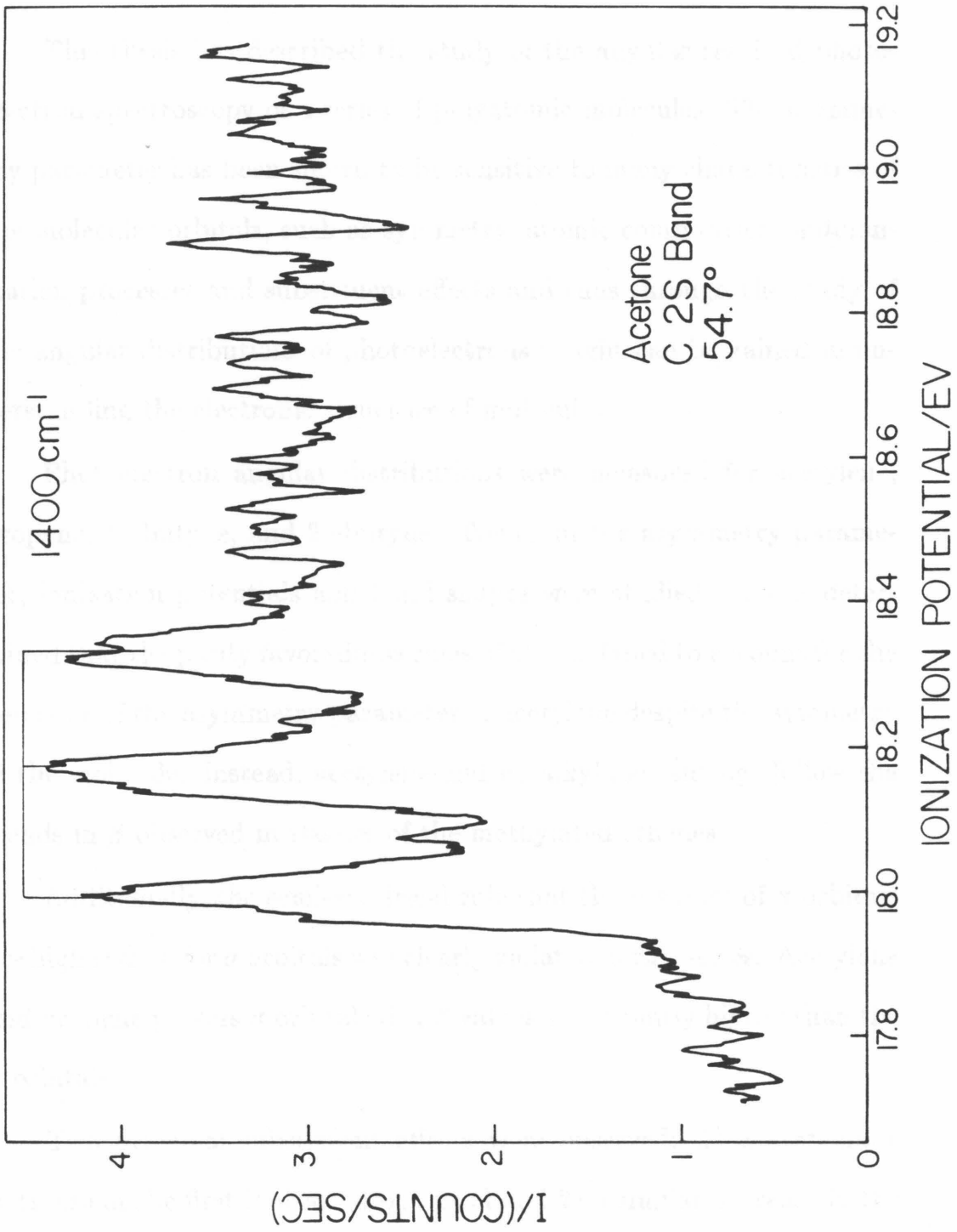
1400 cm⁻¹
Acetone
C 2S Band
54.7°
I/(COUNTS/SEC)
0
1
2
3
4
17.8
18.0
18.2
18.4
18.6
18.8
19.0
19.2
IONIZATION POTENTIAL/EV

CHAPTER 7

SUMMARY AND CONCLUSIONS

This thesis has described the study of the angular resolved photoelectron spectroscopy of a series of polyatomic molecules. The asymmetry parameter has been shown to be sensitive to many characteristics of the molecular orbitals, such as symmetry, atomic composition, autoionization processes and substituent effects and thus through the study of the angular distributions of photoelectrons insight can be gained in understanding the electronic structure of molecules.

Photoelectron angular distributions were measured for acetylene, propyne, 1−butyne, and 2−butyne. Trends in the asymmetry parameter, ionization potentials and band shapes were studied. It was determined that the parity favoredness rules of Chang failed to account for the behavior of the asymmetry parameter of acetylene despite the symmetry of the molecule. Instead, acetylene and its alkylated analogs follow the trends in β observed in studies of the methylated ethenes.

Additionally, the semi-empirical rule that the β values of π orbitals are higher than for σ orbitals was clearly violated in this series. Acetylene and propyne possess σ orbital with β values significantly higher than the π orbitals.

Two principal substituent effects were observed: 1) a systematic decrease in the first ionization potential and 2) a similar decrease in the asymmetry parameter of the $\tilde{X}$ band with increasing alkylation.

The photoelectron angular distributions of formaldehyde, acetaldehyde, and acetone were subsequently examined. In this study, it was determined that, within experimental error, the beta values of the nonbonding $\tilde{X}$ bands of these molecules were invariant with substitution while the C=O π bonding $\tilde{A}$ bands in this homologous series showed a strong decrease in the asymmetry parameter of approximately 0.2 per methylation, in a manner similar to that observed in the methylated ethenes and alkylated ethynes. The correlation of the other orbitals was not sufficiently certain to permit further conclusions to be drawn about the other orbitals measured. Finally, the expected systematic decreases in ionization potential with substitution were also observed.

HAM/3 calculations were performed to determine the ionization potentials of some substituted carbonyls, and to examine the excitation energies of ethylene and its methyl and fluoro derivatives to determine the methods to studies in electron impact spectroscopy.

There was generally good agreement between the ionization potential calculated by this method and experimentally determined values. Agreement between the calculated values of the excitation energies and the experimental were reasonable but the method was not sensitive enough to reproduce the trends observed with increasing substitution of the chromophore.

APPENDIX 1

RESULTS AND DISCUSSION

Paper 3: The Angle Resolved Photoelectron Spectroscopy of Cyclopropane, Ethylene Oxide, and Ethyleneimine.

The Angle Resolved Photoelectron Spectroscopy of Cyclopropane, Ethylene Oxide, and Ethyleneimine[a]

C. F. Koerting,[b] D. J. Flanagan, and A. Kuppermann

Arthur Amos Noyes Laboratory of Chemical Physics,[c]

California Institute of Technology, Pasadena, CA 91125

(received)

Abstract

Photoelectron angular distributions have been measured for the first time for ethylene oxide and ethyleneimine using He I radiation. The determined anisotropy parameters, β, along with those for cyclopropane were used to confirm orbital correlations and photoelectron spectrum band assignments. The β for the high-lying Walsh or Förster-Coulson-Moffitt orbitals did not have the large values characteristic of π orbital ionizations in the alkenes.

---

[a] This work was supported in part by the U. S. Department of Energy, Contract No. DE-AM03-F00767, Project Agreement No. DE-AT03-76ER72004.

[b] Work performed in partial fulfillment of the requirements for the Ph.D. degree in Chemistry at the California Institute of Technology.

[c] Contribution No. 7156.

I. INTRODUCTION

It has been previously shown that the measurement of the angular distributions of photoelectrons can be used to analyze the orbital assignments of the corresponding photoelectron.[1-3] These angular distributions furnish more information about the electronic structure of the molecules than do the fixed angle spectra alone.

The angular distribution of the photoelectrons resulting from the interaction of unpolarized light with a randomly oriented target can be described in terms of the differential cross section, $\frac{d\sigma_{if}}{d\Omega}$, of the process which is given as[4,5]

$$\frac{d\sigma_{if}}{d\Omega} = \frac{Q_{if}}{4\pi}[1 - \frac{\beta_{if}}{2}P_2(\cos\theta)]$$

where Q_{if} is the total ionization cross section from initial target state i to the ionic target state f, θ is the angle between the directions of the ejected electron and the incident photon beam, β_{if} is the asymmetry or anisotropy parameter for the process, and $P_2(\cos\theta)$ is the second order Legendre polynomial. Due to the fact that the cross section must be positive β_{if} is restricted to values between -1 and 2. This quantity is dependent on the kinetic energy of the photoelectron as well as on the characteristics of the orbital from which it was removed, including its angular momentum.[6] This makes β a sensitive probe of some of the details of the electronic structure of the target molecule. Previous work has shown that differences in β can be used to distinguish between ionization processes involving σ- and π-type orbitals.[1,7-11]

The three-membered ring compounds considered in this paper possess unusual chemical and structural properties. Much work has been done in exploring the conjugative properties of cyclopropane.[12,13] In those studies, the similarities between cyclopropane and alkenes in terms of reactivities have been discussed. Even the Auger electron spectra[14] of cyclopropane more closely resemble those of an alkene than of an alkane. Several bonding schemes have been proposed by Walsh,[15–17] Förster[18] and Coulson and Moffitt.[19–20] These schemes have been examined in detail by Honegger *et al.*[21–22] who have concluded that the alkene-like behavior of cyclopropane is due to the high orbital energies of its highest occupied molecular orbitals.

In this work the results of measurements of the asymmetry parameters for the He I photoionization of cyclopropane, ethylene oxide, and ethyleneimine are presented. The photoelectron spectra of these molecules have been published previously[26–40] but the asymmetry parameter measurements provide additional information concerning the bonding in this series of compounds and help elucidate the similarities and differences in this series of molecules.

II. EXPERIMENTAL

The apparatus used in these studies is essentially the one described previously,[10] and will only be briefly described here. A block diagram of the instrument is given in Figure 1. A helium discharge lamp is used to produce the 584 Å radiation which then interacts with the

sample gas present in the scattering chamber. The pressure of this gas is on the order of a few millitorr and is continuously monitored by a calibrated capacitance monometer. The electrons resulting from the photoionization of the sample gas are then energy analyzed by a 6.8 cm mean radius hemispherical electrostatic analyzer, and detected by a spiraltron electron multiplier. The detector and analyzer are mounted on a gear and can be rotated from 45°to 120°with respect to the incident photon beam. The entire spectrometer is located within a vacuum chamber which is lined with a single layer of 0.050" μ metal and surrounded by three pairs of square Helmholtz coils to lower the residual magnetic field to less than 0.2 milligauss. A PDP 8/e minicomputer stores the counts from the electron multiplier, increments the analyzer voltages, monitors the sample pressure, and scans the scattering angle. Background counts are subtracted from the spectra before β is calculated. The performance of the instrument is checked by its ability to reproduce a β of 0.88[10] for the $^2P_{3/2}$ state of argon which has previously been obtained using this instrument. The energy resolution of the work presented here is typically between 40 and 50 meV as measured by the FWHM of the $^2P_{3/2}$ peak of argon.

Samples of cyclopropane and ethylene oxide were obtained as gases from Matheson Gas Products and had stated purities of 99% and 99.7%, respectively. These were used without further purification. Ethyleneimine was obtained from Columbia Organics and had a stated purity of >97%. This liquid was degassed by application of several freeze-pump-

thaw cycles and vacuum distilled prior to use. No extraneous peaks due to impurities were observed in any of the spectra.

III. RESULTS AND DISCUSSION

A. Cyclopropane

Cyclopropane has been the most studied member of the three-membered ring series. A number of previous photoelectron spectroscopy (PES) studies exist[23–29,37,38,40] for this molecule and the relevant ones are summarized in Table I along with the results of the present work. The asymmetry parameters for cyclopropane have been previously determined[23] and are also summarized in Table I. The He I spectrum along with the β spectrum are shown in Figure 2. The He I spectrum agrees well in general appearance with previously published ones.[23,24,26,36,37,39] Minor differences exist in the relative intensities of some of the bands but this is most likely due to the different electron transmission functions of the electron energy analyzers used in the various studies. In addition, the published spectra were all recorded at a 90°angle. The spectra displayed in this paper are recorded at 54.7°, the so-called "magic angle" for which $\frac{d\sigma_{if}}{d\Omega}$ is proportional to Q_{if} because $P_2(\cos\theta)$ in equation 2 vanishes. For non isotropic distributions, the differential cross sections at 90°and 54.7°are different, and therefore, so are the corresponding band intensities.

The first band of the cyclopropane photoelectron spectrum is Jahn-Teller split into two components[41–43] having vertical ionization

potentials (IP) at 10.51 and 11.26 eV. The measured β for these two components are $0.46 \pm .07$ and $0.44 \pm .10$, respectively, and no appreciable change in β across them is observed. Similar results were reported by Carlson for the Jahn-Teller split first band of methane[44] where no significant variation of β over the split band was observed. In benzene, on the other hand, a significant variation over a Jahn-Teller split band was observed.[8] Our result also confirms the observations of Leng and Nyberg[23] even though their values for β are higher than those reported here, possibly due to instrumental artifacts in their apparatus.

The second band in the spectrum is also theoretically predicted to be Jahn-Teller split.[42,43] The calculated splitting is small and has so far not been observed, because of overlapping vibrational progressions. Haselbach[42] has also concluded that since the $1e''$ orbital is primarily composed of p_π(C-H)-type "outer" orbitals, the distortion of the carbon skeleton will affect that orbital to a much lesser extent than the p_σ (C-C) "inner" orbitals which compose the $3e'$ orbital. The measured β for this band is 0.32 ± 0.05, in approximate agreement with the value of 0.43 ± 0.05 obtained previously.[23]

There is some question regarding the assignments of the overlapping bands observed at 15.74 and 16.66 eV. All of the theoretical calculations done so far,[27,45–54] both semi-empirical and *ab initio*, assign the lower band to ionization from the $1a_2''$ orbital. Evans *et al.*[36] have suggested that the assignments of the third and fourth bands should be reversed.

This was done on the basis of comparison with the PES spectra of P_4 and a vibrational analysis of the fourth band. Schweig and Thiel[28] have also supported this assignment on the basis of intensity variations between the He I and He II spectra of cyclopropane and some of its heterocyclic derivatives. Our measured β's are quite different for the two bands, 1.18±0.05 and 0.67±0.04 for the third and fourth bands, respectively. This agrees with the values of 1.26 ± 0.05 and 0.65±0.10 obtained by Leng and Nyberg,[23] which also supports the initial assignments. Their argument was based on the nodal properties of the two orbitals involved. The $3a'$ orbital is "internal" C-C bonding and may contain appreciable carbon 2s character.[36] The nodal properties of this orbital resemble closely an atomic s-type orbital which would account for the high β observed for this C-C σ type orbital. This argument is consistent with the orbital diagrams of Jorgensen and Salem[55] We concur with the conclusions reached by Leng and Nyberg[23] that support the theoretical predictions of the order of these two states.

For the fifth band at 19.51 eV a β of 0.40±0.08 is obtained which is substantially lower than the value of 0.90±0.10 observed previously.[23] Measurements in this region of the spectrum are difficult since the background is large and signals small. This band lies in the portion of the spectrum for which the energy of the photoelectrons is low and instrumental effects can become pronounced and produce a large difference in the values obtained for β. No autoionization effects as postulated by Lindholm[52] manifested themselves in the angular

distributions. A thorough study of β vs. photoelectron energy is needed for the third and fourth bands in order to further clarify their assignments.

B. Ethylene oxide

The observed IP's and β's are summarized in Table 2. The PES spectrum and β's are shown in Figure 3. This spectrum agrees quite well with previous ones.[27,33,38–40] The first band appears as a sharp set of vibrational progressions with a vertical IP at 10.57 eV. This band has been assigned previously[27] to the $2b_1$ orbital since the latter is nonbonding in character and calculations show that it is primarily localized on the lone-pair orbitals of the oxygen atom. Our measured vertical β for this band is 0.36±0.05 which is reasonably close to that obtained for the lone-pair ionization in furan ($\beta_{vert} = 0.56 \pm 0.11$).[1]

Band II has a maximum at 11.77 eV and a $\beta_{vert} = 0.38 \pm 0.07$. The originating orbital has been assigned as the σ a_1 orbital.[27] According to the correlation diagram of Basch et al.,[27] this orbital correlates with the $3e'$ orbital in cyclopropane which is primarily σ(C-C) in character. The β's would then be expected to be similar, which they are, namely, 0.38 vs. 0.45 in cyclopropane.

Bands III and IV occur between 13.5 and 15.5 eV and overlapped strongly. They have been assigned to the $3b_2$ and $1a_2$ orbitals,[27] which are primarily σ(C-O) and π(C-H). They correlate with the $3e'$ and $1e'$ states of cyclopropane, respectively. Our β_{vert} for the two bands are

0.11±0.06 and 0.27±0.03. As seen from Figure 3 there is no appreciable variation in β across both bands with β ranging from 0.1 to 0.3 over the entire region. The assignment for band III is consistent with the β's observed in cyclopropane. Examination of β as a function of electron energy over the first band of cyclopropane yields a slope of -0.14/eV. Extrapolating to the IP of the $3b_2$ orbital of ethylene oxide gives a β of about 0.1 which is consistent with the observed one. This argument makes the assumption that β is a smooth function of energy over this photoelectron energy range. For the second band of cyclopropane the slope is 0.05/eV giving an extrapolated β of about 0.37 which is slightly higher than observed for the $1a_2$ orbital but not inconsistent with its assignment.

Bands V and VI occur between 16 eV and 18 eV. In appearance this band is very similar to the 15-17 eV band system in cyclopropane. As in cyclopropane the β's for these two bands are quite different, being 0.99±0.06 for the first band and 0.65±0.10 for the second. The value for the first band is about 0.2 lower than that for the corresponding cyclopropane orbital. Since bands III and IV in cyclopropane overlap, accurate slopes for β as a function of energy were not determined so the lower β of the V band in ethylene oxide may be due to the variation of β with photoelectron energy. It is also possible that this is a manifestation of the influence of the oxygen atom, but we cannot clearly distinguish between these two effects. The probability density map for the $5a_1$ orbital shows great similarity to that for the correlated $3a'$ orbital of

cyclopropane.[55] The β's of band VI are virtually identical to the $^1b_1$ π(C-H) orbital of ethylene oxide and the $1a_2''$ π(C-H) orbital of cyclopropane to which it is correlated 0.65±0.1 vs. 0.68±0.04, respectively. This indicates that either β is independent of energy in this region or that the effect of oxygen substitution fortuitously cancels the electron energy variation of β; the data are not sufficiently clear to distinguish between the two effects. As in cyclopropane Schweig and Thiel[28] have used intensity arguments to suggest that the assignment of the last two bands be reversed, but by analogy to cyclopropane we concur with the generally accepted assignments as predicted by both *ab initio* and semi-empirical calculations.[27,48,50,51,54,56]

C. Ethyleneimine

With ethyleneimine the symmetry is further reduced when compared to cyclopropane or ethylene oxide. Accordingly, the photoelectron spectrum shown in Figure 4 becomes more complex. Table 3 summarizes the IP's and β's as determined by the present study as well as previous IP measurements.[27,32,35,38]

Band I of the ethyleneimine spectrum appears at 9.85 eV with a $\beta_{vert} = 0.43 \pm 0.09$. It has been previously assigned to the $8a'$ orbital.[27] This correlates with the $1e''$ state of cyclopropane (band II) and displays a similar value of β. Our value of β for this band of ethyleneimine is much lower than that of the analogous band in pyrrole[1] ($\beta_{vert} = 1.09 \pm 0.06$). The difference between these values may be due to lack of π contributions

to the orbital which may be present in pyrrole.

From approximately 11 eV to 14 eV there is a broad band with three distinct maxima at 11.81 (band II), 12.70 (band III) and 13.47 (Band IV) eV. These have been assigned to the $4a''$, $7a'$, and $3a''$ orbitals, respectively. β drops over this region with the successive β_{vert} being 0.55±0.06, 0.55±0.03, and 0.17±0.07 for the three bands. The $4a''$ and $7a'$ σ-type orbitals both correlate with the cyclopropane $3e'$ band I and thus it is not unreasonable to expect them to display similar β's. The β's for bands II and III of ethyleneimine also agree with that for the cyclopropane $3e'$ band if the energy dependence of β observed in the latter is taken into account. The predicted value of the ethyleneimine β using an energy extrapolation of the cyclopropane results is about 0.59 which is within experimental error equal to the observed value. Band IV has been assigned to the $3a''$ π(CH) orbital and displays a β of 0.17±0.07. This measurement is lower than the value of 0.32±0.05 for the $1e''$ cyclopropane band II to which it is correlated[27] but is closer to the 0.27±0.03 observed for the $1a_2$ band IV in ethylene oxide to which it is also correlated.[27] From the molecular electron density diagrams[55] these orbitals are almost exclusively localized on the CH_2 groups and are probably unaffected by the presence of the hetero atoms. It may be that the lowering of the β values is just a manifestation of the dependence of β on electron energy although the energy change between the correlated states in this series is rather small (1.1 eV).

Bands V and VI correlate with the $3a_1'$ and $1a_2''$ states in cyclo-

propane (III and IV, Fig. 2) and the $5a_1$ and $1b_2$ states in ethylene oxide (V and VI, Fig. 3).[27] These states have been assigned to the $6a'$ and $5a'$ orbitals. They do not overlap in this molecule in contrast to cyclopropane and ethylene oxide. These states correspond to internal σ(C-C) and $\sigma(CH_2)$ orbitals. Observation of the orbital diagrams[55] shows similar behavior to the states to which they correlate in cyclopropane and ethylene oxide. The β's for band V is 0.83 ± 0.04 and for band VI 0.84 ± 0.07. Surprisingly, the large differences in the corresponding β values for the other two molecules in the series are not present here. It is possible that this is due to the energy dependence of β but is most likely associated with some as yet undetermined effect of the NH substituent. Again we concur with the energy ordering predicted by the theoretical calculations.[27,45,48,50,51,54]

IV. SUMMARY AND CONCLUSION

We have obtained the photoelectron spectra of cyclopropane, ethylene oxide, and ethyleneimine using He I radiation, at scattering angles ranging from 45°to 120°. The anisotropy parameter, β, has been determined for ethylene oxide and ethyleneimine for the first time and has been used to confirm the previous orbital assignments and correlation diagrams within this series.[27] These asymmetry parameters suggest that π-type bonding does not significantly affect the overall electronic structure of these molecules and support the idea that many of the "conjugative" properties observed for these three-membered rings may be

purely due to the high energy levels of the orbitals involved. No effects of autoionization on the angular distributions were observed.

REFERENCES

1. J. A. Sell and A. Kuppermann, *Chem. Phys.*, **33**, 367 (1978).

2. C. Utsunomiya, T. Kobayashi, and S. Nagakura, *Bull. Chem. Soc. Jap.*, **51**, 3482 (1978).

3. M. N. Piancostelli, P. R. Keller, J. W. Taylor, F. A. Grimm and T. A. Carlson, *J. Amer. Chem. Soc.*, **105**, 4235 (1983).

4. J. Cooper and R. N. Zare, *J. Chem. Phys.*, **48**, 942 (1968).

5. J. Cooper and S. T. Manson, *Phys. Rev.*, **177**, 157 (1969).

6. J. Cooper and R. N. Zare in *Lectures in Theoretical Physics*, edited by S. Gelfman, K. Mahanthappa, and N. Britten (Gordon and Breach, New York, 1969) p. 317.

7. R. M. White, T. A. Carlson, and D. P. Spears, *J. Electron Spectroscopy*, **3**, 59 (1974).

8. T. A. Carlson and C. P. Anderson, *Chem. Phys. Lett.*, **10**, 561 (1971).

9. D. M. Mintz, Ph. D. Thesis, California Institute of Technology, Pasadena, CA 1976.

10. D. C. Mason, D. M. Mintz, and A. Kuppermann, *Rev. Sci. Instrum.*, **48**, 926 (1977).

11. D. Mehaffy, P. R. Keller, J. W. Taylor, T. A. Carlson, M. O. Kraus, F. A. Grimm and J. D. Allen, *J. Electron Spectroscopy*, **26**, 213 (1982).

12. A. de Meigere, *Angew. Chem. Int. Ed.*, **19**, 809 (1979).

13. R. Gleiter, *Topics Curr. Chem.*, **86**, 197 (1979).

14. J. E. Houston and R. R. Rye, *J. Chem. Phys.*, **74**, 71 (1981).

15. A. D. Walsh, *Nature*, **159**, 167 (1947).

16. A. D. Walsh, *Nature*, **159**, 712 (1947).

17. A. D. Walsh, *Trans. Farad. Soc.*, **45**, 179 (1949).

18. Th. Förster, *Z. Phys. Chem.*, **B43**, 58 (1939).

19. C. A. Coulson and W. E. Moffitt, *J. Chem. Phys.*, **15**, 151 (1947).

20. C. A. Coulson and W. E. Moffitt, *Philos. Mag.*, **40**, 1 (1949).

21. E. Honegger, E. Heilbronner, A. Schmelzer, and W. Jian-Qi, *Isr. J. Chem.*, **22**, 3 (1982).

22. E. Honegger, E. Heilbronner, and A. Schmelzer, *Nouv. Chem.*, **6**, 519 (1982).

23. F. J. Leng and G. L. Nyberg, *J. Electron Spectroscopy*, **11**, 293 (1977).

24. D. W. Turner, C. Baker, A. D. Baker, and C. R. Brundle, *Molecular Photoelectron Spectroscopy* (Wiley-Interscience, New York, 1970) pp. 203-213.

25. G. Bieri. F. Burger, E. Heilbronner and J. P. Maier, *Helv. Chem. Acta*, **60**, 223 (1977).

26. M. J. S. Dewar and S. P. Worley, *J. Chem. Phys.*, **50**, 654 (1969).

27. H. Basch, M. B. Robin, N. A. Kuebler, C. Baker, and D. W. Turner, *J. Chem. Phys.*, **51**, 52 (1969).

28. A. Schweig and W. Thiel, *Chem. Phys. Lett.*, **21**, 541 (1973).

29. A. W. Potts and D. G. Streets, *J. Chem. Soc. Farad. Trans. II*, **70**,

875 (1974).

30. A. W. Potts, T. A. Williams, and W. C. Price, *Farad. Disc. Chem. Soc.*, **54**, 104 (1972).

31. N. Bodor, M. J. S. Dewar, W. B. Jennings, and S. D. Worsley, *Tetrahedron*, **26**, 4109 (1970).

32. K. Yoshikawa, M. Hashimoto, and I. Morishimo, *J. Amer. Chem. Soc.*, **96**, 288 (1974).

33. D. S. C. Yee, A. Hamnett, and C. E. Brion, *J. Electron Spectroscopy*, **8**, 291 (1976).

34. M. I. Al-Joboury and D. W. Turner, *J. Chem. Soc.*, , 4434 (1964).

35. D. H. Ave, H. M. Webb, W. R. Davidson, M. Vidal, M. T. Bowers, H. Goldwhite, L. E. Vertal, J. E. Vertal, J. E. Douglas, P. A. Kollman, and G. L. Kenyon, *J. Amer. Chem. Soc.*, **102**, 5151 (1980).

36. S. Evans, P. J. Joachim, A. F. Orchard and D. W. Turner, *Int. J. Mass. Spec. and Ion Phys.*, **9**, 41 (1972).

37. E. Lindholm, C. Fridh, and L. Åsbrink, *Farad. Disc. Chem. Soc.*, **54**, 127 (1972).

38. G. Bieri, L. Åsbrink, and W. Von Niessan, *J. Electron Spectroscopy*, **27**, 129 (1982).

39. R. Krässig, D. Rienke and H. Barmgärtel, *Ber. Buns. Gells.*, **79**, 116 (1975).

40. K. Johnson, I. Powis, and C. J. Danby, *Chem. Phys.*, **70**, 329 (1982).

41. J. R. Collins and G. A. Gallup, *J. Amer. Chem. Soc.*, **104**, 1530

(1982).

42. E. Haselbach, *Chem. Phys. Lett.*, **7**, 428 (1970).

43. C. G. Rowland, *Chem. Phys. Lett.*, **9**, 169 (1971).

44. F. A. Carlson, G. E. McGuire, A. E. Jonas, K. L. Cheng, C. P. Anderson, C. C. Lu, and B. P. Pullen in *Electron Spectroscopy*, edited by D. A. Shirley (North-Holland, Amsterdam 1972) p. 207.

45. D. T. Clark, *Theo. Chem. Acta*, **15**, 225 (1969).

46. E. Kochanski and J. M. Lehn, *Theo. Chem. Acta*, **14**, 281 (1969).

47. A. Skancke, *J. Molec. Struct.*, **30**, 95 (1976).

48. W. Von Niessen, L. S. Cederbaum, and W. P. Kraemer, *Theor. Chim. Acta*, **44**, 85 (1977).

49. H. Marsman, *Tetrahedron*, **27**, 4377 (1971).

50. D. T. Clark, *Theo. Chem. Acta*, **10**, 111 (1968).

51. C. Fridh, *J. Chem. Soc. Farad. Disc. 2*, **75**, 993 (1979).

52. E. Lindholm, C. Fridh, and L. Åsbrink, *Farad. Disc. Chem. Soc.*, **54**, 127 (1972).

53. G. Bieri, L. Åsbrink, and W. Von Niessan, *J. Electron Spectroscopy*, **27**, 129 (1982).

54. P. D. Mollere and K. N. Houk, *J. Amer. Chem. Soc.*, **99**, 3226 (1977).

55. W. L. Jorgensen and L. Salem, *The Organic Chemistry Book of Orbitals* (Academic Press, New York, 1973) pp. 153-159.

56. D. P. Chang, F. G. Herring, and D. McWilliams, *J. Chem. Soc.*

Farad. Trans. 2, **70**, 193 (1974).

TABLE 1. Cyclopropane

Band/Orbital	Vertical IP (eV)		β		
	This Work	Other Work	β_{vertical}	β range across band	β_{vert} (other work)[a]
I/3e′	[10.51,11.26][b]	[10.53,11.3][c] [10.6,11.3][d,e] [10.3,11.3][f]	0.46±.07 0.44±.10	0.21±.09 to 0.71± 0.15	(0.60–0.50)±.05
II/1e″	12.94	13.2[c,d] 13.0[e,f]	0.32±.05	0.23±.08 to 0.56±.10	0.43±.05
III/3a′	15.74	15.7[c,d,e] 15.6[f]	1.18±.05	0.43±.15 to 1.31±.15[g]	1.25±.05
IV/1a″	16.66	16.7[c] 16.5[d] 16.6[e,f]	0.67±.04		0.65±.10
V/2e′	19.51	19.3[d] 19.5[e,f]	0.40±.08	0.25±.10 to 0.64±.10	0.90±.10

a) Reference 23.
b) Numbers in brackets refer to both components of Jahn-Teller split band.
c) Reference 27.
d) Reference 36.
e) Reference 25.
f) Reference 37.
g) Range is for both bands III and IV since they overlap.

TABLE 2. Ethylene Oxide

Band/Orbital	Vertical IP (eV)		β	
	This work	Other Work	β_{vertical}	β range across band
I/$2b_2$	10.57	10.57[a,b] 10.56[c]	0.36±.05	0.31±.04 to 0.40±.06
II/$6a_1$	11.77	11.7[a] 11.85[b,c]	0.38±.07	0.17±.11 to 0.52±.14
III/$2b_1$	13.75	13.7[a] 14.0[b] 13.73[c]	0.11±.06	0.02±.09 to 0.26±.14[d]
IV/$1a_2$	14.23	14.2[a] 14.0[b] 14.16[c]	0.27±.03	
V/$5a_1$	16.51	16.6[a,b] 16.52[c]	0.99±.06	0.40±.04 to 1.17±.09[e]
VI/$1b_2$	17.31	17.4[a,b] 17.2[c]	0.65±.10	

a) Reference 27.
b) Reference 38.
c) Reference 35
d) Range is for both bands III and IV since they overlap.
e) Range is for both bands V and VI since they overlap.

TABLE 3. Ethyleneimine

Band/Orbital	Vertical IP (eV)		β	
	This work	Other Work	β_{vertical}	β range across band
I/8a′	9.85	9.8[a] 9.85[b,c] 9.83[d]	0.43±.09	0.13±.23 to 0.65±.05
II/4a″	11.81	11.8[a] 11.9[b,c] 11.79[d]	0.55±.06	0.08±.11 to 0.71±.05[e]
III/7a′	12.70	12.5[a] 12.16[d] 12.7[c]	0.55±.03	
IV/3a″	13.47	13.5[a] 13.45[d] 13.6[c]	0.17±.07	
V/6a′	15.93	15.9[a] 15.69[d] 16.0[c]	0.83±.09	0.50±.10 to 0.83±.09
VI/5a′	17.47	17.4[a] 17.19[d] 17.5[c]	0.84±.07	0.65±.07 to 0.86±.06

a) Reference 27.
b) Reference 32.
c) Reference 38.
d) Reference 35.
e) Range is for bands II, III, and IV since they overlap.

FIGURE CAPTIONS

Figure 1. Block diagram of the variable angle photoelectron spectrometer. He, cylinder of ultra high purity helium; ZT, liquid nitrogen cooled zeolite trap for lamp helium supply; RB, lamp ballast resistor; LPS, lamp dc power supply; SC, sample chamber, PC, photocathode for light flux measurements; CL, chamber side electron lens elements; ANALYZER, hemispherical electron energy analyzer; ML, electron multiplier side electron lens element; S, Spiraltron electron multiplier; CPS, Spiraltron cathode power supply; APS, Spiraltron anode power supply; R. C., resistance and capacitance of differentiating network for Spiraltron.

Figure 2. Photoelectron spectrum (b) and variation of β with ionization potential (a) for cyclopropane using He I (21.22 eV) radiation. The spectrum was obtained at a detector angle of 54.7 degrees.

Figure 3. Photoelectron spectrum (b) and variation of β with ionization potential (a) for ethylene oxide using He I (21.22 eV) radiation. The spectrum was obtained at a detector angle of 54.7 degrees.

Figure 4. Photoelectron spectrum (b) and variation of β with ionization potential (a) for ethyleneimine using He I (21.22 eV) radiation. The spectrum was obtained at a detector angle of 54.7 degrees.

FIGURE 1.

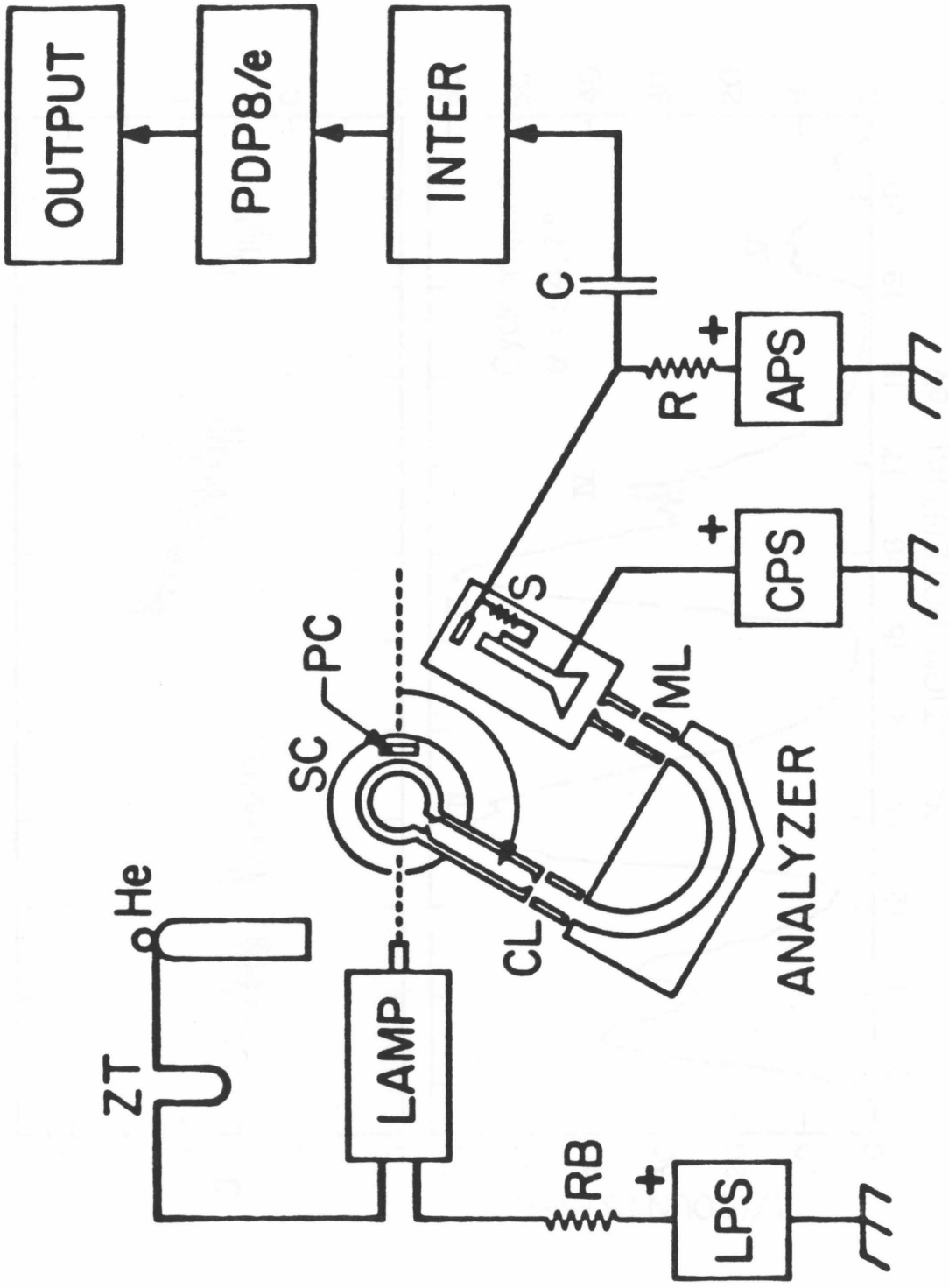
OUTPUT
PDP8/e
INTER
C
R
APS
CPS
S
PC
SC
ML
ANALYZER
CL
He
ZT
LAMP
RB
LPS

FIGURE 2.

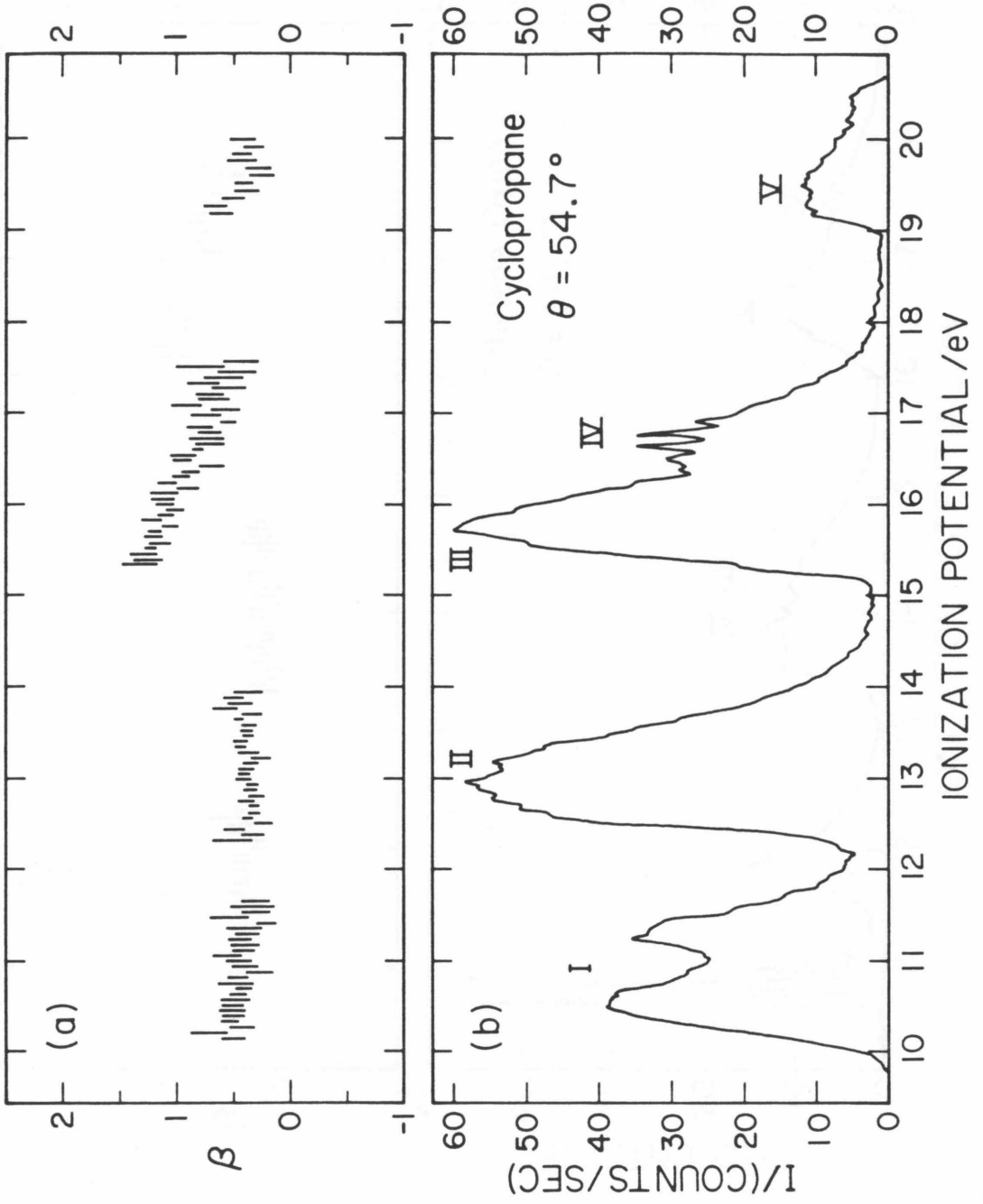
(a)
β
(b)
Cyclopropane
θ = 54.7°
I
II
III
IV
V
I/(COUNTS/SEC)
IONIZATION POTENTIAL/eV

FIGURE 3.

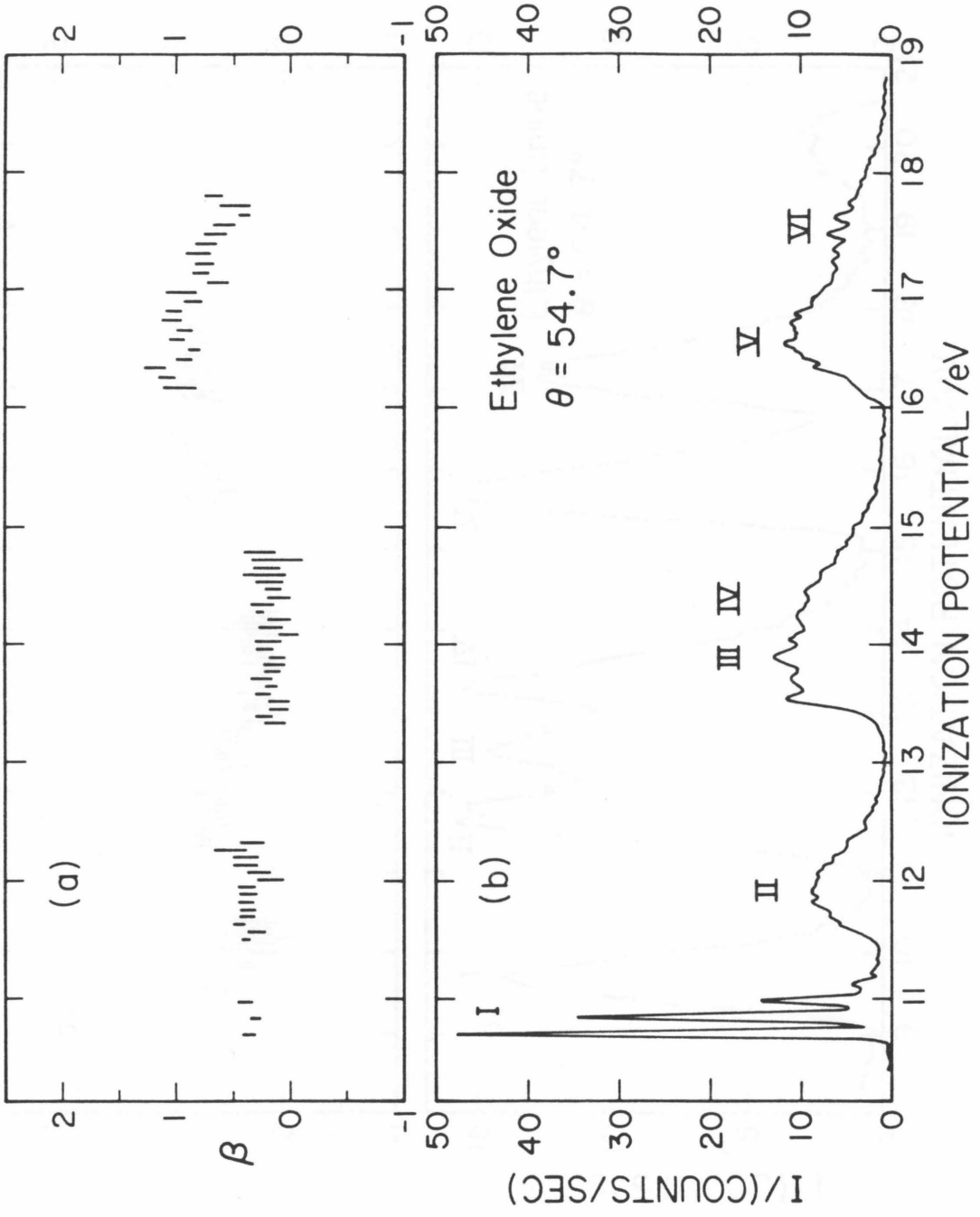
(a)
β
(b)
Ethylene Oxide
θ = 54.7°
I
II
III IV
V
VI
I /(COUNTS/SEC)
IONIZATION POTENTIAL /eV

FIGURE 4.

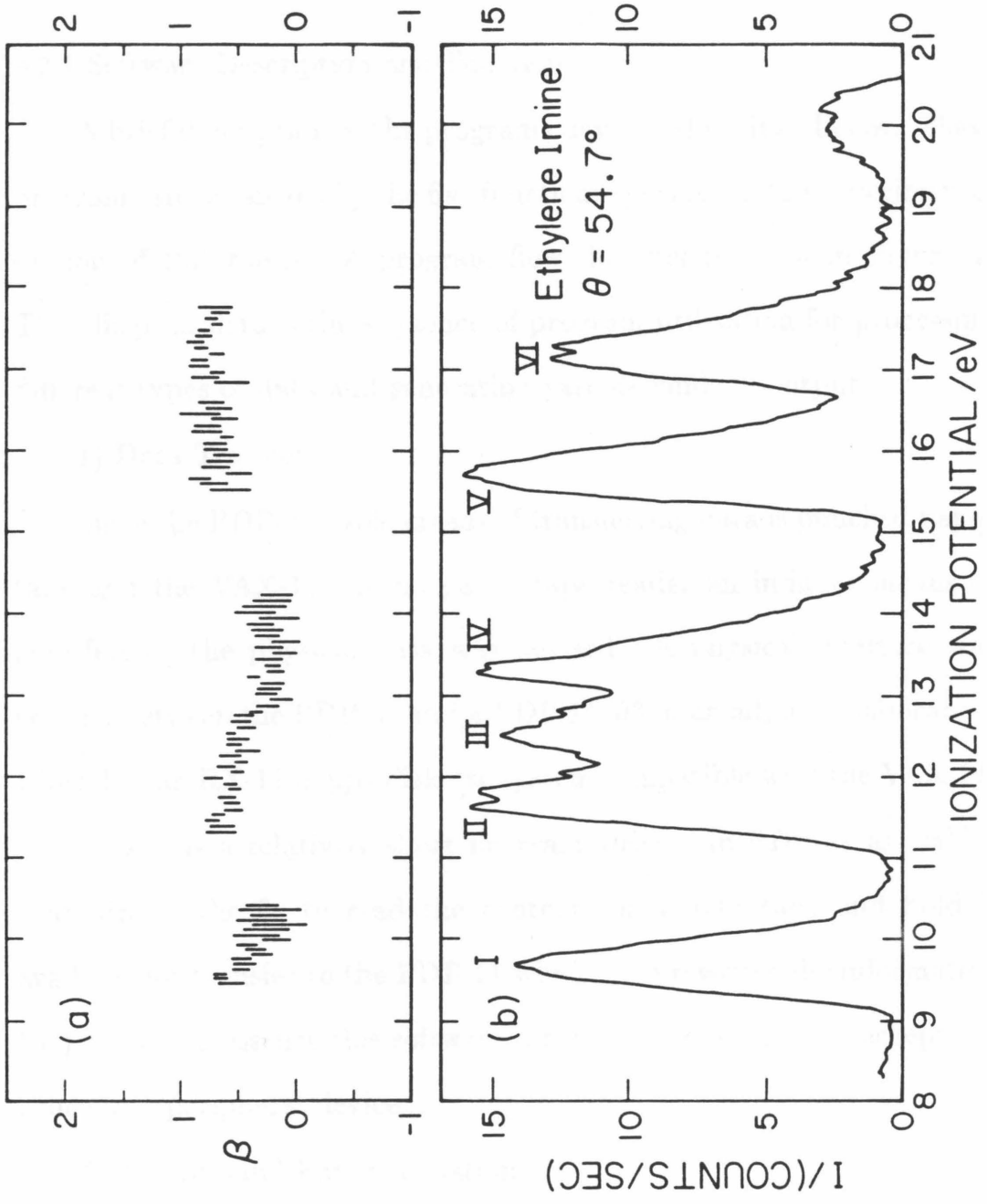
(a)
β
(b)
I
II
III
IV
V
VI
Ethylene Imine
θ = 54.7°
I/(COUNTS/SEC)
IONIZATION POTENTIAL/eV

APPENDIX 2

SOFTWARE

A2.1 Software Description and Function

A brief description of the programs developed is given below. These programs are organized by the five functions specified in the experimental section of this thesis. A program flow diagram is given in Figure 1. This diagram details the sequence of program utilization for processing different types of data and generating various kinds of output.

1) Data Transfer

Since the PDP-8e's sole means of transferring data is punched paper tape and the VAX-11 has no paper tape reader an indirect means of transferring the physical data was devised. A physical interface was erected between the PDP-8e and a PDP 11/03 in an adjacent laboratory which has an RX-11 floppy diskette system compatible with the VAX-11.

Link11 is a relatively short program written in PDP-8e assembler that directs the 8e to read the contents of a data tape and hold it available for transfer to the PDP 11 which then rewrites the information to diskette. In essence this software directs each computer to accept the other as a peripheral device.

2) Background Parametrization

BACK.FOR. This program reads in the background spectra, smooths the data according to the smoothing routine of Savitzky and Golay,[1] and performs a weighted least squares fit to an n^{th} order polynomial.[2] Test-

ing has yielded that the best fits are generally obtained with a fifth order polynomial. The principal output from this program is the polynomial coefficients and the χ^2s, the goodness of fit parameter.

This represents a profound improvement in background handling. Previous procedure involved a visual fitting of the data to three line segments which frequently yielded less then optimal results. In addition, the smoothing routine's capacity was increased from 13 channels to a maximum of 25 in the Fortran version.

3) Spectral Reorganization

In order to calculate the asymmetry parameter, it is first necessary to reorganize the spectral data.

BETVSIP.FOR This program reads in the spectra and smooths the data. The background coefficients are read in and the appropriate background subtracted if desired by the user.

The program then restructures the data from a sequence of intensities organized by angle to a sequence of arrays organized by channel number (ionization potential.)

The chief improvements, besides the expanded smoothing routine and the inherent advantages of Fortran, are the program's abilities to process every channel of data in a spectrum and to greatly increase the number of channels permitted in each band. Former limits were a 125 channel maximum per band with only odd numbered channels being processed. Currently all data is usable with a limit of 511 channels imposed only by the storage capabilities of the PDP-8e.

MULTMAX.FOR This is an ancillary program of BETVSIP.FOR and performs an analogous function for bands with well-resolved structure. The spectra are read in as above but only spectral data for peak maxima are outputted. An algorithm determines the maxima of each spectrum and a matching routine then determines those maxima which exist in all angles of the distribution. Only channels corresponding to matched maxima are reorganized.

In the case of bands with well-defined maxima, it is possible to use the partially reduced data from the data taking program to bypass spectral reorganization. Such data can be inserted manually into the interactive version of the β calculating program described below.

4) β Calculation

There are two programs for calculation β, BETA.FOR which accepts the reorganized output of BETVSIP or MULTMAX, and INTERBETA.FOR which calculates β interactively. Both use the relationships described in section 3.6. Two output files are created, one containing the complete data, calculated betas and extensive statistics, and another abbreviated file for plotting purposes. Additionally, the interactive version displays the results at the terminal.

By using the VAX-11, analysis that used to take 45 minutes can be obtained in a tenth of the time with more complete statistics.

5) Plotting Programs

There are currently four plotting programs for displaying data on the VAX-11.

QUICKPLOT.FOR This program utilizes the terminal graphics capabilities of the VAX-11 to plot any chosen spectrum on any terminal that has advanced graphics capabilities compatible with Digital's VT-100 series CRT terminals, thus providing the means to quickly scan a spectrum for transmission errors, noise spikes or simple identity verification before processing.

HRSPLOT.FOR This program provides a means of plotting a high resolution vibrational spectrum (or any other individual spectrum). The spectrum is read in and smoothed. A background is subtracted and the resultant intensities plotted within a 8.5 x 11 inch format with labeled axis. The program also provides options to expand any chosen portion of the spectrum by any user selected scale factor and to externally input a title for the plot at the time of execution.

The XY plotter on the 8e has no labelling capacity and produced variable sized plots.

CHIMERA.FOR This is a program written specifically to plot the background spectra and the values generated from the background coefficients together on the same graph. This program provides a quick visual check on the fits produced by BACK.FOR and is useful for comparing the results generated by different order polynomials. The program itself is very similar to HRSPLOT except that it lacks the expansion and external labeling options and produces a plot for each of the nine spectra in the background.

BPLOT.FOR This is the most important plotting program. It

creates a labelled two panel display. The upper panel contains a plot of beta values with error bars calculated from BETA.FOR. The lower panel contains a user selected base spectrum appropriate to the ionization range of the betas. As in HRSPLOT, options exist to expand any chosen portion of the base spectrum and to externally provide a title.

A2.2 Software Utilization and Program Listings

1)DATA TRANSFER

LINK11.ASM This assembler program for the PDP-8e controls the transfer of data to a PDP-11 computer.

Starting Address=200
Program control is achieved through the panel switches of the 8e, or from the 11 by transmission of control characters:
G= start transmission
S= restart program
F= immediate halt

```
*200
0200    7300    OPDIR,  CLA CLL
0201    6321    FLAG,   KSF2
0202    7410            SKP
0203    5273            JMP KB2
0204    6031            KSF
0205    7410            SKP
0206    5270            JMP KB
0207    5201            JMP FLAG
0210    7000    OPG,    NOP
0211    4260            JMS SERV
0212    6020            PCE
0213    6014            RFC
0214    6011            RSF
0215    5214            JMP.-1
0216    7300            CLA CLL
0217    6012            RRB
0220    0230            AND MASK
0221    6336            TLS2
0222    6331            TSF2
0223    5222            JMP.-1
0224    7300            CLA CLL
0225    4260            JMS SERV
0226    5210    RETURN, JMP OPG
0227    0200    MASK,   200
0230    7577    NMASK,  7577
0231    0000    ACNOW,  0
0232    0307    G,      307
0233    0306    F,      306
0234    0323    S,      323

*260
0260    0000    SERV,   0
0261    6321            KSF2
0262    7410            SKP
0263    5273            JMP KB2
0264    6031            KSF
0265    7410            SKP
0266    5270            JMP KB
0267    5326            JMP EXIT
0270    6032    KB,     KCC
0271    6036            KRB
0272    5277            JMP CHAR
0273    6322    KB2,    KCC2
```

```
0274    6326            KRB2
0275    1227            TAD MASK
0276    5277            JMP CHAR
0277    3231    CHAR,   DCA ACNOW
0300    1231            TAD ACNOW
0301    7041            CIA
0302    1233            TAD F
0303    7450            SNA
0304    5324            JMP OPF
0305    7300            CLA CLL
0306    1231            TAD ACNOW
0307    7041            CIA
0310    1234            TAD S
0311    7450            SNA
0312    5323            JMP OPS
0313    7300            CLA CLL
0314    1231            TAD ACNOW
0315    7041            CIA
0316    1232            TAD G
0317    7450            SNA
0320    5210            JMP OPG
0321    5326            JMP EXIT
0322    7000            NOP
0323    5200    OPS,    JMP OPDIR
0324    7402    OPF,    HLT
0325    7000            NOP
0326    7300    EXIT,   CLA CLL
0327    5660            JMP I SERV
0330    7402            HLT
```

2) BACKGROUND PARAMETERIZATION

This program, BACK.FOR, will parameterize the background.
All spectra must be concatenated into for003 or its logical equivalent.

input:

'external'*****for002
NANGLE, AV, MODE, NTERMS
(I2/I2/I2/I2)
NANGLE =the number of angles to be parameterized
AV =average per; the convolution parameter for the smoothing
rountine-use any odd number between 5 and 25.
MODE =determines the statistical weighting of the data
0-equal weights for all points
nonzero-instrumental weights of the points
NTERMS =the order of the polynomial function

'internal'*****for003
all data taken from spectrum file as transmitted

'output'*****for008
NTERMS
ANGLE, A(I), I=1, NTERMS, (CHISQR)
Output file is exactly compatible for input into
BETA.EXE without modification. CHISQR is not read
by BETA but is printed for inspection purposes only.
A =array of coefficients of the polynomial

```
C*****************************************************************
      DIMENSION COUNTS(511), XDATA(511), XARRAY(511), YARRAY(511), A(10)
      DOUBLE PRECISION SUMX, SUMY, XTERM, YTERM, ARRAY, CHISQ, SAVE
      DIMENSION SUMX(19), SUMY(10), ARRAY(10, 10)
      INTEGER AV, GATE
      REAL IP1, IP2
C     READ INPUTS
C*************************************************************
C     READ EXTERNAL INPUTS ON FOR002.DAT
      READ (2, 100) NANGLE, AV, MODE, NTERMS
100   FORMAT (I2/I2/I2/I2)
      WRITE(8, 35) NTERMS
35    FORMAT(I2)
C*****************************************************************
C     READ INTERNAL DATA
      DO 105 N=1, NANGLE
      IF (N.NE.1) GO TO 107
      READ (3, 108) IP1, IP2, ANGLE
108   FORMAT(///, 11X, F7.4, 4X, F7.4, 4X, F6.2, 11X, F6.3)
      GO TO 106
107   READ (3, 101) IP1, IP2, ANGLE
101   FORMAT(/, 11X, F7.4, 4X, F7.4, 4X, F6.2, 11X, F6.3)
106   READ (3, 102) SCAN, MV, MULT, GATE, IDWELL
102   FORMAT(F8.4/I5/I5/I5/I5//)
      DWELL=IDWELL*GATE/120.
      NWIDTH=MV*MULT
      NCHAN=SCAN*1000/NWIDTH
      READ (3, 103) (COUNTS(I), I=1, NCHAN)
```

```
103       FORMAT(F10.2)
C         END INPUT SEQUENCE
C*************************************************************
C         CALL THE SMOOTHING ROUTINE
          CALL SGSMOOTH(AV, NCHAN, COUNTS, XDATA)
          DO 225 MX=1, NCHAN
          COUNTS(MX)=XDATA(MX)
225       CONTINUE
C*************************************************************
C         SET UP TWO ARRAYS FOR POLFIT: IP AND COUNTS
          DO 5 NN=1, NCHAN-(av+1)/2
          YARRAY(NN)=COUNTS(NN-1+(AV+1)/2)/(DWELL)
          XARRAY(NN)=IP1+((NN-2+(AV+1)/2)*NWIDTH)/1000.
          IF (XARRAY(NN).LE.(21.00)) GO TO 5
          NCHAN=NN-1
          GO TO 7
5         CONTINUE
7         CALL POLYFIT(XARRAY, YARRAY, NCHAN, NTERMS, MODE, A, CHISQR)
          WRITE(8, 40) ANGLE, (A(I), I=1, NTERMS), CHISQR
40        FORMAT(F10.2, 10(E15.8))
105       CONTINUE
          END
C*************************************************************
          SUBROUTINE SGSMOOTH(NAV, N, DATA, XDATA)
          DIMENSION DATA(511), XDATA(511), P(25), COEFF(11, 15)
          DIMENSION NORM(11)
          DATA (COEFF(1, L), L=1, 3)/17, 12, -3/
          DATA (COEFF(2, L), L=1, 4)/7, 6, 3, -2/
          DATA (COEFF(3, L), L=1, 5)/59, 54, 39, 14, -21/
          DATA (COEFF(4, L), L=1, 6)/89, 84, 69, 44, 9, -36/
          DATA (COEFF(5, L), L=1, 7)/25, 24, 21, 16, 9, 0, -11/
          DATA (COEFF(6, L), L=1, 8)/167, 162, 147, 122, 87, 42, -13, -78/
          DATA (COEFF(7, L), L=1, 9)/43, 42, 39, 34, 27, 18, 7, -6, -21/
          DATA (COEFF(8, L), L=1, 10)/269, 264, 249, 224, 189, 144, 89, 24, -51, -136/
          DATA (COEFF(9, L), L=1, 11)/329, 324, 309, 284, 249, 204, 149, 84, 9, -76, -171/
          DATA (COEFF(10, L), L=1, 12)/79, 78, 75, 70, 63, 54, 43, 30, 15, -2, -21, -42/
          DATA (COEFF(11, L), L=1, 13)/467, 462, 447, 422, 387, 322, 287, 222, 147, 62, -33,
     *-138, -253/
          DATA NORM/35, 21, 231, 429, 143, 1105, 323, 2261, 3059, 8059, 5175/
          M=N-(NAV-1)
          NCOEFF=(NAV+1)/2
          LCOEFF=NCOEFF-2
C         TO GET THE CORRECT MEMBER OF THE COEFF AND NORM ARRAYS
C         LOAD POINTS INTO P ARRAY
C         ARRAY INITIALLY OFFSET FOR CHANNEL ADVANCE SEQUENCE
          DO 10 I=1, NAV-1
10        P(I+1)=DATA(I)
C         SMOOTHING LOOP
          DO 200 I=1, M
          J=I+(NAV-1)
          DO 11 K=1, NAV-1
11        P(K)=P(K+1)
          P(NAV)=DATA(J)
C         SET UP LOOP TO DO SUM
          SUM=COEFF(LCOEFF, 1)*P(NCOEFF)
```

```
      DO 22 L=2, NCOEFF
22    SUM=SUM+COEFF(LCOEFF, L)*(P(NCOEFF-(L-1))+P(NCOEFF+(L-1)))
      XDATA(I+NCOEFF-1)=SUM/FLOAT(NORM(LCOEFF))
200   CONTINUE
      RETURN
      END
C*************************************************************
      SUBROUTINE POLYFIT(X, Y, NPTS, NTERMS, MODE, A, CHISQR)
      DOUBLE PRECISION SUMX, SUMY, XTERM, YTERM, ARRAY, CHISQ
      DIMENSION X(1), Y(1), A(1)
      DIMENSION SUMX(19), SUMY(10), ARRAY(10, 10)
C     ACCUMULATE WEIGHTED SUMS
C*************************************************************
11    NMAX=2*NTERMS-1
      DO 13 N=1, NMAX
13    SUMX(N)=0.
      DO 15 J=1, NTERMS
15    SUMY(J)=0.
      CHISQ=0.
21    DO 50 I=1, NPTS
      XI=X(I)
      YI=Y(I)
31    IF(MODE) 32, 37, 37
32    IF(YI) 35, 37, 33
33    WEIGHT=1./YI
      GO TO 41
35    WEIGHT=1./(-YI)
      GO TO 41
37    WEIGHT=1.
41    XTERM=WEIGHT
      DO 44 N=1, NMAX
      SUMX(N)=SUMX(N)+XTERM
44    XTERM=XTERM*XI
45    YTERM=WEIGHT*YI
      DO 48 N=1, NTERMS
      SUMY(N)=SUMY(N)+YTERM
48    YTERM=YTERM*XI
49    CHISQ=CHISQ+WEIGHT*YI**2
50    CONTINUE
C
C     CONSTRUCT MATRICES AND CALCULATE COEFFICIENTS
C
51    DO 54 J=1, NTERMS
      DO 54 K=1, NTERMS
      N=J+K-1
      ARRAY(J, K)=SUMX(N)
54    CONTINUE
      DELTA=DETERM(ARRAY, NTERMS)
      IF (DELTA) 61, 57, 61
57    CHISQR=0.
      DO 59 J=1, NTERMS
59    A(J)=0.
      GO TO 80
61    DO 70 L=1, NTERMS
62    DO 66 J=1, NTERMS
      DO 65 K=1, NTERMS
```

```
          N=J+K-1
65        ARRAY(J, K)=SUMX(N)
66        ARRAY(J, L)=SUMY(J)
70        A(L)=DETERM(ARRAY, NTERMS)/DELTA
C
C         CALCULATE CHI SQUARE
C
71        DO 75 J=1, NTERMS
          CHISQ=CHISQ-2.*A(J)*SUMY(J)
          DO 75 K=1, NTERMS
          N=J+K-1
75        CHISQ=CHISQ+A(J)*A(K)*SUMX(N)
76        FREE=NPTS-NTERMS
77        CHISQR=CHISQ/FREE
80        RETURN
          END
C*************************************************************
C         PURPOSE:
C         CALCULATE THE DETERMINATE OF A SQUARE MATRIX
C
C         USAGE:
C         DET=DETERM(ARRAY, NORDER)
C
C         DESCRIPTION OF PARAMETERS:
C         ARRAY-MATRIX
C         NORDER-DEGREE OF MATRIX(ORDER OF DETERMINATE)
C
C         COMMENTS: THIS SUBROUTINE DESTROYS THE INPUT MATRIX ARRAY
C         VALID FOR NORDER UP TO 10
          FUNCTION DETERM(ARRAY, NORDER)
          DOUBLE PRECISION ARRAY, SAVE
          DIMENSION ARRAY(10, 10)
10        DETERM=1.
11        DO 50 K=1, NORDER
          IF (ARRAY(K, K)) 41, 21, 41
21        DO 23 J=K, NORDER
          IF (ARRAY(K, J)) 31, 23, 31
23        CONTINUE
          DETERM=0.
          GO TO 60
31        DO 34 I=K, NORDER
          SAVE=ARRAY(I, J)
          ARRAY(I, J)=ARRAY(I, K)
34        ARRAY(I, K)=SAVE
          DETERM=-DETERM
C
C         SUBTRACT ROW K FROM LOWER ROWS TO GET DIAGONAL MATRIX
C
41        DETERM=DETERM*ARRAY(K, K)
          IF(K-NORDER) 43, 50, 50
43        KI=K+1
          DO 46 I=KI, NORDER
          DO 46 J=KI, NORDER
46        ARRAY(I, J)=ARRAY(I, J)-ARRAY(I, K)*ARRAY(K, J)/ARRAY(K, K)
50        CONTINUE
60        RETURN
          END
```

3) SPECTRAL REORGANIZATION

This program, BETVSIP.FOR, is designed to smooth and reorganize spectral data for rapid calculation of betas in BETA.EXE.
All spectra must be concatenated into for003 or its logical equivalent.

Input:

'External'*****for002

The bulk of this file is written through to 'main' output for use in BETA.EXE

N, AV, PNS, THRESH, IBACK, ARGON
(I2/I2/F6.2/I3/I2/I2)
N=number of angles in the distribution
AV=average per; the convolution parameter-use any positive odd number between 5 and 25.
PNS=pressure no sample in microns
THRESH=threshold counts; the minimum counts to calculate a beta
IBACK=background parameter
1-include a background
non1-do not include a background
ARGON=is the sample argon?
0-no
1-yes

'Internal'*****for003

All data taken from spectrum file as transmitted
IP1, IP2, ANGLE(N), PRESS(N)
(///, 11X, F7.4, 4X, F7.4, 4X, F6.2, 11X, F6.3)
IP1=starting ip in eV
IP2=ending ip in eV
ANGLE=angle of spectrum in degrees
PRESS=pressure (uncorrected) in microns

SCAN, MV, MULT, DWELL
(F8.4/I5/I5//I5//)
SCAN=length of scan in eV
MV=channel step size in meV
MULT=channel step multiplier
GATE= time per channel per scan
DWELL=number of scans per spectrum

(COUNTS(I, N), I=1, NCHAN)
(F10.2)

Output:

'Main'*****for005

Note: this file must be assigned since for005 is default read

N, AV, PNS, THRESH, IBACK, ARGON
(I2/I2/F6.2/I3/I2/I2)
N=number of angles in the distribution
AV=average per; the convolution parameter-use any positive odd number between 5 and 25.
PNS=pressure no sample in microns
THRESH=threshold counts; the minimum counts to calculate a beta
IBACK=background parameter

```
          1-include a background
          non1-do not include a background
ARGON=is the sample argon
          0-no
          1-yes

SCAN, MV, MULT, IP1, DWELL
(F8.4/I5/I5/F8.4/I5)
SCAN=length of scan in eV
MV=channel step size in meV
MULT=channel step multiplier
IP1=starting ip in eV
DWELL=duration of time in each channel in sec

THETA(I), PRESS(I), COUNTS(I)
(F6.2, 4X, F6.2, 4X, F10.2)
THETA=angle in degrees
PRESS=pressure uncorrected in microns
COUNTS=counts(smoothed)

C*************************************************
C         THIS PROGRAM WILL PERFORM THE TASK BETA VS IP
C         DOES ON THE PDP 8E NAMELY REORGANIZE THE SPECTRAL
C         DATA FOR RAPID INPUT INTO BETA.FOR
C*************************************************
          COMMON COUNTS(511, 9), ANGLE(9), PRESS(9)
          DIMENSION XDATA(511)
          INTEGER THRESH, AV, GATE, ARGON
          REAL IP1, IP2
C         READ INPUTS
C*********************************************************
C         READ EXTERNAL INPUTS ON FOR002.DAT
C         AND PRINT THEM THROUGH TO PRIMARY OUTPUT FILE
          READ (2, 100) NANGLE, AV, PNS, THRESH, IBACK, ARGON
          WRITE (5, 100) NANGLE, AV, PNS, THRESH, IBACK, ARGON
100       FORMAT (I2/I2/F6.2/I3/I2/I2)
C*************************************************************
C         READ INTERNAL DATA
          DO 105 N=1, NANGLE
          IF (N.NE.1) GO TO 107
          READ (3, 108) IP1, IP2, ANGLE(N), PRESS(N)
108       FORMAT(///, 11X, F7.4, 4X, F7.4, 4X, F6.2, 11X, F6.3)
          GO TO 106
107       READ (3, 101) IP1, IP2, ANGLE(N), PRESS(N)
101       FORMAT(/, 11X, F7.4, 4X, F7.4, 4X, F6.2, 11X, F6.3)
106       READ (3, 102) SCAN, MV, MULT, GATE, IDWELL
102       FORMAT(F8.4/I5/I5/I5/I5//)
          DWELL=IDWELL*GATE/120.
          NWIDTH=MV*MULT
          NCHAN=SCAN*1000/NWIDTH
          READ (3, 103) (COUNTS(I, N), I=1, NCHAN)
103       FORMAT(F10.2)
105       CONTINUE
          WRITE(5, 109) SCAN, MV, MULT, IP1, DWELL
109       FORMAT(F8.4/I5/I5/F8.4/F8.4)
C         END INPUT SEQUENCE
```

```
C*************************************************************
C       CALL THE SMOOTHING ROUTINE
        DO 201 L=1, NANGLE
        CALL SGSMOOTH(AV, NCHAN, COUNTS(1, L), XDATA)
        DO 225 MX=1, NCHAN
        COUNTS(MX, L)=XDATA(MX)
225     CONTINUE
201     CONTINUE
C*************************************************************
C       ENTER PRINT OUT ROUTINE
        DO 300 M=1, NCHAN
        DO 310 N=1, NANGLE
        WRITE (5, 301) ANGLE(N), PRESS(N), COUNTS(M, N)
301     FORMAT (F6.2, 4X, F6.2, 4X, F10.2)
310     CONTINUE
300     CONTINUE
        END
C*************************************************************
        SUBROUTINE SGSMOOTH(NAV, N, DATA, XDATA)
        DIMENSION DATA(511), XDATA(511), P(25), COEFF(11, 15)
        DIMENSION NORM(11)
        DATA (COEFF(1, L), L=1, 3)/17, 12, -3/
        DATA (COEFF(2, L), L=1, 4)/7, 6, 3, -2/
        DATA (COEFF(3, L), L=1, 5)/59, 54, 39, 14, -21/
        DATA (COEFF(4, L), L=1, 6)/89, 84, 69, 44, 9, -36/
        DATA (COEFF(5, L), L=1, 7)/25, 24, 21, 16, 9, 0, -11/
        DATA (COEFF(6, L), L=1, 8)/167, 162, 147, 122, 87, 42, -13, -78/
        DATA (COEFF(7, L), L=1, 9)/43, 42, 39, 34, 27, 18, 7, -6, -21/
        DATA (COEFF(8, L), L=1, 10)/269, 264, 249, 224, 189, 144, 89, 24, -51, -136/
        DATA (COEFF(9, L), L=1, 11)/329, 324, 309, 284, 249, 204, 149, 84, 9, -76, -171/
        DATA (COEFF(10, L), L=1, 12)/79, 78, 75, 70, 63, 54, 43, 30, 15, -2, -21, -42/
        DATA (COEFF(11, L), L=1, 13)/467, 462, 447, 422, 387, 322, 287, 222, 147, 62, -33,
    *-138, -253/
        DATA NORM/35, 21, 231, 429, 143, 1105, 323, 2261, 3059, 8059, 5175/
        M=N-(NAV-1)
        NCOEFF=(NAV+1)/2
        LCOEFF=NCOEFF-2
C       TO GET THE CORRECT MEMBER OF THE COEFF AND NORM ARRAYS
C       LOAD POINTS INTO P ARRAY
C       ARRAY INITIALLY OFFSET FOR CHANNEL ADVANCE SEQUENCE
        DO 10 I=1, NAV-1
10      P(I+1)=DATA(I)
C       SMOOTHING LOOP
        DO 200 I=1, M
        J=I+(NAV-1)
        DO 11 K=1, NAV-1
11      P(K)=P(K+1)
        P(NAV)=DATA(J)
C       SET UP LOOP TO DO SUM
        SUM=COEFF(LCOEFF, 1)*P(NCOEFF)
        DO 22 L=2, NCOEFF
22      SUM=SUM+COEFF(LCOEFF, L)*(P(NCOEFF-(L-1))+P(NCOEFF+(L-1)))
        XDATA(I+NCOEFF-1)=SUM/FLOAT(NORM(LCOEFF))
200     CONTINUE
        RETURN
```

```
      END
C*****************************************************
```

MULTMAX.FOR performs a function similar to that of
BETVSIP.FOR for bands with well resolved maxima.
The input files are identical. The output is also
the same except that parmeters associated with peak
maxima are returns.

One additional output file is created. This file
for007, contains a list of the maxima found for each
angle of the distribution.

```
C*****************************************************
C       THIS PROGRAM WILL PICK OUT THE MAXIMA OF A BAND
C*****************************************************
        COMMON COUNTS(511, 9), MAXDATA(102, 9), ANGLE(9), PRESS(9)
        COMMON XDATA(511), CMAX(9), NUMMAX(9), JINDEX(9)
        COMMON THRESH, AV, DWELL, ARGON, NANGLE
        INTEGER THRESH, AV, GATE, ARGON
        REAL IP1, IP2
C       READ INPUTS
C*****************************************************
C       READ EXTERNAL INPUTS ON FOR002.DAT
        READ (2, 100) NANGLE, AV, PNS, THRESH, IBACK, ARGON
100     FORMAT (I2/I2/F6.2/I3/I2/I2)
C*****************************************************
C       READ INTERNAL DATA
        DO 105 N=1, NANGLE
        IF (N.NE.1) GO TO 107
        READ (3, 108) IP1, IP2, ANGLE(N), PRESS(N)
108     FORMAT(///, 11X, F7.4, 4X, F7.4, 4X, F6.2, 11X, F6.3)
        GO TO 106
107     READ (3, 101) IP1, IP2, ANGLE(N), PRESS(N)
101     FORMAT(/, 11X, F7.4, 4X, F7.4, 4X, F6.2, 11X, F6.3)
106     READ (3, 102) SCAN, MV, MULT, GATE, IDWELL
102     FORMAT(F8.4/I5/I5/I5/I5//)
        DWELL=IDWELL*GATE/120.
        NWIDTH=MV*MULT
        NCHAN=SCAN*1000/NWIDTH
        READ (3, 103) (COUNTS(I, N), I=1, NCHAN)
103     FORMAT(F10.2)
105     CONTINUE
C       END INPUT SEQUENCE
C*****************************************************
C       CALL THE SMOOTHING ROUTINE
        DO 201 L=1, NANGLE
        CALL SGSMOOTH(AV, NCHAN, COUNTS(1, L), XDATA)
        DO 225 MX=1, NCHAN
        COUNTS(MX, L)=XDATA(MX)
225     CONTINUE
        NDERIV=5
        CALL MAXX(NCHAN, NDERIV, COUNTS(1, L), MAXDATA(1, L), NUMMAX(L))
201     CONTINUE
C*****************************************************
C       LOOK AT THE CHANNELS OF THE MAXIMA FOUND BY MAX
C       DETERMINE IF THEY ALIGN FOR THE ANGLES WITHIN A CERTAIN ERROR
        DO 303 KK=1, NANGLE
```

```
303       JINDEX(KK)=1
          DO 266 JCHAN=1, NUMMAX(1)
C         SET CHANMIN TO CHANMAX-1/2CHANWIDTH +1
C         CHANMAX TO CHAN MAX+1/2CHANWIDTH+1
          JINDEX(1)=JCHAN
          JCHANMIN=MAXDATA(JCHAN, 1)-(NDERIV+1)/2
          JCHANMAX=MAXDATA(JCHAN, 1)+(NDERIV+1)/2
          DO 267 JANG=2, NANGLE
          DO 46 K=JINDEX(JANG), NUMMAX(JANG)
          IF((MAXDATA(K, JANG).GE.JCHANMIN).AND.(MAXDATA(K, JANG)
     X.LE.JCHANMAX))THEN
          JINDEX(JANG)=K
          GO TO 267
          ENDIF
46        CONTINUE
          GO TO 266
267       CONTINUE
          GO TO 500
266       CONTINUE
          MOST=1
          DO 217 KJ=1, NANGLE
217       IF (NUMMAX(KJ).GT.MOST) MOST=NUMMAX(KJ)
          WRITE (7, 134)((MAXDATA(I, J), J=1, NANGLE), I=1, MOST)
134       FORMAT(1X, 9I5)
          GO TO 600
C*****************************************************************
C         WRITE OUT DATA FOR BETA PROGRAM
C         NEED AN IP SO AVERAGE THE CHANNELS TO CALCULATE
500       JSUM=0
          DO 510 LK=1, NANGLE
          JT=JINDEX(LK)
510       JSUM=MAXDATA(JT, LK)
          JAVE=JSUM/NANGLE
          PMAX=IP1+(JAVE-1)*NWIDTH/1000.
          WRITE (5, 100) NANGLE, AV, PNS, THRESH, IBACK, ARGON
C         SET SCAN SO ONLY ONE CHANNEL IS EXPECTED
          SCAN=FLOAT(NWIDTH)/1000.
          WRITE(5, 109) SCAN, MV, MULT
109       FORMAT(F8.4/I5/I5)
          WRITE (5, 305) PMAX, DWELL
305       FORMAT(F8.4/F8.4)
          DO 310 N=1, NANGLE
          WRITE (5, 301) ANGLE(N), PRESS(N), COUNTS(MAXDATA(JINDEX(N), N), N)
     *, MAXDATA(JINDEX(N), N)
301       FORMAT (F6.2, 4X, F6.2, 4X, F10.2, I5)
310       CONTINUE
          GO TO 266
600       END
C*************************************************************
          SUBROUTINE SGSMOOTH(NAV, N, DATA, XDATA)
          DIMENSION DATA(511), XDATA(511), P(25), COEFF(11, 15)
          DIMENSION NORM(11)
          DATA (COEFF(1, L), L=1, 3)/17, 12, -3/
          DATA (COEFF(2, L), L=1, 4)/7, 6, 3, -2/
          DATA (COEFF(3, L), L=1, 5)/59, 54, 39, 14, -21/
```

```
      DATA (COEFF(4, L), L=1, 6)/89, 84, 69, 44, 9, -36/
      DATA (COEFF(5, L), L=1, 7)/25, 24, 21, 16, 9, 0, -11/
      DATA (COEFF(6, L), L=1, 8)/167, 162, 147, 122, 87, 42, -13, -78/
      DATA (COEFF(7, L), L=1, 9)/43, 42, 39, 34, 27, 18, 7, -6, -21/
      DATA (COEFF(8, L), L=1, 10)/269, 264, 249, 224, 189, 144, 89, 24, -51, -136/
      DATA (COEFF(9, L), L=1, 11)/329, 324, 309, 284, 249, 204, 149, 84, 9, -76, -171/
      DATA (COEFF(10, L), L=1, 12)/79, 78, 75, 70, 63, 54, 43, 30, 15, -2, -21, -42/
      DATA (COEFF(11, L), L=1, 13)/467, 462, 447, 422, 387, 322, 287, 222, 147, 62, -33,
     *-138, -253/
      DATA NORM/35, 21, 231, 429, 143, 1105, 323, 2261, 3059, 8059, 5175/
      M=N-(NAV-1)
      NCOEFF=(NAV+1)/2
      LCOEFF=NCOEFF-2
C     TO GET THE CORRECT MEMBER OF THE COEFF AND NORM ARRAYS
C     LOAD POINTS INTO P ARRAY
C     ARRAY INITIALLY OFFSET FOR CHANNEL ADVANCE SEQUENCE
      DO 10 I=1, NAV-1
10    P(I+1)=DATA(I)
C     SMOOTHING LOOP
      DO 200 I=1, M
      J=I+(NAV-1)
      DO 11 K=1, NAV-1
11    P(K)=P(K+1)
      P(NAV)=DATA(J)
C     SET UP LOOP TO DO SUM
      SUM=COEFF(LCOEFF, 1)*P(NCOEFF)
      DO 22 L=2, NCOEFF
22    SUM=SUM+COEFF(LCOEFF, L)*(P(NCOEFF-(L-1))+P(NCOEFF+(L-1)))
      XDATA(I+NCOEFF-1)=SUM/FLOAT(NORM(LCOEFF))
200   CONTINUE
      RETURN
      END
C*****************************************************
      SUBROUTINE MAXX(NCHAN, NDERIV, DATA, NMAXDATA, IMAX)
      DIMENSION DATA(511), NMAXDATA(102), DELTA(25)
      IMAX=0
      DO 10 N=1, NCHAN-NDERIV
      DO 20 I=1, NDERIV-1
      DELTA(I)=DATA(N+I)-DATA(N+I-1)
20    CONTINUE
      DO 30 II=1, NDERIV-1
C     CONDITION FOR THE MAXIMA IS DELTA(1) THROUGH (NDERIVE-1)/2
C     IS POSITIVE AND THE REST ARE NEGATIVE.
      IF((II.LE.((NDERIV-1)/2)).AND.(DELTA(II).GT.0).OR.
     *(II.GT.((NDERIV-1)/2)).AND.(DELTA(II).LT.0))THEN
      GO TO 30
      ELSE
      GO TO 10
      ENDIF
30    CONTINUE
      IMAX=IMAX+1
      NMAXDATA(IMAX)=N+((NDERIV-1)/2)
10    CONTINUE
      RETURN
      END
C*****************************************************
```

4) BETA CALCULATION

This program, BETA.FOR is designed to calculate betas.
For a band, the spectra should be processed throught
BETVSIP.EXE; for band with resolvable structure
MULTMAX.EXE should be used to pick out the peak maxima.

Input:
'main'*****for005
Note: this file must be assigned since for005 is default read.
Under normal conditions this file is provided in exactly
compatible form by BETVSIP.EXE or MULTMAX.EXE.

N, AV, PNS, THRESH, IBACK, ARGON
(I2/I2/F6.2/I3/I2/I2)
N=number of angles in the distribution
AV=average per; the convolution parameter-use any positive odd
number between 5 and 25
PNS=pressure no sample in microns
THRESH=threshold counts; the minimum counts to calculate a beta
IBACK=background parameter
1-include a background
non1-do not include a background
ARGON=is the sample argon
0-no
1-yes

SCAN, MV, MULT, IP1, DWELL
(F8.4/I5/I5/F8.4/I5)
SCAN=length of scan in eV
MV=channel step size in meV
MULT=channel step multiplier
IP1=starting ip in eV
DWELL=duration of time in each channel in sec

THETA(I), PRESS(I), COUNTS(I)
(F6.2, 4X, F6.2, 4X, F10.2)
THETA=angle in degrees
PRESS=pressure uncorrected in microns
COUNTS=counts(smoothed from betvsip)

'BACKGROUND'*****FOR008
This file is provided in exactly compatible form by BACK.EXE
NTERMS
(I2)
ANG(I), (ARRAY(M, I), M=1, NTERMS)
(F10.2, 10(F10.4))

OUTPUT:
'BETAS'*****FOR004
A== warning: norm not found; fortran stop!
B==primary output file of statistics and betas

'PLOT'*****FOR010
Plot file for insertion into a plotting routine
ICHAN, IP, BETA, DB
(I5, 5X, F6.3, 4X, F8.5, 2X, F8.5)

```
ICHAN=channel number
IP=ip in eV of the channel
BETA=calculated beta of the channel
DB=the calculated deviation of the betas

C*************************************************************
      COMMON C(9), THETA(9), PRESS(9), P(9), X(9), Y(9), G(9)
      COMMON CORP(9), OFF1(9), OFF(9), CALC(9), COUNTS(9), ANG(9)
      COMMON/BCK/BACK(9), IANG(9), ARRAY(10, 9)
      COMMON N, BETA, JINDEX(9)
      INTEGER ARGON, THRESH, AV
      REAL IP, IP1
C*****************************************************************
C     INPUT EXTERNAL VARIABLES
9000  READ (5, 2000, END=8000) N, AV, PNS, THRESH, IBACK, ARGON
2000  FORMAT(I2/I2/F6.2/I3/I2/I2)
      READ (5, 2002) SCAN, MV, MULT, IP1, DWELL
2002  FORMAT(F8.4/I5/I5/F8.4/F8.4)
C*****************************************************************
      IF (IBACK .NE. 1) GO TO 210
C     READ BACKGROUND PARAMETERS: IF IBACK=1 INCLUDE BACKGRND
C     NINE BACKGROUND ANGLES ARE EXPLICITLY ASSUMED
C     PARAMETERS ARE FOR ONE SECOND DWELL
      READ(8, 200) NTERMS
200   FORMAT (I2)
      DO 203 L=1, 9
      READ(8, 205) ANG(L), (ARRAY(M, L), M=1, NTERMS)
205   FORMAT(F10.2, 10(E15.8))
203   CONTINUE
210   CONTINUE
C     END OF BACKGROUND PARAMETERS
      REWIND 8
C*************************************************************
      NWIDTH=MV*MULT
      NCHAN=SCAN*1000/NWIDTH
      DO 5000 LL=1, NCHAN
      IP=IP1+((LL-1)*NWIDTH)/1000.
      ICHAN=LL
      JSUM=0
      DO 890 M=1, N
      READ (5, 2001) THETA(M), PRESS(M), COUNTS(M), JINDEX(M)
2001  FORMAT(F6.2, 4X, F6.2, 4X, F10.2, I5)
      P(M)=PRESS(M)-PNS
      JSUM=JSUM+JINDEX(M)
890   CONTINUE
C*************************************************************
      IF (IBACK .NE. 1) GO TO 230
      IF (LL .NE. 1 ) GO TO 220
C     DETERMINE ORDER OF ANGLES BUT ONLY ONCE
C     ARRAY IANG CONTAINS ORDERING OF BACKGRND W.R.T. INPUT
C     JNINT=NEXT NEAREST INTEGER-BE WITHIN .5 DEG OF THE SAME ANGLE
      DO 300 LN=1, N
      DO 310 MM=1, 9
310   IF (JNINT(THETA(LN)).EQ.JNINT(ANG(MM))) IANG(LN)=MM
300   CONTINUE
220   CONTINUE
```

```
      DO 230 IM=1, N
      CALL BCKGND(IM, NTERMS, DWELL, IP)
      C(IM)=COUNTS(IM)-BACK(IM)
      IF(C(IM).LE.FLOATJ(THRESH)) GO TO 5000
C     IF COUNTS LESS THAN THRESHOLD SKIP TO NEXT CHANNEL
230   CONTINUE
      IF (IBACK.EQ.1) GO TO 240
      DO 905 IN=1, N
      C(IN)=COUNTS(IN)
      IF(C(IN).LE.FLOATJ(THRESH)) GO TO 5000
905   BACK(IN)=0.0
240   CONTINUE
C*****************************************************
C     CALCULATE THE VARIANCE FACTOR G(I)
      SUMC=0.0
      DO 900 J=1, N
      SUMC=SUMC +1/C(J)
900   CONTINUE
      DO 910 I=1, N
      G(I)= N/(C(I)*SUMC)
910   CONTINUE
C     FIND THE NORM
      DO 920 L=1, N
      IF (JNINT(THETA(L)).EQ.90) GO TO 930
920   CONTINUE
      GO TO 1000
930   CO=C(L)
      PO=P(L)
      GO TO 940
1000  WRITE(4, 1001)
1001  FORMAT(' NORM NOT FOUND')
      STOP
940   CONTINUE
C     CALCULATE X(I) AND Y(I)
      DO 950 K=1, N
      X(K)=(SIN(THETA(K)*3.14159/180))**2
      Y(K)=(C(K)*PO*SIN(THETA(K)*3.14159/180))/(CO*P(K))
950   CONTINUE
C     CALCULATE INTERMEDIATE SUMS
      SX=0.0
      SY=0.0
      DX=0.0
      XY=0.0
      DO 960 L=1, N
      SX=SX+G(L)*X(L)
      SY=SY+G(L)*Y(L)
      DX=DX+G(L)*(X(L)**2)
      XY=XY+G(L)*X(L)*Y(L)
960   CONTINUE
      Q=N*DX-(SX)**2
      A=(SY*DX-SX*XY)/Q
      B=(N*XY-SX*SY)/Q
      BETA=4*B/(3*A+2*B)
C     STATISTICS I VARIANCE
      DBA=-12*B/((3*A+2*B)**2)
      DBB=12*A/((3*A+2*B)**2)
```

```
      SUMT=0.0
      DO 970 J=1, N
      SUMT=SUMT+G(J)*((Y(J)-A-B*X(J))**2)
970   CONTINUE
      SIGA2=DX*SUMT/(Q*(N-2))
      SIGB2=N*SUMT/(Q*(N-2))
      DB2=SIGA2*(DBA)**2+SIGB2*(DBB)**2
      DB=SQRT(DB2)
C     STATISTICS II POISSON
      PDB2=0.0
      DO 980 I=1, N
      PART1=(B*X(I)+A)*Q*(X(I)*SY-XY)
      PART2=(-DX-N*(X(I)**2)+2*X(I)*SX)*(B*(SY*DX-XY*SX)+A*(SY*SX-XY
     X*N))
      DELBC2=(12*G(I)*(PART1+PART2)/(((3*A+2*B)**2)*(Q**2)*C(I)))**2
980   PDB2=PDB2+DELBC2*C(I)
      PDB=SQRT(PDB2/AV)
      GUESSB=BETA
      IF (ARGON .EQ. 1) GUESSB=.88
      DO 1500 K=1, N
      CORP(K)=Y(K)/(A+B)
      CALC(K)=(A+B*X(K))/(A+B)
      OFF1(K)=(2-GUESSB+GUESSB*1.5*X(K))*(A+B)/(2+GUESSB/2)
      OFF(K)=(Y(K)-OFF1(K))/OFF1(K)
1500  CONTINUE
C*****************************************************************
C     PRINT OUTPUT
      IF (JSUM.NE.0) THEN
      JSUM=JSUM/N
      ICHAN=JSUM
      ENDIF
      WRITE(4, 1004) ICHAN, IP
1004  FORMAT(1X, 'CHANNEL:', I4/1X, 'IP:'F8.3)
      WRITE(4, 1005)
1005  FORMAT(' ANGLE', 5X, 'PRESSURE', 5X, 'COUNTS', 8X, ' BACK', 8X,
     X'CORRPK', 7X, 'CALC', 6X, 'OFF')
      DO 990 I=1, N
      WRITE(4, 1006) THETA(I), P(I), COUNTS(I), BACK(I), CORP(I), CALC(I)
     X, OFF(I)
1006  FORMAT(1X, F6.2, 5X, F6.2, 5X, F8.2, 4(5X, F8.4))
990   CONTINUE
      WRITE(4, 1007) BETA, DB, PDB
1007  FORMAT(' BETA=', F8.5, 3X, 'DB=', F8.5, 3X, 'POISDB=', F8.5)
C*****************************************************************
C     PRINT FOR PLOT FILE
      WRITE (10, 1010) ICHAN, IP, BETA, DB
1010  FORMAT( I5, 5X, F6.3, 4X, F8.5, 2X, F8.5)
5000  CONTINUE
      GO TO 9000
8000  END
      SUBROUTINE BCKGND(IM, NTERMS, DWELL, IP)
      COMMON/BCK/BACK(9), IANG(9), ARRAY(10, 9)
      REAL IP
      BACK(IM)=ARRAY(NTERMS, IANG(IM))
      DO 111 I=1, NTERMS-1
```

```
111       BACK(IM)=ARRAY(NTERMS-I, IANG(IM))+BACK(IM)*IP
          BACK(IM)=BACK(IM)*DWELL
          RETURN
          END
C*************************************************
```

INTERBETA.FOR is an interactive version of the beta calculating program. The inputs are the same except they are inserted manually rather than read from files with the exception of the background parameters which must be assigned prior to running the program. Output is written to the terminal as well as to the files described in BETA.FOR.

The program has a sophisticated feedback loop which permits alteration of spectral data and parameters on line without having to reinitiate the program and reinput all data.

Instructions for running the program are provided at run time.

```
C*************************************************************
          COMMON C(9), THETA(9), PRESS(9), P(9), X(9), Y(9), G(9)
          COMMON CORP(9), OFF1(9), OFF(9), CALC(9), COUNTS(9), ANG(9)
          COMMON N, BETA
          COMMON/BCK/BACK(9), IANG(9), ARRAY(10, 9)
          INTEGER ARGON, GATE, THRESH, AV
          REAL IP, IP1
          PRINT 11
11        FORMAT( ' THIS IS AN INTERACTIVE VERSION OF THE BETA PROGRAM'/
     * ' ALL INPUTS ARE UNFORMATTED UNLESS OTHERWISE STATED')
          IFLAG=0
C*************************************************************
C         INTERACTIVE INPUT OF EXTERNAL VARIABLES
C         INPUT EXTERNAL VARIABLES
C*************************************************************
888       CONTINUE
          PRINT 12
12        FORMAT(' INPUT EXTERNAL PARAMETERS:', $)
413       PRINT 13
13        FORMAT(' NUMBER OF ANGLES>', $)
          READ (5, *, ERR=413) N
414       PRINT 14
14        FORMAT(' CONVOLUTION PARAMETER>', $)
          READ (5, *, ERR=414) AV
415       PRINT 15
15        FORMAT(' PRESSURE NO SAMPLE>', $)
          READ (5, *, ERR=415) PNS
416       PRINT 16
16        FORMAT(' THRESHOLD>', $)
          READ (5, *, ERR=416) THRESH
410       PRINT 10
10        FORMAT(' GATE>', $)
          READ (5, *, ERR=410) GATE
419       PRINT 19
19        FORMAT(' DWELL>', $)
          READ (5, *, ERR=419) IDWELL
          DWELL=IDWELL*GATE/120.
417       PRINT 17
```

```
17      FORMAT(' INCLUDE A BACKGROUND, 0=NO, 1=YES>', $)
        READ (5, *, ERR=417) IBACK
418     PRINT 18
18      FORMAT(' IS THIS SAMPLE ARGON, 0=NO, 1=YES>', $)
        READ (5, *, ERR=418) ARGON
423     PRINT 23
23      FORMAT(' EXECUTE OPTION TO CHANGE EXTERNAL INPUTS,
   X0=NO, 1=YES:', $)
        READ (5, *, ERR=423) ICHANGEX
        IF (ICHANGEX) 899, 899, 888
C*****************************************************************
899     CONTINUE
        PRINT 20
20      FORMAT(' INPUT CHANNEL PARAMETERS:'/
   *' NOTE IF BACK=1 THEN AN IP *MUST* BE INCLUDED!')
421     PRINT 21
21      FORMAT(' CHANNEL NUMBER>', $)
        READ (5, *, ERR=421) NCHAN
422     PRINT 22
22      FORMAT(' IP>', $)
        READ (5, *, ERR=422) IP1
424     PRINT 24
24      FORMAT(' EXECUTE OPTION TO CHANGE CHANNEL PARAMETERS,
   X0=NO, 1=YES:', $)
        READ (5, *, ERR=424) ICHANCH
        IF (ICHANCH) 879, 879, 899
879     CONTINUE
C*****************************************************************
        IF (IBACK .NE. 1) GO TO 210
C       READ BACKGROUND PARAMETERS: IF IBACK=1 INCLUDE BACKGRND
C       NINE BACKGROUND ANGLES ARE EXPLICITLY ASSUMED
C       PARAMETERS ARE FOR ONE SECOND DWELL
        READ(8, 200) NTERMS
200     FORMAT (I2)
        DO 203 L=1, 9
        READ(8, 205) ANG(L), (ARRAY(M, L), M=1, NTERMS)
205     FORMAT(F10.2, 10(E15.8))
203     CONTINUE
210     CONTINUE
C       END OF BACKGROUND PARAMETERS
C*************************************************************
874     IF (IFLAG.NE.0) THEN
425     PRINT 25
25      FORMAT(' EXECUTE OPTION TO CHANGE SPECTRUM INPUTS,
   X0=NO, 1=YES:', $)
        READ (5, *, ERR=425) ICHANSP
        IF (ICHANSP.NE.1) GO TO 875
        CALL WRITEOPT
        GO TO 876
        ENDIF
C*****************************************************************
875     CONTINUE
        DO 890 M=1, N
426     PRINT 26
26      FORMAT(' ANGLE>', $)
        READ (5, *, ERR=426) THETA(M)
```

```
427       PRINT 27
27        FORMAT(' PRESSURE>', $)
          READ (5, *, ERR=427) PRESS(M)
428       PRINT 28
28        FORMAT(' COUNTS>', $)
          READ (5, *, ERR=428) COUNTS(M)
890       CONTINUE
          DO 891 M=1, N
          WRITE (6, 2001) THETA(M), PRESS(M), COUNTS(M)
2001      FORMAT(1X, F6.2, 4X, F6.2, 4X, F10.2)
891       CONTINUE
400       PRINT 25
          READ (5, *, ERR=400) ICHANSP
          IF (ICHANSP.NE.1) GO TO 876
          CALL WRITEOPT
876       CONTINUE
          DO 44 M=1, N
44        P(M)=PRESS(M)-PNS
C*************************************************************
          IF (IBACK .NE. 1) GO TO 230
C         DETERMINE ORDER OF ANGLES BUT ONLY ONCE
C         ARRAY IANG CONTAINS ORDERING OF BACKGRND W.R.T. INPUT
C         JNINT=NEXT NEAREST INTEGER-BE WITHIN .5 DEG OF THE SAME ANGLE
          DO 300 LN=1, N
          DO 310 MM=1, 9
310       IF (JNINT(THETA(LN)).EQ.JNINT(ANG(MM))) IANG(LN)=MM
300       CONTINUE
220       CONTINUE
          DO 230 IM=1, N
          CALL BCKGND(IM, NTERMS, DWELL, IP1)
          C(IM)=COUNTS(IM)-BACK(IM)
          IF(C(IM).LE.FLOATJ(THRESH)) GO TO 5000
C         IF COUNTS LESS THAN THRESHOLD SKIP TO NEXT CHANNEL
230       CONTINUE
          IF (IBACK.EQ.1) GO TO 240
          DO 905 IN=1, N
          C(IN)=COUNTS(IN)
          IF(C(IN).LE.FLOATJ(THRESH)) GO TO 5000
905       BACK(IN)=0.0
240       CONTINUE
C*************************************************************
C         CALCULATE THE VARIANCE FACTOR G(I)
          SUMC=0.0
          DO 900 J=1, N
          SUMC=SUMC +1/C(J)
900       CONTINUE
          DO 910 I=1, N
          G(I)= N/(C(I)*SUMC)
910       CONTINUE
C         FIND THE NORM
          DO 920 L=1, N
          IF (JNINT(THETA(L)).EQ.90) GO TO 930
920       CONTINUE
          GO TO 1000
930       CO=C(L)
          PO=P(L)
```

```
      GO TO 940
1000  WRITE(4, 1001)
1001  FORMAT(' NORM NOT FOUND')
      STOP
940   CONTINUE
C     CALCULATE X(I) AND Y(I)
      DO 950 K=1, N
      X(K)=(SIN(THETA(K)*3.14159/180))**2
      Y(K)=(C(K)*PO*SIN(THETA(K)*3.14159/180))/(CO*P(K))
950   CONTINUE
C     CALCULATE INTERMEDIATE SUMS
      SX=0.0
      SY=0.0
      DX=0.0
      XY=0.0
      DO 960 L=1, N
      SX=SX+G(L)*X(L)
      SY=SY+G(L)*Y(L)
      DX=DX+G(L)*(X(L)**2)
      XY=XY+G(L)*X(L)*Y(L)
960   CONTINUE
      Q=N*DX-(SX)**2
      A=(SY*DX-SX*XY)/Q
      B=(N*XY-SX*SY)/Q
      BETA=4*B/(3*A+2*B)
C     STATISTICS I VARIANCE
      DBA=-12*B/((3*A+2*B)**2)
      DBB=12*A/((3*A+2*B)**2)
      SUMT=0.0
      DO 970 J=1, N
      SUMT=SUMT+G(J)*((Y(J)-A-B*X(J))**2)
970   CONTINUE
      SIGA2=DX*SUMT/(Q*(N-2))
      SIGB2=N*SUMT/(Q*(N-2))
      DB2=SIGA2*(DBA)**2+SIGB2*(DBB)**2
      DB=SQRT(DB2)
C     STATISTICS II POISSON
      PDB2=0.0
      DO 980 I=1, N
      PART1=(B*X(I)+A)*Q*(X(I)*SY-XY)
      PART2=(-DX-N*(X(I)**2)+2*X(I)*SX)*(B*(SY*DX-XY*SX)+A*(SY*SX-XY
     X*N))
      DELBC2=(12*G(I)*(PART1+PART2)/(((3*A+2*B)**2)*(Q**2)*C(I)))**2
980   PDB2=PDB2+DELBC2*C(I)
      PDB=SQRT(PDB2/AV)
      GUESSB=BETA
      IF (ARGON .EQ. 1) GUESSB=.88
      DO 1500 K=1, N
      CORP(K)=Y(K)/(A+B)
      CALC(K)=(A+B*X(K))/(A+B)
      OFF1(K)=(2-GUESSB+GUESSB*1.5*X(K))*(A+B)/(2+GUESSB/2)
      OFF(K)=(Y(K)-OFF1(K))/OFF1(K)
1500  CONTINUE
C*****************************************************************
      PRINT 29
```

```
29      FORMAT(' A SECOND COPY OF THIS OUTPUT FILE IS CREATED IN FOR004')
C       PRINT OUTPUT
        WRITE(6, 1004) NCHAN, IP1
        WRITE(4, 1004) NCHAN, IP1
1004    FORMAT(1X, 'CHANNEL:', I4/1X, 'IP:', F8.3)
        WRITE(6, 1005)
        WRITE(4, 1005)
1005    FORMAT(' ANGLE', 5X, 'PRESSURE', 5X, 'COUNTS', 8X, ' BACK', 8X,
   X'CORR PK', 7X, 'CALC', 6X, 'OFF')
        DO 990 I=1, N
        WRITE(6, 1006) THETA(I), P(I), COUNTS(I), BACK(I), CORP(I), CALC(I)
   X, OFF(I)
        WRITE(4, 1006) THETA(I), P(I), COUNTS(I), BACK(I), CORP(I), CALC(I)
   X, OFF(I)
1006    FORMAT(1X, F6.2, 5X, F6.2, 5X, F8.2, 4(5X, F8.4))
990     CONTINUE
        WRITE(6, 1007) BETA, DB, PDB
        WRITE(4, 1007) BETA, DB, PDB
1007    FORMAT(' BETA=', F8.5, 3X, 'DB=', F8.5, 3X, 'POISDB=', F8.5)
C*****************************************************************
C       PRINT FOR PLOT FILE
        WRITE (10, 1010) NCHAN, IP1, BETA, DB
1010    FORMAT( I5, 5X, F6.3, 4X, F8.5, 2X, F8.5)
5000    CONTINUE
430     PRINT 30
30      FORMAT(' GO AGAIN, 0=NO, 1=YES:', $)
        READ (5, *, ERR=430) IFLAG
        IF (IFLAG) 6000, 6000, 5500
5500    PRINT 31
31      FORMAT(' SAME EXTERNAL PARAMETERS, 0=NO, 1=YES:', $)
        READ (5, *, ERR=5500) ISAME
        IF (ISAME) 888, 888, 892
892     PRINT 32
32      FORMAT(' SAME CHANNEL PARAMETERS, 0=NO, 1=YES:', $)
        READ (5, *, ERR=892) NSAME
        IF (NSAME) 899, 899, 874
6000    END
        SUBROUTINE BCKGND(IM, NTERMS, DWELL, IP)
        COMMON/BCK/BACK(9), IANG(9), ARRAY(10, 9)
        REAL IP
        BACK(IM)=ARRAY(NTERMS, IANG(IM))
        DO 111 I=1, NTERMS-1
111     BACK(IM)=ARRAY(NTERMS-I, IANG(IM))+BACK(IM)*IP
        BACK(IM)=BACK(IM)*DWELL
        RETURN
        END
        SUBROUTINE WRITEOPT
        CHARACTER*1 CHAR1, CHAR2
        COMMON C(9), THETA(9), PRESS(9), P(9), X(9), Y(9), G(9)
        COMMON CORP(9), OFF1(9), OFF(9), CALC(9), COUNTS(9), ANG(9)
        COMMON N, BETA
        IFLAG=0
5       DO 891 M=1, N
        WRITE (6, 2001) M, THETA(M), PRESS(M), COUNTS(M)
```

```
2001    FORMAT(1X, I2, 1X, F6.2, 4X, F6.2, 4X, F10.2)
891     CONTINUE
        IF (IFLAG.NE.0) GO TO 50
10      PRINT 40
40      FORMAT(' INSTRUCTIONS FOR CHANGE OPTION'/
     * ' THIS IS A FORMATTED INPUT *NO* EXTRA SPACES ALLOWED!'/
     * 3X, ' EE= EXIT THIS OPTION'/
     * 3X, ' II= WRITE OUT THESE INTRUCTIONS'/
     * 3X, ' PP= PRINT OUT THE ANGLE, PRESSURE, AND COUNTS ARRAYS'/
     * 3X, ' NZ= TO CHANGE AN INPUT; WHERE N=THE LINE NUMBER (1-9)'/
     * 3X, ' AND Z=THE FIRST LETTER OF THE ARRAY (A, P, C)')
        IF (IFLAG.NE.0) GO TO 50
50      PRINT 12
12      FORMAT(' ENTER OPTION')
        READ (5, 100, ERR=50) CHAR1, CHAR2
100     FORMAT (2A1)
        IFLAG=1
        IF (CHAR1 .EQ. 'E') GO TO 3000
        IF (CHAR1 .EQ. 'I') GO TO 10
        IF (CHAR1 .EQ. 'P') GO TO 5
        IF (CHAR2 .EQ. 'A') GO TO 15
        IF (CHAR2 .EQ. 'P') GO TO 20
        IF (CHAR2 .EQ. 'C') GO TO 25
        GO TO 50
15      J=ICHAR(CHAR1)-48
        IF ((J.LT.1).OR.(J.GT.N)) GO TO 50
445     PRINT 45
45      FORMAT(' ANGLE>', $)
        READ (5, *, ERR=445) THETA(J)
        GO TO 50
20      J=ICHAR(CHAR1)-48
        IF ((J.LT.1).OR.(J.GT.N)) GO TO 50
444     PRINT 44
44      FORMAT(' PRESSURE>', $)
        READ (5, *, ERR=444) PRESS(J)
        GO TO 50
25      J=ICHAR(CHAR1)-48
        IF ((J.LT.1).OR.(J.GT.N)) GO TO 50
446     PRINT 46
46      FORMAT(' COUNTS>', $)
        READ (5, *, ERR=446) COUNTS(J)
        GO TO 50
3000    RETURN
        END
```

5) PLOTTING

This file, BPLOT.FOR, describes the use of the bplot program for plotting beta vs ip over a base plot usually but not necessarily the full spectrum at 54.7 degrees.

'Parameter'*****for002
This file contains the parameters for bplot.
IBACK, CPS
(I1, F5.3)
IBACK-a logical switch: non1=no background
1=include background in base plot
CPS-the contact potential shift of the base plot with respect to the energy calibration N.B. This and all other cps are inherently additive.

ELOW, EHIGH, MAGFACT
(F6.2/F6.2/I2)
ELOW= low energy limit of range to be expanded
EHIGH= high energy limit of range
MAGFACT= scale factor of magnified range

'Background'*****for008
This file is provided in exactly compatible form by BACK.EXE
NTERMS
(I2)
ANG(I), (ARRAY(M, I), M=1, NTERMS)
(F10.2, 10(E15.8))

'internal'*****for003
All data taken from spectrum file as transmitted
IP1, IP2, ANGLE, PRESS
(///, 11X, F7.4, 4X, F7.4, 4X, F6.2, 11X, F6.3)
IP1=starting ip in eV
IP2=ending ip in eV
ANGLE=angle of spectrum in degrees
PRESS=pressure (uncorrected) in microns

SCAN, MV, MULT, DWELL
(F8.4/I5/I5//I5//)
SCAN=length of scan in eV
MV=channel step size in meV
MULT=channel step multiplier
GATE=time per channel per scan
DWELL=number of scans per spectrum
(COUNTS(I, N), I=1, NCHAN)
(F10.2)

'Plot'*****for010
Plot file for insertion into plotting routine
STAR, IP, BETA, DB
(A1, 9X, F6.3, 4X, F8.5, 2X, F8.5)
STAR=if star equals '*' read cpsband
IP=ip in eV of the channel
BETA=calculated beta of the channel
DB=the calculated deviation from beta

CPSBAND
(F6.4)
CPSBAND=contact potential shift for the band or data set being plotted

Since there is an indeterminate number of betas to be read
the reading is terminated by an end of file on unit 10.
Read ips, betas, dbs, ignore channel numbers.
A word about contact potential shifts:
since the cps of a band may not be known at the time
of the beta calculation, I have elected for manual insertion
into the data file for010. This should be done as follows:
column 1 should contain an asterisk (*) at the beginning of
each data set. The next line should contain the contact potential
shift with respect to the base plot in eV(f6.4). The sign convention
is as follows: the cps is inherently additive so if the band
has an ip greater than that in the base plot the sign in the cps should
be negative, if the ip is lower the sign should be positive.

'Label'****for007
A title for the plot may be used if desired.
The character string may be typed directly in for007 or its
logical equivalent or may be passed from a parameter list
using open and write commands.

```
C*************************************************************
      COMMON COUNTS(511), ANGLE, PRESS, IP(511)
      COMMON/BTRD/ARRAY(10), AR(10), XMIN, XSCALE, CPS
      DIMENSION XDATA(511)
      INTEGER THRESH, AV, GATE, ARGON
      REAL IP1, IP2, IP
C*************************************************************
C     READ INPUTS
C     READ PROGRAM CONTROL PARAMETERS
      READ (2, 52) IBACK, AV, CPS
52    FORMAT(I1/I2/F5.3)
C     READ INTERNAL DATA
      READ (3, 101) IP1, IP2, ANGLE, PRESS
101   FORMAT(///, 11X, F7.4, 4X, F7.4, 4X, F6.2, 11X, F6.3)
      READ (3, 102) SCAN, MV, MULT, GATE, IDWELL
102   FORMAT(F8.4/I5/I5/I5/I5//)
      DWELL=IDWELL*GATE/120.
      NWIDTH=MV*MULT
      NCHAN=SCAN*1000/NWIDTH
      READ (3, 103)(COUNTS(I), I=1, NCHAN)
103   FORMAT(F10.2)
C     END INPUT SEQUENCE FOR COUNTS
C*************************************************************
C     CALL THE SMOOTHING ROUTINE
      CALL SGSMOOTH(AV, NCHAN, COUNTS, XDATA)
      DO 225 MX=1, NCHAN
      COUNTS(MX)=XDATA(MX)
225   CONTINUE
C*************************************************************
      IF (IBACK .NE. 1) GO TO 210
C     READ BACKGROUND PARAMETERS: IF IBACK=1 INCLUDE BACKGRND
C     NINE BACKGROUND ANGLES ARE EXPLICITLY ASSUMED
```

```
C       PARAMETERS ARE FOR ONE SECOND DWELL
        READ(8, 200) NTERMS
200     FORMAT (I2)
C       INTIALIZE BACKGROUND ARRAYS
        DO 206 LJ=1, NTERMS
206     AR(LJ)=0.0
        DO 207 L=1, 9
        READ(8, 205) ANG, (ARRAY(M), M=1, NTERMS)
205     FORMAT(F10.2, 10(E15.8))
        IF ((JNINT(ANG).NE.(50.0)).AND.(JNINT(ANG).NE.(60.0))) GO TO 207
        DO 203 JB=1, NTERMS
203     AR(JB)=AR(JB)+ARRAY(JB)*(0.5)
207     CONTINUE
210     CONTINUE
C       END OF BACKGROUND PARAMETERS
C*************************************************************
        DO 123 N=1, NCHAN
C       SET UP ARRAY IP AND SUBTRACT OFF THE CONTACT POTENTIAL
C       OF THE BASE PLOT THE CONVENTION IS POSITIVE IE IF THE
C       APPARENT IP IS TOO HIGH CPS SHOULD BE NEGATIVE IF TOO LOW
C       CPS SHOULD BE POSITIVE TO CORRECT IT.
        IP(N)=IP1+((N-1)*NWIDTH)/1000.+CPS
C       SCALE COUNTS BY DWELL TO GET COUNTS/SEC
        COUNTS(N)=COUNTS(N)/DWELL
        IF ( IBACK .NE. 1) GO TO 220
        CALL BCKGRND(NTERMS, IP(N), BACK)
        COUNTS(N)=COUNTS(N)-BACK
        IF(COUNTS(N).LE.0.0) COUNTS(N)=0.0
220     CONTINUE
123     CONTINUE
        CALL BOX(NCHAN, NWIDTH)
        CALL BETARD
        STOP
        END
C*************************************************************
        SUBROUTINE SGSMOOTH(NAV, N, DATA, XDATA)
        DIMENSION DATA(511), XDATA(511), P(25), COEFF(11, 15)
        DIMENSION NORM(11)
        DATA (COEFF(1, L), L=1, 3)/17, 12, -3/
        DATA (COEFF(2, L), L=1, 4)/7, 6, 3, -2/
        DATA (COEFF(3, L), L=1, 5)/59, 54, 39, 14, -21/
        DATA (COEFF(4, L), L=1, 6)/89, 84, 69, 44, 9, -36/
        DATA (COEFF(5, L), L=1, 7)/25, 24, 21, 16, 9, 0, -11/
        DATA (COEFF(6, L), L=1, 8)/167, 162, 147, 122, 87, 42, -13, -78/
        DATA (COEFF(7, L), L=1, 9)/43, 42, 39, 34, 27, 18, 7, -6, -21/
        DATA (COEFF(8, L), L=1, 10)/269, 264, 249, 224, 189, 144, 89, 24, -51, -136/
        DATA (COEFF(9, L), L=1, 11)/329, 324, 309, 284, 249, 204, 149, 84, 9, -76, -171/
        DATA (COEFF(10, L), L=1, 12)/79, 78, 75, 70, 63, 54, 43, 30, 15, -2, -21, -42/
        DATA (COEFF(11, L), L=1, 13)/467, 462, 447, 422, 387, 322, 287, 222, 147, 62, -33,
    *-138, -253/
        DATA NORM/35, 21, 231, 429, 143, 1105, 323, 2261, 3059, 8059, 5175/
        M=N-(NAV-1)
        NCOEFF=(NAV+1)/2
        LCOEFF=NCOEFF-2
C       TO GET THE CORRECT MEMBER OF THE COEFF AND NORM ARRAYS
```

```
C       LOAD POINTS INTO P ARRAY
C       ARRAY INITIALLY OFFSET FOR CHANNEL ADVANCE SEQUENCE
        DO 10 I=1, NAV-1
10      P(I+1)=DATA(I)
C       SMOOTHING LOOP
        DO 200 I=1, M
        J=I+(NAV-1)
        DO 11 K=1, NAV-1
11      P(K)=P(K+1)
        P(NAV)=DATA(J)
C       SET UP LOOP TO DO SUM
        SUM=COEFF(LCOEFF, 1)*P(NCOEFF)
        DO 22 L=2, NCOEFF
22      SUM=SUM+COEFF(LCOEFF, L)*(P(NCOEFF-(L-1))+P(NCOEFF+(L-1)))
        XDATA(I+NCOEFF-1)=SUM/FLOAT(NORM(LCOEFF))
200     CONTINUE
        RETURN
        END
C*************************************************
C       NOTE: THIS FRAME IS DRAWN SIDEWAYS WITH RESPECT TO THE PLOTTER
C       ORIENTATION IS COUNTS AND BETAS ARE POSITIVE XAXIS (PLOTTER)
C       IP ARE ON THE NEGATIVE YAXIS(PLOTTER) N.B. THIS PROGRAM IS NOT
C       ALWAYS CONSISTANT ABOUT THE REFERENCE IE PLOTTER VS PLOT.
C       PEN LOCUS IS INITIAL ORIGIN
        SUBROUTINE BOX(NCHAN, NWIDTH)
        COMMON COUNTS(511), ANGLE, PRESS, IP(511)
        COMMON/BTRD/ARRAY(10), AR(10), XMIN, XSCALE, CPS
        DIMENSION XIP(511), YCOUNTS(511), MODN(6), MODX(4)
        INTEGER*2 LABELPLOT(35)
        REAL IP, MODX, MODXS
        DATA (MODN(L), L=1, 6)/1, 2, 5, 10, 20, 50/
        DATA (MODX(M), M=1, 4)/0.10, 0.20, 0.50, 1.00/
        CALL PLOTS(53, 0, 15)
C       PLOT FILE IS FOR0015
C       REPOSITION ORIGIN-PEN UP
        READ (7, 978, END=979) LABELPLOT
978     FORMAT(35A1)
979     CONTINUE
        CALL SPEED(5)
        CALL PLOT(.5, .5, -3)
C       DRAW BOX
        CALL PLOT(4., 0., 2)
        CALL PLOT(4.25, 0., 3)
        CALL PLOT(7.75, 0., 2)
        CALL PLOT(7.75, 9., 2)
        CALL PLOT(4.25, 9., 2)
        CALL PLOT(4., 9., 3)
        CALL PLOT(0., 9., 2)
        CALL PLOT(0., 0., 2)
C       RAISE PEN FOR CROSSBAR
        CALL PLOT(4., 0., 3)
        CALL PLOT(4., 9., 2)
        CALL PLOT(4.25, 9., 3)
        CALL PLOT(4.25, 0., 2)
C       PLOT LABEL
```

```
      CALL SYMBOL(4.25, 10.25, -.10, LABELPLOT, 0.00, 20)
C     LABEL PLOT
      CALL PLOT(0., 9., -3)
C*********************************************************************
C     OFFSET IP ARRAY AND SCALE IT
      XMIN=IP(1)
      XMAX=IP(NCHAN)
      DELTA=1.05*(XMAX-XMIN)
C     FIND SCALE IN UNITS/INCH
      XSCALE=DELTA/9.0
C     DEFINE NEW XMAX, XMIN
C     ALLOWS 5% FOR BORDERS
      XMIN=XMIN-(.025*DELTA)
      XMAX=XMAX+(.025*DELTA)
C     OFFSET THE ARRAY AND NEGATE IT TO FIT IN THE AREA
      DO 333 NX=1, NCHAN
333   XIP(NX)=-(IP(NX)-XMIN)/XSCALE
C*********************************************************************************
C     SCALE COUNTS TO FIT
C     FIND THE MAXIMUM COUNT
      CMAX=0.
      DO 332 IC=1, NCHAN
      IF (COUNTS(IC).GT.CMAX) CMAX=COUNTS(IC)
332   CONTINUE
C     FIND THE SCALE FOR THE COUNTS
      CSCALE=1.05*CMAX/4.0
C     CREATE NEW ARRAY FOR PLOTTING
      DO 336 K=1, NCHAN
336   YCOUNTS(K)=COUNTS(K)/CSCALE
C*********************************************************************************
C     DETERMINE INTENSITY SCALING
      DO 40 MD=1, 6
      IF((CMAX/MODN(MD)).GT.8) GO TO 40
      IF((CMAX/MODN(MD)).LT.3)THEN
      IF (MD.EQ.1) GO TO 41
      MODS=MODN(MD-1)
      ELSE
      MODS=MODN(MD)
      GO TO 42
      ENDIF
40    CONTINUE
C     CASE IF I LESS THAN 3 COUNTS/SEC TO BE DETERMINE LATER
41    CONTINUE
C     DETERMINE NUMBER OF TICKS WITH SPACING MODS
42    NTICK=JINT(1.05*CMAX/MODS)
      DO 46 NA=1, 2
C     LABEL ZERO
      IF (NA.EQ.1) THEN
      CALL NUMBER(-0.045, 0.1825, 0.09, 0.0, -90., -1)
      ELSE
      CALL NUMBER(-0.045, -9.09, 0.09, 0.0, -90., -1)
      ENDIF
      DO 44 NT=1, NTICK
      ZT=NT*MODS/CSCALE
      ZT1=NT*MODS
C     NUMBER THE TICKMARK
```

```
C       DETERMINE NUMBER OF DIGITS IN LABEL
C       CASE OF LESS THAN ONE POSTPONED TO A LATER TIME
        IF(ZT1.GE.1.) NDIG=1
        IF(ZT1.GE.10.) NDIG=2
        IF(ZT1.GE.100.) NDIG=3
        IF(ZT1.GE.1000.) NDIG=4
        IF (NA.EQ.1) THEN
        CALL NUMBER(ZT-0.045, NDIG*0.09+.0025, 0.09, ZT1, -90., -1)
C       PLACE THE TICKMARK
        CALL SYMBOL(ZT, -0.04, .08, 13, 0., -1)
        ELSE
C       NOW THE OTHER SIDE
        CALL NUMBER(ZT-0.045, -9.09, 0.09, ZT1, -90., -1)
        CALL SYMBOL(ZT, -8.96, 0.08, 13, 0., -1)
        ENDIF
44      CONTINUE
46      CONTINUE
        CALL SYMBOL(1.0625, 0.37, .125, 14HI/(COUNTS/SEC), 0., 14)
C*****************************************************************
C       WORK ON THE ENERGY AXIS
C       DETERMINE SCALING
        DO 60 MD=1, 4
C       FIND THE FIRST TICKMARK GT XMIN
        ZX=JINT(XMIN/MODX(MD))+1.00
        FIRST=ZX*MODX(MD)
C       FIND NEW DELTA
        DELTA1=XMAX-FIRST
C       DETERMINE NUMBER OF TICKS AT THIS MOD
        XTICK=DELTA1/MODX(MD)
        IF(XTICK.GT.8) THEN
        IF(MD.EQ.4) THEN
        MODXS=MODX(MD)
        GO TO 62
        ENDIF
        GO TO 60
        ENDIF
        IF(XTICK.LT.3) THEN
        IF (MD.EQ.1) THEN
        MODXS=MODX(MD)
        GO TO 62
        ENDIF
        MODXS=MODX(MD-1)
        ELSE
        MODXS=MODX(MD)
        GO TO 62
        ENDIF
60      CONTINUE
C       LABEL FIRST
62      NXTICK=JINT(XTICK)
        ZXF=-(FIRST-XMIN)/XSCALE
        CALL SYMBOL(-0.04, ZXF, 0.08, 13, -90., -1)
        IF(MODXS.EQ.1.00) THEN
        CALL NUMBER(-0.25, ZXF+0.09, 0.09, FIRST, -90., -1)
        ELSE
        CALL NUMBER(-0.25, ZXF+.1825, 0.09, FIRST, -90., 1)
        ENDIF
```

```
      DO 64 NT=1, NXTICK
      ZXT1=FIRST+NT*MODXS
      ZXT=-(ZXT1-XMIN)/XSCALE
      CALL SYMBOL(-0.04, ZXT, 0.08, 13, -90., -1)
      IF(MODXS.EQ.1.00) THEN
      CALL NUMBER(-0.25, ZXT+0.09, 0.09, ZXT1, -90., -1)
      ELSE
      CALL NUMBER(-0.25, ZXT+.18, 0.09, ZXT1, -90., 1)
      ENDIF
64    CONTINUE
      CALL SYMBOL(-.45, -3.063, .125, 23HIONIZATION POTENTIAL/EV, -90., 23)
C     MOVE TO FIRST POINT WITH PEN UP
      CALL PLOT(YCOUNTS(1), XIP(1), 3)
      DO 334 NPL=2, NCHAN
      IF ((NPL.LE.5.OR.(NCHAN-NPL).LE.5).AND.(YCOUNTS(NPL).EQ.(0.0)).OR.
     X(YCOUNTS(NPL-1).EQ.(0.0))) THEN
      CALL PLOT(YCOUNTS(NPL), XIP(NPL), 3)
      GO TO 334
      ENDIF
      CALL PLOT(YCOUNTS(NPL), XIP(NPL), 2)
334   CONTINUE
C     MOVE BACK TO ORIGIN PEN UP
      CALL PLOT(0., 0., 3)
C*********************************************************************
C     READ BLOWUP
71    READ(2, 72, END=79) ELOW, EHIGH, MAGFACT
72    FORMAT(F6.2/F6.2/I2)
C     DETERMINE THE CHANNEL NUMBERS OF THE RANGE
      LOWCHAN=JNINT((ELOW-IP(1))*1000./NWIDTH)
      IF (LOWCHAN.LT.1) LOWCHAN=1
      LHICHAN=JNINT((EHIGH-IP(1))*1000./NWIDTH)
      IF (LHICHAN.GT.NCHAN) LHICHAN=NCHAN
C     MOVE PEN TO FIRST POINT PEN UP
C     CHECK FOR OVERFLOW
      BF=YCOUNTS(LOWCHAN)*MAGFACT
      IF(BF.GT.3.50) BF=3.50
      CALL PLOT(BF, XIP(LOWCHAN), 3)
C     PLOT THE RANGE
      DO 73 NB=LOWCHAN, LHICHAN
      BY=YCOUNTS(NB)*MAGFACT
      IF (BY.GT.3.50) BY=3.50
      IF (((BY.GE.3.50).AND.(YCOUNTS(NB-1)*MAGFACT).GE.3.50).AND.(NB.GE.2))
     1THEN
      CALL PLOT(BY, XIP(NB), 3)
      ELSE
      CALL PLOT(BY, XIP(NB), 2)
      ENDIF
73    CONTINUE
      GO TO 71
C     MOVE BACK TO ORIGIN PEN UP
79    CALL PLOT(0., 0., 3)
C*********************************************************************
C     REPOSITION ORIGIN FOR BETA AXIS
      CALL PLOT(5.25, 0., -3)
      CALL SYMBOL(0.35, 0.37, 0.125, 4HBETA, 0., 4)
C     PLACE TICK MARKS EVERY HALF UNIT
```

```
C       AND LABEL EVERY UNIT
        DO 50 NB=1, 7
        Z=-1.00+(NB-1)*(0.500)
        IF (JMOD((NB-1), 2).EQ.0) CALL NUMBER(Z-.045, 0.1825, 0.09, Z, -90., -1)
        CALL SYMBOL(Z, -0.04, 0.08, 13, 0., -1)
50      CONTINUE
C       CHANGE THE ORIGIN FOR THE OTHER SIDE
        CALL PLOT(0., -9., -3)
C       PLACE TICK MARKS EVERY HALF UNIT
C       AND LABEL EVERY UNIT
        DO 55 NB=1, 7
        Z=-1.00+(NB-1)*(0.500)
        IF (JMOD((NB-1), 2).EQ.0) CALL NUMBER(Z-.045, -0.09, 0.09, Z, -90., -1)
        CALL SYMBOL(Z, 0.04, 0.08, 13, 0., -1)
55      CONTINUE
C       RESTORE THE ORIGIN FOR PLOTTING
        CALL PLOT(0., 9., -3)
        RETURN
        END
C*******************************************************
        SUBROUTINE BCKGRND (NTERMS, BKIP, BACK)
        COMMON/BTRD/ARRAY(10), AR(10), XMIN, XSCALE, CPS
        BACK=AR(NTERMS)
        DO 111 I=1, NTERMS-1
111     BACK=AR(NTERMS-I)+BACK*BKIP
        RETURN
        END
C*******************************************************
        SUBROUTINE BETARD
        COMMON/BTRD/ARRAY(10), AR(10), XMIN, XSCALE, CPS
C       SINCE THERE ARE AN INDETERMINATE NUMBER OF BETAS TO BE READ
C       THE READING IS TERMINATED BY AN EOF ON UNIT 10. READ IPS,
C       BETAS, DBS, IGNORE CHANNEL NUMBERS. A WORD ABOUT CONTACT
C       POTENTIAL SHIFTS: SINCE THE CPS OF A BAND MAY NOT BE KNOWN
C       AT THE TIME OF THE BETA CALCULATION I HAVE ELECTED FOR
C       MANUAL INSERTION INTO THE DATA FILE FOR010. THIS SHOULD BE
C       DONE AS FOLLOWS: COLUMN 1 SHOULD CONTAIN A STAR (*) AT THE
C       BEGINNING OF EACH DATA SET. THE NEXT LINE SHOULD CONTAIN THE
C       CONTACT POTENTIAL SHIFT WITH RESPECT TO THE BASE PLOT IN
C       EV.(F6.4). THE SIGN CONVENTION IS AS FOLLOWS: THE CPS IS
C       INHERENTLY POSITIVE, SO IF THE BAND HAS AN IP GREATER THAN
C       THAT IN THE BASE PLOT THE SIGN IN THE CPS SHOULD BE NEGATIVE
C       IF THE IP IS LOWER THE SIGN SHOULD BE POSITIVE.
400     READ(10, 401, END=490) STAR, BIP, BETA, DB
401     FORMAT(A1, 9X, F6.3, 4X, F8.5, 2X, F8.5)
        IF (STAR.EQ.'*') THEN
        READ(10, 450) CPSBAND
450     FORMAT(F6.4)
        GO TO 400
        END IF
        IF (BETA.GT.2 .OR. BETA.LT.-1) GO TO 400
C       CONVERT BIP FOR PLOTTING
        BIP=-((BIP+CPS+CPSBAND)-XMIN)/XSCALE
C       BETAS ARE ALREADY SCALED 1 UNIT/INCH
        CALL ERRBAR(BIP, BETA, DB)
C       REMEMBER THE PLOT IS SIDEWAYS RELATIVE TO THE PLOTTER
        GO TO 400
```

```
C       END PLOT
490     CALL PLOT(2.74999, -9.500, 999)
        RETURN
        END
C*********************************************************************
        SUBROUTINE ERRBAR(X, Y, DY)
C       MOVE TO POINT PEN UP
        CALL PLOT(Y+DY, X, 3)
C       MAKE STRAIGHT LINE TO Y-DY, X
        CALL PLOT(Y-DY, X, 2)
        RETURN
        END
C*********************************************************************
```

The program HRSPLOT.FOR produces a plot in an 8.5x11 format
of any single spectrum.
With the exception of file for010 containing the beta
values, the inputs of HRSPLOT.FOR are identical with those
of BPLOT.FOR.

```
C*************************************************************
        COMMON COUNTS(511), ANGLE, PRESS, IP(511)
        COMMON/BTRD/ARRAY(10), AR(10), XMIN, XSCALE, CPS
        DIMENSION XDATA(511)
        INTEGER THRESH, AV, GATE, ARGON
        REAL IP1, IP2, IP
C*************************************************************
C       READ INPUTS
C       READ PROGRAM CONTROL PARAMETERS
        READ (2, 52) IBACK, AV, CPS
52      FORMAT(I1/I2/F5.3)
C       READ INTERNAL DATA
        READ (3, 101) IP1, IP2, ANGLE, PRESS
101     FORMAT(///, 11X, F7.4, 4X, F7.4, 4X, F6.2, 11X, F6.3)
        READ (3, 102) SCAN, MV, MULT, GATE, IDWELL
102     FORMAT(F8.4/I5/I5/I5/I5//)
        DWELL=IDWELL*GATE/120.
        NWIDTH=MV*MULT
        NCHAN=SCAN*1000/NWIDTH
        READ (3, 103)(COUNTS(I), I=1, NCHAN)
103     FORMAT(F10.2)
C       END INPUT SEQUENCE FOR COUNTS
C*************************************************************
C       CALL THE SMOOTHING ROUTINE
        CALL SGSMOOTH(AV, NCHAN, COUNTS, XDATA)
        DO 225 MX=1, NCHAN
        COUNTS(MX)=XDATA(MX)
225     CONTINUE
C*************************************************************
        IF (IBACK .NE. 1) GO TO 210
C       READ BACKGROUND PARAMETERS: IF IBACK=1 INCLUDE BACKGRND
C       NINE BACKGROUND ANGLES ARE EXPLICITLY ASSUMED
C       PARAMETERS ARE FOR ONE SECOND DWELL
        READ(8, 200) NTERMS
200     FORMAT (I2)
C       INTIALIZE BACKGROUND ARRAYS
        DO 206 LJ=1, NTERMS
```

```
206       AR(LJ)=0.0
          DO 207 L=1, 9
          READ(8, 205) ANG, (ARRAY(M), M=1, NTERMS)
205       FORMAT(F10.2, 10(E15.8))
          IF ((JNINT(ANG).NE.(50.0)).AND.(JNINT(ANG).NE.(60.0))) GO TO 207
          DO 203 JB=1, NTERMS
203       AR(JB)=AR(JB)+ARRAY(JB)*(0.5)
207       CONTINUE
210       CONTINUE
C         END OF BACKGROUND PARAMETERS
C*************************************************************
          DO 123 N=1, NCHAN
C         SET UP ARRAY IP AND SUBTRACT OFF THE CONTACT POTENTIAL
C         OF THE BASE PLOT THE CONVENTION IS POSITIVE IE IF THE
C         APPARENT IP IS TOO HIGH CPS SHOULD BE NEGATIVE IF TOO LOW
C         CPS SHOULD BE POSITIVE TO CORRECT IT.
          IP(N)=IP1+((N-1)*NWIDTH)/1000.+CPS
C         SCALE COUNTS BY DWELL TO GET COUNTS/SEC
          COUNTS(N)=COUNTS(N)/DWELL
          IF ( IBACK .NE. 1) GO TO 220
          CALL BCKGRND(NTERMS, IP(N), BACK)
          COUNTS(N)=COUNTS(N)-BACK
          IF(COUNTS(N).LE.0.0) COUNTS(N)=0.0
220       CONTINUE
123       CONTINUE
          CALL BOX(NCHAN, NWIDTH)
          STOP
          END
C*************************************************************
          SUBROUTINE SGSMOOTH(NAV, N, DATA, XDATA)
          DIMENSION DATA(511), XDATA(511), P(25), COEFF(11, 15)
          DIMENSION NORM(11)
          DATA (COEFF(1, L), L=1, 3)/17, 12, -3/
          DATA (COEFF(2, L), L=1, 4)/7, 6, 3, -2/
          DATA (COEFF(3, L), L=1, 5)/59, 54, 39, 14, -21/
          DATA (COEFF(4, L), L=1, 6)/89, 84, 69, 44, 9, -36/
          DATA (COEFF(5, L), L=1, 7)/25, 24, 21, 16, 9, 0, -11/
          DATA (COEFF(6, L), L=1, 8)/167, 162, 147, 122, 87, 42, -13, -78/
          DATA (COEFF(7, L), L=1, 9)/43, 42, 39, 34, 27, 18, 7, -6, -21/
          DATA (COEFF(8, L), L=1, 10)/269, 264, 249, 224, 189, 144, 89, 24, -51, -136/
          DATA (COEFF(9, L), L=1, 11)/329, 324, 309, 284, 249, 204, 149, 84, 9, -76, -171/
          DATA (COEFF(10, L), L=1, 12)/79, 78, 75, 70, 63, 54, 43, 30, 15, -2, -21, -42/
          DATA (COEFF(11, L), L=1, 13)/467, 462, 447, 422, 387, 322, 287, 222, 147, 62, -33,
     *-138, -253/
          DATA NORM/35, 21, 231, 429, 143, 1105, 323, 2261, 3059, 8059, 5175/
          M=N-(NAV-1)
          NCOEFF=(NAV+1)/2
          LCOEFF=NCOEFF-2
C         TO GET THE CORRECT MEMBER OF THE COEFF AND NORM ARRAYS
C         LOAD POINTS INTO P ARRAY
C         ARRAY INITIALLY OFFSET FOR CHANNEL ADVANCE SEQUENCE
          DO 10 I=1, NAV-1
10        P(I+1)=DATA(I)
C         SMOOTHING LOOP
          DO 200 I=1, M
```

```
      J=I+(NAV-1)
      DO 11 K=1, NAV-1
11    P(K)=P(K+1)
      P(NAV)=DATA(J)
C     SET UP LOOP TO DO SUM
      SUM=COEFF(LCOEFF, 1)*P(NCOEFF)
      DO 22 L=2, NCOEFF
22    SUM=SUM+COEFF(LCOEFF, L)*(P(NCOEFF-(L-1))+P(NCOEFF+(L-1)))
      XDATA(I+NCOEFF-1)=SUM/FLOAT(NORM(LCOEFF))
200   CONTINUE
      RETURN
      END
C*****************************************************
C     NOTE: THIS FRAME IS DRAWN SIDEWAYS WITH RESPECT TO THE PLOTTER
C     ORIENTATION IS COUNTS AND BETAS ARE POSITIVE XAXIS (PLOTTER)
C     IP ARE ON THE NEGATIVE YAXIS(PLOTTER) N.B. THIS PROGRAM IS NOT
C     ALWAYS CONSISTANT ABOUT THE REFERENCE IE PLOTTER VS PLOT.
C     PEN LOCUS IS INITIAL ORIGIN
      SUBROUTINE BOX(NCHAN, NWIDTH)
      COMMON COUNTS(511), ANGLE, PRESS, IP(511)
      COMMON/BTRD/ARRAY(10), AR(10), XMIN, XSCALE, CPS
      DIMENSION XIP(511), YCOUNTS(511), MODN(6), MODX(4)
      INTEGER*2 LABELPLOT(35)
      REAL IP, MODX, MODXS
      DATA (MODN(L), L=1, 6)/1, 2, 5, 10, 20, 50/
      DATA (MODX(M), M=1, 4)/0.10, 0.20, 0.50, 1.00/
      READ (7, 978, END=979) LABELPLOT
978   FORMAT(35A1)
979   CONTINUE
      CALL PLOTS(53, 0, 15)
C     PLOT FILE IS FOR0015
C     REPOSITION ORIGIN-PEN UP
      CALL SPEED(5)
      CALL PLOT(.5, .5, -3)
C     DRAW BOX
      CALL PLOT(7., 0., 2)
      CALL PLOT(7., 9., 2)
      CALL PLOT(0., 9., 2)
      CALL PLOT(0., 0., 2)
C     PLOT LABEL
      CALL SYMBOL(4.25, 10.25, -.10, LABELPLOT, 0.00, 20)
C     LABEL PLOT
      CALL PLOT(0., 9., -3)
C*****************************************************************
C     OFFSET IP ARRAY AND SCALE IT
      XMIN=IP(1)
      XMAX=IP(NCHAN)
      DELTA=1.05*(XMAX-XMIN)
C     FIND SCALE IN UNITS/INCH
      XSCALE=DELTA/9.0
C     DEFINE NEW XMAX, XMIN
C     ALLOWS 5% FOR BORDERS
      XMIN=XMIN-(.025*DELTA)
      XMAX=XMAX+(.025*DELTA)
C     OFFSET THE ARRAY AND NEGATE IT TO FIT IN THE AREA
```

```
      DO 333 NX=1, NCHAN
333   XIP(NX)=-(IP(NX)-XMIN)/XSCALE
C*********************************************************************
C     SCALE COUNTS TO FIT
C     FIND THE MAXIMUM COUNT
      CMAX=0.
      DO 332 IC=1, NCHAN
      IF (COUNTS(IC).GT.CMAX) CMAX=COUNTS(IC)
332   CONTINUE
C     FIND THE SCALE FOR THE COUNTS
      CSCALE=1.05*CMAX/7.0
C     CREATE NEW ARRAY FOR PLOTTING
      DO 336 K=1, NCHAN
336   YCOUNTS(K)=COUNTS(K)/CSCALE
C*********************************************************************
C     DETERMINE INTENSITY SCALING
      DO 40 MD=1, 6
      IF((CMAX/MODN(MD)).GT.8) GO TO 40
      IF((CMAX/MODN(MD)).LT.3)THEN
      IF (MD.EQ.1) GO TO 41
      MODS=MODN(MD-1)
      ELSE
      MODS=MODN(MD)
      GO TO 42
      ENDIF
40    CONTINUE
C     CASE IF I LESS THAN 3 COUNTS/SEC TO BE DETERMINE LATER
41    CONTINUE
C     DETERMINE NUMBER OF TICKS WITH SPACING MODS
42    NTICK=JINT(1.05*CMAX/MODS)
      DO 46 NA=1, 2
C     LABEL ZERO
      IF (NA.EQ.1) THEN
      CALL NUMBER(-0.045, 0.1825, 0.09, 0.0, -90., -1)
      ELSE
      CALL NUMBER(-0.045, -9.09, 0.09, 0.0, -90., -1)
      ENDIF
      DO 44 NT=1, NTICK
      ZT=NT*MODS/CSCALE
      ZT1=NT*MODS
C     NUMBER THE TICKMARK
C     DETERMINE NUMBER OF DIGITS IN LABEL
C     CASE OF LESS THAN ONE POSTPONED TO A LATER TIME
      IF(ZT1.GE.1.) NDIG=1
      IF(ZT1.GE.10.) NDIG=2
      IF(ZT1.GE.100.) NDIG=3
      IF(ZT1.GE.1000.) NDIG=4
      IF (NA.EQ.1) THEN
      CALL NUMBER(ZT-0.045, NDIG*0.09+.0025, 0.09, ZT1, -90., -1)
C     PLACE THE TICKMARK
      CALL SYMBOL(ZT, -0.04, .08, 13, 0., -1)
      ELSE
C     NOW THE OTHER SIDE
      CALL NUMBER(ZT-0.045, -9.09, 0.09, ZT1, -90., -1)
      CALL SYMBOL(ZT, -8.96, 0.08, 13, 0., -1)
      ENDIF
```

```
44      CONTINUE
46      CONTINUE
        CALL SYMBOL(2.5625, 0.37, .125, 14HI/(COUNTS/SEC), 0., 14)
C*****************************************************************
C       WORK ON THE ENERGY AXIS
C       DETERMINE SCALING
        DO 60 MD=1, 4
C       FIND THE FIRST TICKMARK GT XMIN
        ZX=JINT(XMIN/MODX(MD))+1.00
        FIRST=ZX*MODX(MD)
C       FIND NEW DELTA
        DELTA1=XMAX-FIRST
C       DETERMINE NUMBER OF TICKS AT THIS MOD
        XTICK=DELTA1/MODX(MD)
        IF(XTICK.GT.8) THEN
        IF(MD.EQ.4) THEN
        MODXS=MODX(MD)
        GO TO 62
        ENDIF
        GO TO 60
        ENDIF
        IF(XTICK.LT.3) THEN
        IF (MD.EQ.1) THEN
        MODXS=MODX(MD)
        GO TO 62
        ENDIF
        MODXS=MODX(MD-1)
        ELSE
        MODXS=MODX(MD)
        GO TO 62
        ENDIF
60      CONTINUE
C       LABEL FIRST
62      NXTICK=JINT(XTICK)
        ZXF=-(FIRST-XMIN)/XSCALE
        CALL SYMBOL(-0.04, ZXF, 0.08, 13, -90., -1)
        IF(MODXS.EQ.1.00) THEN
        CALL NUMBER(-0.25, ZXF+0.09, 0.09, FIRST, -90., -1)
        ELSE
        CALL NUMBER(-0.25, ZXF+.1825, 0.09, FIRST, -90., 1)
        ENDIF
        DO 64 NT=1, NXTICK
        ZXT1=FIRST+NT*MODXS
        ZXT=-(ZXT1-XMIN)/XSCALE
        CALL SYMBOL(-0.04, ZXT, 0.08, 13, -90., -1)
        IF(MODXS.EQ.1.00) THEN
        CALL NUMBER(-0.25, ZXT+0.09, 0.09, ZXT1, -90., -1)
        ELSE
        CALL NUMBER(-0.25, ZXT+.18, 0.09, ZXT1, -90., 1)
        ENDIF
64      CONTINUE
        CALL SYMBOL(-.45, -3.063, .125, 23HIONIZATION POTENTIAL/EV, -90., 23)
C       MOVE TO FIRST POINT WITH PEN UP
        CALL PLOT(YCOUNTS(1), XIP(1), 3)
        DO 334 NPL=2, NCHAN
        IF ((NPL.LE.5.OR.(NCHAN-NPL).LE.5).AND.(YCOUNTS(NPL).EQ.(0.0)).OR.
```

```
    X(YCOUNTS(NPL-1).EQ.(0.0))) THEN
          CALL PLOT(YCOUNTS(NPL), XIP(NPL), 3)
          GO TO 334
          ENDIF
          CALL PLOT(YCOUNTS(NPL), XIP(NPL), 2)
334       CONTINUE
C         MOVE BACK TO ORIGIN PEN UP
          CALL PLOT(0., 0., 3)
C*************************************************************************
C         READ BLOWUP
71        READ(2, 72, END=79) ELOW, EHIGH, MAGFACT
72        FORMAT(F6.2/F6.2/I2)
C         DETERMINE THE CHANNEL NUMBERS OF THE RANGE
          LOWCHAN=JNINT((ELOW-IP(1))*1000./NWIDTH)
          IF (LOWCHAN.LT.1) LOWCHAN=1
          LHICHAN=JNINT((EHIGH-IP(1))*1000./NWIDTH)
          IF (LHICHAN.GT.NCHAN) LHICHAN=NCHAN
C         MOVE PEN TO FIRST POINT PEN UP
C         CHECK FOR OVERFLOW
          BF=YCOUNTS(LOWCHAN)*MAGFACT
          IF(BF.GT.6.00) BF=6.00
          CALL PLOT(BF, XIP(LOWCHAN), 3)
C         PLOT THE RANGE
          DO 73 NB=LOWCHAN, LHICHAN
          BY=YCOUNTS(NB)*MAGFACT
          IF (BY.GT.6.00) BY=6.00
          IF (((BY.GE.6.00).AND.(YCOUNTS(NB-1)*MAGFACT).GE.6.00).AND.(NB.GE.2))
          1THEN
          CALL PLOT(BY, XIP(NB), 3)
          ELSE
          CALL PLOT(BY, XIP(NB), 2)
          ENDIF
73        CONTINUE
          GO TO 71
C         END PLOT
79        CALL PLOT(7.99999, -9.5, 999)
          RETURN
          END
C*************************************************************
          SUBROUTINE BCKGRND (NTERMS, BKIP, BACK)
          COMMON/BTRD/ARRAY(10), AR(10), XMIN, XSCALE, CPS
          BACK=AR(NTERMS)
          DO 111 I=1, NTERMS-1
111       BACK=AR(NTERMS-I)+BACK*BKIP
          RETURN
          END
C*************************************************************
```

The program CHIMERA.FOR tests the fit of the background parameters by plotting the background spectra and the values calculated from the coefficients on the same plot.

Inputs:

'Parameter'****for005

This must be assigned or it will default to sys$input.

NSPECTRA

(I1)

NSPECTRA= the number of spectra to be plotted

```
          'Internal'****for003
This file must contain the background spectra as transmitted.

          'Background'***for008
This file must contain the background parameters generated
by BACK.FOR

C*************************************************************
          COMMON COUNTS(511), ANGLE, PRESS, IP(511), BACKK(511)
          COMMON/BTRD/ARRAY(10), AR(10), XMIN, XSCALE
          DIMENSION XDATA(511)
          INTEGER THRESH, AV, GATE, ARGON
          REAL IP1, IP2, IP
          CALL PLOTS(53, 0, 15)
C*************************************************************
C         CREATE A LOOP TO PLOT OUT AS MANY SETS OF DATA
C         AS DESIRED
          READ (5, 23) NSPECTRA
23        FORMAT(I1)
          DO 4444 MNSP=1, NSPECTRA
C*************************************************************
C         READ INTERNAL DATA
          IF (MNSP.NE.1) GO TO 107
          READ (3, 108) IP1, IP2, ANGLE, PRESS
108       FORMAT(///, 11X, F7.4, 4X, F7.4, 4X, F6.2, 11X, F6.3)
          GO TO 106
107       READ (3, 101) IP1, IP2, ANGLE, PRESS
101       FORMAT(/, 11X, F7.4, 4X, F7.4, 4X, F6.2, 11X, F6.3)
106       READ (3, 102) SCAN, MV, MULT, GATE, IDWELL
102       FORMAT(F8.4/I5/I5/I5/I5//)
          DWELL=IDWELL*GATE/120.
          NWIDTH=MV*MULT
          NCHAN=SCAN*1000/NWIDTH
          READ (3, 103)(COUNTS(I), I=1, NCHAN)
103       FORMAT(F10.2)
C         END INPUT SEQUENCE FOR COUNTS
C*************************************************************
C         CALL THE SMOOTHING ROUTINE
          AV=5
          CALL SGSMOOTH(AV, NCHAN, COUNTS, XDATA)
          DO 225 MX=1, NCHAN
          COUNTS(MX)=XDATA(MX)
225       CONTINUE
C*************************************************************
C         PARAMETERS ARE FOR ONE SECOND DWELL
          READ(8, 200) NTERMS
200       FORMAT (I2)
C         INTIALIZE BACKGROUND ARRAYS
          DO 206 LJ=1, NTERMS
206       AR(LJ)=0.0
          DO 207 L=1, 9
          READ(8, 205) ANG, (ARRAY(M), M=1, NTERMS)
205       FORMAT(F10.2, 10(E15.8))
          IF (JNINT(ANG).NE.JNINT(ANGLE)) GO TO 207
          DO 203 JB=1, NTERMS
```

```
203       AR(JB)=AR(JB)+ARRAY(JB)
207       CONTINUE
210       CONTINUE
          REWIND 8
C         END OF BACKGROUND PARAMETERS
C*************************************************************
          DO 123 N=1, NCHAN
C         SET UP ARRAY IP AND SUBTRACT OFF THE CONTACT POTENTIAL
          IP(N)=IP1+((N-1)*NWIDTH)/1000.-CP1
C         SCALE COUNTS BY DWELL TO GET COUNTS/SEC
          COUNTS(N)=COUNTS(N)/DWELL
          CALL BCKGRND(NTERMS, IP(N), BACK)
          BACKK(N)=BACK
220       CONTINUE
123       CONTINUE
          CALL BOX(NCHAN)
4444      CONTINUE
          CALL PLOT(8.0, -10.5, 999)
          STOP
          END
C*************************************************************
          SUBROUTINE SGSMOOTH(NAV, N, DATA, XDATA)
          DIMENSION DATA(511), XDATA(511), P(25), COEFF(11, 15)
          DIMENSION NORM(11)
          DATA (COEFF(1, L), L=1, 3)/17, 12, -3/
          DATA (COEFF(2, L), L=1, 4)/7, 6, 3, -2/
          DATA (COEFF(3, L), L=1, 5)/59, 54, 39, 14, -21/
          DATA (COEFF(4, L), L=1, 6)/89, 84, 69, 44, 9, -36/
          DATA (COEFF(5, L), L=1, 7)/25, 24, 21, 16, 9, 0, -11/
          DATA (COEFF(6, L), L=1, 8)/167, 162, 147, 122, 87, 42, -13, -78/
          DATA (COEFF(7, L), L=1, 9)/43, 42, 39, 34, 27, 18, 7, -6, -21/
          DATA (COEFF(8, L), L=1, 10)/269, 264, 249, 224, 189, 144, 89, 24, -51, -136/
          DATA (COEFF(9, L), L=1, 11)/329, 324, 309, 284, 249, 204, 149, 84, 9, -76, -171/
          DATA (COEFF(10, L), L=1, 12)/79, 78, 75, 70, 63, 54, 43, 30, 15, -2, -21, -42/
          DATA (COEFF(11, L), L=1, 13)/467, 462, 447, 422, 387, 322, 287, 222, 147, 62, -33,
     *-138, -253/
          DATA NORM/35, 21, 231, 429, 143, 1105, 323, 2261, 3059, 8059, 5175/
          M=N-(NAV-1)
          NCOEFF=(NAV+1)/2
          LCOEFF=NCOEFF-2
C         TO GET THE CORRECT MEMBER OF THE COEFF AND NORM ARRAYS
C         LOAD POINTS INTO P ARRAY
C         ARRAY INITIALLY OFFSET FOR CHANNEL ADVANCE SEQUENCE
          DO 10 I=1, NAV-1
10        P(I+1)=DATA(I)
C         SMOOTHING LOOP
          DO 200 I=1, M
          J=I+(NAV-1)
          DO 11 K=1, NAV-1
11        P(K)=P(K+1)
          P(NAV)=DATA(J)
C         SET UP LOOP TO DO SUM
          SUM=COEFF(LCOEFF, 1)*P(NCOEFF)
          DO 22 L=2, NCOEFF
22        SUM=SUM+COEFF(LCOEFF, L)*(P(NCOEFF-(L-1))+P(NCOEFF+(L-1)))
```

```
      XDATA(I+NCOEFF-1)=SUM/FLOAT(NORM(LCOEFF))
200   CONTINUE
      RETURN
      END
C*************************************************************
C     NOTE: THIS FRAME IS DRAWN SIDEWAYS WITH RESPECT TO THE PLOTTER
C     ORIENTATION IS COUNTS AND BETAS ARE POSITIVE XAXIS (PLOTTER)
C     IP ARE ON THE NEGATIVE YAXIS(PLOTTER) N.B. THIS PROGRAM IS NOT
C     ALWAYS CONSISTANT ABOUT THE REFERENCE IE PLOTTER VS PLOT.
C     PEN LOCUS IS INITIAL ORIGIN
      SUBROUTINE BOX(NCHAN)
      COMMON COUNTS(511), ANGLE, PRESS, IP(511), BACKK(511)
      COMMON/BTRD/ARRAY(10), AR(10), XMIN, XSCALE
      DIMENSION XIP(511), YCOUNTS(511), YBACK(511)
      REAL IP
C     PLOT FILE IS FOR0015
C     REPOSITION ORIGIN-PEN UP
      CALL SPEED(5)
      CALL PLOT(.5, .5, -3)
C     DRAW BOX
      CALL PLOT(7., 0., 2)
      CALL PLOT(7., 10., 2)
      CALL PLOT(0., 10., 2)
      CALL PLOT(0., 0., 2)
C     LABEL PLOT
      CALL PLOT(0., 10., -3)
C*************************************************************
C     OFFSET IP ARRAY AND SCALE IT
C     FIND THE INTEGER CLOSEST TO THE MINIMUM BUT DOES NOT EXCEDE IT
      XMIN=AINT(IP(1))
C     FIND THE NEXT LARGEST INTEGER TO THE MAXIMUM
      XMAX=AINT(IP(NCHAN))
      IF (XMAX .LT. IP(NCHAN)) XMAX=XMAX+1.00
      DELTA=XMAX-XMIN
C     FIND SCALE IN UNITS/INCH
      XSCALE=DELTA/10.0
C     OFFSET THE ARRAY AND NEGATE IT TO FIT IN THE AREA
      DO 333 NX=1, NCHAN
333   XIP(NX)=-(IP(NX)-XMIN)/XSCALE
C*************************************************************
C     SCALE COUNTS TO FIT
C     FIND THE MAXIMUM COUNT
      CMAX=0.
      DO 332 IC=1, NCHAN
      IF (COUNTS(IC).GT.CMAX) CMAX=COUNTS(IC)
332   CONTINUE
C     FIND THE SCALE FOR THE COUNTS
      CSCALE=CMAX/6.
C     CREATE NEW ARRAY FOR PLOTTING
      DO 336 K=1, NCHAN
      YBACK(K)=BACKK(K)/CSCALE
336   YCOUNTS(K)=COUNTS(K)/CSCALE
C     SINCE THE XAXIS STARTS AND ENDS ON AN INTEGER TICK
C     MARK EACH INTEGER AND LABEL EVERY EVEN ONE
      XL=XMIN
233   XLP=-(XL-XMIN)/XSCALE
```

```
      CALL SYMBOL(-.04, XLP, .08, 13, -90., -1)
C     IF XL IS EVEN LABEL IT
      IF (AMOD(XL, 2.).EQ. 0.) CALL NUMBER(-.2, XLP+.2, .1, XL, -90., 2)
      XL=XL+1.00
      IF(XL.LE.XMAX) GO TO 233
      CALL SYMBOL(-.45, -3.563, .125, 25HIONIZATION POTENTIAL (EV), -90., 25)
      CALL AXIS(0., 0., 14HI (COUNTS/SEC), 14, 5.99, 0., 0., CSCALE)
C     MOVE TO FIRST POINT WITH PEN UP
      CALL PLOT(YCOUNTS(1), XIP(1), 3)
      DO 334 NPL=2, NCHAN
334   CALL PLOT(YCOUNTS(NPL), XIP(NPL), 2)
      DO 338 NBL=1, NCHAN
      YB=YBACK(NBL)
      IF (YB.GE.7.) YB=7.
      IF (YB.LE.0.) YB=0.
338   CALL SYMBOL(YB, XIP(NBL), .05, 4, 0., -1)
      CALL PLOT(8.0, -10.5, -3)
      RETURN
      END
C*************************************************************
      SUBROUTINE BCKGRND (NTERMS, BKIP, BACK)
      COMMON/BTRD/ARRAY(10), AR(10), XMIN, XSCALE
      BACK=AR(NTERMS)
      DO 111 I=1, NTERMS-1
111   BACK=AR(NTERMS-I)+BACK*BKIP
      RETURN
      END
C*************************************************************
This program, QUICKPLOT.FOR plots up to nine spectra in
sucession to the terminal screen of any VT-100 terminal
equipped with advanced video capacity.
Input:
      'External'***for003
All parameters are read directly from the spectrum file.
No modification is needed.

      'Control'****for005=sys$input
Interactive control:
N= display the new spectrum
Q= quit

C*************************************************************
      CHARACTER*80 TITLE
      CHARACTER*20 TITLE1
      CHARACTER*1 SP, TITLE2, TITLE3
      COMMON COUNTS(511), IP(511)
      REAL IP1, IP2, IP
      INTEGER GATE
C*************************************************************
      DATA TITLE1/'INTENSITY VS. IP '/
      SP=CHAR(32)
C     READ INPUTS
C     READ INTERNAL DATA
      DO 110 JI=1, 9
      IF (JI.NE.1) THEN
90    READ(5, 99) NEXT
```

```
99      FORMAT(A1)
        IF (NEXT.EQ.'Q') GO TO 111
        IF (NEXT.NE.'N') GO TO 90
        END IF
        IF (JI.NE.1) GO TO 106
        READ (3, 101) IP1, IP2, ANG
101     FORMAT(///, 11X, F7.4, 4X, F7.4, 4X, F6.2)
        GO TO 105
106     READ (3, 104) IP1, IP2, ANG
104     FORMAT(/, 11X, F7.4, 4X, F7.4, 4X, F6.2)
105     READ (3, 102) SCAN, MV, MULT, GATE, IDWELL
102     FORMAT(F8.4/I5/I5/I5/I5//)
        DWELL=IDWELL*GATE/120.
        NWIDTH=MV*MULT
        NCHAN=SCAN*1000/NWIDTH
        READ (3, 103)(COUNTS(I), I=1, NCHAN)
103     FORMAT(F10.2)
C       END INPUT SEQUENCE FOR COUNTS
C*************************************************************
        DO 10 N=1, NCHAN
10      IP(N)=IP1+((N-1)*NWIDTH)/1000.
        IANG=NINT(ANG)
        IANG1=IANG/10
        IF(IANG1.GE.10)THEN
        IANG2=IANG1-10
        TITLE2=CHAR(IANG2+48)
        TITLE=TITLE1//'1'//TITLE2//'0'//' DEGREES'
        ELSE
        TITLE2=CHAR(IANG1+48)
        IANG2=IANG-(IANG1*10)
        TITLE3=CHAR(IANG2+48)
        TITLE=TITLE1//SP//TITLE2//TITLE3//' DEGREES'
        ENDIF
        CALL VTPLOT(NCHAN, IP, COUNTS, 0, 0.0, TITLE)
110     CONTINUE
111     END
```

REFERENCES

1. A. Savitzky and M. Golay, *Anal. Chem.*, **36**, 1627 (1962).

2. P. Bevington, *Data Reduction and Error Analysis for the Physical Sciences* (McGraw-Hill, New York, 1969).

FIGURE CAPTIONS

Figure 1. A program flow diagram for using the software developed for data reduction on the VAX-11/780.

FIGURE 1.

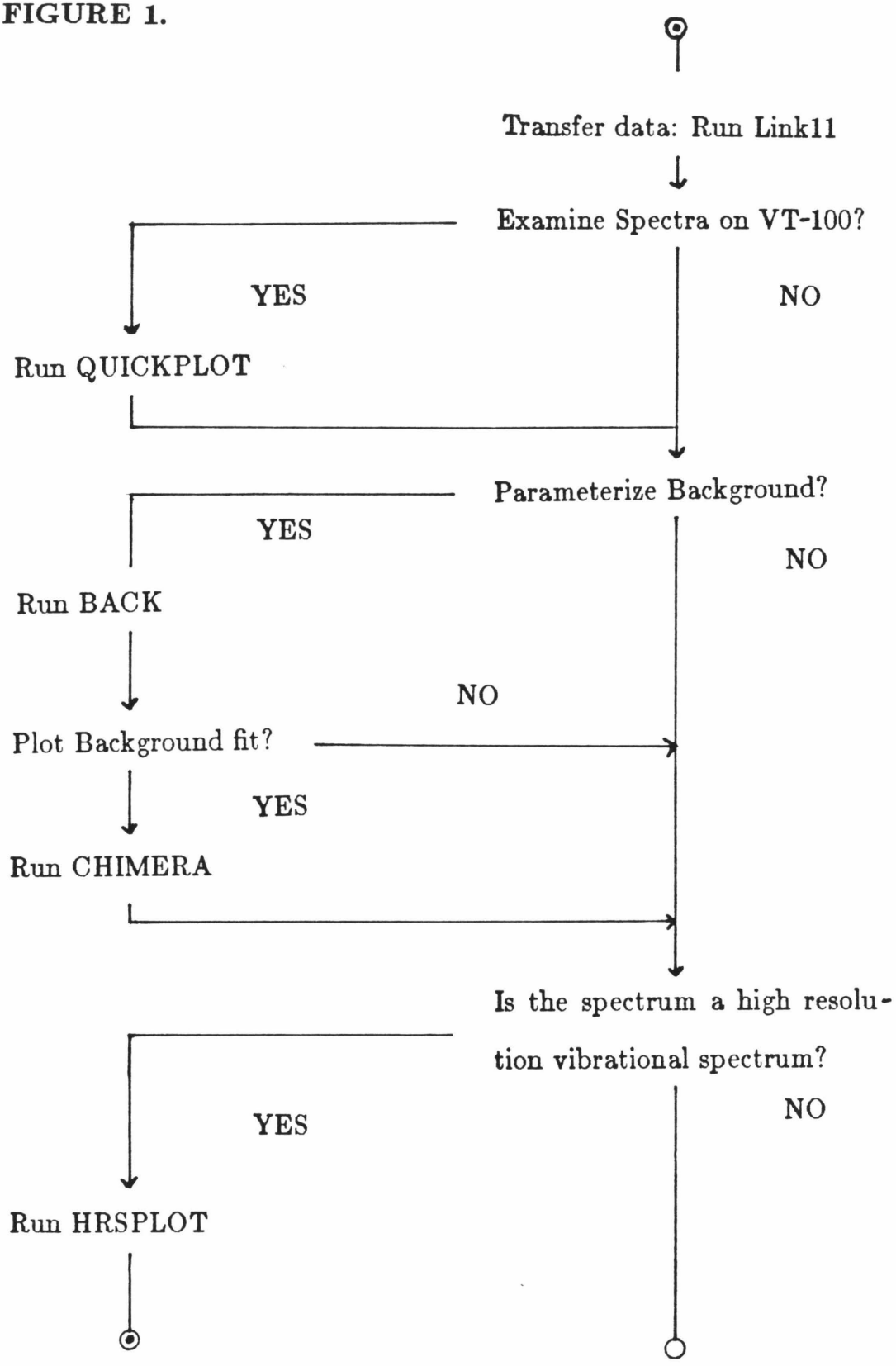
Transfer data: Run Link11
Examine Spectra on VT-100?
YES
NO
Run QUICKPLOT
Parameterize Background?
YES
NO
Run BACK
NO
Plot Background fit?
YES
Run CHIMERA
Is the spectrum a high resolution vibrational spectrum?
YES
NO
Run HRSPLOT

FIGURE 1: continued